UNIVERSIDAD AUTÓNOMA DE MADRID
Departamento de Biología Molecular

INSTITUTO NACIONAL DE TÉCNICA AEROESPACIAL –
CONSEJO SUPERIOR DE INVESTIGACIONES CIENTÍFICAS
Centro de Astrobiología

Isolation and characterization of *Acidiphilium* sp. PM, a nickel-resistant electricigen from Río Tinto

DOCTORAL THESIS

Patxi San Martín Úriz

Madrid, 2015

Universidad Autónoma de Madrid

Facultad de Ciencias

Departamento de Biología Molecular

Instituto Nacional de Técnica Aeroespacial –
Consejo Superior de Investigaciones Científicas

Centro de Astrobiología

Isolation and characterization of *Acidiphilium* sp. PM, a nickel-resistant electricigen from Río Tinto

DOCTORAL THESIS

Patxi San Martín Úriz

Madrid, 2015

A thesis presented to the Facultad de Ciencias, Universidad Autónoma de Madrid, in fulfillment of the requirements for the degree of Doctor of Philosophy

The research here presented was carried out at the Centro de Astrobiología (Instituto Nacional de Técnica Aeroespacial - Consejo Superior de Investigaciones Científicas) under the supervision of Professor Ricardo Amils.

Patxi San Martín Úriz was supported by the Consejo Superior de Investigaciones Científicas through an I3P fellowship and by the Instituto Nacional de Técnica Aeroespacial in the form of a Rafael Calvo Rodés fellowship.

D. Ricardo Amils Pibernat, Catedrático de Microbiología de la Universidad Autónoma de Madrid,

Certifica:

Que la Tesis Doctoral titulada “Isolation and characterization of *Acidiphilium* sp. PM, a nickel-resistant electricigen from Río Tinto”, de la que es autor Patxi San Martín Úriz, ha sido realizada bajo su dirección en el Centro de Astrobiología y cumple los requisitos exigidos para optar al grado de Doctor en Ciencias

Para que conste, lo firmo en Madrid, a cinco de enero de 2015.

Dr. Ricardo Amils Pibernat

A la mirada de mi padre, al latido de mi madre.

"Quizá podría dividirse la suma de los seres humanos, de toda cultura y toda raza, entre los que se alquilan y los que se dan (…)".

—Gonzalo Sánchez Terán. *Los silencios de Dios y otras metáforas*

ACKNOWLEDGEMENTS

Gracias a todos aquellos que pagan sus impuestos, porque su dinero se materializó en dos becas que me permitieron vivir y en el material que permitió llevar a cabo esta investigación.

A Ricardo Amils, que me permitió hacer la tesis en su laboratorio, equivocarme incontables veces y me enseñó a buscarme la vida y a asumir el rumbo de esta tesis.

Gracias a Kirsten Küsel (Friedrich Schiller University Jena) por el cultivo de *Acp. cryptum* JF-5 y a Moustafa Malki (Instituto de Catálisis y Petroleoquímica) por el de *Acidiphilium* sp. 3.2 Sup 5, que desató esta tesis. A Monike Oggerin le debo el aprendizaje del campo pulsado, y a Elena González Toril el de CARD-FISH. A Nuria Rodríguez y a la dedicación de Mari Paz Martín debo las cuantificaciones de metales pesados. La filogenia de *Acidiphilium* es obra de Elena González Toril y Alejandro Palomo. Todo lo que sé sobre *microarrays* se lo debo a Pedro Alcolea y Mercedes Moreno y a su infinita paciencia. La caracterización de las fuentes de energía de *Acidiphilium* sp. PM es fruto de la generosidad de Irene Sánchez Andrea. Sin el trabajo laborioso y meticuloso de Manuel Gómez, Rafa Bargiela y Aida Arcas no hubiera salido un solo dato sobre el genoma de *Acidiphilium*. Y sin la ayuda de Olga Zafra, Vero Morgante, Eugenia Guazzaroni, Carolina González, pero sobre todo de Salvador Mirete y Eduardo González Pastor, aún seguiría peleándome por sacar adelante el *screening* funcional de la genoteca. A la diligencia y profesionalidad de Marina Postigo debo miles de lecturas de secuenciación y la utilización del robot epMotion que me ahorró equivocaciones y muchas horas de trabajo. Los protocolos y el empuje de David Lara permitieron extracciones proteicas de calidad y Montse Martínez Gomáriz (Parque Científico de Madrid – UCM) consiguió que las 2D-DIGE fueran un éxito. El consejo siempre amable de Chus García y Encarna de Miguel (Life Technologies) y de Alberto Mudarra y Sandra Gonzalo (CBM), contribuyó a llevar a buen puerto las qPCRs.

Hay veces que a uno le gustaría gastar sombrero para poder quitárselo delante de ciertas personas. Pedro Alcolea comenzó a reunirse conmigo hace siete años para aconsejarme sobre cómo hacer una genoteca simplemente porque él sabía cómo hacerlo. La última reunión fue este mismo 2015. Manuel Gómez ha dedicado literalmente cientos de horas a trabajar en *Acidiphilium* sp. PM, no sólo en la parte de análisis bioinformático sino

también discutiendo mis experimentos. Sus contribuciones a esta tesis han sido definitivas. ¡MUCHAS GRACIAS a los dos!

Esta tesis está basada en consejos desinteresados y muchas horas de discusión con personas que no tenían ninguna responsabilidad para conmigo. Mi agradecimiento a todas ellas, y en especial a Eduardo González Pastor, Francisco López de Saro, Jaime Iranzo y Mercedes Moreno, es enorme.

Gracias a toda la gente del C-101, el 104 y el laboratorio de extremofilia. Especialmente a Antonio, porque le pidieron que me "enseñara el oficio" y lo hizo con dedicación y paciencia; a Lilia porque su capacidad de trabajo y pasión por la ciencia nos movieron a muchos a aprender; a Nico, Carlotta, Ine y Monike junto a los que inicié camino. Gracias a los estudiantes de módulo, de máster o de grado con los que he tenido la suerte de compartir poyata (especialmente a Raúl y Alex), porque vuestro entusiasmo es recordatorio constante de lo fascinante que puede ser la ciencia. Mi deuda con Ángeles dista mucho de estar saldada. Por los papers, consejos desinteresados y cientos de kilómetros de coche, ¡gracias! Compartir horas de laboratorio, de discusiones científicas o "filosóficas", de montaña o de cena con Fran, David, Enoma y Cristina conforman algunos de los mejores recuerdos de esta tesis, ¡GRACIAS, chicos!

Sin la buena disposición y la sonrisa del personal de gerencia (Maite, Gloria, Tatiana, Macarena y Esther incluidas), de Rosa y de Pedro, el CAB sería un lugar más sombrío y gris. Mi tesis no hubiera siquiera empezado sin los préstamos, consejos y ayuda constante de multitud de personas de otros laboratorios a los que sería interminable nombrar. Gracias a todos por hacer el CAB más solidario, más habitable. Mi agradecimiento es especial a Graciela, Fernando Puente, Héctor, Laura García, Celia, Ana García, Luis Mora, Fernando Camps, Luis Cuesta, Antonio Pérez, Zoubir, David Bermejo, Paco Najarro… porque su disposición a ayudar y sus ánimos hicieron esta etapa más sencilla.

Gracias a María Serrano, María Lamprecht y Vicky, por muchas risas y ánimos en un laboratorio a horas absurdas, en un despacho inundado de papers o en cualquier terraza de Madrid.

Durante estos años he tenido la suerte de sentarme a la mesa con un grupo de personas magníficas cuyas conversaciones terminaron por derrocar algunos de mis prejuicios, templar mis ánimos y afianzar algunas convicciones. Gracias a Eva, Francisco, Michael, Delphine, Manuel, Virginia, Andrew, Jakob, Aurora, Javier, Maria Rosa, Elena Puga, Carlos, Montse… por tantas y tan buenas conversaciones.

Gracias a Jacobo Aguirre, por esa clase de astronomía “suelta” que se transformó en siete cursos y algunos de mis mejores recuerdos de Madrid, por acercarme a la física teórica y participarme de tu filosofía de vida.

Gracias a Urtzi, por los consejos, por los planes, por descubrirme Madrid recién llegado. Por seguir ahí, pese a la distancia y los años. A Pat, por los ánimos y las confidencias. Por apretarme de vez en cuando.

A mis compañeros de piso, Alex, Carlos, Raquel, Rubén y Siria, que se convirtieron casi en familia. Porque hay que poner mucho de cada uno para convivir tantos años y eso no se olvida.

Pocas veces tiene uno la fortuna de encontrar gente que se entrega sin reservas. GRACIAS Patri, por darte a bocajarro a cuantas personas hemos tenido la fortuna de cruzarnos en tu vida.

A la gente de Cruz Roja, en particular a los voluntarios de Bravo 11, por docenas de guardias llenas de humanidad y compromiso.

A Amaya, por dos años preciosos. Por su idealismo y sus ganas de coherencia.

Mis años de tesis están salpicados de recuerdos de montaña. Sin la energía y claridad que me proporciona, esta tesis y quien la escribe probablemente hubieran naufragado. Gracias a Juanillo, Luis, Gabriel y Pablo Merino por muy buenos momentos en la montaña, de travesía, escalando o esquiando. Gracias, a Jaime por las travesías por Dolomitas, Alpes o por cualquier tachuela, por los increíbles paisajes y mejores conversaciones. Gracias a Roberto, por atardeceres en la sierra, bailes regionales calzando crampones y por tu gran sentido del humor y de la amistad. Gracias a Iñaki, Aitor, Txipa y Alex por palizas épicas con sonrisas de dos palmos.

Gracias a la kuadrilla (a Gari, Goñi, Ángel, Iván, Luisma, Maria Pilar y Lorea), por aguantar “minutos culturales” que duraban media noche… ¡y los que os quedan! A Marcos y su acidez sin paliativos, que supieron estar en horas altas y bajas. Gracias, porque vuestro sentido de la lealtad ennoblece la palabra kuadrilla.

A los biolocos (Iñaki, Migueltxo, Garbiñe, Erik, Charly, Antonio, Miren, Ana Pardo, Jonathan, Ana Albéniz, Oroz, Ali, Cris…), por su extraordinario sentido del humor y de la responsabilidad. Porque me conocen y tienen la paciencia de recordarme mi melodía cuando se me olvida. Por miles de kilómetros de viaje, por okupaciones, cenas y conversaciones con poso. Porque cada uno elige su patria y la mía son ellos.

Gracias a Laura, a sus ojos luminosos, a su sonrisa fácil y transparente. Gracias por combatir mi perfeccionismo con paciencia y besos. Por lo que nos queda por vivir juntos.

A mis primos y tíos. A la memoria de mis tías Mari Jose Elcano y Lola San Martín, por su ejemplo de fortaleza y lucha.

A mi hermano Pablo, por estar ahí. Siempre. Por liderar con el ejemplo. Porque treinta y tres años contigo han terminado por convencerme de que, es verdad, “la vida es de los constantes”.

A mis padres, por la vida. Por auparme a la montaña, a la honradez, y al esfuerzo. A mi padre, que me transmite cada día la alegría desbordante de vivir. Por enseñarme a mirar. A mi madre, por su cariño irreductible y su entrega incondicional.

ABSTRACT

Acidiphilium is a conspicuous member of acidic environments, where it grows heterotrophically using O_2 and Fe^{3+} as electron acceptors. In 2008, a Río Tinto *Acidiphilium* isolate was identified that coupled glucose oxidation with direct transfer of electrons to graphite electrodes even in the presence of oxygen. This opened the door to the use of aerobic anodes in microbial fuel cells, which would greatly simplify their design. This PhD thesis is part of a long-term, trans-disciplinar, multi-laboratory plan to characterize this *Acidiphilium* isolate.

As part of this thesis, the genome of *Acidiphilium* sp. PM has been sequenced and annotated and its metabolism has been partially reconstructed. This has allowed the identification of central metabolic pathways and has permitted comparative genomic studies with other *Acidiphilium* strains. In addition, a DNA genomic microarray has been constructed that enables whole-genome transcriptional studies as well as comparative genomic hybridizations.

Furthermore, this work has seeked to characterize *Acidiphilium* sp. PM resistance to heavy metals. In particular, its remarkable ability to withstand Ni has been examined using different approaches. On the one hand, a functional screening of a genomic library of *Acidiphilium* sp. PM allowed the identification of Ni-resistance determinants. On the other hand, whole-genome transcriptomics and proteomics revealed the rapid programmed response triggered by Ni, which ultimately leads to cell growth arrest. Differential gene expression analysis also allowed the identification of certain enzymes as potential primary targets of Ni toxicity.

RESUMEN

Acidiphilium es un habitante habitual de ambientes ácidos, donde crece heterotróficamente usando O_2 y Fe^{3+} como aceptores de electrones. En 2008, se aisló de Río Tinto una cepa de *Acidiphilium* capaz de acoplar la oxidación de glucosa con la transferencia directa de electrones a electrodos de grafito. Este descubrimiento abrió la puerta al uso de ánodos aerobios en pilas de combustible microbianas, lo que simplificaría significativamente su diseño. Esta tesis forma parte de un plan a largo plazo llevado a cabo por un grupo transdisciplinar de laboratorios que intenta caracterizar en profundidad esta cepa.

Como parte de esta tesis, el genoma de *Acidiphilium* sp. PM ha sido secuenciado y anotado y su metabolismo ha sido parcialmente reconstruido. Esto ha permitido la identificación de rutas del metabolismo central y la comparación del genoma de *Acidiphilium* sp. PM con los de otras cepas del género. Además, se ha construído un *microarray* de ADN genómico que permite realizar estudios transcripcionales a nivel de todo el genoma, así como hibridaciones comparativas entre genomas.

Por otra parte, este trabajo ha perseguido caracterizar la resistencia de *Acidiphilium* sp. PM a metales pesados. En concreto, se ha examinado su inusual capacidad de resistir Ni mediante distintas metodologías. Por un lado, el análisis funcional de una librería genómica de *Acidiphilium* sp. PM ha permitido identificar genes involucrados en resistencia a Ni. Por otro lado, estudios de transcriptómica y proteómica a nivel de todo el genoma han revelado que el Ni desencadena una rápida respuesta programada que, en última instancia, lleva a una parada del crecimiento celular. Los análisis de expresión diferencial de genes también han llevado a la identificación de varias enzimas como potenciales dianas principales de la toxicidad causada por el Ni.

INDEX

INDEX OF FIGURES

INDEX OF TABLES

ABBREVIATIONS

2DE: two-dimensional electrophoresis
2-MC: 2-methylcitrate
Acc. No: accession number
Amp: ampicillin
ANOVA: analysis of variance
Atm: atmosphere(s) (unit of pressure equivalent to 101 325 Pa)
ATP: adenosine triphosphate
BC: before Christ
BCAA: branched-chain amino acid
BChl: bacteriochlorophyll
BLAST: basic local alignment search tool
Bp: base pair
ca.: *circa* (approximately)
CAI: codon adaptation index
CGH: comparative genomic hybridization
CHAPS: 3-[(3-Cholamidopropyl)dimethylammonio]-1-propanesulfonate
Clp: caseinolytic proteases
CFU: colony forming unit
CRISPR: clustered regularly interspaced short palindromic repeats
Da: dalton
DAPI: 4',6-diamidino-2-phenylindole
DksA: DnaK suppressor protein
DIGE: differential in-gel electrophoresis
DM: defined medium
dNTP: deoxynucleotide
ddNTP: dideoxynucleotide
DSMZ: *Deutsche Sammlung von Mikroorganismen und Zellkulturen* (German Collection of Microorganisms and Cell Cultures)
DTT: dithiothreitol
EC: enzyme commission number
EDTA: ethylenediaminetetraacetic acid
etc.: *et cetera* (and the rest)
e.g.: exempli gratia (for instance)
EMBOSS: European molecular biology open software suite
et al.: *et alii* (and co-workers)
F: fold change (fluorescence intensity ratio Cy5/Cy3 when Cy5 > Cy3 or –Cy3/Cy5 when Cy5 < Cy3)
FAM: 6-carboxyfluorescein
FDR: false discovery rate
FU: fluorescence unit
Glimmer: gene locator and interpolated Markov modeler
GYE: glucose, yeast extract
h: hour(s)
Hsl: heat shock locus
ICP-MS: inductively coupled plasma-mass spectrometry
IEF: isoelectric focusing
i.e.: id est (that is)
IPTG: isopropyl β-D-1-thiogalactopyranoside
Kb: kilo base pairs

LB-Ap: Luria Bertani-Ampicillin
LOWESS: locally weighted scatterplot smoothing
LPS: lipopolysaccharide
MALDI-TOF: matrix-assisted laser desorption/ionization-time of flight
Mb: mega base pairs
MFS: major facilitator superfamily
MGB-NFQ: minor groove binder-nonfluorescent quencher
MIC: minimum inhibitory concentration
Min: minute(s)
MITE: miniature inverted-repeat transposable element
NCBI: National Center for Biotechnology Information
N.D.: not detected / not measured
Ni^r: nickel resistant
OD: optical density
ORF: open reading frame
PBS: phosphate buffered saline
PCIA: phenol-chloroform-isoamyl alcohol
PCR: polymerase chain reaction
PFGE: pulsed field gel electrophoresis
PGC: photosynthesis gene cluster
PHA: polyhydroxyalkanoates
PHB: poly-β-hydroxybutyrate
qPCR: real-time quantitative polymerase chain reaction
qRT-PCR: quantitative reverse-transcription polymerase chain reaction
RE: restriction enzyme
RMSD: root mean square deviation
RND: resistance-nodulation-cell division
RPS BLAST: reversed position specific basic local alignment search tool
RuBisCO: Ribulose-1,5-bisphosphate carboxylase/oxygenase
SAP: shrimp alkaline phosphatase
Sec: second(s)
SD: standard deviation
SDS-PAGE: sodium dodecyl sulphate-polyacrylamide gel electrophoresis
SE: standard error
ssDNA: single strand DNA
T: temperature
TA: toxin-antitoxin
TCA: tricarboxylic acid
Tris: tris(hydroxymethyl)aminomethane)
U: unit
USD: United States dollar
UV: ultraviolet
V: volt
Vhs: volt-hours
v/v: volume/volume
w/v: mass/volume
X-gal: 5-bromo-4-chloro-3-indolyl-β-D-galactopyranoside

1. INTRODUCTION

1.1. RÍO TINTO

Río Tinto is a naturally acidic river located in the province of Huelva (South-western Spain). It springs up in Peña de Hierro, at the heart of the Iberian Pyritic Belt, one of the world's largest metallic sulphide deposits (Leistel *et al.*, 1997). The bacterial leaching of these sulphides (via thiosulphate or via polysulphides and sulphur) ultimately generates sulphuric acid, which lowers the pH and favours the solubilisation of the heavy metals present in the rock (Schippers and Sand, 1999). The acidic waters of Río Tinto (average pH 2.3) harbour a plethora of metals of which iron is the most abundant, reaching concentrations as high as 20 g/l (Gonzalez-Toril *et al.*, 2003). Indeed, these large amounts of solubilized Fe^{3+} ions are responsible for the intense red colour of Río Tinto (Figure 1).

Figure 1. Sampling points 3.1 and 3.2 in the initial course of Río Tinto. Sampling point 3.2 (in the background) is often referred to as RT8 following nomenclature in (Garcia-Moyano *et al.*, 2012). Image courtesy of Mercedes Moreno.

Río Tinto has attracted the interest of astrobiology, a multidisciplinary approach to the study of the origin, evolution and distribution of life in the universe. On the one hand, understanding the adaptations of life to extreme physico-chemical conditions broadens the so-called habitability zone, which comprises the bodies where life could potentially arise. On the other hand, the similarities in the sulphate- and hematite-rich minerals of the Río Tinto basin and of Mars' Meridiani Planum has led to the proposal of Río Tinto as a geochemical and mineralogical terrestrial analog of Mars (Fernández-Remolar *et al.*, 2005; Amils *et al.*, 2007).

1.1.1. Microbial diversity and ecology of Río Tinto

The combination of high acidity and toxic metal concentrations in the waters of Río Tinto restricts the presence of life to microbial forms. Paradoxically, the diversity of eukaryotes is far greater than that of prokaryotes, and accounts for over 65% of the biomass in the water column. Eukaryotes found in Río Tinto include members of the phyla Bacillariophyta, Chlorophyta and Euglenophyta as well as ciliates, cercomonads, amoebae, stramenopiles, fungi, heliozoans and rotifers (Lopez-Archilla *et al.*, 2001; Aguilera *et al.*, 2006).

Prokaryotic abundance in the water column is in the order of 10^6 cells per ml, less than 2% of which correspond to Archaea (mainly Thermoplamatales) (Gonzalez-Toril *et al.*, 2003). Around 80% of these prokaryotes belong to three Bacterial groups: *Acidithiobacillus ferrooxidans*, *Leptospirillum ferrooxidans* and *Acidiphilium* spp., all of which are involved in the iron cycle. The relative proportions of the three vary throughout the river in response to physico-chemical conditions (*e.g.* total iron content or Fe^{3+}/Fe^{2+} ratio) (Gonzalez-Toril *et al.*, 2003; Garcia-Moyano *et al.*, 2012).

Planktonic bacterial cells sometimes aggregate forming bacterial-only macroscopic filaments. The microbial composition of these biofilms roughly follows that of the surrounding water, which strongly suggests that they originate in the rock bed and detach when they reach certain buoyancy (Garcia-Moyano *et al.*, 2007). Bacterial cells can also be found in algal photosynthetic biofilms. As in the case of prokaryotic filaments, the three most abundant groups colonize these biofilms. Their relative proportions vary depending on the algal composition (Souza-Egipsy *et al.*, 2008).

Microbial community composition varies across sediments depending on the pH and redox potential. Where these are similar to those of the water column (pH 2.5 and +300mV conductivity), iron reducers *Acidithiobacillus* and *Acidiphilium* dominate the sediment. In contrast, places with higher pH (4.2 - 6.2), more reducing redox potential (from +50 to -210 mV) and lower iron solubility, are colonized by sulphate-reducing *Syntrophobacter*, *Desulfurella* and *Desulfosporosinus* (Sanchez-Andrea *et al.*, 2011; Garcia-Moyano *et al.*, 2012; Sanchez-Andrea *et al.*, 2012).

Earlier works in our laboratory have focused on the ecology and physiology of *Leptospirillum* and *Acidithiobacillus* (Malki, 2003; Garcia-Moyano, 2007). Both *L. ferrooxidans* and *A. ferrooxidans* were found to couple iron oxidation to the respiration of

oxygen, but only *A. ferrooxidans* could respire iron (using sulphur as electron donor). Regarding the genus *Leptospirillum*, *L. ferrooxidans* was the most abundant species, *L. ferriphilum* and *L. ferrodiazotrophum* representing only 1% of the cell counts. Moreover, *Leptospirillum* was found to dominate over *Acidithiobacillus* at higher temperatures. A model was proposed in which *Leptospirillum* and *Acidithiobacillus* drive a complete iron cycle and contribute to the input of carbon in the system by fixating CO_2 (Malki, 2003). The relevance of *L. ferrooxidans* to Río Tinto's nitrogen cycle was also confirmed when the *nif* operon of *L. ferrooxidans* L3.2 was identified and expressed in N-starved cultures (Parro and Moreno-Paz, 2003). Most of the work on these microorganisms was performed on strains isolated from a sampling point named "3.2", a 6 m-deep dam in the initial course of the river (Figure 1) [RT8 in the nomenclature used by Garcia-Moyano *et al.* (Garcia-Moyano *et al.*, 2012)].

On the other hand, little research has dealt with Río Tinto's *Acidiphilium* species other than studying its distribution along Río Tinto (Gonzalez-Toril *et al.*, 2003; Garcia-Moyano *et al.*, 2012). *Acidiphilium* cell counts are low near the source of the river but it dominates downstream (especially in deeper waters) both in the water column and in the sediments (Garcia-Moyano *et al.*, 2012). Members of this genus can respire Fe in the presence of various oxygen concentrations and, at least one species (*Acp. acidophilum*), is capable of growing on reduced sulphur compounds. This makes *Acidiphilium* a relevant member of the iron and sulphur cycles and worthy of further study. Interestingly, an *Acidiphilium* isolate from Río Tinto has been identified that can couple glucose oxidation with the transfer of electrons to graphite electrodes in the presence of oxygen, an unusual ability with interesting biotechnological applications (Malki *et al.*, 2008) (see 1.2.2.2).

1.2. THE GENUS *Acidiphilium*

1.2.1. Genus description

In 1975, Guay and Silver reported the isolation of *Thiobacillus acidophilus* (currently *Acidiphilium acidophilum*), a facultative autotroph growing in co-culture with *Thiobacillus ferrooxidans* (currently *Acidithiobacillus ferrooxidans*) (Guay and Silver, 1975). Yet, the description of the genus *Acidiphilium* corresponds to Harrison (1981). *Acidiphilium* was named after the Latin *acidum* (an acid) and the Greek *philus* (loving), for its requirement of low pH. The first *Acidiphilium* species was termed *Acp. cryptum* (from the Greek *krytpos*, hidden), for it was found "hidden" in cultures of *Thiobacillus ferrooxidans* (Harrison, 1981). Currently, the genus *Acidiphilium* comprises five species: *Acp. cryptum* (Harrison, 1981),

Acp. acidophilum [formerly *Thiobacillus acidophilus* (Guay and Silver, 1975; Harrison, 1983; Hiraishi *et al.*, 1998)], *Acp. organovorum* (Lobos *et al.*, 1986), *Acp. angustum* / *Acp. rubrum* (Wichlacz *et al.*, 1986) and *Acp. multivorum* (Wakao *et al.*, 1994). Taxonomically, the genus *Acidiphilium* belongs to the family *Acetobacteraceae*, order *Rhodospirillales*, *Alphaproteobacteria* class within the phylum *Proteobacteria* of the *Bacteria* domain. *16S rRNA*-based phylogenetic trees show that *Acidiphilium* forms a major cluster with *Acidocella*, *Acetobacter*, *Gluconobacter* and *Rhodophila* species. This cluster is deeply-branched off from the *Alphaproteobacteria* (Imhoff and Hiraishi, 2005). *Acidiphilium* species fall into two separate clusters: one which includes *Acp. acidophilum* and *Acp. angustum* / *Acp. rubrum* and another accommodating *Acp. multivorum*, *Acp. cryptum* and *Acp. organovorum* (Figure 2).

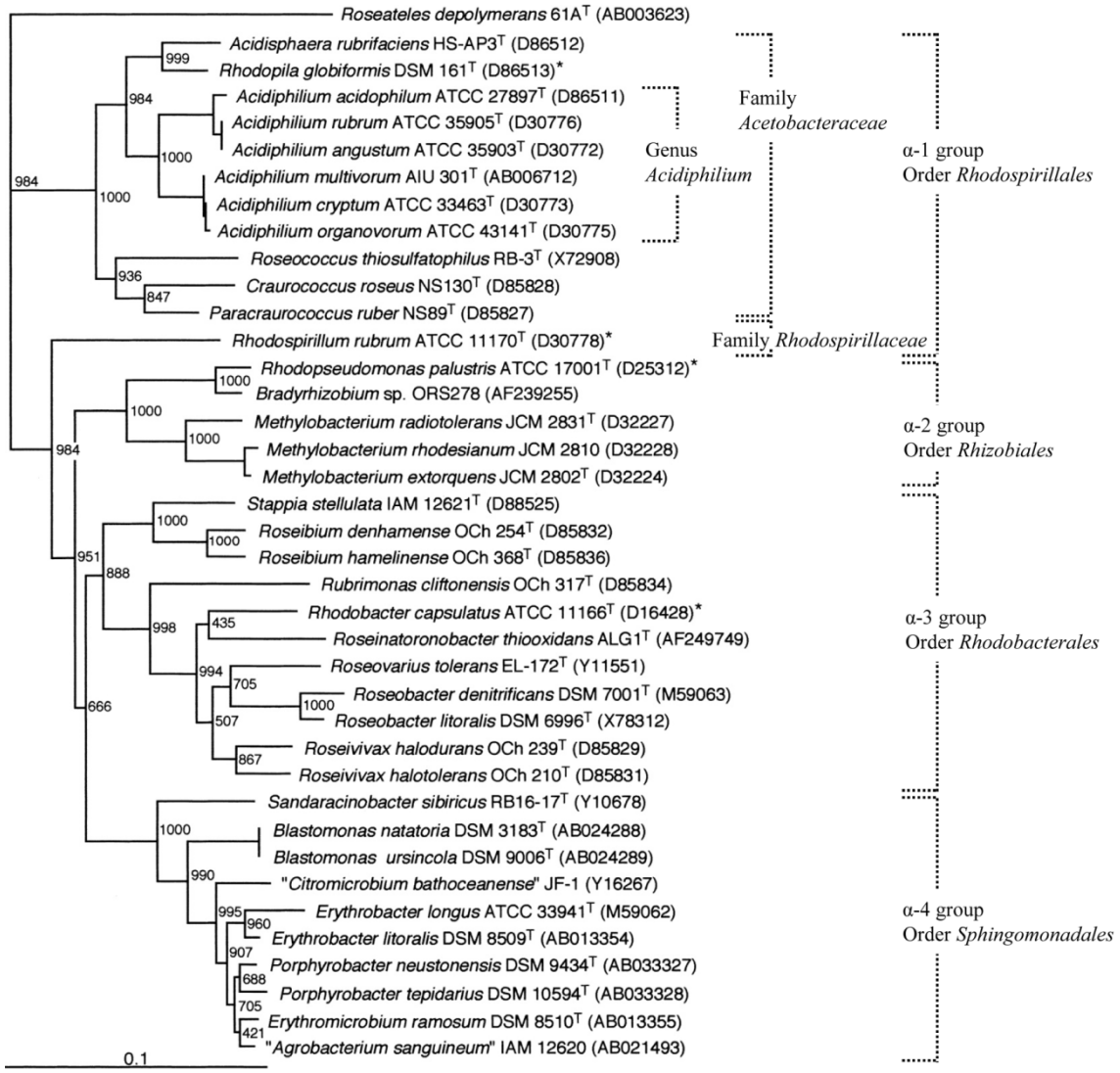

Figure 2. *16S rRNA*-based phylogenetic tree of aerobic anoxygenic BChl-containing bacteria. *Acidiphilium* species fall into two different clusters within the *Acetobacteraceae*. Asterisks indicate facultative phototrophic bacteria. Modified from Hiraishi and Shimada (2001).

Morphologically, *Acidiphilium* cells are gram-negative, straight rods, 0.3–1.2 x 4.2 μm in size. The size and shape vary depending on the carbon sources and on the pH of the medium. Cells may or may not be motile, with one or two polar or subpolar flagella and do not form endospores or capsules. Poly-β-hydroxybutyrate (PHB) and polyphosphate granules are frequent in *Acidiphilium* cells, but no intracellular membranes have been described (Figure 3). *Acidiphilium* colonies may be white to cream, yellow, pink, red, or brown. Straight-chain monounsaturated $C_{18:1}$ acid is the major component of cellular fatty acids and Q-10 is the major ubiquinone (Hiraishi and Imhoff, 2005).

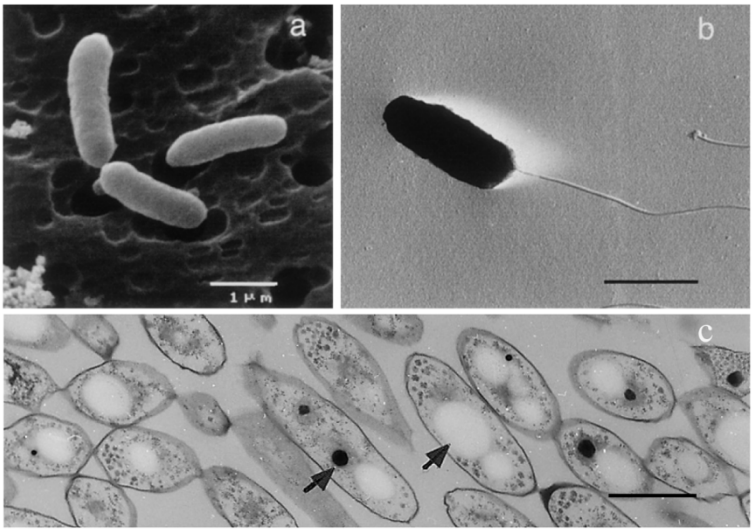

Figure 3. Cell morphology and ultrastructure of *Acidiphilium* species. A) Scanning electron micrograph of *Acp. rubrum* ATCC 35905^T; B) transmission electron micrograph of *Acp. cryptum* ATCC 33463^T showing a cell with a single polar flagella; C) Transmission electron micrograph of a thin-section of *Acp. rubrum* ATCC 35905T cells. Arrows indicate polyphosphate (dark) and poly-β-hydroxybutyrate (white) granules. All scale bars represent 1 μm. Reproduced from Hiraishi and Shimada (2001).

Members of this genus are aerobic, mesophilic and acidophilic bacteria (pH range 2.0-5.9). All known *Acidiphilium* species can grow chemoorganotrophically but only *Acp. acidophilum* can sustain growth using reduced inorganic sulphur. *Acidiphilium* species can grow on simple organic compounds as both carbon sources and electron donors (*e.g.* D-glucose, D-fructose, D-xylose or mannitol), but low concentrations of acetate (0.25 mM) and lactate (2 mM) inhibit their growth. The list of usable carbon sources and inhibiting compounds varies from one species to another. *Acp. multivorum* (from the Latin *multus* and *varare*, devouring many) is unusually versatile and can grow on a wide variety of sugars, certain short aliphatic alcohols (methanol, ethanol and propanol) and a large number of amino acids (Wakao *et al.*, 1994).

Acidiphilium species utilize the pentose phosphate and Entner-Doudoroff pathways for glucose metabolism instead of the more widespread Embden-Meyerhoff-Parnas pathway (Shuttleworth *et al.*, 1985). When grown in nutrient-rich media cells accumulate PHB in discrete, refractive granules, causing cells to swell. Studies with *Acp. cryptum* DX1-1 revealed that the greatest accumulation of PHB occurs with initial C:N ratios of 2.4 (Xu *et al.*, 2010). Yet, PHB also accumulated through CO_2 fixation when sulphur was added to the medium (Xu *et al.*, 2013a).

All *Acidiphilium* species use oxygen as electron acceptor and several species, including *Acp. cryptum*, can respire (*i.e.* dissimilatory reduce) Fe^{3+} in the presence of various oxygen concentrations (Johnson and McGinness, 1991; Kusel *et al.*, 1999; Johnson and Bridge, 2002; Kusel *et al.*, 2002; Coupland and Johnson, 2008). On the other hand, Fe^{2+} cannot be used as electron donor, although it has been observed to stimulate growth (Lobos *et al.*, 1986; Wakao *et al.*, 1994). *Acp. cryptum* JF-5 is also capable of reducing Cr^{6+} to Cr^{3+} both in the presence and in the absence of oxygen. Yet, Cr^{6+} reduction does not seem to be an energy-linked process, but rather a detoxification mechanism (Cummings *et al.*, 2007).

Interestingly, the genus was amended to accommodate only those species capable of synthesizing zinc-chelated bacteriochlorophyll *a* (Zn-Bchl *a*) (Kishimoto *et al.*, 1995b). Zn-Bchl *a* has been shown to be more resistant to acid than Mg-Bchl *a*, which would explain why this form of Bchl was selected in highly acidic environments (Kobayashi *et al.*, 1998). *Acidiphilium* species are included in the group of the aerobic anoxygenic BChl-containing bacteria, most of which also belong to the *Alphaproteobacteria* (Hiraishi and Shimada, 2001). The *puf* operon, which encodes polypeptides of the photosynthetic reaction centre and the core light-harvesting complex, has been identified in all *Acidiphilium* species (Hiraishi *et al.*, 1998). The synthesis of Zn-Bchl *a* is strongly inhibited by light and lack of oxygen. Paradoxically, light-induced $^{14}CO_2$ incorporation has been reported in *Acp. rubrum* in the absence of glucose or its metabolites, although this CO_2 fixation proved insufficient to sustain growth (Kishimoto *et al.*, 1995a). It has been speculated that this pseudo-photosynthesis could afford *Acidiphilium* greater survival in oligotrophic environments. In this sense, Hiraishi and Shimada observed increased survival of starved cells in the presence of light as well as accumulation of BChl under carbon limitation (Hiraishi and Shimada, 2001).

Acidiphilium genomes have a high GC content, ranging from 63.2% in *Acp. rubrum* to 68.1% in the case of *Acp. multivorum* AIU 306, as determined experimentally (Wakao *et*

al., 1994). The repertoire of genetic tools available for the manipulation of *Acidiphilium* genomes is scarce. An attempt to establish a genetic system in *Acidiphilium* was made in the early nineties. However, early works on electroporation, conjugation and the characterization of RecA were performed in different strains of *Acidiphilium facilis*, which was later transferred to the genus *Acidocella* (Glenn *et al.*, 1992; Inagaki *et al.*, 1993b; Inagaki *et al.*, 1993a). A lysogenic bacteriophage (φAc1) was discovered that could integrate into *Acidiphilium* genome (Ward *et al.*, 1992; Ward *et al.*, 1993). However, no transduction system has been developed since, possibly because strains used in that study are now suspected *Acidocella*. Conversely, genetic transfer from *Escherichia coli*, *Pseudomonas putida*, and *Acidocella* strains to certain *Acidiphilium* isolates have been achieved through conjugation (Quentmeier and Friedrich, 1994; Mahapatra *et al.*, 2003; Singh and Banerjee, 2007). Electroporation has also proved successful in transforming some *Acidiphilium* strains using *Acidocella* plasmids (Ghosh *et al.*, 1997). However promising these results may be, many technical challenges need to be addressed before a functional genetic system is established: conjugation and transformation efficiencies vary widely depending on the recipient strain, some plasmids readily integrate the genome, others tend to recombine, *et cetera*.

Acidiphilium species have been isolated from acidic mineral environments, including acid mine drainage and acidic soils (Wichlacz *et al.*, 1986; Kishimoto and Tano, 1987; Wakao *et al.*, 1994), where they are suspected to feed on the organic matter produced by primary producers (such as iron-oxidizers *L. ferrooxidans* and *A. ferrooxidans*). Acidic environments are often rich in heavy metals, which is why several *Acidiphilium* isolates are among the most metal-resistant prokaryotes (see section 1.3.2).

1.2.2. Biotechnological interest of *Acidiphilium*

1.2.2.1. *Acidiphilium* in biomining

Microorganisms from acidic, metal-rich environments have been used by the mining industry for over 50 years. Biomining benefits from the ability of some microbes to solubilize metals from metal sulphides into the water, from which they can be readily recovered. This process, termed bioleaching, allows the profitable extraction of metals (typically Cu, Au and U) from low-grade ores with less energy costs and environmental impact compared to traditional physico-chemical processes like smelting and roasting (Rawlings, 2002).

Traditionally, metal solubilization is achieved by the attack of Fe^{3+} on the sulphides. Fe^{3+} ions are generated in large amounts by acidophilic, iron-oxidizing bacteria and archaea. *Acidiphilium* species are incapable of oxidizing Fe^{2+}, yet they are often found in biotanks as part of the leaching consortia, where they presumably engage in mutualistic interactions with iron-oxidizers like *A. ferrooxidans* and *L. ferrooxidans* (Johnson, 1998). Only recently, a novel method was devised that allows the extraction of Ni from Ni laterites by reductive dissolution of goethite (instead of the traditional solubilization by iron oxidation). This reduction of Fe^{3+} to Fe^{2+} has been successfully tested in *A. ferrooxidans*, *Acidicaldus organivorans* (both in complete anaerobiosis) and *Acidiphilium* SJH (only in microaerobiosis) (du Plessis *et al.*, 2011; Hallberg *et al.*, 2011).

Understandably, the success of bioleaching is bound to the ability of these microorganisms to resist the toxic metals found in the leachate (Sampson and Phillips, 2001; Rawlings, 2002). Metal concentrations in heaps can vary from 2-6 g/l Cu, 2-5 g/l Ni and up to 23 g/l in the case of Zn. However, in tank reactors, metal concentrations can build up to 19 g/l Cu, 23 g/l Ni or a staggering 65 g/l Zn (Watkin *et al.*, 2009). The adaptation of pre-existent mild-resistant bacteria to such extreme conditions is not well understood although two mechanisms have been postulated: i) mutations in genes already existing in a bacterium or ii) acquisition of new metal resistance genes by horizontal gene transfer (Rawlings, 2007). With the current knowledge, predicting a bacterium maximum resistance for bioleaching purposes is unfeasible. However, the identification of resistance determinants from axenic cultures of natural metal resisters can contribute to shed some light on how bacteria adapt to toxic metal concentrations and on the limits of such adaptations.

As described above, *Acidiphilium* is among the most metal-resistant microorganisms, which makes it a good candidate for the identification of metal resistance determinants. In addition, as opposed to acidophilic iron-oxidizers, *Acidiphilium* can be grown to high cell densities and is easy to manipulate. On the other hand, genetic transfer systems are still rudimentary and limited to certain strains. Pioneering studies in the transfer of metal resistance determinants using *Acidiphilium* strains include the heterologous expression of plasmid-mediated arsenic resistance genes from *Acidiphilium multivorum* AIU301 in *E. coli* (Suzuki *et al.*, 1997; Suzuki *et al.*, 1998a), or the cloning of cadmium and zinc resistance determinants from *Acidocella* spp. into *Acp. multivorum* and *E. coli* (Ghosh *et al.*, 1997).

1.2.2.2. *Acidiphilium* as an electricigen

Microorganisms have evolved to use a wide range of natural electron acceptors. Recently, a number of microorganisms have been found that can also couple the oxidation of organic matter with direct electron transfer to artificial electrodes. For their ability to generate electric currents, these microorganisms have been named electricigens. Most electricigens are versatile anaerobic metal reducers and possess a wide variety of cytochromes. *Geobacter* is very likely the most extensively characterized of them. It has been proposed that these bacteria gain electrons from central metabolic pathways (*e.g.* the tricarboxylic acid cycle) and then transfer these electrons to the anode via electron transport proteins (possibly c-type cytochromes) or conductive pilli (Figure 4) [reviewed in (Lovley, 2006; Lovley, 2012)].

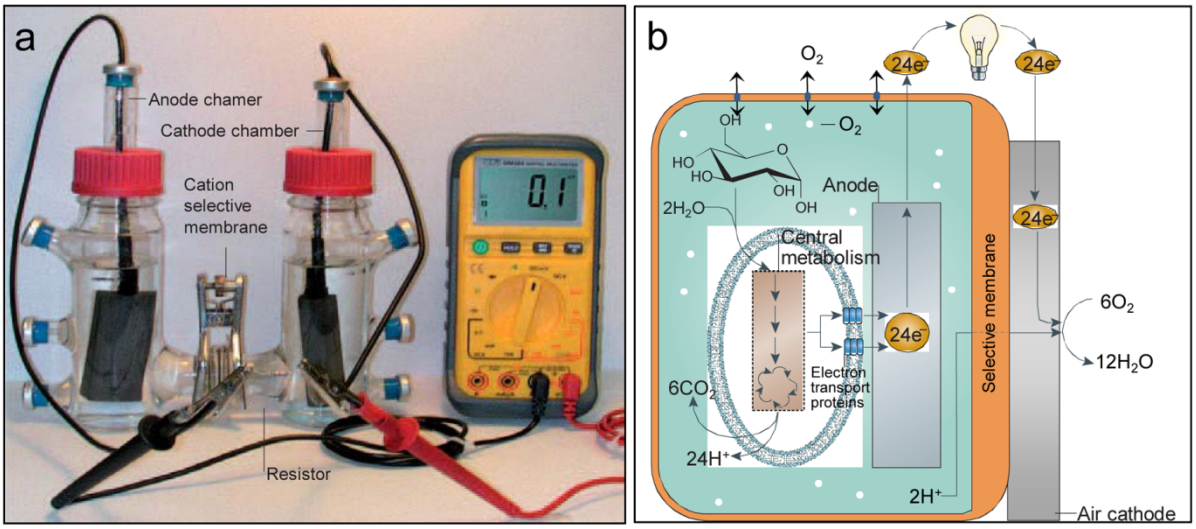

Figure 4. Certain *Acidiphilium* strains can behave as electricigens. A) An electricigen operating in a microbial fuel cell. B) Schematic representation of the possible electron transfer in energy-producing *Acidiphilium* strains when grown on glucose. Glucose is oxidized by the cell to carbon dioxide via the pentose phosphate and Entner-Doudoroff pathways and the tricarboxylic acid cycle. Electrons released in the process are transferred to the anode via electron transport proteins, possibly c-type cytochromes. Modified from Lovley (2006).

In 2008, two studies reported on the ability of two *Acidiphilium* strains to transfer electrons to graphite electrodes. One article described the production of electricity in *Acidiphilium cryptum* ATCC 33463, which was found to be mediated by iron and not through direct electron transfer (Borole *et al.*, 2008). However, the other study, performed with an *Acidiphilium* isolate from Río Tinto, described the direct transfer of electrons to graphite electrodes even in the presence of oxygen (one of *Acidiphilium*'s electron acceptors) (Malki *et al.*, 2008). These data suggests that the generation of electricity in *Acidiphilium* might be strain-specific.

The aerobic production of current by this Río Tinto *Acidiphilium* isolate opened the door to the use of aerobic anodes, which would greatly simplify the design of microbial fuel cells. A consortium of research teams was established and financed under the name PICOMICRO with the aim of studying and ultimately optimizing the electron transfer process (Fernandez *et al.*, 2006).

This Río Tinto isolate rapidly became the reference working strain in our (and others') laboratory and a thorough characterization of the strain was planned. Early works with this isolate faced the challenges of working with an uncommon genus: available genetic systems were rudimentary (inefficient and highly dependent on the strain), genomic information was absent (only some plasmid and 16S rRNA sequences were available), and there was a lack of commercial or custom-made high-throughput technologies such as DNA microarrays. For this reason, goals were set to develop genomic tools that would facilitate the study of the strain. This thesis in particular seeked i) to sequence and annotate the genome of the electricigen, and ii) to construct a DNA microarray that would allow genome-wide transcriptional studies as well as comparative genomic hybridizations with other *Acidiphilium* strains.

Alongside with the development of genetic tools, different goals were set to characterize the strain. Given the interest of our group in the ecological aspects of acidic environments, our work focused on the characterization of the strain's heavy metal resistance.

1.3. HEAVY METALS IN PROKARYOTES

1.3.1. The role of heavy metals in prokaryotes

A handful of elements (H, C, O, N, P, Fe and S) are essential and required in large amounts by all microorganisms. Others, so-called essential elements, are also required although in smaller proportions; these include Na, K, Ca and Mg among others. Finally, some elements are required in trace amounts and only by some groups of microorganisms for very specific purposes. The latter include many heavy metals, such as Co, Cu, Ni and Zn. The unusual reactivity of these heavy-metals affords bacteria great catalytic versatility, enables transfer reactions and contributes to protein stability. Heavy metal cations may serve as co-factors or may be incorporated in the catalytic site of proteins. In the latter case proteins are often referred to as metalloproteins.

The main downside to the increase in catalytic versatility afforded by heavy metals is their high toxicity. Heavy metal concentrations in the millimolar (and sometimes the submillimolar) range can be lethal to most microorganisms, even to those craving them. In addition, many heavy metal cations such as Hg^{2+}, Ag^{+} or Pb^{2+} are not required by any known organism, yet they are toxic to all forms of life. Heavy metals can enter the cell through unspecific, constitutively expressed transport systems such as the magnesium uptake system or through metal inorganic transport protein CorA. Once inside the cell, free metal cations can wreak havoc. Depending on the heavy metal, they may disrupt membrane integrity, inhibit transport systems or generate toxic free radicals [reviewed in (Nies, 1999)]. An additional problem to the use of heavy metals by organisms is the natural order of stability of divalent metals (often referred to as the Irving-Williams series), which complicates the formation of tight complexes for elements such as Ca and Mg in favour of Cu, Ni or Zn (Irving and Williams, 1953). This can result in the incorporation of unsuitable cations to metalloenzymes, ruining their catalytic activities.

In order to cope with the toxicity of heavy metals, deal with their shortage or excess, and avoid incorrect incorporations in metalloproteins, organisms have evolved a network of highly-specific metal sensors, transporters, chelators, and metal detoxification systems that ensures the correct use or disposal of these heavy metals.

1.3.2. Heavy metal resistance in prokaryotes

Prokaryotes have evolved various mechanisms to reduce heavy metal toxicity: i) enzymatic detoxification of the cation to a less toxic form (primarily through a change in the oxidation state, *e.g.* Hg^{2+} reduction to volatile Hg^{0}), ii) complexation with thiol-containing molecules (primarily for sulphur-binding cations Hg^{2+}, Cd^{2+} and Ag^{+}), iii) modification of cation transport systems to make them more impermeable to heavy metals, iv) reduction in the sensitivity of cellular targets to metal ions, or v) active efflux through metal-specific transport systems. Of these mechanisms, inducible, operon-encoded, metal-specific efflux systems have been the most extensively studied. These include members of the resistance-nodulation-cell division (RND) superfamily and P_1-type ATPases—both of which are energy dependent— as well as cation-diffusion facilitators (which probably operate through proton antiport) (illustrated in Figure 5). Indeed, microorganisms often rely on several of these mechanisms to resist a particular heavy metal [reviewed in (Nies, 1999; Bruins *et al.*, 2000; Nies, 2003; Silver and Phung le, 2005)].

Operon-encoded efflux systems have been consistently found in plasmids of many microorganisms, although they are also present in the chromosome of some microorganisms. Arguably the most paradigmatic example is that of *Cupriavidus* (formerly *Ralstonia*) *metallidurans* (Goris *et al.*, 2001; Vandamme and Coenye, 2004), a metal-resistant betaproteobacterium isolated from a zinc decantation tank in Belgium (Mergeay *et al.*, 1985). *C. metallidurans* harbours two large plasmids: plasmid pMOL28 (171 kb), which contains genes involved in resistance to Ni^{2+}, Co^{2+}, CrO_4^{2-} and Hg^{2+}, and plasmid pMOL30 (234 kb), which carries genes for Ag^{+}, Cd^{2+}, Co^{2+}, Cu^{2+}, Hg^{2+}, Pb^{2+} and Zn^{2+} resistance (Mergeay *et al.*, 2003; Monchy *et al.*, 2007).

Heavy metal solubility increases with acidity, which is why many of the most metal-resistant microorganisms are found in acidic environments, including acid mine and acid rock drainage (Table 1). For instance, different strains of *A. ferrooxidans* have been found to resist up to 1 M Ni, 0.8 M Cu or 1.071 M Zn. Paradoxically, most of our understanding of metal resistance at the molecular level comes from studies performed in (far less resistant) neutrophiles (Dopson *et al.*, 2003; Silver and Phung le, 2005).

The genus *Acidiphilium* harbours particularly metal-resistant members: *Acp. cryptum* is capable of growing in the presence of 700 mM Cd^{2+}, 300 mM Al^{3+} or 125 mM Zn^{2+} whereas *Acp. multivorum* grows in concentrations as high as 350 mM Ni^{2+} or 30 mM As^{3+} (Table 1). Growth in these conditions usually requires extended lag phases and longer doubling times, and induces morphological changes in the cells (Mahapatra and Banerjee, 1996; Fischer *et al.*, 2002; Chakravarty and Banerjee, 2008). Little information is known on the mechanisms that afford *Acidiphilium* these metal resistances. Exceptions to these are the finding that resistance to Cd^{2+} and Zn^{2+} in "*Acidiphilium symbioticum*" KM2 is mediated by plasmids (Mahapatra *et al.*, 2002a), or, more notably, the thorough characterization of the As-resistance operon *arsRDABC* found in plasmid pKW301 of *Acp. multivorum* AIU301 (Chen and Rosen, 1997; Suzuki *et al.*, 1997; Suzuki *et al.*, 1998a; Suzuki *et al.*, 1998b; Rastorguev *et al.*, 2001).

As shown in the Results (see section 4.1.3), the characterization of the metal resistance in *Acidiphilium* sp. PM uncovered an unusual tolerance to Ni. While similar Ni resistance had been observed in other *Acidiphilium* strains (Table 1), the underlying mechanisms had not been described. For this reason, alongside with the development of genetic tools, this thesis seeked to understand *Acidiphilium* sp. PM response to Ni and the mechanisms that afford it this resistance.

Microorganism	Metal concentration whereby metabolic activity occurs (mM)									
	Ag(I)	Al(III)	As(III)	Cd(II)	Co(II)	Cu(II)	Mo(VI)	Ni(II)	U(VI)	Zn(II)
Neutrophilic bacteria										
Escherichia coli	0.02[a]	2[a]	4[b]	0.5[a]	1[a]	1[a]	1[c]	1[a]	2[a]	1[a]
Acidophilic bacteria										
Acidiphilium acidophilum	ND	200[d]	ND	ND	ND	ND	ND	ND	ND	ND
"Acidiphilium capsulatum"	ND	200[d]	ND	ND	ND	ND	ND	ND	ND	ND
Acidiphilium cryptum	< 0.005[e]	300[d]	ND	700[g]	ND	50[e]	0.1[e]	20[f]	0.5[e]	125[f]
Acidiphilium multivorum	ND	ND	30[h]	20[f]	ND	10[f]	ND	350[f]	ND	40[f]
"Acidiphilium symbioticum" KM2	ND	ND	ND	700[f]	ND	20[f]	ND	20[f]	ND	150[f]
"Acidiphilium symbioticum" H8	ND	ND	ND	700[f]	ND	15[f]	ND	30[f]	ND	150[f]
Acidiphilium angustum	ND	ND	ND	< 0.2[f]	ND	5[f]	ND	10[f]	ND	8[f]
Acidiphilium sp. strain GS18h	ND	ND	ND	10[f]	ND	15[f]	ND	30[f]	ND	60[f]
Acidocella aminolytica	ND	ND	ND	200[g]	ND	30[g]	ND	150[g]	ND	500[g]
Acidocella facilis	ND	ND	ND	< 1[g]	ND	< 1[g]	ND	1[g]	ND	100[g]
Acidocella sp. strain GS19h	ND	ND	ND	700[g]	ND	15[g]	ND	150[g]	ND	900[g]
Acidithiobacillus ferrooxidans	0.01[i]	371[j]	93[k]	500[l]	170[j]	800[m]	1.25[n]	1000[o]	1-8[p]	1071[q]
Acidithiobacillus thiooxidans	ND	200d	ND	ND	ND	ND	ND	300r	ND	ND
Leptospirillum ferrooxidans	< 0.002[e]	ND	ND	ND	ND	5[e]	0.2[e]	ND	5[e]	ND
Leptospirillum ferriphilum	ND	ND	60[s]	<5[t]	5[t]	<5[t]	ND	100[r]	ND	20[t]
Sulfobacillus thermosulfidooxidans	ND	ND	ND	ND	ND	6[u]	ND	25[v]	ND	43[u]
Acidophilic archaea										
"Ferroplasma acidarmanus"	ND	ND	13[w]	4[x]	ND	312[y]	ND	ND	ND	ND
Metallosphaera sedula	<0.9[z]	ND	1[z]	1[z]	1[z]	200[aa]	1[z]	1.7[z]	0.4[z]	150[z]
Sulfolobus acidocaldarius	ND	ND	ND	10[ab]	ND	1[ab]	ND	1[ab]	ND	10[ab]
Sulfolobus solfataricus	ND	ND	ND	10[ab]	ND	1[ab]	ND	0.1[ab]	ND	10[ab]
Sulfolobus metallicus strain BC	0.009[ac]	ND	19[ac]	ND	90[ac]	ND	2[ac]	ND	ND	ND

Table 1. Heavy metal resistance of some acidophiles. The table shows the upper metal concentrations at which growth or a defined enzyme activity (*e.g.* Fe (II) oxidation) still occurs in axenic cultures under controlled conditions. Higher metal resistances have been reported in bioleaching tanks (Torma, 1977). Values for the neutrophilic *E. coli* are given for comparison. ND, not determined. Data from: a, (Nies, 1999); b, (Carlin *et al.*, 1995); c, (Campbell *et al.*, 1985); d, (Fischer *et al.*, 2002); e, (Johnson *et al.*, 1992); f, (Mahapatra and Banerjee, 1996); g, (Ghosh *et al.*, 1997); h, (Suzuki *et al.*, 1997); i, (Sugio *et al.*, 1984); j, (Tuovinen *et al.*, 1971); k, (Harvey and Crundwell, 1996); l, (Baillet *et al.*, 1997); m, (Holmes and Haq, 1989); n, (Yong *et al.*, 1997); o, (Dew *et al.*, 1999); p, (Leduc *et al.*, 1997); q, (Kondratyeva *et al.*, 1995); r, (Xu *et al.*, 2013b); s, (Tuffin *et al.*, 2006); t, (Tian *et al.*, 2007); u, (Vartanyan *et al.*, 1990); v, (Watling, 2008); w, (Gihring *et al.*, 2003); x, (Dopson *et al.*, 2004); y, (Baker-Austin *et al.*, 2005); z, (Huber *et al.*, 1989); aa, (Maezato *et al.*, 2012); ab, (Miller *et al.*, 1992); ac, (Mier *et al.*, 1996).

1.4. NICKEL

Ni can occur as Ni^0 or Ni^{2+}, although Ni^+ and Ni^{3+} can exist under certain conditions. Nearly all of Earth's Ni is suspected to be forming part of the Earth's core. The presence of Ni on the Earth's crust is scarce (*ca.* 80 μg g^{-1}) (Adriano, 2001), the abundance being higher in ultramafic rocks such as peridotite and serpentine (reaching 2000 μg g^{-1}) (Nriagu, 1990). Iron meteorites are also an abundant source of Ni (5-65%), where it is found as kamacite and taenite. The bulk of Ni on Earth is found in ores of laterites (primarily composed of nickeliferous limonite [(Fe,Ni)O(OH)] and garnierite [$(Ni,Mg)_3Si_2O_5(OH)_4$] and in magmatic sulphide deposits, where the principal ore mineral is pentlandite [$(Ni, Fe)_9S_8$]. Volcanoes and soil particles carried by the wind account for most of the natural Ni emissions. On the other hand, mining activities and the combustion of oil are the main anthropogenic sources of Ni emission. Ni levels in non-polluted areas are low: in open ocean water 0.2 – 0.7 μg/l, and in fresh water generally less than 2 μg/l (Reimann *et al.*, 1998).

The main Ni producers are Canada, Russia, Indonesia and Australia (Nieminen *et al.*, 2007). Ni is used in the manufacture of stainless steels, alloys, (Al-Ni-Co) magnets, coins and rechargeable batteries among others (Nieminen *et al.*, 2007). As of November 2014, a metric ton of Ni is sold at around 15500 USD (according to the London Metal Exchange), but in May 2007 the price peaked to 54000 USD per ton. Paradoxically, under these circumstances, US 5 cent coins (also known as "nickels") had a manufacturing cost almost double its own face value. This situation forced the US government to pass a law criminalizing the "exportation, melting and treatment" of US 5 and 1 cent coins (Moy, 2007).

1.4.1. Nickel utilization by microorganisms

To the best of our knowledge, there is no report on the utilization of Ni by *Acidiphilium* or any acidophilic species. Current information regarding Ni uptake, homeostasis, intracellular transport or assembly in Ni-metallocenters derives from works performed on neutrophilic species over the last 50 years. Bartha and Ordal pioneered the field in 1965 with a report describing the requirement of Ni by two hydrogen-oxidizing strains growing chemolithotrophically (Bartha and Ordal, 1965). A decade later, jack bean's (*Canavalia ensiformis*) urease became the first identified enzyme requiring Ni for catalysis (Dixon *et al.*, 1975). To date, nine Ni-dependent enzymes have been described: urease (Dixon *et al.*, 1975), carbon monoxide dehydrogenase, acetyl-CoA decarbonylase/synthase (Drake *et al.*, 1980; Ferry, 1995; Ragsdale and Kumar, 1996), methyl-Coenzyme M reductase

(Diekert *et al.*, 1980; Whitman and Wolfe, 1980; Ellefson *et al.*, 1982), Ni-Fe hydrogenases (Graf and Thauer, 1981), Ni-dependent superoxide dismutase (Youn *et al.*, 1996a; Youn *et al.*, 1996b), Ni-dependent glyoxalase I (Clugston *et al.*, 1998), acireductone dioxygenase (Dai *et al.*, 1999) and lactate racemase (Boer *et al.*, 2014). Other enzymes, such as glycerol-1-phosphate dehydrogenase AraM from *Bacillus subtilis* (Guldan *et al.*, 2008) or the quercetinase QueD of *Streptomyces* sp. FLA (Merkens *et al.*, 2008), present higher activities when Ni is added; however, the physiological relevance of this metal specificity remains to be understood.

In spite of being rare, Ni enzymes are key to the colonization of highly specific niches. For instance, methanogenic archaea require up to eight Ni-containing enzymes to grow on H_2 and CO_2 as sole energy and carbon sources (Jaun and Thauer, 2007). Schönheit and co-wokers calculated that *Methanobacterium thermoautotrophicum* requires as much as 1 μmol (58.7 μg) of Ni per g of cells to synthesize its eight Ni metalloenzymes (Schönheit *et al.*, 1979). Another paradigmatic example is the colonization of the human gastric mucosa by the pathogenic *Helicobacter pylori* (an infection associated with enhanced risk of gastric cancer). To achieve a favourable circumneutral pH, *H. pylori* synthesizes urease to hydrolyze urea into CO_2 and NH_3, neutralizing the gastric acid (Eaton *et al.*, 1991). This crucial enzyme constitutes up to 10% of the total protein content (Bauerfeind *et al.*, 1997), each active molecule requiring 24 coordinated Ni^{2+} ions (Ha et al, 2001).

The unusual requirements for Ni observed in *H. pylori* and other Ni-dependent bacteria need to be met in environments where Ni is present only in trace amounts and in a manner that avoids cellular damage caused by free Ni ions in the cytoplasm. To achieve this, organisms have evolved a network of proteins that regulate the main actors involved in Ni import and export, its transport within the cell and the assembly of Ni-metallocenters (Figure 5).

Ni ions are suspected to reach the periplasm through nonspecific transmembrane porins in the outer membrane, although Ni-binding TonB-dependent transporters have been discovered in *Helicobacter* species. Once in the periplasm, Ni can enter the cells through non-specific systems (primarily the CorA Mg^{2+} transporter), yet many microorganisms have developed Ni-specific uptake systems to meet their Ni requirements. Examples of the latter are ATP-binding cassette transporters (such as that encoded by operon *nikABCDE* of *E. coli*) or permeases of the NiCoT family (*e.g.* NixA from *H. pylori*). In *E. coli*, Ni uptake systems

allow the intracellular accumulation of *ca*. 30 µM Ni from media containing scarcely 1 µM Ni (Macomber *et al.*, 2011).

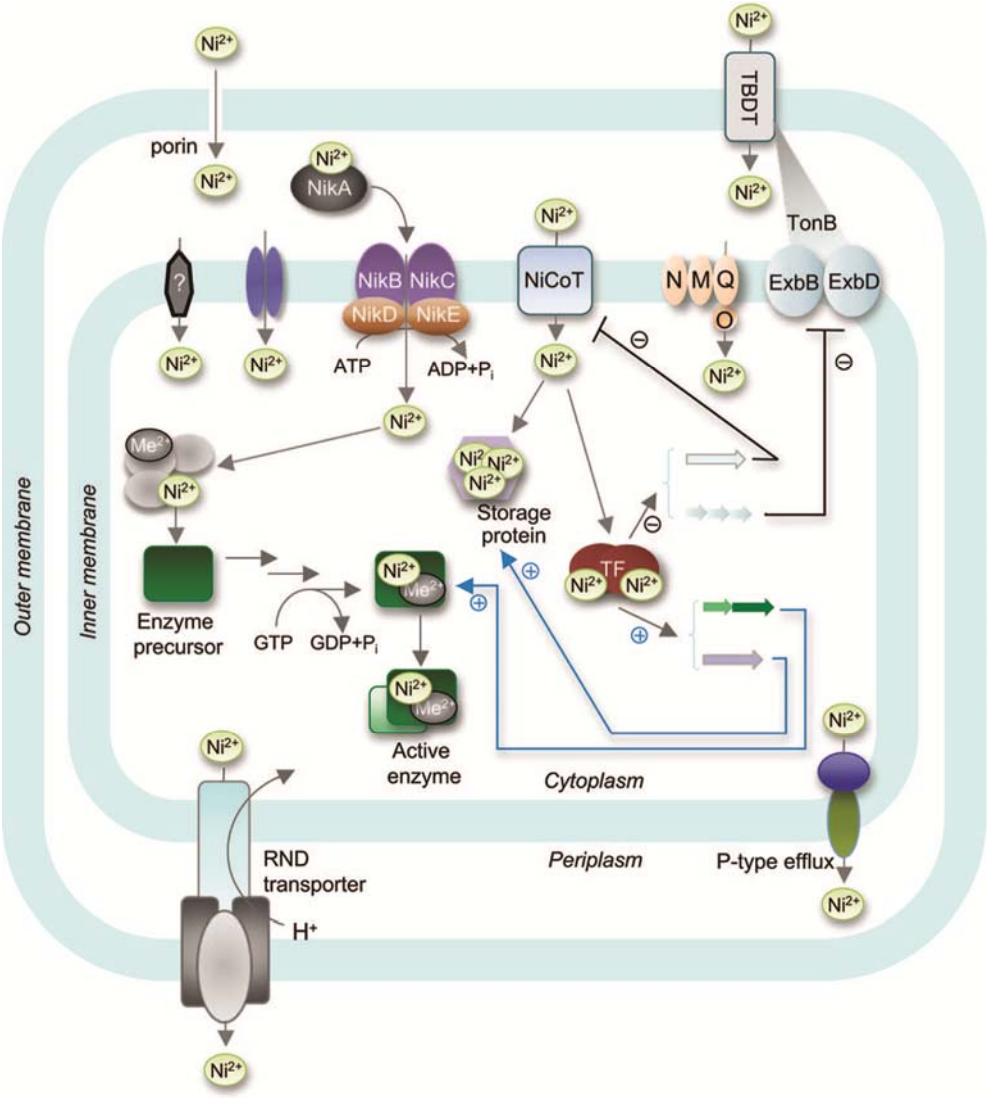

Figure 5. Systems involved in Ni homeostasis and trafficking in the cell. TF indicates transcription factor, blue arrows represent upregulation and black arrows, downregulation. Reproduced from (Li and Zamble, 2009).

Ni homeostasis in the cell is tightly regulated by transcription factors that act on the expression of genes involved in Ni uptake, sequestration, utilization and efflux. The first- (and best-) characterized Ni regulator was NikR. In *E. coli*, this regulator inhibits Ni uptake by repressing the transcription of *nikABCDE* operon. Other Ni-dependent regulators control the efflux of Ni cations, such as *E. coli*'s RcnR, which represses the transcription of *rcnA* (a gene encoding a Ni-efflux pump) in the absence of Ni. In *Streptomyces griseus*, when Ni is present, the two-component metalloregulator SrnRQ represses the transcription of the Fe-

superoxide dismutase in favour of the Ni-containing superoxide dismutase (Mulrooney and Hausinger, 2003; Li and Zamble, 2009).

Ni atoms present in metalloenzymes are usually deeply buried within the structure of the protein. While this strategy guarantees the incorporation of the correct metal (and avoids misincorporation of more abundant/more stable cations) it demands the use of accessory proteins for the assembly of the metallocenter. As an example *H. pylori* urease apoprotein $(UreABC)_3$ requires the participation of four accessory proteins (UreDEFG) for its activation. Similar accessory proteins have been described for the biosynthesis of NiFe-hydrogenases and carbon monoxide dehydrogenases (Mulrooney and Hausinger, 2003; Li and Zamble, 2009; Kaluarachchi *et al.*, 2010).

1.4.2. Nickel resistance mechanisms

In contrast to eukaryotes, where Ni toxicity (including its carcinogenic effects on humans) has been widely studied, the mechanisms for Ni toxicity in prokaryotes, and particularly in acidophiles, are still poorly understood. Four mechanisms have been proposed to explain Ni toxicity: i) replacement of the active metal in metalloproteins, ii) binding to catalytic residues of non-metalloenzymes, iii) allosteric inhibition of enzymes, and iv) induction of oxidative stress (Macomber and Hausinger, 2011). Ni displacement of other metal ions (especially Fe) from metalloenzymes is probably the most studied. The presence of submillimolar concentrations of Ni can result in enzymatic inactivations of 50% or higher. For instance, the activity of *E. coli* Mg-dependent DNA polymerase I is reduced to half in the presence of 370 μM Ni (Snow *et al.*, 1993) [a list of microbial enzymes inhibited by Ni can be found in (Macomber and Hausinger, 2011)].

Because Ni is toxic in minute amounts, even microorganisms which require Ni for growth have developed mechanisms to export Ni cations (Table 2). Of these mechanisms, inducible operon-encoded, energy-dependent specific efflux systems are the most common and have been extensively studied in the past. Examples of these Ni efflux systems are: CnrCBA from the metal-resistant *C. metallidurans* CH34 (Liesegang *et al.*, 1993; Grass *et al.*, 2000; Tibazarwa *et al.*, 2000), the CznCBA efflux system of the pathogen *H. pylori* (Stahler *et al.*, 2006), locus *nccYXHCBAN* in *Achromobacter xylosoxidans* 31A (Schmidt and Schlegel, 1994), and the *ncrABCY* operon of the acidophilic *L. ferriphilum* UBK03 (Tian *et al.*, 2007; Zhu *et al.*, 2011). Most of these efflux systems belong to the RND superfamily, and are composed of three components: a RND protein, a member of the membrane fusion

protein family (abbreviated MFP) and an outer membrane factor (OMF). These three proteins form a complex that actively exports Ni from the cytoplasm or the periplasm, across the outer membrane and to the outside of the cell (Nies, 2003). This tripartite complexes constitute a first line of defense against Ni toxicity but are rather unspecific and commonly export at least one other heavy metal (often Co) (Table 2). A second layer of resistance is provided by cation diffusion facilitators and proteins of the major facilitator superfamily, which often rely on electrochemical gradients to operate. For instance, *Achromobacter xylosoxidans* 31A NreB pumps out Ni cations (Grass *et al.*, 2001) allowing growth in concentrations up to 3 mM Ni (Table 2).

Microorganism	Operon	Metal specificity	Ni resistance (in mM)	Efflux type	Ref.
Neutrophilic bacteria					
Achromobacter xylosoxidans 31A	*nccYXHCBAN*	Ni, Co, Cd	40	RND	a, b
Achromobacter xylosoxidans 31A	*nreB*	Ni	3	MFS	c
Cupriavidus metallidurans CH34	*cnrYXHCBA*	Co, Ni	3	RND	d, e, f
Cupriavidus metallidurans CH34	*dmeF*	Zn, Co, Cd, Ni	0.4	CDF	g
Escherichia coli MC4100	*rcnAB*	Ni, Co	0.01	rcnA	h, i
Hafnia alvei 5-5	*ncrABCYX*	Ni, Co	30	MFS	j
Helicobacter pylori 26695	*cznCBA*	Co, Zn, Ni	1.2	RND	k
Klebsiella oxytoca CCUG 15788	*nirABCD*	Ni	10	MFS?	l, m
Pseudomonas aeruginosa KT2440	*mrdH*	Cd, Zn, Ni	4	Hybrid	n
Rhizobium leguminosarum bv viciae	*dmeRF*	Co, Ni	1	CDF	o
Serratia marcens C-1	*ncrABC*	Ni, Co	20	MFS	p
Acidophilic bacteria					
Leptospirillum ferriphilum UBK03	*ncrABCY*	Ni	30-40	?	q, r

Table 2. Mechanisms of Ni resistance in prokaryotes. Mechanisms of Ni efflux are divided in: resistance-, nodulation, cell-division efflux systems (RND); major facilitator superfamily proteins (MFS); cation diffusion facilitators (CDF) or a mixture of them (hybrid) (*P. aeruginosa* MrdH is a protein with domains similar both to RcnA and to CzcB homologs). Data from: a, (Schmidt *et al.*, 1991); b, (Schmidt and Schlegel, 1994); c, (Grass *et al.*, 2001); d, (Liesegang *et al.*, 1993); e, (Grass *et al.*, 2000); f, (Tibazarwa *et al.*, 2000); g, (Munkelt *et al.*, 2004); h, (Rodrigue *et al.*, 2005); i, (Blériot *et al.*, 2011); j, (Park *et al.*, 2004); k, (Stahler *et al.*, 2006); l, (Stoppel *et al.*, 1995); m, (Park *et al.*, 2008); n, (Haritha *et al.*, 2009); o, (Rubio-Sanz *et al.*, 2013); p, (Marrero *et al.*, 2007); q, (Tian *et al.*, 2007); r, (Zhu *et al.*, 2011).

Although cation efflux is the most common mechanism among natural Ni resisters, microorganisms have evolved other ways to avoid Ni toxicity. For instance, *E. coli* develops a chemotactic response away from Ni (Tso and Adler, 1974; Englert *et al.*, 2010), the gammaproteobacterium *Thiocapsa rosepersicina* reduces Ni^{2+} to Ni^{0} (elemental Ni) (Zadvornyy *et al.*, 2009) and a Ni-resistant strain of the sulphate reducer *Desulfotomaculum*

complexes Ni in dark-brown soluble NiS compounds, effectively decreasing the amount of free toxic Ni ions (Fortin *et al.*, 1994). Eukaryotic microorganisms have developed further strategies not yet reported in prokaryotes. In Ni-resistant strains of *Saccharomyces cerevisiae*, these strategies include extracellular chelation with glutathione, sequestering Ni cations in histidine-rich vacuoles, and reducing intracellular accumulation of Ni through changes in Mg^{2+} uptake protein CorA [reviewed in (Joho *et al.*, 1995a)].

Ni efflux systems were traditionally discovered in bacteria thriving in Ni-rich environments (both naturally occurring and anthropogenically contaminated) and were thus considered a limited problem in nature. However, the identification of *E. coli rcnAB* (encoding a Co and Ni efflux system) and several putative homologs throughout the bacterial and archaeal domains (Rodrigue *et al.*, 2005; Blériot *et al.*, 2011), suggests that Ni might be indeed an extended concern of many microorganisms.

As seen in Table 2, most of these Ni efflux systems have been described in neutrophiles rather than in more Ni-resistant acidophiles. This raises the question of whether coping mechanisms used by neutrophiles are actually suitable for acidophiles standing metal concentrations one or two orders of magnitude higher. Additional interest in understanding Ni resistance mechanisms in acidophiles may come from the biomining industry after recent reports that certain acidophiles can be used to leach nickel through reductive dissolution of Ni-containing ferric iron ores (du Plessis *et al.*, 2011; Hallberg *et al.*, 2011).

The fact that *Acidiphilium* sp. PM withstands large Ni concentrations (see section 4.1.3), grows to high cell densities and is easy to manipulate compared to acidophilic iron-oxidizers, makes it an optimal model for the study of Ni resistance in acidophiles.

2. OBJECTIVES

This thesis is part of a long-term, trans-disciplinar, multi-laboratory plan to characterize a Río Tinto *Acidiphilium* strain capable of producing electricity. This work pursued two distinct goals:

1. The development of genomic tools to facilitate the study of the strain.
   - 1.1 Genome sequencing and annotation of *Acidiphilium* PM. Reconstruction of its basic metabolism and comparative analysis with other *Acidiphilium* strains.
   - 1.2 Construction of a shotgun DNA genomic microarray of *Acidiphilium* PM of use both in whole-genome transcriptional studies and in comparative genomic hybridization.
2. The characterization of the heavy metal resistance in *Acidiphilium* PM.
   - 2.1. General characterization of the heavy metal resistance in *Acidiphilium* sp. PM.
   - 2.2. Identification of Ni-resistance determinants in *Acidiphilium* PM.
   - 2.3. Understanding the early response to Ni in *Acidiphilium* sp. PM.

3. MATERIALS AND METHODS

Unless stated otherwise, the following apply: i) protocols were performed at room temperature, and ii) whenever protocols involved the use of commercial kits, these were carried out as recommended by the manufacturers. Common molecular biology techniques were performed as described in (Sambrook and Russell, 2001). Nucleic acid accession numbers refer to NCBI's GenBank database (http://www.ncbi.nlm.nih.gov/genbank).

3.1. CHEMICAL AND BIOCHEMICAL MATERIAL

3.1.1. Buffer solutions

The composition of buffers routinely used in this work is detailed in Table 3.

Name	Composition	Use
PBS 1X	137 mM NaCl, 2.7 mM KCl, 10 mM Na_2HPO_4, 1.8 mM KH_2PO_4	Washing cell pellets
TE 1X	10 mM Tris-HCl pH 8.0, 1 mM EDTA	Suspending DNA
TAE 1X	40 mM Tris-acetate, 1 mM EDTA	Agarose gel electrophoresis
TBE 0.5X	45 mM Tris-borate, 1 mM EDTA	Agarose gel electrophoresis
DNA Loading buffer 10X	TAE 1X, 50% glycerol, 0.25% bromophenol blue, 0.25% xylene cyanol	DNA loading in gels
SSC 1X	150 mM NaCl, 15 mM sodium citrate	Washing DNA microarrays
SDS-PAGE 10X	25 mM Tris pH 8.3, 192 mM glycine, 0.1% SDS	Denatured protein gel electrophoresis

Table 3. Buffers and solutions used in this work.

3.1.2. Oligonucleotides

Oligonucleotides were synthesized by Bonsai Technologies or Applied Biosystems. Below is a list of the oligonucleotides used in this work. Oligos used in qPCR assays are listed separately in Table A 1 (APPENDIX IV).

Name	Sequence (5' - 3')	Ta (ºC)	Annealing region
8F	AGAGTTTGATCMTGGC	46.0	Initial portion of the *16S rRNA* gene of Bacteria.
1492R	TACGGYTACCTTGTTACGACTT	46.0	Final portion of the *16S rRNA* gene of Bacteria.
M13F	GTAAAACGACGGCCAG	50.0	Terminator of lacZ α fragment. Opposite sense to transcription.
M13R	CAGGAAACAGCTATGAC	50.0	Initial portion of the β-gal α-fragment. Same sense as transcription as pLac.
pSRNi16_*orf3*-2_F	CAGGTTCTAGATCAACATATTCGTGACCTGATCG	52.9	Promoter region of the RND efflux transporter. Inserts a XbaI restriction site.
pSRNi16_*orf3*-2_R	CAGGTAAGCTTGCCGGTTACTATAGGGTCAGGAC	52.9	Terminal region of the hypothetical protein. Inserts a HindIII restriction site.
Not I/KAN-3 FP-2	ACCTACAACAAAGCTCTCATCAACC	50.0	3' end of <Not I/KAN-3> Transposon.
Not I/KAN-3 RP-2	TCCCGTTGAATATGGCTCATAAC	50.0	5' end of <Not I/KAN-3> Transposon.
M13pUC F23	C^6-NH_2-CCCAGTCACGACGTTGTAAAACG	54.2	Terminator of lacZ α fragment. Opposite sense to transcription.
M13pUC R23	C^6-NH_2-AGCGGATAACAATTTCACACAGG	54.2	Initial portion of the β-gal α-fragment. Same sense as transcription as pLac.
16S rRNA_F	C^6-NH_2-TGTCAGTGGCGGACGGGTGAGTAA	61.2	*16S rRNA* gene of *Acidiphilium* species
16S rRNA_R	C^6-NH_2-GGCTGCCTCCCTTGCGGGTTA	61.2	*16S rRNA* gene of *Acidiphilium* species
AsRED_F	C^6-NH_2-GCCGGCATCGAACCCACGATCA	61.8	Arsenate reductase
AsRED_R	C^6-NH_2-GCCCAGCGGCGTCACCACGAT	61.8	Arsenate reductase
atpB_F	C^6-NH_2-CATGCAGGGCCTCGCCGAGATCA	62.5	*atpB*
atpB_R	C^6-NH_2-GCCCGCGAACACCTCCCACATCA	62.5	*atpB*
COX3_F	C^6-NH_2-TCGGCGCGGTCAGCACCATGTT	63.6	cytochrome C oxidase subunit 3
COX3_R	C^6-NH_2-AGTACCACGCGGCGGCCTCGAA	63.6	cytochrome C oxidase subunit 3
GAPDH_F	C^6-NH_2-CCCCGGCACGGTCGAGGTGAA	64.9	*GAPDH*
GAPDH_R	C^6-NH_2-CAGGGCGGCGGTGTCGCTCAT	64.9	*GAPDH*
rpoD_F	C^6-NH_2-GGACACCGCGACGCTCGACAT	65.5	*rpoD*
rpoD_R	C^6-NH_2-GCGCGAGGGGTGCTTGAGCTT	65.5	*rpoD*
bchL_F	C^6-NH_2-AGCGTGCAGGTCGCCCTCGAT	66.3	*bchL*
bchL_R	C^6-NH_2-GCGACGCGGCGAGATCGAGATA	66.3	*bchL*
trpB_F	C^6-NH_2-TCGGCGGCGCCAAGGTCTATTTCA	66.4	*trpB*
trpB_R	C^6-NH_2-TTGTCCATGCCGGGGGCGATCTT	66.4	*trpB*
S reductase_F	C^6-NH_2-CCCTTTCGCCCCCGAGGACAT	67.0	Flavodoxin/nitric oxide synthase
S reductase_R	C^6-NH_2-CCGCATCGCCCACGAGCTTCT	67.0	Flavodoxin/nitric oxide synthase
AsOX_F	C^6-NH_2-GTCCCGCTGCCACCGAAGAAT	61.3	Arsenite oxidase large subunit
AsOX_R	C^6-NH_2-TGCCGACGCGAGTTCCCTTGT	61.3	Arsenite oxidase large subunit
dnaK_F	C^6-NH_2-TCGACCTCGGCACCACGAATT	61.3	*dnaK*
dnaK_R	C^6-NH_2-GCCGACTTGATCGCCTCGAGAT	61.3	*dnaK*
mer_F	C^6-NH_2-GCATAGCCGAGAAAGCCCTCAA	63.0	Mercuric reductase
mer_R	C^6-NH_2-AAAGGTCTGTGCCGCAAGCTT	63.0	Mercuric reductase
pufL_F	C^6-NH_2-CGGCGGGGACCTGTTCGATTT	63.8	*pufL*
pufL_R	C^6-NH_2-GAACGGGCCGGAGAGCAGGAT	63.8	*pufL*
FBPase_F	C^6-NH_2-GCGACGCTCTGAGGCTCGATA	64.4	*FBP*
FBPase_R	C^6-NH_2-AGGCTGCCCTGCCCTTTCATA	64.4	*FBP*
hydA_F	C^6-NH_2-CAGCCGCCGCTCGTTCCTGAAAT	65.5	*hydA*
hydA_R	C^6-NH_2-TCGTCCGCCGTCGCCTCGAT	65.5	*hydA*
MCAT_F	C^6-NH_2-CGCGCGAGGTGTTCGAGGAAGT	66.3	*MCAT*
MCAT_R	C^6-NH_2-AGGTGTGCCGCAGGACAATGCTT	66.3	*MCAT*
bchC_F	C^6-NH_2-GCCGGCTGGGCGAGACGGTGTT	66.4	*bchC*
bchC_R	C^6-NH_2-GCGCGGCGACATCGGCGAGAT	66.4	*bchC*
idh_F	C^6-NH_2-CGGATCATCTGGGGGTTCATCAA	63.0	*idh*
idh_R	C^6-NH_2-TTCGAGATCAGCAGCGCGAGA	63.0	*idh*
dnaE_F	C^6-NH_2-TCGTCCATCTCCGCGTCCACT	64.4	*dnaE*
dnaE_R	C^6-NH_2-GGTGGCGAGGAGTTCGGAGAA	64.4	*dnaE*
bchH_F	C^6-NH_2-CCGCCGACCATCCCGGCCTGAT	66.6	*bchH*
bchH_R	C^6-NH_2-CGGACCGAGGCCACCGGGTTCA	66.6	*bchH*
FUR_F	C^6-NH_2-TGGCAAACGGGCTCAGGATGA	63.0	FUR family protein
FUR_R	C^6-NH_2-GCGGCCGAACAGCTCGATCTT	63.1	FUR family protein
MoOX_F	C^6-NH_2-CGTCGCCAACAAGCTGATGAA	65.0	Molybdopterin oxidoreductase
MoOX_R	C^6-NH_2-TGGCGGAGAAATCCCTTCAGTT	65.0	Molybdopterin oxidoreductase

Table 4. Oligonucleotides used in this work. Restriction sites are underlined. T_a indicates annealing temperatures.

3.2. BIOLOGICAL MATERIAL

3.2.1. Bacterial strains

The bacterial strains used in this work are listed in Table 5.

Strain	Genotype	Reference
Acidiphilium sp. strain 3.2 Sup 5	Wildtype	(Malki *et al.*, 2008)
Acidiphilium sp. strain PM		(This work)
Acidiphilium cryptum JF-5	Wildtype	(Kusel *et al.*, 1999)
Acidiphilium multivorum AIU301	Wildtype	(Wakao *et al.*, 1994)
Escherichia coli DH10B	F- *mcrA* Δ(*mrr-hsdRMS-mcrBC*) φ80*lacZ*Δ*M15* Δ*lacX74 recA1 endA1 araD139* Δ(*ara*, *leu*)*7697 galU galK* λ- *rpsL nupG* /pMON14272 / pMON7124	Invitrogen
Escherichia coli One Shot® TOP10	*F- mcrA Δ(mrr-hsdRMS-mcrBC) φ80lacZΔM15 ΔlacX74 recA1 araD139 Δ(ara-leu) 7697 galU galK rpsL (StrR) endA1 nupG λ-*	Invitrogen

Table 5. *E. coli* and *Acidiphilium* strains used in this work.

Acidiphilium sp. strain 3.2 Sup 5 and *Acp. cryptum* JF-5 were kindly provided by Moustafa Malki (Instituto de Catálisis y Petroleoquímica, Madrid, Spain) and Kirsten Küsel (Friedrich Schiller University Jena, Jena, Germany) respectively. *Acp. multivorum* AIU301 was purchased from the Japan Collection of Microorganisms.

3.2.2. Plasmids

The plasmids used in this work are listed in Table 6.

Name	Marker and use	Reference
pUC19	Amp^R, P*lac-lacZ*' used as control in transformation	Invitrogen
pCR®2.1-TOPO®	Amp^R, Kan^R, P*lac-lacZ*' used as cloning vector	Invitrogen
pBluescript® II SK+	Amp^R, P*lac-lacZ*' used as cloning vector	Stratagene
pTRI-Actin	Amp^R, SP6, T7, T3 promoters used for *in vitro* transcription of ß-actin gene fragment	Ambion
pTRI-Xef1	Amp^R, SP6, T7, T3 promoters used for *in vitro* transcription of *Xenopus* elongation factor 1α	Ambion

Table 6. Plasmids used in this work.

3.3. MICROBIOLOGICAL METHODS

3.3.1. Media, growth conditions, cell counting and preservation of the strains

Three different media recipes were used for the growth of *Acidiphilium* species.

a) GYE medium

Acidiphilium strains were routinely cultivated in GYE medium, which is composed of a mineral salt solution (0.2% $(NH_4)_2SO_4$, 0.01% KCl, 0.033% $K_2HPO_4 \cdot 3H_2O$, 0.025% $MgSO_4 \cdot 7H_2O$, 0.0014% $Ca(NO_3)_2 \cdot 4H_2O$) supplemented with 0.2% (w/v) glucose and 0.01% (w/v) yeast extract (Harrison, 1984). The pH was adjusted to 2.5 with 1 N H_2SO_4 prior to autoclaving at 111 ºC and 0.5 atm overpressure for 30 min.

b) Defined medium

A defined medium (DM) was successfully tested and used to grow *Acidiphilium* with metals. This medium is identical to GYE except that yeast extract is replaced by 1 ml of 100X Modified Wolfe's Mineral solution and 1 ml of 1000X Wolfe's Vitamin Solution (Wolin *et al.*, 1963) (Table 7). Minerals and vitamins are added to the autoclaved medium from filter-sterilized stocks.

Modified Wolfe's Mineral solution. A 100X stock contains (per litre):

Nitriletriacetic acid	1.5 g	$ZnSO_4 \cdot 7H_2O$	0.18 g
$MgSO_4 \cdot 7H_2O$	3.0 g	$CuSO_4 \cdot 5H_2O$	0.01 g
$MnSO_4 \cdot 2H_2O$	0.5 g	$KAl(SO_4)_2 \cdot 12H_2O$	0.02 g
NaCl	1.0 g	H_3BO_3	0.01 g
$FeSO_4 \cdot 7H_2O$	0.1 g	$Na_2MoO \cdot 2H_2O$	0.01 g
$CoSO_4 \cdot 7H_2O$	0.18 g	$NiCl_2 \cdot 6H_2O$	0.025 g
$NaSeO_3 \cdot 5H_2O$	0.3 g	Distilled H_2O	To 1 l

Wolfe's Vitamin Solution. A 1000X stock contains (per litre):

Biotine	20 mg	Folic acid	20 mg
Pyridoxine-HCl	10 mg	Tiamine.HCl$\cdot 2H_2O$	50 mg
Riboflavin	50 mg	Nicotinic acid	50 mg
Calcium D-Pantotenate	50 mg	B_{12} vitamin	50 mg
p-aminobenzoic acid	50 mg	Distilled H_2O	To 1 l

Table 7. Composition of modified Wolfe's mineral and Wolfe's vitamin solutions.

c) Media for iron reduction

Liquid Fe-TSB medium (pH 2.25) (Johnson and McGinness, 1991) was used to test *Acidiphilium*'s ability to reduce Fe^{3+}. This medium is composed of 0.025% tryptic soy broth, 0.2% glucose, and 0.8% $Fe_2(SO_4)_3$. First, a solution with tryptic soy broth and glucose was prepared and autoclaved. After cooling, $Fe_2(SO_4)_3$ was added to the solution from a sterile stock (100 g/l; pH 1.4).

All *Acidiphilium* cultures were grown at 30 ºC. Aerobic cultures were stirred in orbital shakers at 140 rpm whereas microaerobic cultures were incubated with no agitation. For the preparation of anaerobic cultures, Fe-TSB media was heated to boiling point for 5 min (in order to remove dissolved oxygen), then purged with N_2:CO_2 (80:20) while cooling. 60 ml of cold medium were dispensed in 100 ml-bottles and sealed with butyl rubber stoppers. After autoclaving, bottles were further purged with N_2:CO_2 (80:20) for 5 to 10 min and inoculated.

To grow *Acidiphilium* in solid medium (pH ≈ 2.5), a solution of 3 g/l agar was prepared, autoclaved and cooled down to 50 ºC prior to mixing 1:1 (v/v) with a sterile 2X GYE solution (pH 2).

E. coli was grown aerobically in LB (Lennox, 1955) or Terrific Broth modified (Sigma-Aldrich) at 37 ºC. When needed, these media were supplemented with 50-100 µg/ml ampicillin (LB-Ap) or 50 µg/ml kanamycin (LB-Ap-Kan). To select recombinants through screening of β-galactosidase activity, 5-bromo-4-chloro-3-indolyl-β-D-galactopyranoside (X-gal) and isopropyl β-D-1-thiogalactopyranoside (IPTG) were added to a concentration of 70 mg/l and 19 mg/l, respectively. Commercial SOC medium (2% yeast extract, 10 mM NaCl, 2.5 mM KCl, 10 mM $MgCl_2$) (Invitrogen) was added to *E. coli* DH10B cells after transformation by electroporation.

Growth was monitored by measuring optical density at a wavelength of 600 nm (OD_{600}) using a S2000 WPA spectrophotometer (Biochrom Ltd.).

Viable cells were counted by plating serial dilutions on solid GYE. To work out total cell numbers, culture aliquots were fixed with 4% (v/v) formaldehyde for 1 h, then diluted 10-fold and filtered through 0.2-µm pore-size GTTP filters (Millipore). Portions of these filters were stained with 4',6-diamidino-2-phenylindole (DAPI) and visualized under a Zeiss Axioskop 2 microscope (Zeiss).

E. coli was kept at 4 ºC for a maximum of two weeks. For longer periods it was preserved at -80 ºC in 20% glycerol. *Acidiphilium* strains were kept at 30 ºC for two weeks.

For longer storage, they were preserved at room temperature as freeze-dried pellets, or at -80 ºC in 10% DMSO or nutrient broth-glycerol 10%.

3.3.2. Growth with heavy metals

When *Acidiphilium* was grown with heavy metals, these were added to sterile defined media as sulphate salts from filter-sterilized 100 mM or 1 M stock solutions. Metal-containing plates were prepared from three separate solutions: 2X GYE, 4 g/l agar and a 5X heavy metal solution. These solutions were sterilized separately, brought to 50 ºC and mixed in a 5:4:1 proportion.

To test the growth of *E. coli* in the presence of metals, LB agar was autoclaved, cooled down to 50 ºC and supplemented with the appropriate metal from filter-sterilized 100 mM or 1 M stock solutions.

3.3.3. Growth under physico-chemical stresses

Selected Ni-resistant *E. coli* clones from the screening of the genomic library of *Acidiphilium* sp. PM (see section 3.7) were grown under physico-chemical stress (heat-shock, ultraviolet (UV) radiation, strong oxidation or acid stress).

Heat shock. Cells were grown in LB-Ap to early exponential phase. Then, 1 ml aliquots were pelleted by centrifugation (12000 g, 2 min), washed with PBS 1X (pH 7.4) and resuspended in 1 ml PBS 1X. Cells were then exposed to heat-shock (50 ºC) for 0 and 30 min. To determine their viability, serial dilutions of these aliquots were plated on LB-Ap agar and incubated overnight at 37 ºC.

UV radiation. Cells were grown overnight in LB-Ap. Then, 1 ml aliquots were pelleted by centrifugation (12000 g, 2 min), washed with PBS 1X (pH 7.4) and resuspended in 1 ml PBS 1X. Serial dilutions of these aliquots were plated on LB-Ap agar and irradiated at room temperature with UV radiation (λ = 254 nm-lamp operating at 1.55 W/m^2) for 0 and 5 sec. Plates were then incubated overnight at 37 ºC.

Hydrogen peroxide. Cells were grown in LB-Ap to early exponential phase. Then, 1 ml aliquots were removed and exposed to 2.5 mM H_2O_2 for 0 and 30 min (37 ºC). To determine their viability, serial dilutions of these aliquots were plated on LB-Ap agar and incubated overnight at 37 ºC.

Acid. Acid resistance experiments were performed as described by Guazzaroni *et al.* [30]. Briefly, cells were grown overnight in LB-Ap. Then, 1 µl aliquots were transferred to 1

ml of PBS (pH 7.2) and to 1 ml of LB broth (pH 1.8). Cells in LB broth were incubated in a heating block at 37 ºC for 1 h. To determine their viability, serial dilutions of these aliquots were plated on LB-Ap agar and incubated overnight at 37 ºC.

In all cases, rates of survival were calculated as the number of colony forming units per millilitre (cfu/ml) remaining after the treatment divided by the number of cfu/ml at time zero. Each experiment was repeated at least three times.

3.4. NUCLEIC ACID PREPARATIONS, AMPLIFICATION AND ANALYSIS

3.4.1. Preparation of plasmidic DNA

For plasmid preparation of selected clones, cells were grown overnight, then pelleted by centrifugation at 8000 g for 3 min and their plasmids were extracted using the QIAprep Spin Miniprep Kit (Qiagen).

High-throughput alkaline lysis was used for the extraction of recombinant plasmids from clones of the genomic library of *Acidiphilium* sp. PM. For the PCR-amplification of the genomic library, recombinant clones were grown overnight in TB-Amp using 96-deep-well plates. Then 15 µl of these cultures were incubated in 8 mM NaOH for 3 min at 95 ºC, chilled in ice and neutralized with 1.1% HCl. After centrifugation at 800 g for 1 minute, recombinant plasmids were recovered from the supernatant. Alternatively, when recombinant plasmids were extracted for insert sequencing, an automatized system was used where cells were grown in 96-well plates, collected by centrifugation at 2000 g and 4 ºC for 10 min and their plasmids were extracted using the Perfectprep™ Plasmid 96 Vac Kit (5 PRIME) with the aid of a liquid handling robot epMotion® 5075 (Eppendorf).

3.4.2. Extraction of genomic DNA from *Acidiphilium* sp. PM

DNA from *Acidiphilium* was extracted using GNOME® DNA Isolation Kit (MP Biomedicals).

Alternatively, when large preparations of intact DNA were required (*e.g.* for the construction of a genomic library of *Acidiphilium* sp. PM), the protocol approximately followed the detailed by Marmur (Marmur, 1961). Up to 1 l of culture in early stationary phase was pelleted by centrifugation (4300 g for 15 min) and then washed (50 mM Tris-HCl pH 8.0, 5 mM EDTA, 50 mM NaCl). Cells were then resuspended in 8 ml of lysis buffer (50 mM Tris-HCl pH 8.0, 10 mM EDTA, 100 mM NaCl, 25% sucrose, 1 mg/ml lysozyme, 40 µg/ml RNase A) and allowed to lyse for 20 min prior to the addition of 1 volume of 2% SDS.

After gentle mixing by inversion, cells were further lysed with 4 cycles of snap-freezing and thawing. Proteinase K was added at 10 µg/ml and the mixture was incubated for 30 min at 30 ºC. DNA released from cells was recovered with three, 20-ml phenol-chloroform-isoamyl alcohol (PCIA) (25:24:1) extractions, followed by 1 extraction with chloroform-isoamyl alcohol (24:1). DNA precipitation was performed with 0.1 volumes of 3 M sodium acetate pH 5.2 and 2.5 volumes of cold (-20 ºC) absolute ethanol. DNA was then spooled and transferred to a microcentrifuge tube, where it was washed with 70% ethanol and suspended in DNase-free H_20.

DNA preparations for pulsed field gel electrophoresis (PFGE) were carried *in situ* using low-melting point agarose (In Cert agarose, FMC BioProducts), a technique pioneered by Schwartz and Cantor (Schwartz and Cantor, 1984). From a culture grown to mid exponential phase, aliquots containing 10^8, $5x10^8$ and 10^9 cells were collected by centrifugation and suspended in 10 mM Tris-HCl pH 7.6, 1 M NaCl buffer. These solutions were mixed in equal amounts with 1.6% (w/v) low-melting point agarose, poured on plugs and allowed to cool. Plugs were incubated at 37 ºC for 24 h in lysis buffer (6 mM Tris-HCl pH 7.6, 1 M NaCl, 100 mM EDTA, 0.5 (w/v) polyoxyethylene 20 cetyl ether (Brij® 58), 0.2% (w/v) deoxycholate, 0.5% (v/v) sarkosyl, 1 mg/ml lysozyme, 10 µg/ml RNase A). This buffer was replaced by another containing 0.5 M EDTA (pH 9.0), 1% (v/v) sarkosyl, 1 mg/ml proteinase K, in which plugs were incubated for 48 h at 50 ºC. Plugs were then washed with TE 1X before being stored at 4 ºC in fresh TE 1X.

3.4.3. Extraction of total RNA from *Acidiphilium* sp. PM

Cells in early exponential phase were pelleted by centrifugation at 8000 g for 15 min at 4 ºC. Pellets were immediately snap-frozen in liquid nitrogen and stored at -80 ºC until further processing. RNA was extracted using column-based TRIzol® Plus RNA Purification System (Ambion), which includes an on-column DNase treatment. To avoid traces of contaminant DNA, upon elution, RNA was further treated with TURBO™ DNase (Ambion). RNA was then purified and concentrated with the RNeasy® Minelute® Cleanup kit (Qiagen).

The absence of contaminant DNA was verified as the lack of PCR amplification of the glyceraldehyde 3-phosphate dehydrogenase (GAPDH) gene (primer sequences are shown in Table 4). The integrity of the extracted RNA was checked by capillary electrophoresis in an RNA Nano Chip run in a 2100 Bioanalyzer (Agilent Technologies).

Nucleic acids were quantified using a ND-1000 Spectrophotometer (NanoDrop Technologies Inc.).

3.4.4. Polymerase Chain Reaction (PCR) amplification

DNA from *Acidiphilium* sp. PM was PCR-amplified using Expand Long Template PCR system (Roche). Reactions were performed in a final volume of 50 µl with the following mixture: 1 M betaine (Sigma), 350 µM of each dNTP (Roche), 300 nM of each primer (Bonsai Technologies), and 1 U of Expand Long Template PCR System (Roche). Amplifications were typically carried out in a DNA Engine Tetrad® 2 thermal cycler (Bio-Rad) using the following program: initial denaturation at 95 °C, 3 min; 35 cycles of [95 °C, 1 min; annealing temperature (see Table 4), 1 min; 68 °C, 1 min/kb], and a final elongation step at 68 °C, 10 min. However, for the amplification of the genomic library, a variation of this program was used: initial denaturation at 95 °C, 3 min; 17 cycles of [95 °C, 20 sec; 54.2 °C, 30 sec; 68 °C, 8 min], 21 cycles of [95 °C, 20 sec; 54.2 °C, 30 sec; 68 °C, 8 min+20 sec/cycle]; and a final elongation step at 68 °C, 7 min.

Oligonucleotides were designed using OLIGO 4.0 (National Biosciences Inc.) or NCBI's Primer-BLAST (Ye *et al.*, 2012) using an algorithm for melting temperature calculation (SantaLucia, 1998).

3.4.5. DNA labelling

5 µg of DNA were fragmented by sonication at 70% for 15 sec in a Branson Digital Sonifier 250D (Branson). A 0.5 µg-aliquot run in an agarose gel showed a homogeneous smear with fragments ranging from 0.3 to 3 kb. 2.5 µg of the fragmented DNA were mixed with 61 ng/µl random hexamer primers (Invitrogen), denatured at 70 ºC for 10 min, then snap-chilled on ice. Subsequently, 63 µM dATP, dCTP, dGTP, 38 µM dTTP, 75 µM Cy3-dUTP, 50000 U DNA Polymerase I, Large (Klenow) Fragment (New England Biolabs) were added and the mixture was incubated at 37 ºC for 2 h. Labelled cDNA was then purified using the QIAquick PCR Purification kit (Qiagen).

This protocol was used for DNA labelling in comparative genomic hybridizations. In addition, the quality of the spotted microarrays was checked by hybridization with sheared, Cy3-labelled DNA.

3.4.6. Synthesis of RNA by *in vitro* transcription

In vitro transcription reactions were performed using the MEGAscript® kit (Ambion). Transcripts were then purified using MEGAclear™ kit (Ambion) and stored at -80 ºC. *Xenopus laevis* elongation factor-1 alpha-chain and mouse β-actin antisense fragment (codons 303 to 220) were *in vitro* transcribed from T7 promoters in pTRI-Xef and pTRI-β-actin-Mouse (Table 6) using T7 RNA polymerase. Transcripts quality was ascertained both by regular gel electrophoresis and capillary electrophoresis, and quantified by spectrophotometry.

3.4.7. DNA cloning techniques

DNA was digested using restriction enzymes as recommended by the manufacturers (Roche, New England Biolabs).

When required, 5' protruding ends were filled with T4 DNA polymerase (New England Biolabs). Taq polymerase (Promega) and dATP were used to add single A 3' overhangs to blunt DNA fragments.

Prior to ligation, DNA fragments were purified using the QIAquick PCR Purification kit (Qiagen) or by extraction with PCIA (25:24:1) followed by precipitation. Ligation reactions were performed overnight with T4 DNA ligase (Roche) in a volume of 10 µl. Insert to vector ratios were adjusted to 5:1 except for the construction of the genomic library, where a 45:1 ratio was used. 3' A overhangs left by Taq polymerase allowed the ligation of PCR products with 3' T overhangs of pCR®2.1-TOPO® vector (Invitrogen) without further treatment with ligase.

When ORFs were subcloned, *ca*. 200-bp regions upstream of the start codon were also amplified to include their native expression sequences (promoters and ribosome binding sites).

The constructs generated as part of the functional screening for Ni-resistant clones were checked by sequencing with M13F and M13R (Table 4; 3.5).

3.4.8. *In vitro* transposon mutagenesis

In vitro transposon mutagenesis was performed using the EZ-Tn5™ In-Frame Linker Insertion Kit (Epicentre, Madison, WI), which is based on a hyperactive Tn5 transposition system (Goryshin and Reznikoff, 1998). <Not I/KAN-3> transposon contains a kanamycin resistance selection marker and specific sequences that allow the mapping of insertions.

Products of transposon insertion reactions were transformed in *E. coli* DH10B by electroporation as described in 3.4.9, and selected in LB-Ap-Kan plates. Approximately two hundred transformants from each reaction were patched on LB-Ap-Kan plates. After an overnight incubation they were re-streaked on LB-Ap-Kan plates with 2.25 mM Ni. Ni-sensitive transformants contained an interrupted ORF that was involved in Ni resistance. The insertions sites were mapped by sequencing using transposon-specific primers Not I/KAN-3 FP-2 and Not I/KAN-3 RP-2 (Table 4). In addition, several Ni-resistant transformants had their insertions mapped to verify that the remaining ORFs were not involved in Ni-resistance.

3.4.9. Transformation of *E. coli*

Recombinant plasmids were precipitated and resuspended in ultrapure H_2O prior to transformation of *E. coli* cells.

Chemically-competent *E. coli* One Shot® TOP10 (Table 5) were purchased from Invitrogen. *E. coli* DH10B cells were made competent using cold $CaCl_2$ as described by Cohen (Cohen *et al.*, 1972). Chemically-competent cells were transformed by heat-shock using the Hanahan method (Hanahan, 1983) as modified by Inoue (Inoue *et al.*, 1990). The transformation efficiency of these cells was verified by transformation with commercial pUC19 (Invitrogen) (Table 6).

For the construction of a genomic library of *Acidiphilium* sp. PM, *E. coli* ElectroMAX™ DH10B™ Cells (Invitrogen) (Table 5) were transformed by electroporation. Briefly, recombinant plasmidic DNA was mixed with 20 µl of *E. coli* ElectroMAX DH10B cells and transferred to ice-chilled 1 mm-gap cuvettes (Cell projects). A MicroPulser™ (Bio-Rad) was used to apply one 1800 V pulse for approximately 5.2 milliseconds. Immediately afterwards, 1 ml of SOC medium was added to the cells. After being incubated for 1 h at 37 ºC, 10-20 µl aliquots were plated in LB-Ap agar supplemented with X-gal and IPTG.

3.4.10. DNA electrophoresis

Separation of DNA fragments was routinely performed on 0.8-1% agarose gels (low EEO, Sigma) prepared with and run in TAE 1X or TBE 0.5X. To purify DNA fragments, bands were excised with a sterile razor blade and DNA was extracted with the QIAquick Gel Extraction Kit (Qiagen). Given the large number of PCR reactions that needed to be checked for the construction of the microarray, an alternative high-throughput electrophoresis system was used. About half of all PCR reactions were analyzed in pre-stained 96-well Ready-To-

Run 1.2% Agarose gels (GE Healthcare) run in a Ready-To-Run™ Separation Unit (GE Healthcare).

For PFGE, intact or RE-digested genomic DNAs were separated in 1% PFGE-grade agarose (SeaKem GTG or SeaPlaque® GTG® Agaroses, FMC BioProducts) using TBE 0.5X (14 ºC) as the running buffer. One third or one half of a plug was loaded into each well, which was then sealed with 0.8% low-melting point agarose. CHEF Mapper® XA and CHEF-DR® II Pulsed Field Electrophoresis Systems (Bio-Rad) were used to run 24-hour electrophoresis at 6 V/cm, and pulses ramping from 10 to 50 sec (for 50 to 500 kb fragments) or from 60 to 120 sec (for 200 to 1600 kb fragments).

Depending on the size range of the fragments examined, different molecular weight markers were used: Lambda Ladder (New England Biolabs) and *Saccharomyces cerevisiae* chromosomal DNA (Bio-Rad) were used for PFGE analysis, whereas 1 Kb DNA Ladder (New England Biolabs), 1 Kb Plus DNA Ladder (Invitrogen) and phage φ 29 digested with HindIII were used for conventional gel electrophoresis.

3.5. DNA SEQUENCING AND GENE ANNOTATION

3.5.1. Sequencing and annotation of the genome of *Acidiphilium* sp. PM

The genomic sequence of *Acidiphilium* PM was determined by pyrosequencing, (also known as 454 sequencing), a high-throughput method based on Ronaghi's technology of "sequencing by synthesis" (Ronaghi, Karamohamed *et al.* 1996; Ronaghi, Uhlén *et al.* 1998). Whole genome sequencing was carried out by Life Sequencing Ltd. (Valencia, Spain) using a 454 Life Sciences GS FLX System (Roche).

Contig assembly was performed using GS De novo Assembler 2.3 (Roche). Contigs longer than 500 bp were annotated by means of an automatic pipeline that uses tRNAscan (Lowe and Eddy, 1997) to predict tRNA genes, Glimmer (Delcher *et al.*, 2007) to predict coding sequences, and BLAST and RPS-BLAST (Altschul *et al.*, 1997) comparisons against several protein sequence and protein family databases to generate functional annotations. Insertion sequences were classified following nomenclature in ISfinder database (Siguier *et al.*, 2006). Annotations were then stored and queried using a Gbrowse-based system (Stein *et al.*, 2002). An automatic metabolic reconstruction was generated with Pathway Tools (Karp *et al.*, 2002). Gene orthologs between *Acidiphilium* species were identified using the stand-alone version of InParanoid 7.0 (Östlund *et al.*, 2010). EMBOSS software package (Rice *et*

al., 2000) was used to examine anomalous codon usage (*cusp*, *cai* and *codcmp* tools) and GC content bias (*geecee* application). Conserved domains in proteins were identified using NCBI's Conserved Domain Database (Marchler-Bauer *et al.*, 2013).

3.5.2. Sequencing and mapping of clones from the genomic library

Clones retrieved in the screening of the genomic library and in differential gene expression studies performed with the microarray had their recombinant plasmids extracted (see section 3.4.1). Inserts were then sequenced using an automatized, fluorescent version of the chain-terminating dideoxynucleotides (ddNTPs) method (Sanger *et al.*, 1977). Plasmid DNA was end-sequenced using M13F and M13R primers (Table 4) and the BigDye® Terminator v3.1 Cycle Sequencing Kit (Applied Biosystems). Runs were performed in an Applied Biosystems 3730xl DNA Analyzer (48-capillary array) (Applied Biosystems).

Sequence reads were then aligned against the draft genome of *Acidiphilium* sp. PM (Acc. No. NZ_AFPR00000000) using BLASTN (Altschul *et al.*, 1990). The output was processed with a custom Perl script that defined the boundaries of each cloned fragment by pairing forward and reverse sequence read matches that fulfilled the following conditions: i) e-value for both alignments < 10^{-100}, ii) convergent orientation of the mapped sequences and iii) 10 kb maximum distance between the 5' ends of the mapped sequences. The annotation of the genome of *Acidiphilium* sp. PM was used to identify ORFs in the clones. Only genes overlapping at least 5% with the clone were considered in the analysis.

3.6. PHYLOGENETIC ANALYSIS

3.6.1. *16S rRNA*-based phylogenetic analysis of *Acidiphilium* sp. PM

16S rRNA gene sequences of eight *Acidiphilium* strains (including 6 type strains) were retrieved from NCBI's Reference Sequence database, a collection of non-redundant, selected and curated genomic, transcriptomic and protein sequence records (Pruitt *et al.*, 2012) (Table 8). These sequences were imported in ARB software package (v. 5.2) (Ludwig *et al.*, 2004) and incorporated to a database of over 50000, 1000 bp-long prokaryotic *16S rRNA* gene sequences. Sequence alignments were manually corrected and alignment uncertainties were omitted in the phylogenetic analysis. Phylogenetic trees of representatives of the *Acetobacteraceae* were generated using parsimony, neighbour-joining and maximum-likelihood algorithms and selecting *Leptospirillum ferrooxidans* as the outgroup to root the

tree. A filter for *Alphaproteobacteria* was used which excluded highly variable positions. A consensus tree was selected based on the stability of the topology of the trees.

Species	Strain	Reference	Ref. Seq. acc. no.
Acp. acidophilum	MS Silver^T (ATCC 27807; DSM 700)	(Guay and Silver, 1975; Harrison, 1983; Hiraishi *et al.*, 1998)	NR_036837
Acp. angustum	KLB^T (ATCC 35903)	(Wichlacz *et al.*, 1986)	NR_025850
Acp. cryptum^T	Lhet2^T (ATCC 33463; DSM 2389; JCM 21277)	(Harrison, 1981)	NR_025851
Acp. cryptum	JF-5	(Kusel *et al.*, 1999)	NR_074281
Acp. multivorum	AIU301^T (AIU301; DSM 11245; JCM 8867)	(Wakao *et al.*, 1994)	NR_074327
Acp. organovorum	TFC^T (ATCC 43141)	(Lobos *et al.*, 1986)	NR_025853
Acp. rubrum	OP^T (ATCC 35905)	(Wichlacz *et al.*, 1986)	NR_025854
Acidiphilium sp.	PM (DSM 24941)	(San Martin-Uriz *et al.*, 2011)	NZ_AFPR01000512

Table 8. *Acidiphilium* strains used in the construction of a *16S rRNA*-based phylogenetic tree. ^{T} designates type strains.

3.6.2. Phylogenetic analysis of *Acidiphilium* sp. PM HslVU

The amino acid sequences of HslV and HslU of 14 acidophilic and 14 non-acidophilic taxa were retrieved from GenBank and then concatenated. An alignment was generated with Clustal W (Thompson *et al.*, 1994) using MEGA5 (Tamura *et al.*, 2011). A phylogenetic tree was inferred using the Maximum Likelihood method based on the Jones–Taylor–Thornton (JTT) amino acid substitution model. The branch support in the phylogenetic tree was assessed with a bootstrap analysis of 1000 replicates.

3.7. CONSTRUCTION OF A SHOTGUN GENOMIC LIBRARY OF *Acidiphilium* sp. PM

A shotgun genomic library of *Acidiphilium* sp. PM was constructed in *E. coli* DH10B cells using pBluescript® II SK+ (Table 6) as the vector (Figure 6).

DNA from *Acidiphilium* sp. PM was extracted by enzymatic and mechanical disruption of the membranes followed by PCIA extraction as explained in section 3.4.2. This DNA was then fragmented by partial digestion with 0.022 U Sau3AI/µg DNA (Roche) (10 min at 37 ºC). A 5 µg aliquot was run in an agarose gel to check the products of the digestion. Digested DNA was then separated in a 10-40% sucrose gradient by isopycnic ultracentrifugation. Fractions were collected and run in agarose gels to verify their size. Fractions containing DNA fragments in the ranges 1.5-4 kb, 2-6 kb and 3-10 kb were pooled, then precipitated and suspended in ultrapure H_2O. This fragmented, sized-sorted *Acidiphilium* sp. PM DNA made up the inserts.

The pBluescript® II SK+ (pSKII+) phagemid was used as the vector in the construction of the genomic library. pSKII+ was digested with BamHI and dephosphorylated

with Shrimp Alkaline Phosphatase (SAP). Then, it was purified by extraction with PCIA, precipitated and suspended in H_2O.

Insert and vector were mixed in a proportion of 45:1 (m/m) and were allowed to ligate overnight using 1000 U of T4-DNA ligase (Roche). The products of the ligation were precipitated and suspended in H_2O. Then, 20 µl of *E. coli* DH10B electrocompetent cells (Invitrogen) were transformed with 100-150 ng of recombinant plasmids by electroporation.

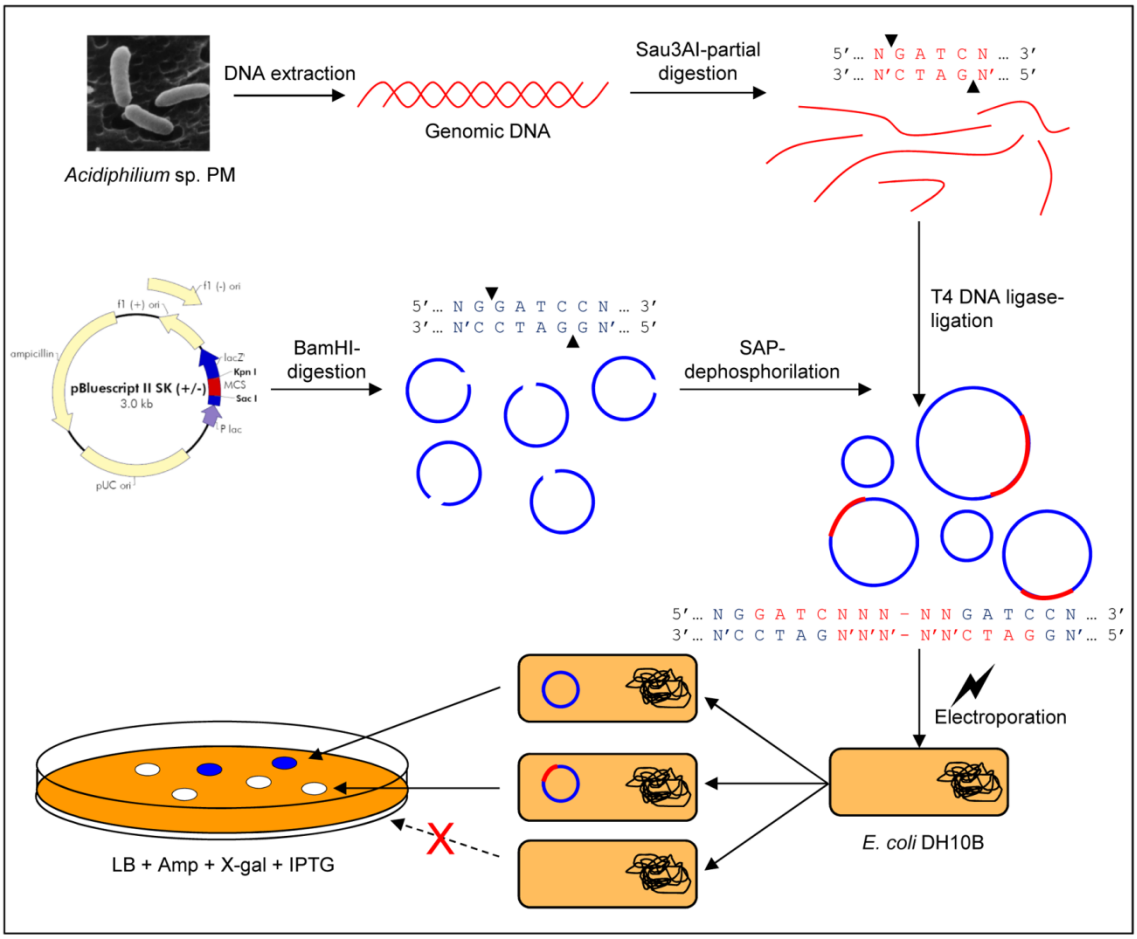

Figure 6. Scheme for the construction of a genomic library of *Acidiphilium* sp. PM.

3.8. CONSTRUCTION OF A SHOTGUN GENOMIC MICROARRAY OF *Acidiphilium* sp. PM

Genomic microarrays of *Acidiphilium* sp. PM were constructed using clones from the library with insert sizes 2-6 kb. A total of 8544 recombinant clones from the genomic library (contained in eighty-nine 96-well plates) were grown overnight in TB-Amp and lysed using alkaline conditions (see section 3.4.1). Inserts from the recombinant plasmids were PCR-amplified using amino-modified oligonucleotides M13pUC F23 and M13pUC R23 (Table 4).

PCR products were checked by agarose gel electrophoresis. Half of these PCR reactions were run in conventional 0.8% agarose gels and were used to estimate the average insert size. The remaining PCRs were checked using pre-stained 96-well Ready-To-Run 1.2% Agarose gels (GE Healthcare). The efficiency of recombination was calculated as the number of positive amplifications divided by the total number of PCR reactions.

A separate 96-well plate (plate 90) was used to accommodate 48 hybridization controls. Positive controls comprised 22 PCR-amplified genes from *Acidiphilium* sp. PM, including several involved in central metabolism, DNA replication, transcription and heavy-metal detoxification. Sau3AI-digested genomic DNA was also used as positive hybridization control (Table 9). PCR-amplified inserts from several clones of a genomic library of *Leishmania infantum* MCAN/ES/98/10445 (kindly provided by Pedro Alcolea, Centro de Investigaciones Biológicas, Madrid, Spain) and 1X MicroSpotting Solution Plus (Telechem International, Inc) served as negative hybridization controls (Table 9).

All PCR reactions were purified using 50 µl, 96-well-plate PCR purification kits (TeleChem International, Inc.), then spun-dried and resuspended in 1X MicroSpotting Solution Plus. Prior to spotting, these products were transferred from 96-well plates to 384-well plates with the aid of a liquid handling robot epMotion® 5075.

A total of 8592 spots (including 48 control spots) constitute an individual array. Arrays were printed in duplicate onto epoxy-coated slides VEPO 25C (CEL associates Inc.) at 21 ºC and 37-44% relative humidity using a MicroGrid-TAS II Arrayer (Digilab Inc.). The microarray configuration was deposited in NCBI's Gene Expression Omnibus database under accession number GPL17306. The quality of the printed microarrays was visually inspected and a microarray from each batch was further hybridized with fragmented, fluorescently-labelled genomic DNA of *Acidiphilium* sp. PM.

Well	Control	GenBank Acc. No.	Primers	Species
90A1	*16S rRNA*	AFPR01000512.1:149..1480	16S rRNA_F & 16S rRNA_R	*Acidiphilium* PM
90A2	Arsenate reductase	AFPR01000513.1:14144..14377	AsRED_F & AsRED_R	*Acidiphilium* PM
90A3	*atpB*	AFPR01000105.1:48980..49385	atpB_F & atpB_R	*Acidiphilium* PM
90A4	Cytochrome C oxidase subunit 3	AFPR01000050.1:2507..3100	COX3_F & COX3_R	*Acidiphilium* PM
90A5	*GAPDH*	AFPR01000557.1:5300..6131	GAPDH_F & GAPDH_R	*Acidiphilium* PM
90A6	*rpoD*	AFPR01000360.1:402..2232	rpoD_F & rpoD_R	*Acidiphilium* PM
90A7	*bchL*	AFPR01000202.1:1979..2747	bchL_F & bchL_R	*Acidiphilium* PM
90A8	*trpB*	AFPR01000186.1:712..1606	trpB_F & trpB_R	*Acidiphilium* PM
90A9	Flavodoxin/nitric oxide synthase	AFPR01000462.1:21417..22543	S reductase_F & S reductase_R	*Acidiphilium* PM
90A10	Arsenite oxidase large subunit	AFPR01000513.1:16057..18541	AsOX_F & AsOX_R	*Acidiphilium* PM
90A11	*dnaK*	AFPR01000043.1:3647..5372	dnaK_F & dnaK_R	*Acidiphilium* PM
90A12	Mercuric reductase	AFPR01000560.1:1816..3365	mer_F & mer_R	*Acidiphilium* PM
90B1	*pufL*	AFPR01000072.1:2837..3548	pufL_F & pufL_R	*Acidiphilium* PM
90B2	Fructose-1,6-Bisphosphatase (FBP)	AFPR01000162.1:3081..4075	FBPase_F & FBPase_R	*Acidiphilium* PM
90B3	*hydA*	AFPR01000118.1:2916..3848	hydA_F & hydA_R	*Acidiphilium* PM
90B4	*MCAT*	AFPR01000148.1:2904..3742	MCAT_F & MCAT_R	*Acidiphilium* PM
90B5	*bchC*	AFPR01000291.1:428..985	bchC_F & bchC_R	*Acidiphilium* PM
90B6	*idh*	AFPR01000194.1:19300..20384	idh_F & idh_R	*Acidiphilium* PM
90B7	*dnaE*	AFPR01000495.1:15295..18353	dnaE_F & dnaE_R	*Acidiphilium* PM
90B8	*bchH*	AFPR01000202.1:2964..6336	bchH_F & bchH_R	*Acidiphilium* PM
90B9	FUR family protein	AFPR01000449.1:1242..1609	FUR_F & FUR_R	*Acidiphilium* PM
90B10	Molybdopterin oxidoreductase	AFPR01000564.1:7085..9349	MoOX_F & MoOX_R	*Acidiphilium* PM
90B11	Spotting solution 1x	-	-	-
90B12	Spotting solution 1x	-	-	-
90C1	Sau3AI-digested genomic DNA	-	-	*Acidiphilium* PM
90C2	*Le. infantum* clone S30C8	GS882475	M13pUC F23 & M13pUC R23	*Le. Infantum*
90C3	*Le. infantum* clone S18H12	GS882328	M13pUC F23 & M13pUC R23	*Le. Infantum*
90C4	*Le. infantum* clone S31A9	-	-	*Le. Infantum*
90C5	*Le. infantum* clone S13C5	GS598893	M13pUC F23 & M13pUC R23	*Le. Infantum*
90C6	*Le. infantum* clone S31F5	GS882516	M13pUC F23 & M13pUC R23	*Le. Infantum*
90C7	*Le. infantum* clone S19D9	GS882338	M13pUC F23 & M13pUC R23	*Le. Infantum*
90C8	*Le. infantum* clone S15F1	GS598968	M13pUC F23 & M13pUC R23	*Le. Infantum*
90C9	*Le. infantum* clone S21H8	GS882523	M13pUC F23 & M13pUC R23	*Le. Infantum*
90C10	Spotting solution 1x	-	-	-
90C11	Spotting solution 1x	-	-	-
90C12	Spotting solution 1x	-	-	-
90D1	Spotting solution 1x	-	-	-
90D2	Spotting solution 1x	-	-	-
90D3	Spotting solution 1x	-	-	-
90D4	Spotting solution 1x	-	-	-
90D5	Spotting solution 1x	-	-	-
90D6	Spotting solution 1x	-	-	-
90D7	Spotting solution 1x	-	-	-
90D8	Spotting solution 1x	-	-	-
90D9	Spotting solution 1x	-	-	-
90D10	Spotting solution 1x	-	-	-
90D11	Spotting solution 1x	-	-	-
90D12	Spotting solution 1x	-	-	-

Table 9. Preparation of the controls of the genomic microarray of *Acidiphilium* sp. PM. *Acidiphilium* sp. PM genes and *Le. infantum* MCAN/ES/98/10445 clones were PCR-amplified using the primers listed (sequences are specified in Table 4). Amplicon sequences are indicated as GenBank coordinates.

3.9. COMPARATIVE TRANSCRIPTOMICS USING GENOMIC MICROARRAYS OF *Acidiphilium* sp. PM

3.9.1. RNA reverse-transcription and cDNA labelling

RNA was reverse-transcribed and cDNA was labelled with N-hydroxysuccinimide esters of cyanine fluorescent dyes (Cy3 and Cy5) using a protocol adapted from (Alcolea *et al.*, 2009). 20 µg of total RNA were mixed with 200 ng/µl random hexamers and 40 U RNase OUT (Invitrogen), then denatured at 70 ºC for 10 min and snap-chilled on ice. Subsequently, 525 µM dATP, dCTP, dGTP, 210 µM dTTP, 630 µM aminoallyl-dUTP, 10 mM DTT, and 600 U of Superscript® III RNase H$^-$ (Invitrogen) were added and the mixture was incubated

at 46 ºC for 3 h to allow cDNA synthesis. RNA was then degraded by incubation in 100 mM NaOH, 10 mM EDTA for 30 min at 70 ºC. The single-stranded cDNA was purified with the QIAquick PCR Purification kit (Qiagen, Valencia, CA) but using phosphate wash buffer (5 mM KPO4, 80% ethanol) and phosphate elution buffer (4 mM KPO4) instead of the kit wash and elution buffers (which Tris-based composition may interfere with free amine residues in the aminoallyl-dUTP-cDNA).

Labelling of the cDNA was carried out in 10 µl 100 mM $NaHCO_3$ (pH 9.0) by adding 5 µl of 12 ng/µl DMSO-dissolved Cy3 or Cy5 monofunctional dyes and allowing the coupling to take place in the dark for 1 h. Labelled cDNA was purified with the regular QIAquick PCR Purification kit (Qiagen) protocol, and quantified by spectrophotometry.

3.9.2. Microarray hybridization

Slides were washed in 2X SSC, 0.1% sarcosyl and 2X SSC, then denatured for 3 min at 95 ºC and fixed in cold absolute ethanol. Before hybridization, microarrays were blocked by incubation at 42 ºC for 45 min with 3X SSC, 60 mM Tris-HCl pH 8.0, 0.3% SDS, 1% BSA, 83 ng/µl denatured salmon sperm DNA (Invitrogen).

Cy3- and Cy5-labelled cDNAs were mixed in approximately equimolar amounts and incubated at 65 ºC for 16 h in 1x HybIt Hybridization Solution (ArrayIt), 75 ng/µl herring sperm ssDNA (Invitrogen).

After hybridization, slides were washed in progressively less stringent conditions (first in 2X SSC, 0.2% SDS at 65 ºC; next in 1X SSC; and finally in 0.2X SSC). Slides were then spun dry in a Galaxy™ Miniarray slide centrifuge (VWR).

3.9.3. Microarray scanning and data analysis

Hybridized microarrays were immediately scanned for Cy3 (532 nm) and Cy5 (635 nm) dyes with a GenePix 4100A scanner (Axon Instruments) setting a saturation tolerance of 0.005%. Local feature background median was subtracted from raw data of average fluorescence intensity values and exported to AlmaZen (BioAlma). Normalization was performed applying LOWESS algorithm (Cleveland *et al.*, 1982) individually to each of the blocks in the microarray (LOWESS per pin) (Yang *et al.*, 2002). Spots were printed in duplicate in each slide but were treated separately during the analysis to maximize sensitivity. Comparative analysis consisted of a paired Student's t-test ($p < 0.05$) for average $\log_2$ratio in each replicate under the null hypothesis of absence of differential gene expression.

Thresholds for the selection of the spots were set *ad hoc* based on the Fold change/A scatter plot ($F = \frac{R}{G}$ for R > G or $F = -\left(\frac{G}{R}\right)$ when R < G; $A = \frac{(\log_2 R + \log_2 G)}{2}$, where R and G are the fluorescence intensities of the tested and reference conditions, respectively). Selected clones were end-sequenced and their reads mapped against the draft genome of *Acidiphilium* sp. PM as detailed in section 3.5.2.

If selected, a given spot could have one or two set of values for F, $\log_2$F±SD and p depending on whether one or the two replicates included in the microarray had met the criteria. Where only one significant replicate was present, the threshold was lowered to a more conservative $p \leq 0.001$ to discard that it had been erroneously selected. When two sets of values were present, single values for F, $\log_2$F±SD and p were calculated as detailed in APPENDIX III. If two replicates were selected, their data was deemed more reliable and statistical significance was kept at $p < 0.05$.

To validate the overall expression data from microarray hybridizations, and to further study the up- or down-regulation of individual genes in clones containing multiple genes, quantitative real time RT-PCR assays (qRT-PCR) were performed.

3.9.4. Validation of microarray data with quantitative real time RT-PCR (qRT-PCR)

RNA was reverse-transcribed to cDNA using Superscript® III RNase H- (Invitrogen) as recommended by the manufacturer. Typical housekeeping genes (*e.g.* GAPDH, DNA polymerase, 16S rRNA) were differentially expressed in response to Ni and Zn; hence they could not be used for the normalization of qRT-PCR data. Instead, 10^6 copies of two external mRNA transcripts (mouse β-actin antisense and *Xenopus laevis* elongation factor 1α) were added to every 2 ng of RNA prior to reverse-transcription and used in subsequent normalization. These RNA transcripts were synthesized *in vitro* from pTRI plasmids using T7 RNA polymerase (3.4.6).

Each qRT-PCR assay was performed using 2 ng of cDNA and 1X TaqMan® Universal Master Mix II (Applied Biosystems) in a final volume of 15 µl. Assays were performed in triplicate using 384-well plates with custom TaqMan® MGB probes (250 nM) and oligonucleotide pairs (900 nM) synthesized by Applied Biosystems. TaqMan® probes contained 6-carboxyfluorescein (FAM) as the reporter dye in 5' and minor groove binder-nonfluorescent quencher (MGB-NFQ) as the quencher in 3'. A complete list of the primers and probes used in qRT-PCR assays is provided in Table A 1 (APPENDIX IV). qRT-PCR

assays were performed in an ABI PRISM® 7900HT (Applied Biosystems). Fold-change and SE values were calculated in ExpressionSuite Software v1.0 (Applied Biosystems) using the comparative cycle time (or ΔΔCt) method (Bookout *et al.*, 2006) and external transcripts mouse β-actin antisense and *Xenopus laevis* elongation factor 1α as reference genes.

3.10. COMPARATIVE PROTEOMICS

3.10.1. Protein extraction and quantification

Cells in mid exponential phase were pelleted by centrifugation (8000 g, 10 min), and then washed with 2 ml cold PBS (pH 2). Pellets were immediately snap-frozen in liquid nitrogen and stored at -80 ºC until further processing.

A protein extraction protocol was optimized: pellets were resuspended in 1 ml extraction buffer (7 M urea, 2 M thiourea, 1 mM EDTA, 10 mM DTT, 5 mM $MgCl_2$, 4% (v/v) Tx100, 15 µl Calbiochem Protease Inhibitor Cocktail Set VI), then disrupted with 250 µl of zirconia beads from RiboPure™-Bacteria Kit (Ambion) using a Fast Prep FP220A Instrument (Q-Bio Gene Inc.) and 3 cycles of: 20 sec at speed 5.0, 5 min in ice. After centrifugation (16000 g for 5 min at 4 ºC), supernatants were collected and cell debris and intact cells were resuspended in extraction buffer and further disrupted (20 sec at speed 6.5). Supernatants were then merged, centrifuged again and stored at -80 ºC.

Protein samples were submitted to a Proteomics Facility (Universidad Complutense de Madrid – Parque Científico de Madrid (UCM-PCM) (Madrid, Spain), a member of ProteoRed-ISCIII), where 2D-DIGE comparative proteomics was performed. Proteins were cleaned up by precipitation using the 2-D Clean-Up Kit (GE Healthcare) and then resuspended in DIGE buffer (10 mM Tris, 7 M urea, 2 M thiourea, 2% (w/v) CHAPS). Protein concentration was determined using the Bradford assay (Bradford, 1976) and their quality was visually inspected in 10% SDS-PAGE gels stained with Coomassie Blue G-250. Precision Plus Protein™ Unstained standard (Bio-Rad) was used as molecular weight marker.

3.10.2. Sample labelling and 2D gel electrophoresis

Proteins were labelled using Cy fluorescent dyes (GE Healthcare) following a procedure described by Moreno and co-workers (Moreno *et al.*, 2009) with minor modifications. 50 µg of protein extracts were labeled in the dark with 400 pmol of

fluorescent dye at 41 ºC for 30 min. The reaction was subsequently stopped by addition of 1 µl of 10 mM Lys.

150 µg of proteins were run in each 2DE gel: 50 µg of Cy3-labelled proteins (condition 1), 50 µg of Cy5-labelled proteins (condition 2) and 50 µg of Cy2-labelled internal standard (a mixture containing equal amounts of protein from all replicates). Prior to being loaded in the gel, the 150 µg mixture was diluted 1:1 with loading buffer (7 M urea, 2 M thiourea, 4% (w/v) CHAPS, 200 mM DTT, 4% Pharmalytes). Isoelectric focusing (IEF) was performed in a non-linear gradient using 24-cm Immobiline DryStrip pH 3-11 NL (GE Healthcare) which had been previously rehydrated [in 8 M urea, 2 M thiourea, 4% (w/v) CHAPS, 2% (v/v) IPGphor buffer 3-11 (GE Healthcare) and 100 mM DeStreak (GE Healtchare)] for 8 h. IEF was carried out at 20 ºC using the following sequential voltages: 120 V for 1 h; 500 V for 2 h; 500-2000 V gradient along 2 h; 1000–5000 V gradient along 6 h; 5000 V for 12 h. Strips were then equilibrated for 12 min in reducing solution (100 mM Tris-HCl (pH 8.0), 6 M urea, 30% (v/v) glycerol, 2% (w/v) SDS, 2% (w/v) DTT) followed by alkylation for 5 min in the same solution supplemented with 2.5% (w/v) iodoacetamide. To perform the separation in the second dimension the strip was applied on top of a 22 x 26 cm homogeneous 12% T, 2.6% C polyacrylamide gel. Electrophoresis runs were carried out at 20 ºC applying 15 W per gel.

3.10.3. Protein visualization and image analysis

After electrophoresis, gels were scanned in a Typhoon 9400 (GE Healthcare) fluorescence scanner with a pixel resolution of 100 µm at the corresponding excitation/emission wavelengths for each dye (Cy3: 532/580 nm; Cy5: 633/670 nm; Cy2: 488/520 nm). Gel images were cropped with ImageQuant v5.1 (GE Healthcare) and analyzed using DeCyder v6.5 software (GE Healthcare). The latter was used to identify spots, calculate their volumes, match spots across gels using a master gel, and for statistical analysis. First, the normalized ratio against the internal standard (Cy3/Cy2 or Cy5/Cy2) was worked out individually for each spot in each gel. Then, the average normalized ratio across replicates was used to compare pairs of experiments (treatment vs control) using Student's t-test. Because 2 variables were tested [treatment (yes/no) and time (1h/5h)], 2-way ANOVA (with False Discovery Rate (FDR) correction) was applied to study the statistical significance of each separate variable as well as their interaction. Protein spots with $p < 0.05$ were considered statistically significant.

3.10.4. Identification of protein spots using MALDI-TOF mass spectrometry

Following statistical analysis, proteins were identified as described elsewhere (Moreno *et al.*, 2009). Briefly, 2-DE gels were stained with Colloidal Coomassie Blue. Then, spots of interest were manually excised, and their proteins were reduced, alkylated and digested with trypsin prior to analysis in a MALDI-TOF/TOF spectrometer 4700 Proteomics Analyzer (PerSeptive Biosystems). Proteins were identified with MASCOT 2.1 (www.matrixscience.com/server.html) (Perkins *et al.*, 1999) using peptide mass fingerprints against a database of predicted proteins of *Acidiphilium* sp. PM.

3.11. MEASUREMENT OF HEAVY METAL CONCENTRATIONS

3.11.1. Determining heavy metal content in water samples

The measurement of trace elements in the waters of Río Tinto was carried out by inductively coupled plasma-mass spectrometry (ICP-MS), as recommended by the U.S. Environmental Protection Agency (Environmental Monitoring Systems Laboratory, 1996).

3.11.2. Determining Ni content in cells

Cells submitted to metal stress were harvested by centrifugation and washed three times with ultrapure H_2O before pellets were lyophilized, pulverized and dissolved in H_2O:HCl:HNO_3:H_2O_2 3:1:4:0.5 (v/v) by closed vessel microwave digestion in a Milestone Ethos Touch Control (Milestone). Ni content was measured by ICP-MS using an ELAN9000® ICP quadrupole mass spectrometer (PerkinElmer).

4. RESULTS AND DISCUSSION

4.1. ISOLATION AND CHARACTERIZATION OF *Acidiphilium* sp. PM

4.1.1. Isolation of *Acidiphilium* sp. PM

Acidiphilium sp. 3.2 Sup 5 was isolated by Moustafa Malki from the surface waters of a 6 m-deep dam in the initial course of Río Tinto [sampling point RT8 according to nomenclature used in (Garcia-Moyano *et al.*, 2012)]. In voltammetry experiments, this isolate proved capable of transferring electrons to artificial electrodes, even in the presence of oxygen (one of its natural electron acceptors) (Malki *et al.*, 2008). Since its isolation on 11 September 2004, it had been maintained by periodic transfer to fresh GYE media. Over time, the culture had yielded progressively lower intensity currents, which was compatible with the initial population accumulating mutations, exhibiting genetic drift, *et cetera*.

To study the homogeneity of the culture, we compared the restriction patterns of SpeI-digested DNA from a single colony and from the whole culture of *Acidiphilium* sp. 3.2 Sup 5 using PFGE. As shown in Figure 7A, *Acidiphilium* sp. 3.2 Sup 5 presented a complex pattern which contained several bands not found in the pattern of the single colony. This suggested that the culture was composed of a mixture of different strains. To isolate them, 20 colonies were grown and their restriction patterns studied by digestion with SpeI followed by separation with PFGE. Three different patterns were observed (Figure 7B). Merging the bands from the three patterns, yielded that of *Acidiphilium* sp. 3.2 Sup 5. This indicated that all possible SpeI patterns had been isolated. Interestingly, colonies corresponding to patterns 1 and 2 were larger than colonies with pattern 3.

To determine whether all three types of colonies belonged to the genus *Acidiphilium*, their *16S rRNA* gene were PCR-amplified and sequenced. A phylogenetic analysis revealed that the representatives of all three patterns are closely-related *Acidiphilium* strains. Indeed, they cluster in a highly similar group (> 99.5%) which also comprises *Acp. cryptum*, *Acp. multivorum* and *Acp. organovorum* species (APPENDIX I).

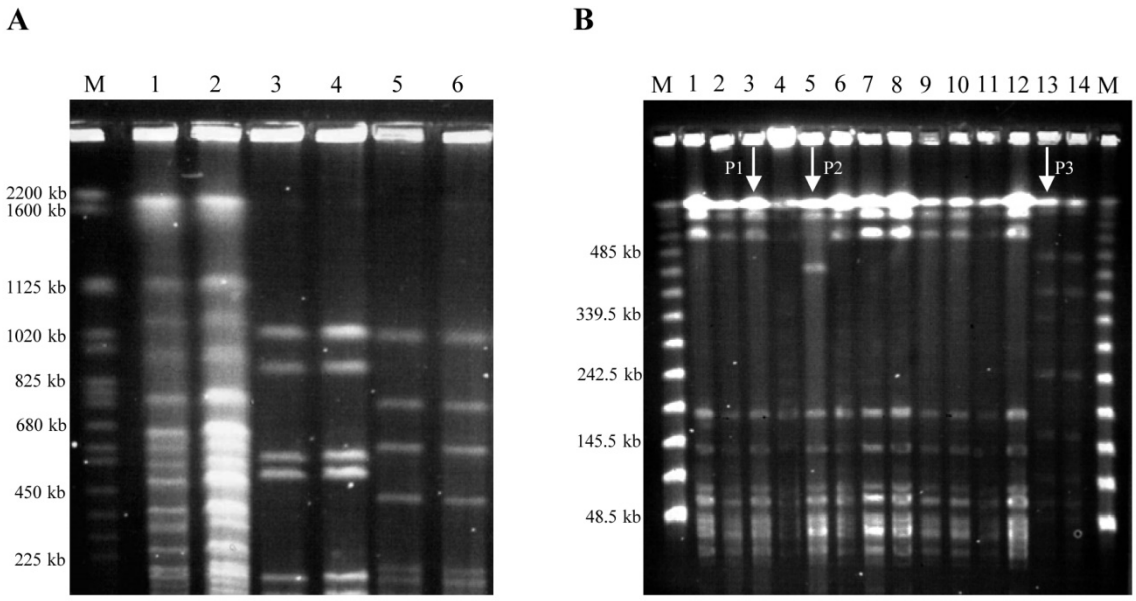

Figure 7. Isolation of *Acidiphilium* sp. PM from a culture of *Acidiphilium* sp. 3.2 Sup 5. A) The restriction pattern of *Acidiphilium* sp. 3.2 Sup 5 (lanes 1-2) is compared with that of a single colony from the culture (lanes 3-4) and that of *Acidiphilium cryptum* JF-5 (lanes 5-6). (B) SpeI-digested DNA from 14 colonies isolated from a culture of *Acidiphilium* sp. 3.2 Sup 5. Arrows indicate the three types of patterns (P) observed. M represents the molecular weight markers: *S. cerevisiae* chromosomal DNA in (A) and λ-phage DNA concatemers in (B).

At that time, *Acidiphilium*'s ability to transfer electrons to electrodes was suspected to correlate with its ability to reduce iron in the presence of various oxygen concentrations (after all, both electron transfers rely on cytochromes). For this reason, the ability to reduce iron reduction under aerobic, anaerobic and microaerobic conditions in all three types of strains was examined. All strains presented similar iron reduction activities (Table 10). However, in voltammetry experiments, representatives of pattern 1 yielded higher current intensities than the rest (M. Malki, personal communication). Strain 3, a representative of pattern 1, was selected for further characterization and became the reference *Acidiphilium* strain from Río Tinto in our laboratory.

	Aerobiosis	Microaerobiosis	Anaerobiosis
Pattern 1 (strain 3)	++	++++	+ / -
Pattern 1 (strain 6)	++	++++	+ / -
Pattern 2 (strain 5)	++	++++	+ / -
Pattern 3 (strain 15)	++	++++	+ / -
Pattern 3 (strain 16)	++	++++	+ / -
Acidiphilium 3.2 Sup 5	++	++++	+ / -

Table 10. Iron reduction of the strains isolated from a culture of *Acidiphilium* 3.2 Sup 5. Iron reduction was tested using Fe-TSB medium as described in 3.3.1. Iron reduction was followed visually as the fading of the reddish colour of the media.

This strain was renamed *Acidiphilium* sp. strain PM after project PICOMICRO, and was deposited in the German Collection of Microorganisms and Cell Cultures under catalogue number DSM 24941. Due to its biotechnological interest as an electricigen, this strain was stored as a safe deposit.

4.1.2. Characterization and preservation of *Acidiphilium* sp. PM

Acidiphilium sp. PM was capable of sustaining growth in a mineral salt solution supplemented with yeast extract and one of the following electron donors (added as 0.1%): glucose, mannitol, maltose, sucrose, citric acid, sorbitol, glutamate, fructose and ethanol. Conversely, acetate, benzoate and pyruvate were not suitable energy sources. Interestingly, only *Acp. cryptum* has been reported to grow on maltose (Hiraishi and Imhoff, 2005).

In GYE medium, *Acidiphilium* sp. PM exhibited a rapid growth (generation time: 8-12 hours) reaching stationary phase within the first 48 hours. A cell density of 1-2 10^9 cells/ml (roughly 5 generations) was reached when 1 g/l of glucose was used as energy source. The growth in GYE is limited by the energy source, as confirmed by the increase in cell density upon doubling the amount of glucose in the medium (Figure 8).

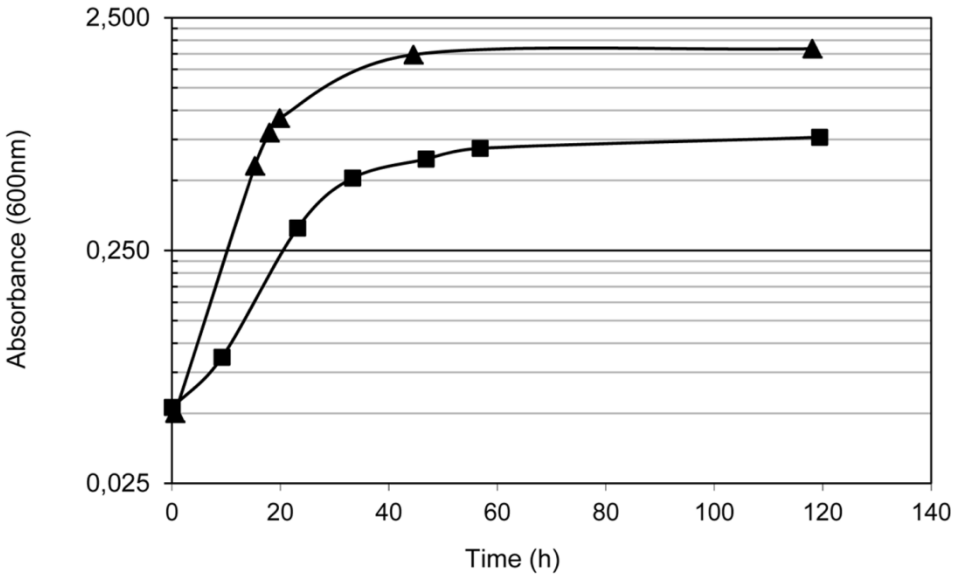

Figure 8. Growth of *Acidiphilium* sp. PM in GYE medium. Higher cell densities were achieved with 2 g/l of glucose (triangles) than with 1 g/l (squares).

A defined medium (DM) (described in 3.3.1) was tested in which yeast extract was replaced by Wolfe's Vitamin Solution and Modified Wolfe's Mineral solution (Wolin *et al.*, 1963). Cell yields and average doubling times were similar to those reported for GYE.

However, *Acidiphilium* sp. PM grew differently in GYE plates than in solid DM. GYE agar produced slightly convex, roundish, opaque, white colonies. These colonies were 1.8-3 mm in diameter, opaque and white after 1 week but turned pale brown after prolonged incubations. Fully grown colonies in DM agar were smaller (0.7-1.5 mm in diameter), less convex, translucent and did not change color when allowed to age (Figure 9). Nonetheless, similar viable numbers were obtained with both media. GYE agar plates were routinely used for colony counting throughout this work. Interestingly, defined solid medium could be used as a baseline for the formulation of a minimal medium, of use in the selection of exconjugants or transformants through auxotrophy-prototrophy.

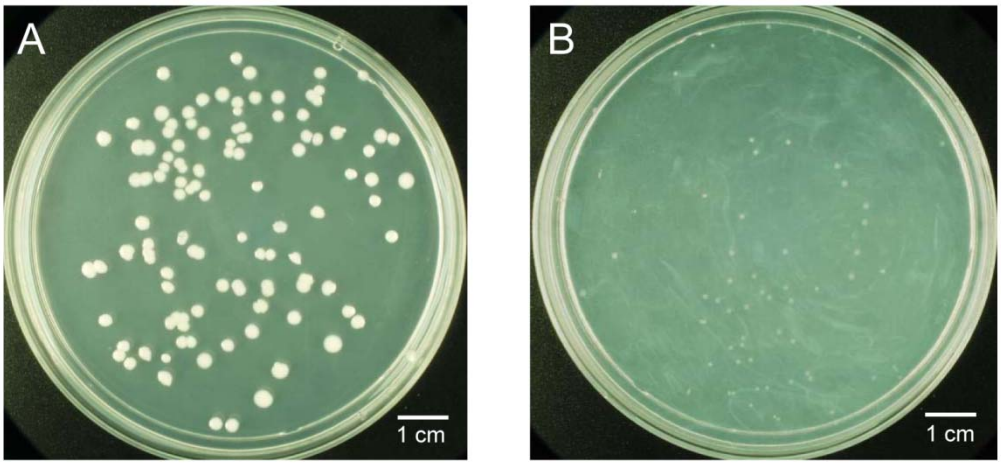

Figure 9. Growth of *Acidiphilium* sp. PM in solid GYE or DM media. A 25 µl aliquot of an *Acidiphilium* sp. PM culture in exponential growth was plated in GYE (A) and DM (B) agar. After one week, GYE agar produced larger, more opaque, more convex colonies than did defined medium agar. Scale bars represent 1 cm.

Acidiphilium sp. PM was capable of using both O_2 and Fe^{3+} as electron acceptors. Paradoxically, the absence of O_2 in the medium prevented the respiration of Fe^{3+}. Aerobic conditions also hindered Fe^{3+} respiration, resulting in partial Fe^{3+} reduction. Microaerobic conditions, however, allowed the complete reduction of 25 mM Fe^{3+} in four days (Figure 10).

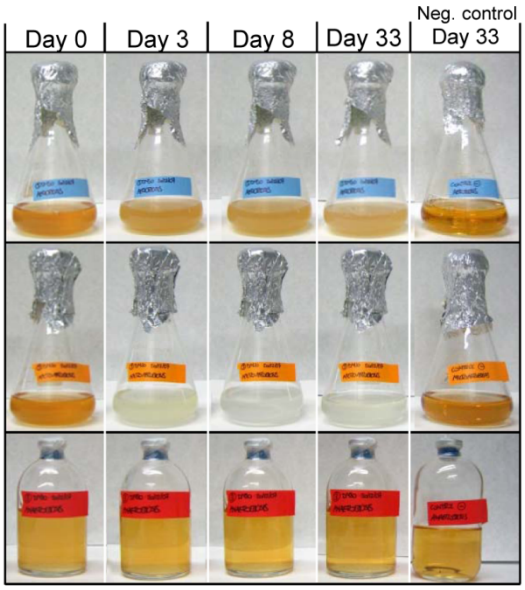

Figure 10. Fe^{3+} respiration in *Acidiphilium* sp. PM. The sequence shows a 33-day evolution of *Acidiphilium* growth under aerobic (top), microaerobic (middle) and anaerobioc (bottom) conditions. Negative control corresponds to uninoculated media.

A phylogenetic analysis based on the *16S rRNA* gene showed that *Acidiphilium* sp. PM falls in a highly homogenous (> 99.5% similarity) cluster which comprises *Acp. cryptum*, Acp. multivorum and Acp. organovorum (Figure 11).

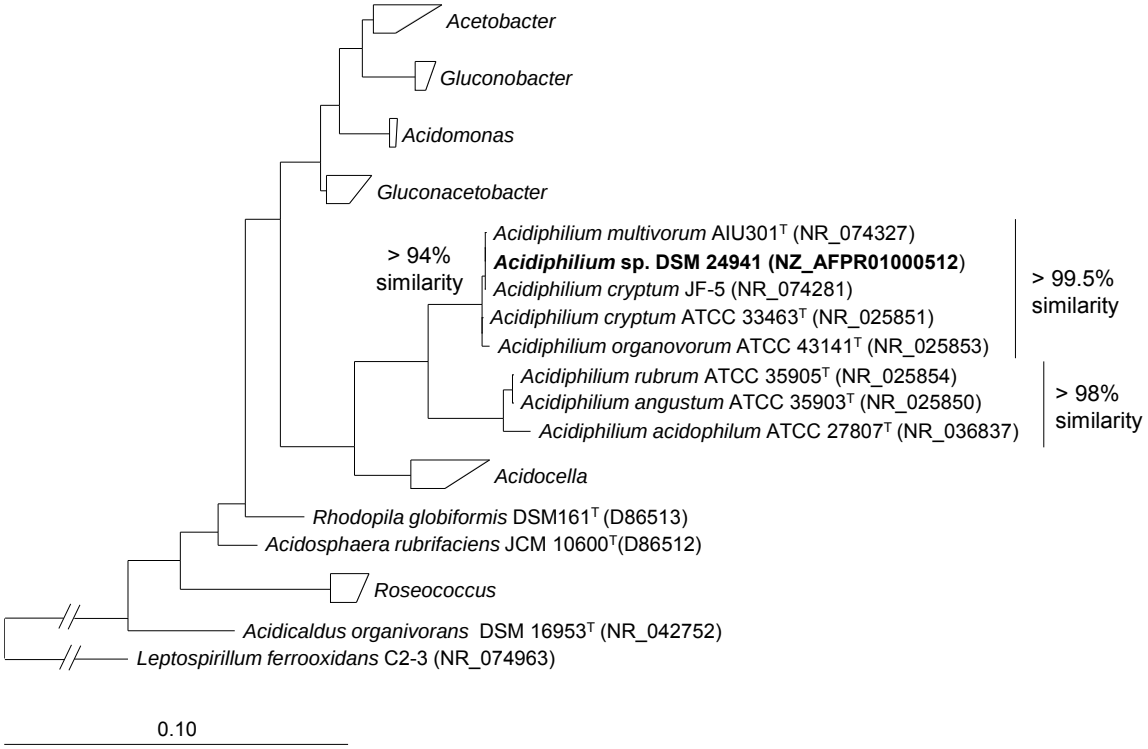

Figure 11. *16S rRNA*-based phylogeny of *Acidiphilium* sp. PM. This tree is based on the complete sequences of the *16S rRNA* genes and includes other genus of the *Acetobacteraceae*. Numbers in brackets indicate NCBI's Ref. Seq. accession numbers. *Acidiphilium* sp. PM is shown in bold type. *L. ferrooxidans* was used as outgroup. The scale bar represents a 10% nucleotide substitution rate.

4.1.3. Characterization of the heavy metal resistance of *Acidiphilium* sp. PM

One interesting aspect of microbes inhabiting acid mine drainage and acid rock drainage is their ability to withstand unusually high metal concentrations. Early studies in Río Tinto reported the presence of large metal concentrations, primarily Fe, which reached 20 g/l near the spring of the river (Gonzalez-Toril *et al.*, 2003). However, metal concentrations throughout the river vary widely (Garcia-Moyano *et al.*, 2012).

The heavy metal content in 3.2, the pond where *Acidiphilium* sp. PM originates from, was measured 10 times over a 46-month period using ICP-MS. The average values for some of the most studied heavy metals are listed in Table 11. Fe stands out as the most abundant element. Aside from Fe, Al and Zn are the only two metals to reach millimolar concentrations. Co, Ni, As, Cd and Pb remain in the low micromollar range.

	Al	Mn	Fe	Co	Ni	Cu	Zn	As	Cd	Pb
Average (μM)	7487.3	940.4	32141.2	38.8	5.3	256.9	1247.9	23.0	3.3	2.2
SD (μM)	3691.7	560.2	18227.6	21.5	3.2	131.0	661.5	16.9	1.7	1.3

Table 11. Average metal concentrations in 3.2.

Acidiphilium sp. PM ability to grow in the presence of some of these heavy metals was tested. After 30 day-incubations, *Acidiphilium* sp. PM was capable of growing in 750 mM Al, 2 mM Co, 1000 mM Ni, 10 mM Cu, 200 mM Zn and 5 mM Cd (Figure 12). In addition, after incubations of more than a month, growth was detected in flasks with 5 mM Co, 20 mM Cu, 250 mM Zn, and (only in some replicates) with 1200 mM Ni. Extended incubations in high metal concentrations led to the aggregation of cells, forming visible clumps in the culture. Growth in the presence of Co, Ni, Cu, Zn and Cd was preceded by long lag phases, which increased with the metal concentration (Figure 12). Extended lag phases upon addition of heavy metals have been reported for various other acidophiles (Tuovinen *et al.*, 1971; Xu *et al.*, 2013b), including some *Acidiphilium* strains (Mahapatra and Banerjee, 1996). The absence of lag phases when *Acidiphilium* sp. PM is grown with Al suggests that this resistance is constitutive in this strain. Similar results (in terms of inhibitory metal concentrations and lag phases) were obtained when GYE or DM were used to test metal resistance.

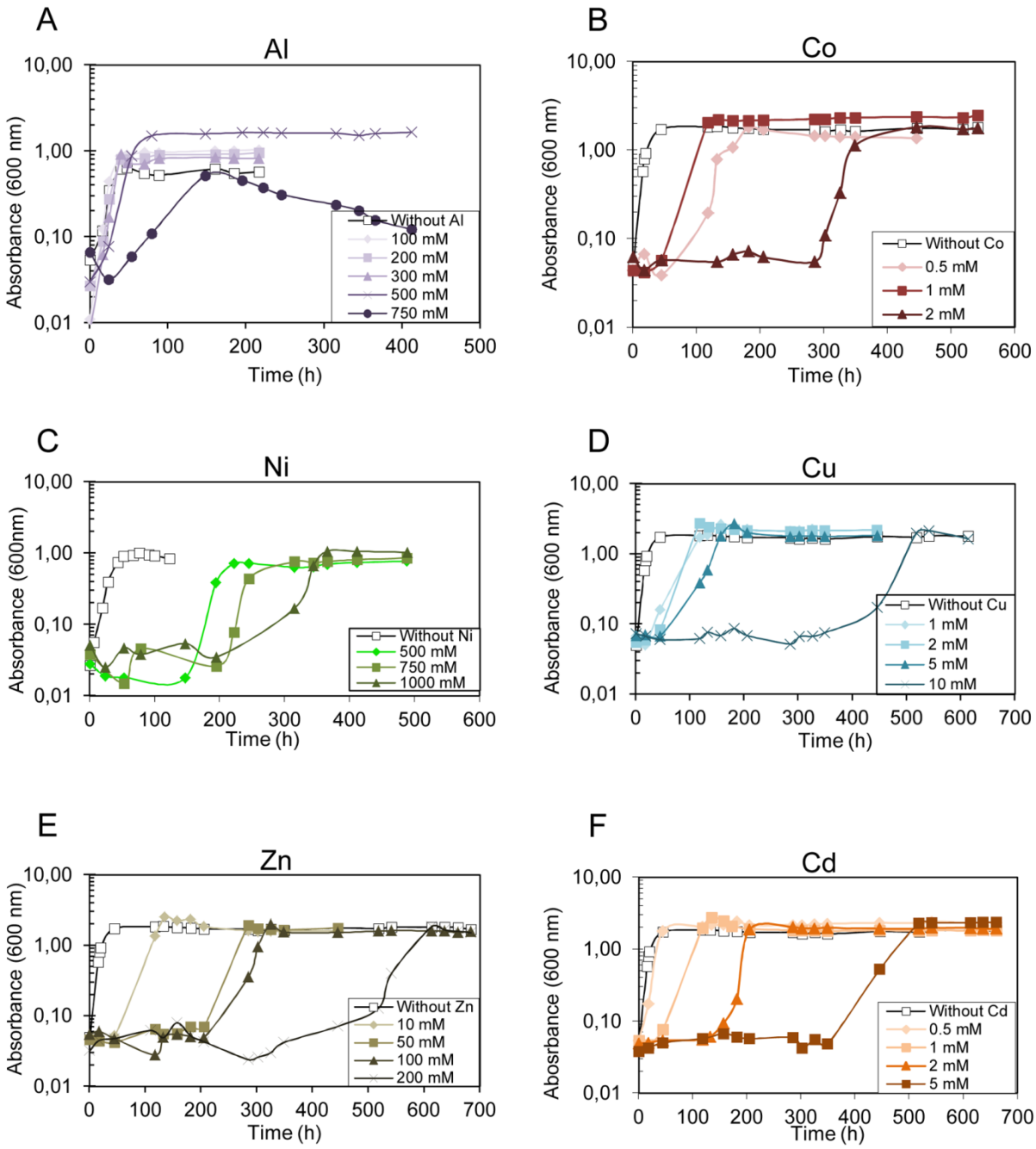

Figure 12. Growth of *Acidiphilium* sp. PM with heavy metals. Graphs depict the growth in increasing concentrations of Aluminum (A), Cobalt (B), Nickel (C), Copper (D), Zinc (E) and Cadmium (F).

To our knowledge, this is the first report for Co resistance in *Acidiphilium*. Al, Ni and Zn resistances in this strain are the highest reported in this genus. Indeed, the outstanding tolerance to Ni of *Acidiphilium* sp. PM is only matched by *A. ferrooxidans* (see Table 1). Paradoxically, Ni concentrations in Río Tinto remain below 1 mM, not only in 3.2 (Table 11) but throughout the river (data not shown). For this reason, we decided to further study the mechanisms behind Ni resistance.

4.1.4. Characterization of the Ni resistance in *Acidiphilium* sp. PM

Quite remarkably, the extreme Ni tolerance of *Acidiphilium* sp. PM did not require preadaptation to progressively larger Ni concentrations; instead, it consistently emerged in unexposed populations. Growth in high concentrations of Ni was preceded by long lag phases (often in excess of ten days), but these were greatly reduced when cells were pre-cultured in Ni-containing media (Figure 13). Quite remarkably, during exponential growth, doubling times in cultures grown with and without Ni remained approximately the same.

Prior to entering exponential growth, tiny aggregates were visible in cultures supplemented with Ni. In addition, growth in extreme Ni concentrations often unfolded in the form of macroscopic cellular aggregates visible to the naked eye. Cell aggregation induced by metals have been reported in other acidophiles, including *Acidiphilium* (Chakravarty and Banerjee, 2008).

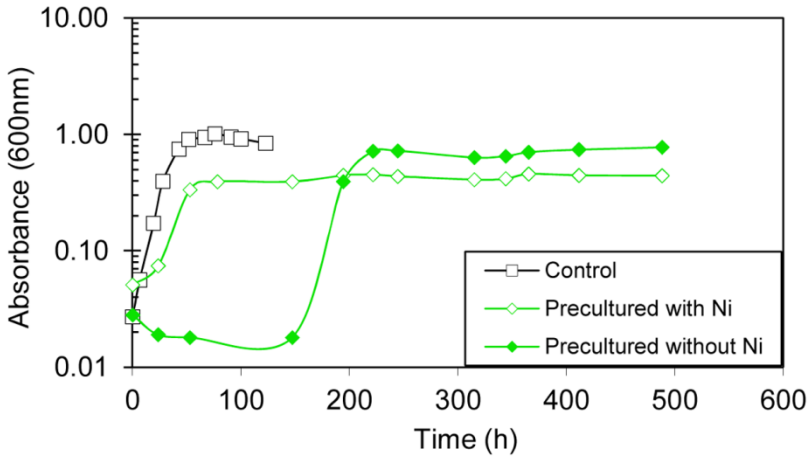

Figure 13. *Acidiphilium* sp. PM growth in Ni when precultured in media with or without Ni. Green lines show the growth of *Acidiphilium* sp. PM in 500 mM Ni when it is pregrown with (empty diamonds) or without 500 mM Ni (green diamonds). A Ni-free culture is shown as a control of normal growth (empty squares).

To test whether the entire population was equally resistant to Ni, the viability of cells exposed to 100 mM Ni was monitored over time by removing aliquots at intervals and plating serial dilutions in (Ni-free) GYE plates. As shown in Figure 14, cell viability dropped sharply upon exposure to Ni. After five days in 100 mM Ni, only 1 in 2 x 10^6 cells were viable. Eventually, this fraction of Ni-resisters (Ni^r) resumed growth yielding a full-grown culture of Ni-resistant *Acidiphilium* sp. PM.

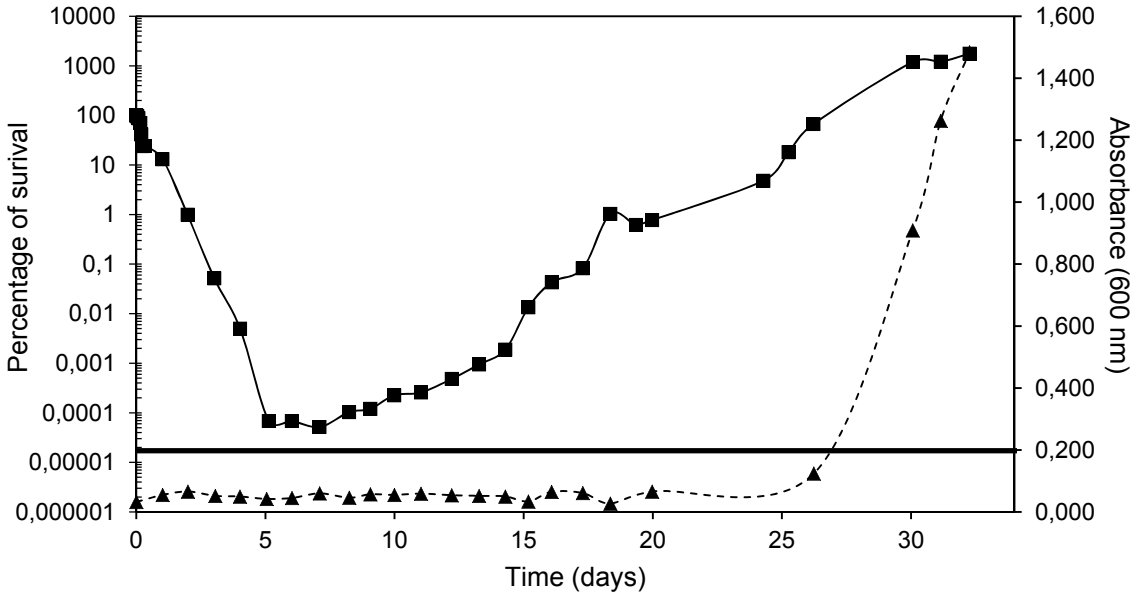

Figure 14. Viability of *Acidiphilium* sp. PM upon exposure to 100 mM Ni. A culture of *Acidiphilium* sp. PM was exposed to 100 mM Ni and the cell viability (squares) and optical density of the culture (triangles) were monitored over time. A percentage of survival higher than 100% was reached when the culture grew fully and the number of cells per ml of culture exceeded that of the inoculum. The black horizontal line represents the limit of detection for cell survival (0.00002% or 7 cells).

Similar results were obtained when serial dilutions of a culture were exposed to different concentrations of Ni in GYE plates. Colony counting revealed that most cells are indeed sensitive to low Ni concentrations and that only a tiny fraction of the population (1 in 10000 cells) resisted 20 mM Ni. Unexpectedly, about the same proportion of cells survived Ni concentrations up to 100 mM (the highest concentration tested) (Figure 15). Although this fraction of Ni resisters was constant regardless of the concentration of Ni, their lag phases were much dependent on the Ni concentration.

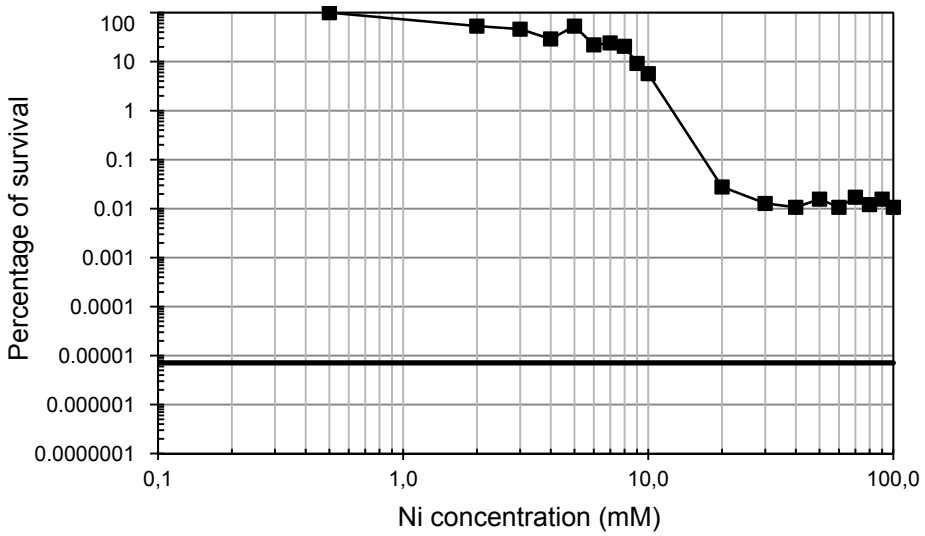

Figure 15. Survival of *Acidiphilium* sp. PM as a function of Ni concentration. The graph represents the survival rate of *Acidiphilium* sp. PM when exposed to increasing Ni concentrations. The black horizontal line represents the limit of detection for cell survival (0.000007% or 33 cells). 0.01% is equivalent to 1 in 10000 cells.

The number of Ni^r cells in plates was *ca.* 100-fold higher than in experiments carried out in liquid media. It was hypothesized that interactions between cells in the two-dimensions of solid media could be causing this discrepancy. To test this hypothesis, a 100-fold dilution of a culture was plated randomly and homogeneously using glass beads. Next, a 25 µl-drop of culture was deposited in the centre of the plate and allowed to dry. Pictures taken at intervals showed that 1 in 10^6 cells became fast-growing Ni^r and grew visible colonies. Notably, these colonies seemed to trigger the growth of other Ni^r cells in their surroundings (Figure 16). Whether the growth of the latter is triggered by quorum-sensing signals or they benefit from the organic matter released by the fast-growers has not been ascertained. Overall, fast-growing colonies accounted for 4% of the total Ni-resistant population and are in the same order of magnitude as the Ni-resistant population in liquid cultures.

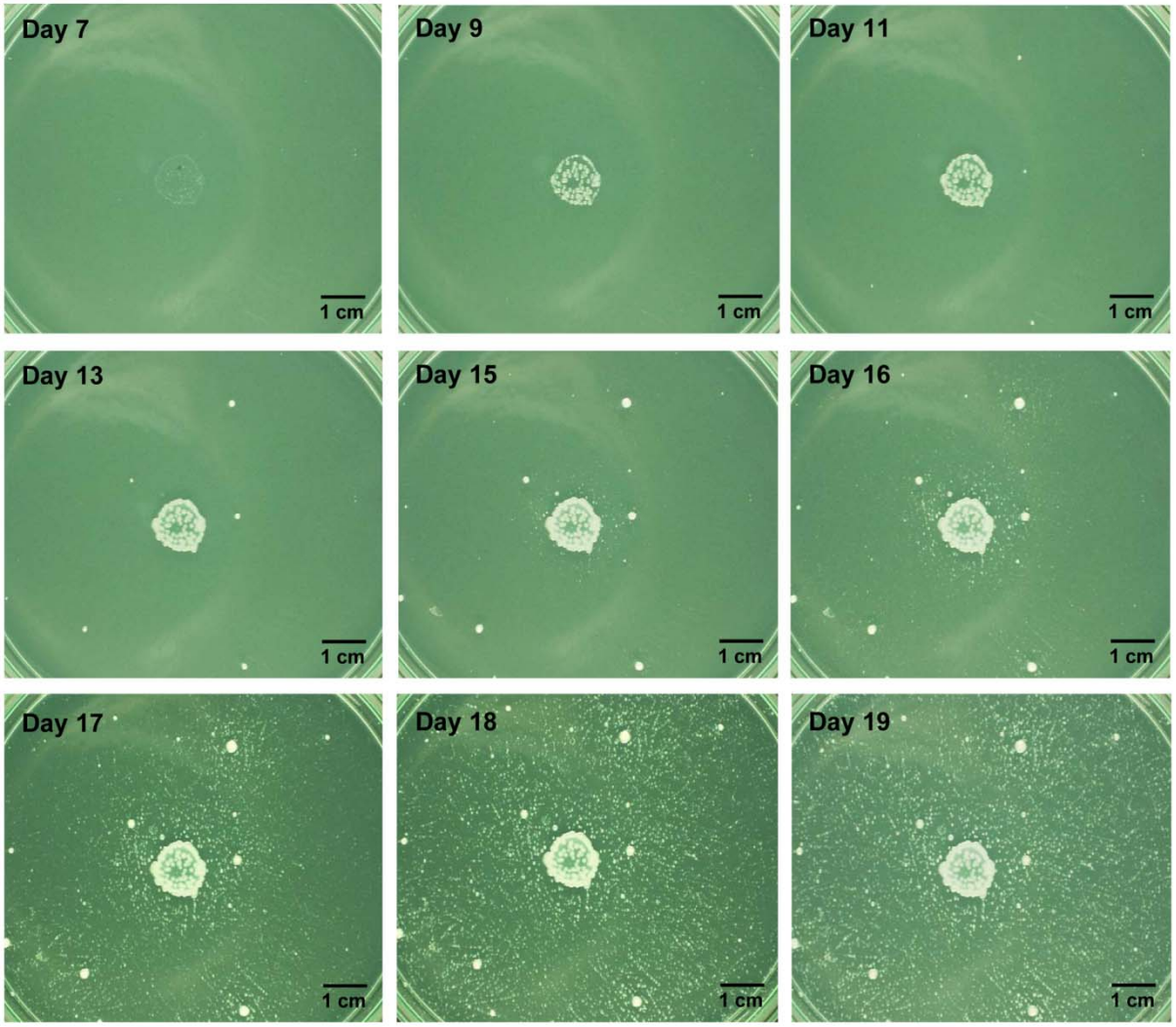

Figure 16. Growth dynamics of *Acidiphilium* sp. PM in Ni-containing solid media. A 100-fold dilution of a culture in mid-log phase was plated randomly and homogeneously using glass beads. A 25 µl-drop of culture was then deposited in the middle of the plate and allowed to dry. Images were collected every 24-48 h. A MATLAB script was used to rotate and resize the images. Basic image processing was performed with Adobe Photoshop CS3. Scale bars represent 1 cm.

This extreme resistance to Ni was consistently observed on multiple cultures started from single colonies, which suggests that *Acidiphilium* sp. PM has the ability to evolve an extreme-Ni^r phenotype. Even though fully resistant mutants could be present in the culture prior to the addition of Ni, their short doubling times (Figure 13) suggest that mutations entail little or no loss of fitness. This is particularly difficult to reconcile with the prolonged lag phases of up to 10 days that preceed the growth of Ni-resistant populations. It is therefore proposed that some form of adaptive evolution is taking place upon exposure to Ni. A similar progressive adaptation may be responsible for the extreme metal resistance of the leaching consortia in heaps and tank reactors.

4.2. SEQUENCING, ANNOTATION AND RECONSTRUCTION OF THE BASIC METABOLISM OF *Acidiphilium* sp. PM

As part of a broader goal to develop genetic tools for the study of *Acidiphilium* sp. PM, the genome of this isolate was sequenced and annotated. Since 2007 several other *Acidiphilium* genomes have been released. The complete genomes of *Acp. cryptum* JF-5 (Acc. No. CP000689 - CP000697, released in May 2007) and *Acp. multivorum* AIU301 (Acc. No. AP012035 - AP012043; released in March 2011) as well as draft genomes of *Acidiphilium* sp. JA12-A1 (Acc. No. JFHO00000000; May 2014) and *Acp. angustum* ATCC 35903 (Acc.. No. JNJH00000000; June 2014) are publicly available in NCBI's Nucleotide database (http://www.ncbi.nlm.nih.gov/nuccore). Quite unexpectedly, this vast information awaits analysis. Indeed, no literature describing their genomic features, such as genome-based metabolic reconstruction, have been released as of December 2014.

DNA from *Acidiphilium* sp. PM was extracted and submitted to Life Sequencing Ltd. (Valencia, Spain), where a library of DNA fragments was prepared and then sequenced using 454 sequencing. The run yielded 252 837 reads, with an average size of 235 bp. Reads were assembled into 814 contigs, 627 of which were longer than 500 bp (lengths ranging from 100 to 114 367 bp; N50 = 12446). Annotation of these contigs and basic metabolic reconstruction were performed as described in section 3.5.1. *Acidiphilium* sp. PM whole genome shotgun project was deposited in NCBI's GenBank database under project accession number AFPR00000000.

4.2.1. General features of the genome of *Acidiphilium* sp. PM

The draft genome of *Acidiphilium* sp. PM contains 3.98 Mb (15-fold coverage) with an average GC content of 68%. In comparison, the genome sizes of *Acp. cryptum* JF-5 (Acc. No. CP000689 - CP000697) and *Acp. multivorum* AIU301 (Acc. No. AP012035 - AP012043) are 3.96 Mb and 4.21 Mb, respectively, and their GC content is 67% (Table 12). These high GC contents are consistent with the 63.2–68.1% GC determined experimentally by Wakao *et al.* for several *Acidiphilium* species (Wakao *et al.*, 1994). Overall, the chromosomes of the three species are largely syntenous as well as highly similar in the aligned regions (average 99% identity at the amino acid level in the 2866 pair of orthologs identified between *Acidiphilium* sp. PM and *Acp. cryptum* JF-5).

Sequence comparison, primarily with *Acidiphilium cryptum* JF-5, allowed the ascription of most contigs to either the chromosome or one of nine predicted plasmids. The

exact size of the plasmids could not be determined on the basis of their sequence. Instead, they were determined experimentally by running undigested DNA from *Acidiphilium* sp. PM both in conventional electrophoresis and in PFGE. The sizes of the plasmids were estimated to be approximately: 650, 270, 190, 90, 70, 50, 20-30, 4.8 and 3 kb (Figure 17). Eight of these plasmids presented similarities with 7 of the 8 plasmids found in *Acp. cryptum* JF-5. Interestingly, an extra plasmid (pAPM09) was found in *Acidiphilium* sp. PM that presented a 91% identity with plasmid pTF4.1 of *A. ferrooxidans*.

Table 12. Genomic comparison of three *Acidiphilium* genomes.

	Acidiphilium sp. PM	*Acp. cryptum* JF-5	*Acp. multivorum* AIU301
Genomic size	*ca.* 3.98 Mb	3.96 Mb	4.21 Mb
GC content	68%	67%	67%
Predicted ORFs	3981	3559	3949
rRNA operons	2	2	2
tRNAs[1]	48	48	48
	Ala Arg Asn Asp Cys	Ala Arg Asn Asp Cys	Ala Arg Asn Asp Cys
	4 4 1 1 1	4 4 1 1 1	4 4 1 1 1
	Gln Glu Gly His Ile	Gln Glu Gly His Ile	Gln Glu Gly His Ile
	2 2 **3** 1 2	2 2 **3** 1 2	2 2 **4** 1 2
	Leu Lys Met Phe Pro	Leu Lys Met Phe Pro	Leu Lys Met Phe Pro
	4 **3** 4 1 3	4 **3** 4 1 3	4 **2** 4 1 3
	Ser Thr Trp Tyr Val	Ser Thr Trp Tyr Val	Ser Thr Trp Tyr Val
	4 3 1 1 3	4 3 1 1 3	4 3 1 1 3
Plasmids[2]	9	8	8
	ca. 650	pACRY01 (203589 bp)	pACMV1 (271573 bp)
	ca. 270	pACRY02 (187422 bp)	pACMV2 (65564 bp)
	ca. 190	pACRY03 (88953 bp)	pACMV3 (54248 bp)
	ca. 90	pACRY04 (37415 bp)	pACMV4 (40588 bp)
	ca. 70	pACRY05 (37155 bp)	pACMV5 (14328 bp)
	ca. 50	pACRY06 (8781 bp)	pACMV6 (12125 bp)
	ca. 25	pACRY07 (5629 bp)	pACMV7 (5178 bp)
	ca. 4.8	pACRY08 (4909 bp)	pACMV8 (1728 bp)
	ca. 3		

[1] Differences in the types of tRNAs are shown in underlined bold letters. [2] Plasmid sizes in *Acidiphilium* sp. PM were estimated from gel electrophoresis.

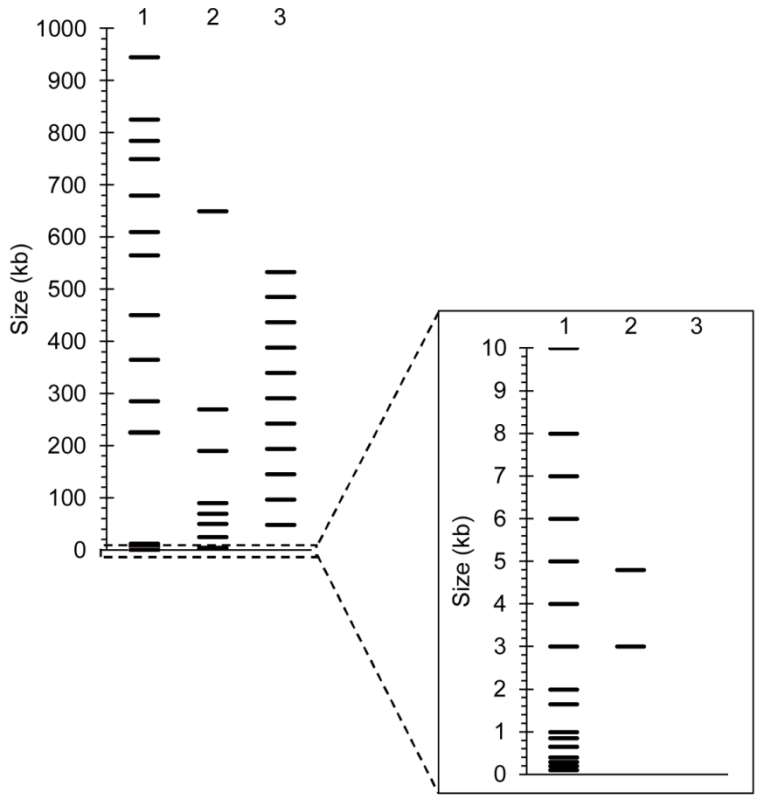

Figure 17. *Acidiphilium* sp. PM plasmid sizes as determined by agarose gel electrophoresis. Undigested DNA from *Acidiphilium* sp. PM was run in conventional and PFGE electrophoresis. The composite above summarizes data from multiple gels. The inset shows DNA plasmids in the 0 to 10 kb range. Lane 1: *Saccharomyces cerevisiae* chromosomal DNA and 1 Kb Plus DNA ladder; Lane 2: Undigested DNA from *Acidiphilium* sp. PM; Lane 3: Lambda ladder.

The origin of replication (*oriC*) in *Acidiphilium* sp. PM was identified in the vicinity of *hemA*. This 280 bp-long region contains three DnaA boxes and presents single mismatches with the *oriC* regions of *Acp. cryptum* JF-5 and *Acp. multivorum* AIU 301 (Figure 18).

gcgacctgcctagcttcaattcgtcttataggaaaggacgggggggagtagtgttagctgt
gaactctggggaaccccgcaatccggtttttctgcacagagTTTTCCACAgcaaaactc
ggcctgcaatctgctgattctgcatcaaaccccccggtTTTTCCACAtatgcgggggatgc
ccgggaaattcatccaccgctcgccgcggtgtgaaattcatccacgctttccaccgcggg
cggtttcgcggcccgagTTATCCACGctatgagaccatgc

Figure 18. Origin of replication of *Acidiphilium* sp. PM. DnaA boxes are shown in capital red letters. Blue and green letters represent mismatches with the *oriC* of *Acp. cryptum* JF-5 and *Acp. multivorum* AIU301, respectively.

A total of 48 tRNA genes were identified, six of which form part of two nearly identical ribosomal RNA operons with the following structure 16S-tRNA(Ile)-tRNA(Ala)-23S-5S-tRNA(Met) (Figure 19). These operons are 99.76% similar to the ribosomal operons in *Acp. cryptum* JF-5 (RefSeq AccNo. NC_009484) and 99.85% identical to those of *Acp. multivorum* AIU301 (RefSeq AccNo. NC_015186). This extraordinary similarity makes the

three strains indistinguishable on the basis of their rRNA, which was readily observable in the *16S rRNA*-based phylogenetic tree of Figure 11.

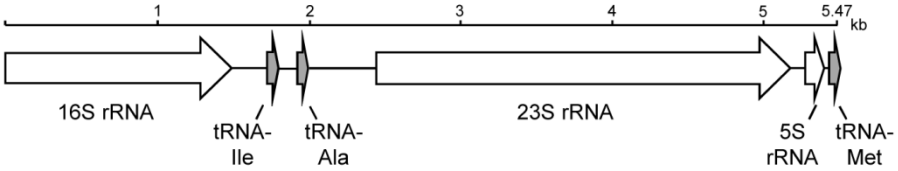

Figure 19. Ribosomal operon structure in *Acidiphilium* sp. PM.

4.2.2. Elements of genomic plasticity

Genomic plasticity is key to bacterial adaptation and survival. Mobile genetic elements (transposons, phages and plasmids) and horizontal gene transfer events confer rapid genomic flexibility and, therefore, are crucial to bacterial evolution. The influence of these phenomena in acidophiles has been reviewed recently (López de Saro *et al.*, 2013).

A remarkable fraction (*ca.* 2.4%) of the genome of *Acidiphilium* sp. PM is made up of repeated regions. Of these, insertion sequences (IS) and other transposable elements are the most abundant. 87 ISs and transposable elements were identified in the genome of *Acidiphilium* sp. PM, IS110 being the most abundant family (Figure 20). Interestingly, after 49 months of periodic transfer to fresh nutrient-rich media, the number of copies of IS1634 in the population increased from 1 to 3 as determined by array hybridization and verified with qPCR (H. Maldonado and F. J. López de Saro, personal communication). Similar IS families are found in two other fully-sequenced *Acidiphilium* strains, although the total numbers of transposable elements varies between them (Figure 20). Other acidophiles show even greater variation in their content of mobile elements. For instance, while the genome of *Sulfolobus acidocaldarius* apparently contains no IS elements or MITEs, mobile elements in *S. solfataricus* add up to more than 10% of its genome (Brugger *et al.*, 2004). Greater mobile element contents could be indicative of recent adaptations to fluctuations in the environment (Moran and Plague, 2004).

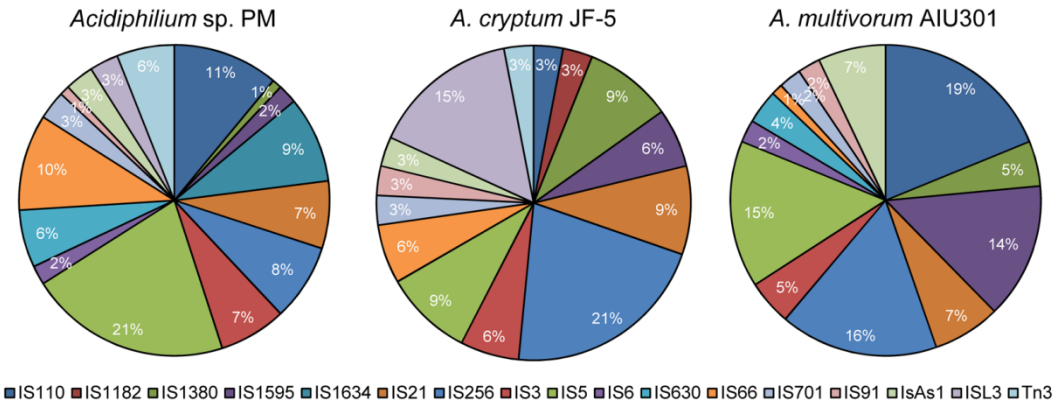

Figure 20. Transposable elements in *Acidiphilium*. The total numbers of IS varies between strains (*Acidiphilium* sp. PM: 87 ISs; *Acp. cryptum* JF-5: 33; *Acp. multivorum* AIU301: 85), but IS families are mostly the same across the three strains. Data from the transposable elements of *Acp. cryptum* JF-5 and *Acp. multivorum* AIU301 were retrieved from López de Saro *et al* (2013).

CRISPR/Cas systems confer resistance to foreign genetic elements, typically viruses (Horvath and Barrangou, 2010). One such CRISPR/Cas system was identified in *Acidiphilium* sp. PM. This CRISPR region consists of 105, 29-bp repetitions interspaced with 93, 30-bp variable spacers. The direct repeats in *Acidiphilium* sp. PM CRISPR are identical to those in *Acp. cryptum* JF5 plasmid pACRY02, and very similar (only one mismatch) to that found in *Acp. multivorum* AIU301 pACMV3. The spacers in this CRISPR/Cas system point to the existence of several bacteriophages of *Acidiphilium* in Río Tinto. Indeed, a candidate phage which infects *Acidiphilium* cells from Río Tinto is the subject of ongoing research in our group (C. Moraru, personal communication). Putative prophages have been identified in the genome of *Acp. cryptum* JF-5 (Andersson and Banfield, 2008), yet no experimental evidence of a lysogenic phage has been reported.

Lateral gene transfer is another major source of genomic plasticity. Some authors have proposed that microorganisms who share the same niche tend to exchange genes at higher frequencies (DeLong, 2000; Papke *et al.*, 2004). In acidophiles, horizontal gene transfer (HGT) has been reported for *Leptospirillum* group II (Lo *et al.*, 2007; Simmons *et al.*, 2008), *A. ferrooxidans* (Valdés *et al.*, 2010), the archeon *Ferroplasma* (Eppley *et al.*, 2007) and between *Thermoplasma acidophilum* and *S. solfataricus* (Ruepp *et al.*, 2000). More recently, Schonknecht and *et al.* suggested that the acidophilic red alga *Galdieria sulphuraria* could have acquired up to 5% of its genome from various bacteria and archaea through horizontal gene transfer, which would imply extraordinary genetic exchange across different domains (Schonknecht *et al.*, 2013). The remarkable similarity between plasmids pTF4.1 of *A. ferrooxidans* and pAPM09 from *Acidiphilium* sp. PM could be indicative of

genetic exchange between the two species. For this reason we aimed at exploring genes that might have been acquired through lateral transfer.

Anomalous codon usage and GC content biases are often considered indicative of recent HGT events. The analysis of these features in *Acidiphilium* sp. PM uncovered 129 ORFs which fulfilled at least two of the three criteria used in the analysis, that is, ≥ 2 standard deviations from the predicted average values in codon usage bias (*i.e.* CAI < 0.483; RMSD > 0.31) and/or GC content bias (*i.e.* 0.567 > %GC > 0.787). Interestingly, many of these "anomalous" ORFs were arranged in clusters, the largest of which comprised 15 biased ORFs. This 15-ORF cluster is located in contig 00592 (Acc. No. AFPR01000464) and includes genes involved in conjugation and type IV secretory pathway (Figure 21). Contig 00592 (GC content: 52.6%) was also the largest contig that could not be ascribed to either the chromosome or one of the plasmids during the annotation phase. We hypothesized that, should this gene cluster had been acquired "recently" (later than the branching of *Acidiphilium*), it was unlikely to be found in *Acidiphilium* isolates outside Río Tinto. The failure to predict orthologs of these ORFs in *Acp. cryptum* JF5 supported this hypothesis.

In addition, to verify that these sequences were indeed exclusive of *Acidiphilium* sp. PM, a whole-genome shotgun microarray of *Acidiphilium* sp. PM was competitively hybridized with fragmented, fluorescently-labelled genomic DNA from *Acidiphilium* sp. PM and from two geographically distant *Acidiphilium* strains (Figure 22). The "foreign" strains selected were: *Acp. cryptum* JF-5 (a strain isolated from an acidic coal mine in Germany) and *Acp. multivorum* AIU301 (isolated from a sulphur-pyrite mine in Japan). It was expected that DNA regions recently acquired by *Acidiphilium* sp. PM through HGT would be absent from foreign strains and therefore would present poor hybridization in selected spots of the microarray. Hybridized microarrays were scanned and analysed for spots with poor signals from foreign *Acidiphilium* DNA. Thresholds were set based on the M/A scatter plot (Figure 22). Selected clones were then end-sequenced and aligned against the draft genome of *Acidiphilium* sp. PM. As shown in Figure 21, several of the sequences presenting poor hybridization with foreign *Acidiphilium* DNA lie within contig 00592. This confirms that this genomic island is indeed exclusive of *Acidiphilium* sp. PM.

A

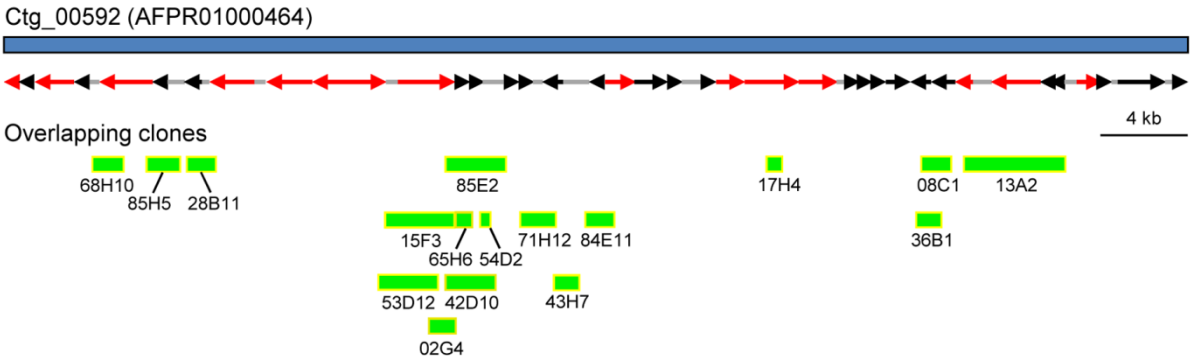

B

Locus tag	Gene	Orthologs in *A. cryptum* JF5	Orthologs in *At. ferrooxidans*	BLASTP first hit (e-value)
APM_2901	**Hypothetical protein**	**No**	**No**	**-**
APM_2902	Conjugal transfer protein	No	No	*Acidithiobacillus ferrivorans* (5e-90)
APM_2903	**Putative plasmid conjugal transfer protein**	**No**	**Yes**	***Acidithiobacillus ferrivorans* (3e-64)**
APM_2904	Conjugal transfer protein TrbJ	No	No	Acidithiobacillus thiooxidans (e-57)
APM_2905	**Conjugal transfer protein TrbE**	**No**	**Yes**	***Acidithiobacillus thiooxidans* (0.0)**
APM_2906	Hypothetical protein	No	No	-
APM_2907	**conjugal transfer protein TrbB**	**No**	**No**	***Acidithiobacillus thiooxidans* (2e-126)**
APM_2908	Hypothetical protein	No	No	-
APM_2909	**DNA topoisomerase III**	**No**	**Yes**	***Thiomonas arsenitoxydans* (0.0)**
APM_2910	**Hypothetical protein**	**No**	**No**	**-**
APM_2911	**Hypothetical protein**	**No**	**No**	***Acidithiobacillus thiooxidans* (4e-85)**
APM_2912	**DNA polymerase I, putative**	**No**	**No**	***Acidithiobacillus thiooxidans* (3e-179)**
APM_2913	Hypothetical protein	No	No	-
APM_2914	Hypothetical protein	No	No	-
APM_2915	Hypothetical protein	No	No	-
APM_2916	Hypothetical protein	No	No	-
APM_2917	Hypothetical protein	No	No	*Methylobacterium extorquens* (3e-78)
APM_2918	Hypothetical protein	No	No	-
APM_2919	**Type IV secretory pathway VirD2 pilin**	**No**	**Yes**	***Acidithiobacillus ferrivorans* (6e-150)**
APM_2920	Putative DNA primase (TraC)	No	Yes	*Leptospirillum ferrodiazotrophum* (1e-78)
APM_2921	Hypothetical protein	No	No	*Acidithiobacillus ferrivorans* (3e-41)
APM_2922	Hypothetical protein	No	No	-
APM_2923	**Hemolysin activation/secretion protein-like protein**	**No**	**No**	***Thioalkalivibrio sp.* ALE16 (1-20)**
APM_2924	**Penicillin-binding protein, 1A**	**No**	**No**	***Bacillus cereus* (6e-17)**
APM_2925	**ribonucleotide-diphosphate reductase subunit**	**No**	**Yes**	***Acidiphilium cryptum* JF-5 (0.0)**
APM_2926	Hypothetical protein	No	No	*Acidithiobacillus ferrivorans* (4e-33)
APM_2927	Hypothetical protein	No	No	-
APM_2928	Involved in type IV secretion complex(VirB1)	No	No	*Acidithiobacillus caldus* (5e-49)
APM_2929	TraB	No	No	*Acidithiobacillus thiooxidans* (5e-77)
APM_2930	Hypothetical protein	No	No	-
APM_2931	Hypothetical protein	No	No	-
APM_2932	**DNA methylase N-4/N-6 domain-containing protein**	**No**	**No**	***Ochrobactrum intermedium* (3e-78)**
APM_2933	**TRAG family protein**	**No**	**Yes**	***Acidithiobacillus thiooxidans* (0.0)**
APM_2934	Hypothetical protein	**No**	**No**	*Arabidopsis thaliana* (1e-6)
APM_2935	Phage transcriptional regulator, AlpA	No	No	*Dickeya* sp. (5e-07)
APM_2936	**Phage integrase family protein**	**No**	**No**	***Celeribacter baekdonensis* (2e-110)**
APM_2937	Hypothetical protein	No	No	*Celeribacter baekdonensis* (5e-9)
APM_2938	Hypothetical protein	No	No	*Nitrobacter winogradskyi* (2e-164)
APM_2939	Hypothetical protein	No	No	*A. cryptum* JF5 (8e-64)

Figure 21. Genes contained in contig 00592. Analysis of horizontal gene transfer. A) Genetic organization of contig 00592. APM_2901 is the first ORF on the left. Arrows depict genes and grey lines represent intergenic regions. Red arrows show genes with "anomalous" codon usage and/or GC content bias. Green boxes represent the clones of the microarray presenting faint hybridization signals with DNA from "foreign" strains (*Acp. cryptum* JF-5 or *Acp. multivorum* AIU 301) in comparative genomic hybridizations. B) Description of the ORFs present in contig 00592. ORFs with anomalous codon usage and/or GC content bias are shown in bold type. Orthologs were searched for using InParanoid. Protein BLAST searches were performed against NCBI's non redundant database. Only first hits with e-values lower than 10^{-6} are shown.

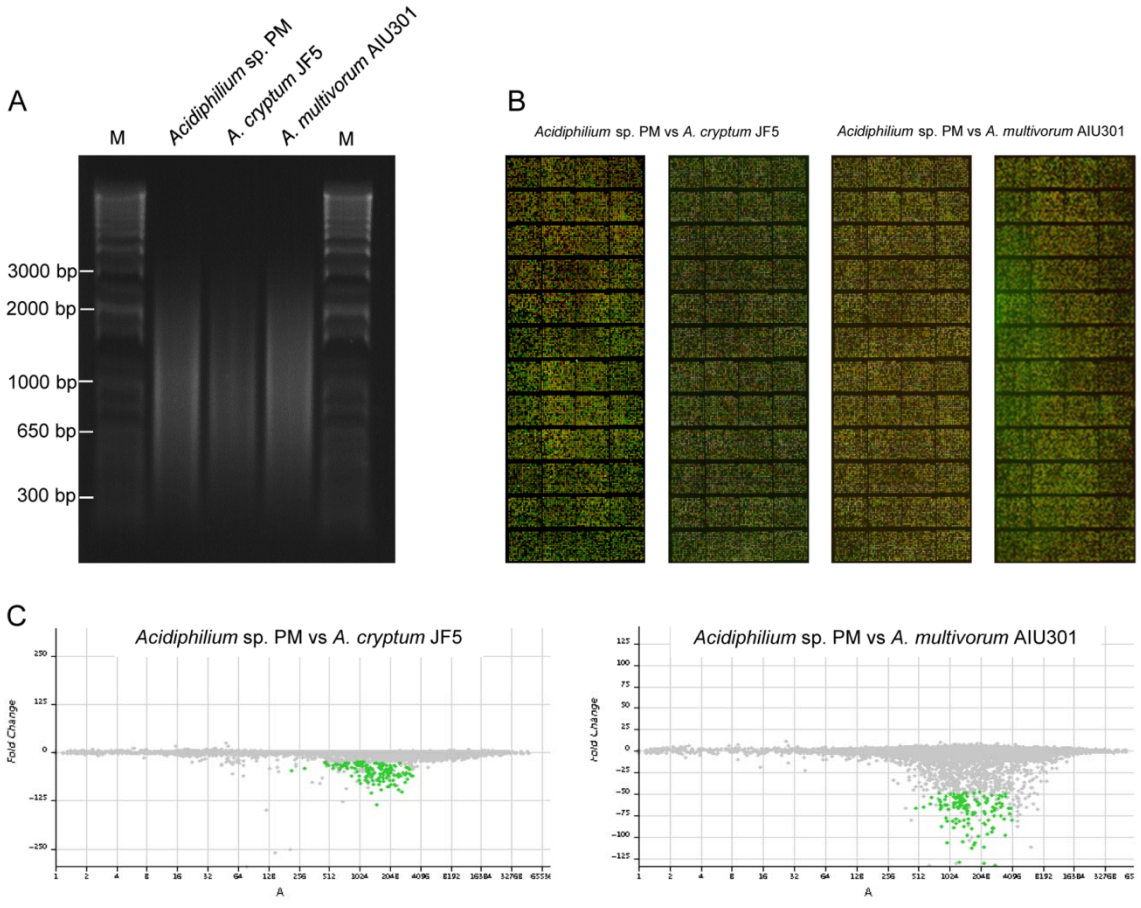

D

	Acidiphilium sp. PM vs *A. cryptum* JF5			*Acidiphilium* sp. PM vs *A. multivorum* AIU301		
Clone	F	Log_2 F ± SE	p	F	Log_2F ± SE	p
02G4	-56.07	-5.8 ± 0.1	0.014	-34.51	-5.1 ± 0.3	0.040
08C1	-70.14	-6.1 ± 0.2	0.000			
13A2				-44.68	-5.5 ± 0.2	0.018
15F3				-25.91	-4.7 ± 0.0	0.002
17H4	-63.33	-6.0 ± 0.1	0.005	-56.40	-5.8 ± 0.4	0.047
28B11	-108.56	-6.8 ± 0.3	0.031	-46.64	-5.5 ± 0.2	0.000
36B1	-88.20	-6.5 ± 0.2	0.024			
42D10	-99.71	-6.6 ± 0.3	0.000	-91.79	-6.5 ± 0.2	0.000
43H7				-44.20	-5.5 ± 0.2	0.000
53D12	-47.81	-5.6 ± 0.1	0.006	-32.68	-5.0 ± 0.1	0.000
54D2				-27.60	-4.8 ± 0.3	0.039
65H6	-69.29	-6.1 ± 0.2	0.016			
68H10	-68.61	-6.1 ± 0.2	0.000	-49.88	-5.6 ± 0.1	0.000
71H12	-94.39	-6.6 ± 0.2	0.000	-87.47	-6.5 ± 0.2	0.000
84E11				-36.92	-5.2 ± 0.0	0.005
85E2				-46.89	-5.6 ± 0.2	0.000
85H5	-82.69	-6.4 ± 0.2	0.000	-61.79	-5.9 ± 0.2	0.019

Figure 22. Comparative genomic hybridizations (CGH) of three *Acidiphilium* isolates. A) Genomic DNA from *Acidiphilium* sp. PM, *Acp. cryptum* JF-5 and *Acp. multivorum* AIU301 was extracted as described in 3.4.2, and then fragmented to 300-3000 bp by sonication. M represents the molecular weight marker (1 Kb Plus DNA Ladder). B) Fragmented DNA was fluorescently labelled as described in 3.4.5. Cy3-labelled genomic DNA from *Acidiphilium* sp. PM was combined with Cy5-labelled gDNA from *Acp. cryptum* JF-5 or *Acp. multivorum* AIU301 and hybridized against a genomic microarray of *Acidiphilium* sp. PM. Dye-swap duplicates were performed to avoid fluorescence biases. C) M/A scatter plots of the CGH of *Acidiphilium* sp. PM vs *Acp. cryptum* JF-5 (left) and *Acidiphilium* sp. PM vs *Acp. multivorum* AIU301 (right). Fold change (F) is the ratio of the fluorescence intensities (negative values indicate higher intensities from *Acidiphilium* sp. PM) and A is the average of the log_2 intensities from each DNA. Thresholds for the selection of the spots were set *ad hoc* based on the cloud of spots. For *Acidiphilium* sp. PM vs *Acp. cryptum* JF-5: $F < -47.8$, *Acp. cryptum* JF-5 signal < 500, $p < 0.05$, and for *Acidiphilium* sp. PM vs *Acp. multivorum* AIU301: $F < -24.8$, *Acp. multivorum* AIU301 signal < 500, $p < 0.05$. Spots fulfilling these criteria are highlighted in

green. These clones were end-sequenced and aligned against the draft genome of *Acidiphilium* sp. PM. D) Hybridization data from the clones aligning with contig 00592. Negative values indicate that the signal from *Acidiphilium* sp. PM was higher than the signal from the foreign *Acidiphilium* strain. SE is the standard error for the $\log_2$F and p is the significance value of the paired Student's t-test.

Neighboring acidophiles were suspected donors of this genomic island. A protein BLAST against NCBI's non-redundant protein database revealed that, in fact, many of the "anomalous" ORFs were remarkably similar to proteins found in *Acidithiobacillus* species (Figure 21). Minor horizontal gene transfer events between members of the *Rhodospirillales* and *Acidithiobacillus* had been reported recently (Acuña *et al.*, 2013).

Overall, this evidence suggests that virtually all DNA contained in contig 00592 was recently acquired, probably from *Acidithiobacillus* species, through lateral gene transfer. Evidence continues to build up around the idea suggested by Lopez de Saro and *et al.* that acidic environments could be rather closed systems where genetic exchange with non-acidophiles is highly restricted (López de Saro *et al.*, 2013).

4.2.3. *In silico* metabolic reconstruction

In silico metabolic reconstruction revealed the presence of a complete Entner-Doudoroff pathway (including key enzymes 6-phosphogluconate dehydratase and 2-keto-3-deoxyphosphogluconate aldolase), instead of the classical Embden-Meyerhof glycolysis (no gene could be found for 6-phosphofructokinase). The pentose phosphate pathway was also found to be complete. These results are in agreement with results from earlier radiospirometry assays conducted in *Acidiphilium* strains using [^{14}C]glucose (Shuttleworth *et al.*, 1985). A complete tricarboxylic acid cycle was also detected that allows the complete oxidation of glucose to CO_2. In addition, the prediction of three enzymes unique to the Calvin-Benson-Bassham cycle (RuBisCO, phosphoribulokinase and sedoheptulose bisphosphatase) suggests that *Acidiphilium* sp. PM is capable of CO_2 fixation (although this fixation has proved insufficient to sustain autotrophic growth). In the early nineties, Pronk and *et al.* reported "significant activities" of the RuBisCO in *Acp. acidophilum* (formerly *Thiobacillus acidophilus*) (Hiraishi *et al.*, 1998) both under organic carbon limitation and excess (Pronk *et al.*, 1990). More recently, Xu and *et al.* reported light-independent fixation of CO_2 resulting in the accumulation of PHB (Xu *et al.*, 2013a). A detailed analysis revealed that *Acidiphilium* sp. PM possesses Type I and Type II RuBisCO enzymes. The simpler type II isozyme is found in only a handful of other bacteria, including several *Alphaproteobacteria* (Tabita *et al.*, 2007). The reason for this redundancy in *Acidiphilium* is unclear. Yet, in other

bacteria such as *Hydrogenovibrio marinus*, structurally different RuBisCO enzymes respond differently to CO_2 concentrations, thus affording rapid adaptation to variable CO_2 availability (Yoshizawa *et al.*, 2004).

Besides the catabolism of glucose, the metabolic routes for the degradation of sorbitol, ethanol, glycerol, fructose, glutamate, 4-aminobutyrate, citric acid and maltose, but not of sucrose, were predicted in the genome of *Acidiphilium* sp. PM. Moreover, a route was predicted that would allow *Acidiphilium* sp. PM to grow on catechol, protocatechuate and, possibly, phenol.

In 1990, Bhattacharyya and *et al.* isolated and characterized a membrane-associated ATP synthase from *Acp. cryptum* Lhet2 which was strongly inhibited by azide and oligomycin but not by vanadate, which is characteristic of F_0F_1 ATP-synthases (Bhattacharyya *et al.*, 1990). Indeed, the genome of *Acidiphilium* sp. PM contains genes for ATP synthases of the F_0F_1-type. However, unlike *E. coli*, (which contains a single operon, proteins of F_0 and F_1 complexes are encoded in two distant operons in *Acidiphilium* sp. PM. Operon *atpHAGDC* encodes F_1 complex subunits δ, α, γ, β and ε, while F_0 complex is codified by *atpI*, *atpB* (subunit a), *atpE* (subunit c), *atpG* (subunit b2) and *atpF* (subunit b1). The presence of two b subunits (b1 and b2), is a common characteristic of photosynthetic species.

Our analysis revealed no genes related to atmospheric nitrogen fixation. Instead, two distinct pathways for ammonium assimilation into glutamate were predicted. The first is a two-step, ATP-driven process catalyzed by glutamine synthetase (EC 6.3.1.2) and glutamate synthase (EC 1.4.1.13). Alternatively, ammonium can be incorporated as glutamate in a one-step, ATP-independent reaction catalyzed by NADH-requiring glutamate dehydrogenase (EC 1.4.1.2). However, the affinity of the latter enzyme is typically 5- to 20-fold weaker, making this pathway suitable only in the presence of millimolar concentrations of ammonium (*e.g.* in laboratory conditions) (Lightfoot *et al.*, 1988). In addition, a gene cluster involved in assimilative nitrate reduction was identified in plasmid pAPM_01. This cluster is similar to that found in *Acidiphilium multivorum* AIU301 plasmid pACMV1.

Sixty-four genes coding for components of the respiratory chain were detected. These included several coding for the four subunits of cytochrome bo oxidase (*cyoABCD*) and the two subunits of two cytochrome bd oxidases (*cydAB*), which afford *Acidiphilium* sp. PM oxygen respiration. Interestingly, unlike other bacteria, *Acidiphilium* genomes harbour two distinct and complete *nuo* operons (*nuoABCDEFGHIJKLMN* and *nuoABC/DEFGHIJKLMN*)

encoding two distinct NADH:ubiquinone-oxidoreductases (also known as respiratory chain complex I). On the other hand, and even though *Acidiphilium* sp. PM ability to respire Fe^{3+} has been determined experimentally in this work (4.1.2) and elsewhere (Malki *et al.*, 2008), we were unable to predict any genes involved in iron respiration.

Acp. cryptum JF5 can reportedly grow anaerobically by coupling H_2 oxidation to the reduction of Fe^{3+} (Kusel *et al.*, 1999). This constitutes the only exception to the strict chemoorganotrophy of *Acidiphilium* representatives outside *Acp. acidophilum*. Our analysis confirms the presence of genes encoding a membrane-bound [Ni-Fe] hydrogenase, a *b*-type cytochrome (that could feed electrons to the respiratory chain) as well as proteins involved in the hydrogenase biosynthesis and maturation. Similarly to what has been reported in other proteobacteria (Schwartz and Friedrich, 2006), these genes appear to be encoded in large polycistronic transcriptional units in the genomes of *Acp. cryptum* JF5 and *Acp. multivorum* AIU301.

The prediction of a complete *narGYJ* cluster involved in nitrate respiration and a polysulphide reductase operon (*psrABC*) leads us to propose that *Acidiphilium* sp. PM might be capable of anaerobic respiration using nitrate or polysulphides as electron acceptors.

4.2.4. The photosynthetic gene cluster

As mentioned in the introduction, *Acidiphilium* species are characterized by their ability to synthesize Zn-BChl *a*. This pigment is part of the machinery that affords them the status of aerobic anoxygenic phototrophs. In many purple photosynthetic bacteria, the genes involved in photosynthesis are arranged in a large cluster, called the photosynthesis gene cluster (PGC). Interestingly, the PGC of *Betaproteobacteria* seems to have been acquired from *Alphaproteobacteria* by HGT and then experienced rearrangement (Igarashi *et al.*, 2001).

Prior to the advent of next-generation sequencing, the *puf* operon of most *Acidiphilium* species had been readily sequenced but only sparse information was available on the carotenoid and chlorophyll biosynthetic genes (Hiraishi and Shimada, 2001). And yet, the existence of a PGC homologous to that of other purple bacteria was long proposed (Igarashi *et al.*, 2001). Recently, the sequencing and annotation of *Acp. multivorum* AIU301 confirmed the existence of a PGC in *Acidiphilium* (Nagashima and Nagashima, 2013). Using the annotation in *Acidiphilium multivorum* (Acc. No. AP012035), we identified 12 contigs of *Acidiphilium* sp. PM genome which (together) contain most of PGC. Overall, the PGCs in

Acidiphilium sp. PM and *Acp. multivorum* present high identity and sinteny. The complete PGC of *Acidiphilium* sp. PM is estimated to exceed 38 kb in size (or 1% of its genome). It contains genes for the reaction center (RC) subunits, light-harvesting (LH) complex I polypeptides (*puf* operon), the assembly of the RC and the LH complexes (*puh* operon), the biosynthesis of carotenoids (*crt* genes) and bacteriochlorophyll (*bch* genes) as well as some ORFs involved in regulation (Figure 23). No genes were predicted for light-harvesting complex II (LH-II) in either *Acidiphilium* genome, which is in agreement with absorption spectra obtained from *Acp. rubrum* membranes (Hiraishi and Shimada, 2001).

Figure 23 shows a comparison of the homologous PGC of *Acidiphilium* sp. PM, *Acp. multivorum* AIU 301 and *Rhodobacter sphaeroides* 2.4.1 [the latter which PGC was one of the first to be sequenced and annotated (Naylor *et al.*, 1999; Kontur *et al.*, 2012)]. Differences in their *puf* operons include the lack of *pufQ* and *pufK* in *Acidiphilium* spp., and the replacement of *R. sphaeroides pufX* (which encodes an unbound cytochrome subunit) by *Acidiphilium pufC* gene (encoding a cytochrome bound to the reaction center). Notably, *Acidiphilium* species have a Glu168 residue instead of the His168 in the otherwise highly-conserved, co-factor binding region of PufL. It has been speculated that this substitution allows the accommodation of the larger Zn atom in the catalytic center (Hiraishi and Shimada, 2001).

All three species contain the same set of genes for bacteriochlorophyll biosynthesis (*bchBCDEFGHIJLMNOPXYZ*), albeit with differences. The directionality of *bchIDO* subcluster in *Acidiphilium* is inverted and, contrary to *R. sphaeroides*, *bchEJ* genes in *Acidiphilium* species are located separately to the main cluster (680 kb upstream of *puhA*). The loss of *tspO* (of unknown function) in *Acidiphilium* species, is rather unexpected for it is conserved in most other purple bacteria (Nagashima and Nagashima, 2013). Our analysis showed no evidence for an extra gene in *Acidiphilium* that would catalyze the exchange of Mg by Zn as the metal center. Therefore, as suggested previously by Hiraishi and Shimada, it is likely that this exchange is non-enzymatic but rather driven by high local concentrations of Zn (Hiraishi and Shimada, 2001).

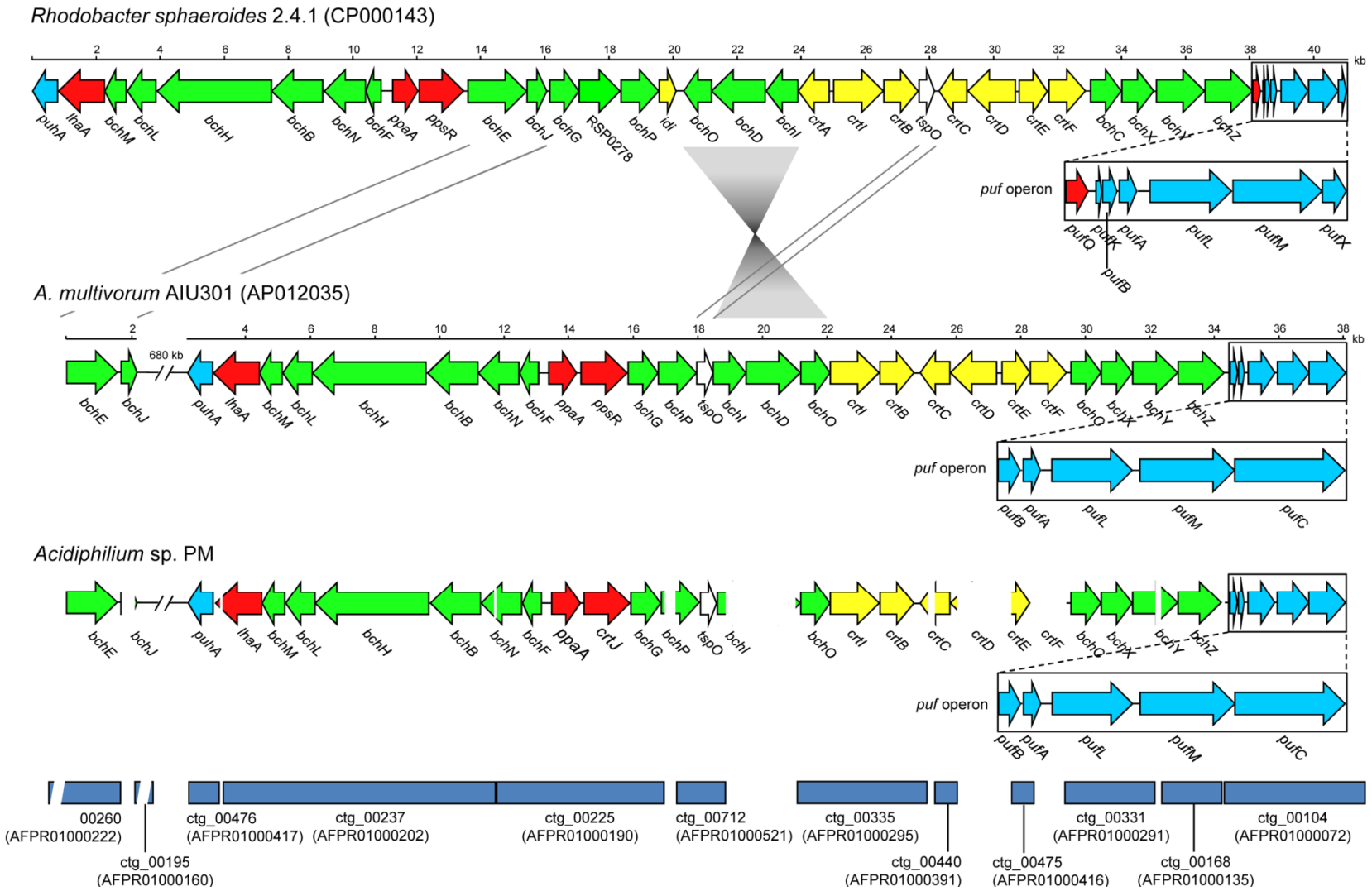

Figure 23. Photosynthetic gene cluster of *Acidiphilium* species. The photosynthetic gene cluster of *Rhodobacter sphaeroides* 2.4.1 (top) is shown for comparison. ORFs were coloured as follows: Turquoise: ORFs belonging to the *puf* operon; yellow: ORFs involved in the carotenoid biosynthetic pathway; Green: ORFs involved in the biosynthesis of bacteriochlorophyll; Red: ORFs with regulatory functions; white: ORFs of unknown function. Grey lines depict gene translocations (straight lines) or gene inversions (shaded triangles). The inset shows *puf* operon magnified three times. Blue rectangles (bottom) represent contigs of the genome of *Acidiphilium* sp. PM. Numbers in brackets indicate GenBank accession numbers.

Oddly enough, the genome of *Acp. cryptum* JF-5 seemed to have lost the PGC altogether. To verify this, we tried to PCR-amplify *pufL* (subunit L of the RC), *bchL* and *bchC* (from Zn-BChl *a* biosynthetic pathway) using genomic DNA from *Acp. cryptum* JF-5 and specific primers designed for *Acidiphilium* sp. PM orthologs (Table 4). Gel electrophoresis of the PCR products showed that these genes (and probably the complete PGC) are indeed present in *Acidiphilium cryptum* JF-5 (Figure 24). To rule out possible errors in the annotation of PGC genes, the genome of *Acp. cryptum* JF-5 was re-annotated using our own annotation pipeline. However, no genes of the PGC could be identified. It is therefore likely that this loss of information is the result of errors during the sequencing or assembly of *Acp. cryptum* JF-5 genome.

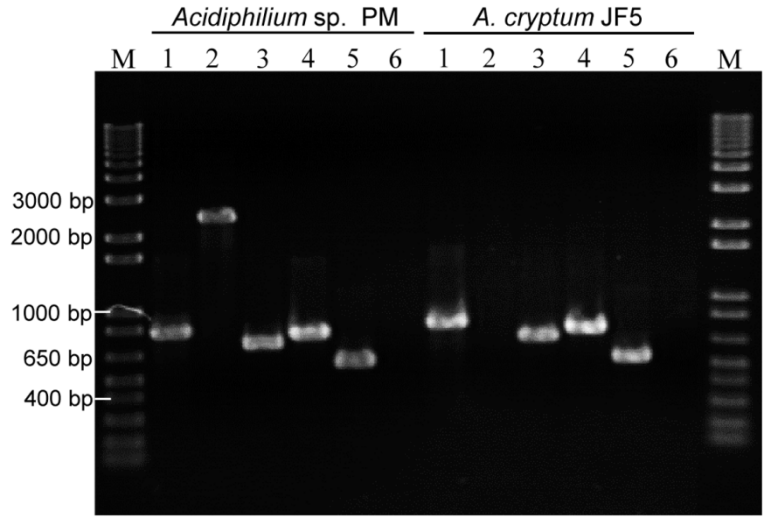

Figure 24. PCR-amplification of PGC genes from *Acp. cryptum* JF-5. GAPDH gene was used as a positive control and arsenite oxidase large subunit was included as a negative control (it was known to be absent in *Acp. cryptum* JF-5). PCR products were run in the following order: Lane 1: *GAPDH*; Lane 2: Arsenite oxidase large subunit; Lane 3: *pufL* (Photosynthetic reaction center L subunit), Lane 4: *bchL* (Light-independent protochlorophyllide reductase iron-sulphur ATP-binding protein); Lane 5: *bchC* (2-desacetyl-2-hydroxyethyl bacteriochlorophyllide A dehydrogenase); Lane 6: negative control; M: molecular weight marker (1 Kb Plus DNA Ladder).

4.2.5. Metal ion homeostasis

As expected of an acidophile inhabiting an acid-rich environment, *Acidiphilium* sp. PM harbours a repertoire of systems involved in the maintenance of metal ion homeostasis.

Metal-uptake regulators present in *Acidiphilium* sp. PM include the DtxR (*e.g.* MntR) and Fur families, which repress the transcription of uptake genes in metal-rich conditions. On the other hand, detoxification of heavy metals is regulated by members of the large MerR and ArsR/SmtB families. Upon binding of the metal, these regulators experience a conformational change that triggers the activation (MerR) or derepression (ArsR/SmtB) of

resistance operons. Metal efflux operons in *Acidiphilium* sp. PM comprise several resistance-nodulation-cell division (RND) proteins, cation-diffusion facilitators and P-type ATPases.

Numerous proteins containing Ni-binding domains were predicted, namely [NiFe] hydrogenase subunits and Hyp/Hup proteins involved in their biosynthesis and maturation. On the other hand, a search for homologs of Ni-resistance determinants from other organisms uncovered several proteins with high similarity. However, these proteins were annotated in *Acidiphilium* sp. PM with a different metal specificity. It should be noted that the binding of a particular metal to an efflux protein cannot be ascertained only on the basis of the protein sequence.

4.3. IDENTIFICATION OF Ni-RESISTANCE DETERMINANTS VIA A FUNCTIONAL SCREENING OF A GENOMIC LIBRARY OF *Acidiphilium* sp. PM

As described in the introduction, most metal resistance mechanisms described to date are based on operon-encoded, energy-dependent efflux systems. Traditionally, these operons have been identified through the screening of genomic libraries and the heterologous expression of metal resistance determinants. Even in bioleaching concentrates, where metals can build up to several grams per litre, adapted strains contain similar genes. Interestingly, these genes are often found in tandem and associated to transposon elements, which allow their expansion and afford increasingly higher metal resistance to their host (Tuffin *et al.*, 2005; Tuffin *et al.*, 2006).

For this reason, to study the mechanisms behind Ni resistance in *Acidiphilium* sp. PM, a functional genomics approach was planned. A shotgun genomic library of *Acidiphilium* sp. PM was constructed and screened for Ni-resistant clones. Then clones were sequenced and the genes involved in Ni-resistance identified through transposon mutagenesis and/or subcloning.

4.3.1. Construction of a genomic library of *Acidiphilium* sp. PM

A shotgun genomic library of *Acidiphilium* sp. PM was constructed in *E. coli* DH10B using the high-copy-number plasmid pBluescript®II SK^+ ($pSKII^+$) as described in 3.7. Briefly, DNA from *Acidiphilium* sp. PM was partially digested with Sau3AI and DNA fragments 2 to 6 kb in size were ligated to BamHI-digested SAP-dephosphorylated $pSKII^+$ and transformed into *E. coli* DH10B. Figure 25 shows intermediate steps in the construction of the library: the preparation of the inserts (A and B) and preparation of the vector (C). The genomic library consisted of approximately 10^5 recombinants, with an average insert size of 2.2 kb (range 0.5 to 7 kb) as determined by PCR amplification.

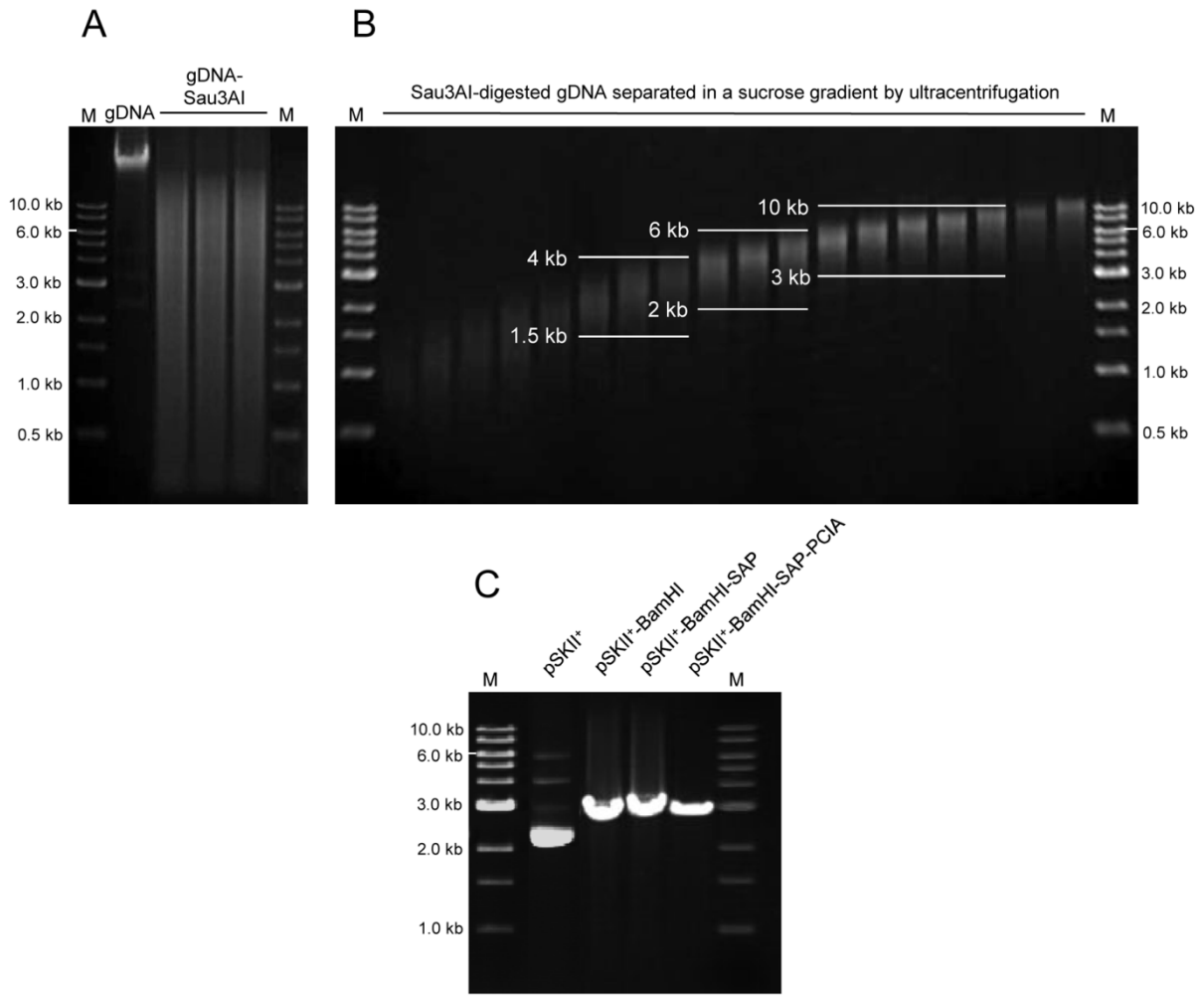

Figure 25. Construction of a shotgun genomic library of *Acidiphilium* sp. PM. (A) Inserts were prepared by partial digestion of genomic DNA (gDNA) with Sau3AI (gDNA-Sau3AI) followed by (B) separation of the fragments in a sucrose gradient by isopycnic ultracentrifugation. (C) The preparation of the vector included digestion of pSKII+ with BamHI, followed by dephosphorylation of 5' ends with Shrimp Alkaline Phosphatase (SAP) and purification by extraction with PCIA (25:24:1) and precipitation. Inserts and vector were ligated and *E. coli* DH10B was transformed with the ligation products. M stands for molecular weight marker (1 Kb DNA Ladder).

4.3.2. Screening of a genomic library of *Acidiphilium* sp. PM for Ni-resistant clones

Prior to performing the functional screening, the minimum inhibitory concentrations for *E. coli* DH10B (pSKII+) were determined. These were found to be: 2.25 mM $NiSO_4 \cdot 6H_20$, 0.8 mM $CdSO_4 \cdot 8/3H_20$, 1.5 mM $ZnSO_4 \cdot 7H_20$, 1.25 mM $CoSO_4 \cdot 7H_20$ and 4.5 mM $CuSO_4 \cdot 5H_20$. *E. coli* DH10B (pSKII+) was used as a negative control throughout these experiments.

To ensure that a representative portion of the genome was screened, *ca*. 12000 recombinant clones were plated onto LB-Ap plates containing 2.25 mM Ni (the MIC for *E. coli* DH10B). These 12000 clones contained an estimated 26 Mb of cloned DNA, which is

equivalent to 6.5 times the size of *Acidiphilium* sp. PM genome (3.98 Mb) (4.2.1). After an overnight incubation at 37 ºC, several nickel-resistant (Ni^r) colonies were recovered. To exclude the possibility that chromosomal mutations in the host were responsible for the resistant phenotype, recombinant plasmids from the Ni^r clones were extracted and transformed again into *E. coli* DH10B. Re-transformed clones were then tested for Ni resistance using drop assays. Some of these re-transformed Ni^r clones were further discarded when sequencing revealed that their inserts were chimeric. These chimeras arose from the ligation of Sau3AI-digested cohesive fragments from distant genome fragments. Eventually four Ni-resistant clones were selected for further analysis.

The selected Ni-resistant clones and the control grew to similar cell densities in the absence of Ni (Figure 26 left). Therefore, the different growths in Ni could only be attributed to the genes encoded in the recombinant plasmids (Figure 26 right). Clones carrying pSRNi5 and pSRNi6 exhibited the highest levels of resistance to Ni.

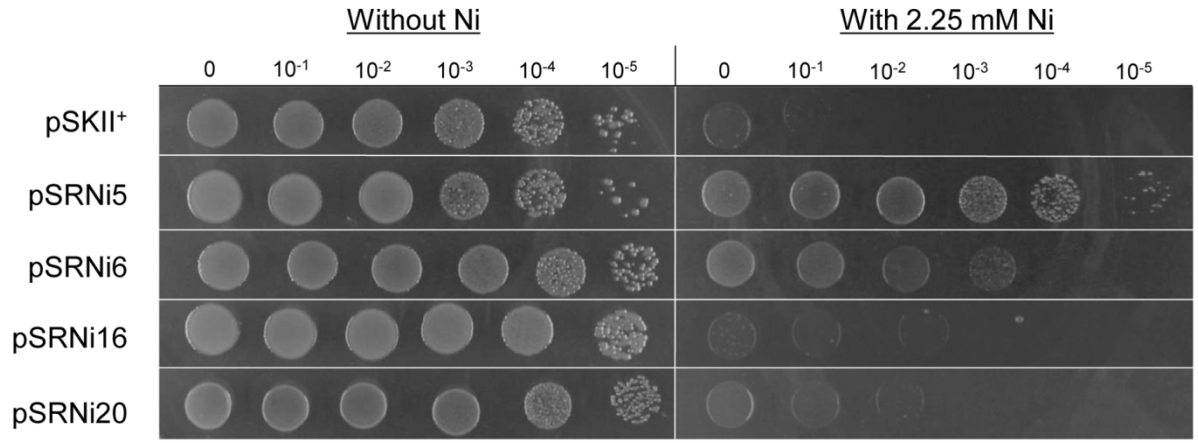

Figure 26. Ni resistance of the clones rescued in the screening of a genomic library of *Acidiphilium* sp. PM. Serial dilutions of overnight-grown cultures were plated on LB-Ap plates with (right) and without 2.25 mM Ni (left).

Earlier works had shown that Ni resistance determinants may also confer resistance to Co and Cd (Mirete *et al.*, 2007). For this reason all four Ni^r clones were tested for cross-resistance to Co(II), Cd(II), Cu(II) and Zn(II). Transformants carrying pSRNi6 were found to tolerate 0.8 mM Cd and all clones except pSRNi20 resisted at least 1.25 mM Co. On the other hand, none of the clones presented significantly higher resistance to Cu or Zn than the control (Figure 27). Similar Ni-Co cross-resistance have been reported previously for Ni-resistance determinants in *Cupriavidus necator* (formerly *Alcaligenes eutrophus*) (Liesegang

et al., 1993), *Klebsiella oxytoca* (Park *et al.*, 2004) and *E. coli* (Liesegang *et al.*, 1993; Park *et al.*, 2004; Rodrigue *et al.*, 2005; Mirete *et al.*, 2007).

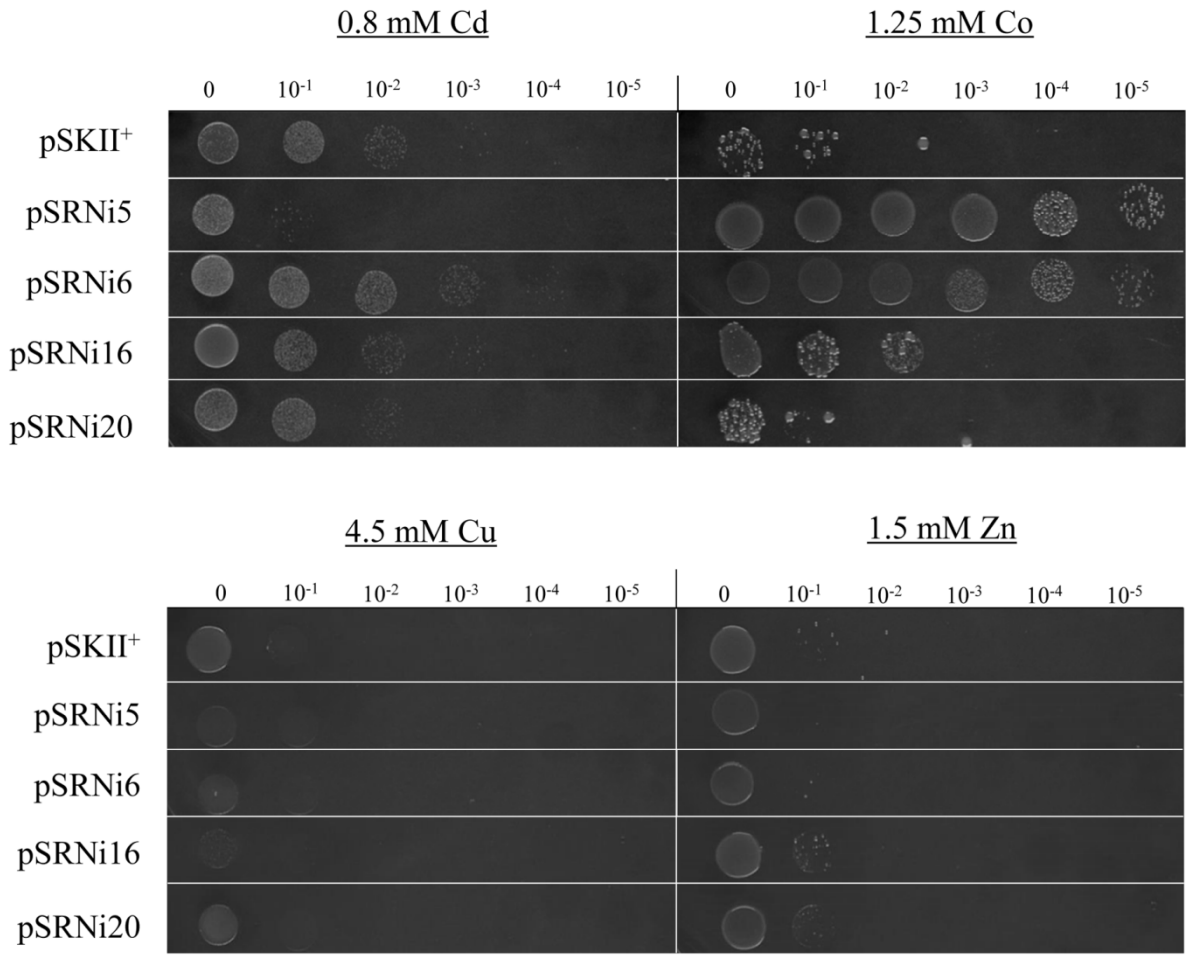

Figure 27. Heavy-metal cross-resistance of the four Ni-resistant clones. Serial dilutions of overnight-grown cultures were plated on LB-Ap containing 0.8 mM Cd, 1.25 mM Co, 4.5 mM Cu, or 1.5 mM Zn [the MICs for *E. coli* DH10B (pSKII+)].

4.3.3. Cellular Ni content of the Ni^r clones

Some metal resistance mechanisms prevent the accumulation of nickel through active transport efflux pumps or by extracellular chelation of the metal. Others tend to favour the intracellular accumulation by sequestering Ni in histidine-rich vacuoles (Joho *et al.*, 1995b; Nies, 1999). To gather information on the mechanism of Ni resistance in our Ni^r clones, the cellular Ni content of the clones was measured.

Cells in early stationary phase were supplemented with 4 mM Ni and incubated at 37 ºC for 1 h. Cells were then harvested by centrifugation, washed and their cellular Ni content measured using inductively coupled plasma-mass spectrometry (ICP-MS) as described in 3.11.2. As shown in Figure 28 cells bearing pSRNi20 seemed to accumulate a substantially

larger amount of cellular Ni compared to control cells (bearing an empty pSKII$^+$). On the other hand, no clones seemed to actively export Ni outside the cell.

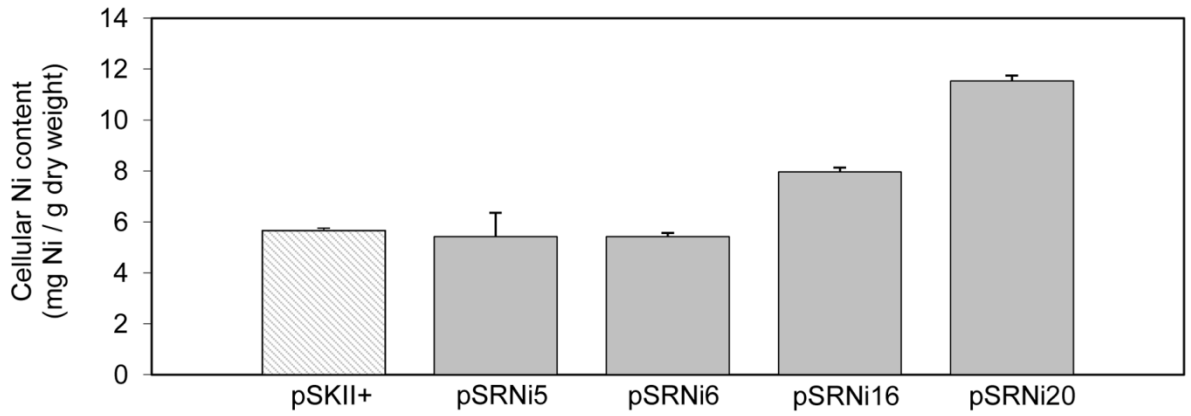

Figure 28. Cellular Ni content of the Ni^r clones. Cellular Ni concentration was measured with ICP-MS after growing cells in stationary phase for 1 h in 4 mM Ni.

4.3.4. Identification of Ni-resistance determinants

In order to identify the ORFs conferring Ni resistance in each recombinant plasmid, their inserts were end-sequenced and then mapped against the draft genome of *Acidiphilium* sp. PM. Surprisingly, all the insert sequences aligned with the bacteria's chromosome and not with the plasmids. Earlier reports on *Acidiphilium* resistance determinants for arsenic (Suzuki *et al.*, 1997), cadmium and zinc (Mahapatra *et al.*, 2002b) revealed that they were plasmid-encoded. Insert sequences had a GC-content ranging between 63% and 70%, comparable to the overall 68% GC-content of *Acidiphilium* sp. PM (4.2.1). The gene organization, protein identification and transmembrane domain predictions of the ORFs contained in the cloned DNA fragments are summarized in Figure 29 and Table 13.

Five ORFs were identified in pSRNi5, four in pSRNi6, three in pSRNi16, and a single ORF was found in pSRNi20 (Figure 29). The identification of the gene(s) responsible for Ni resistance was accomplished by *in vitro* transposon mutagenesis and/or subcloning. Plasmid pSRNi20 contained a single ORF encoding a glycosyl transferase; therefore, we concluded that differences in Ni resistance between this clone and the control were necessarily caused by that single ORF.

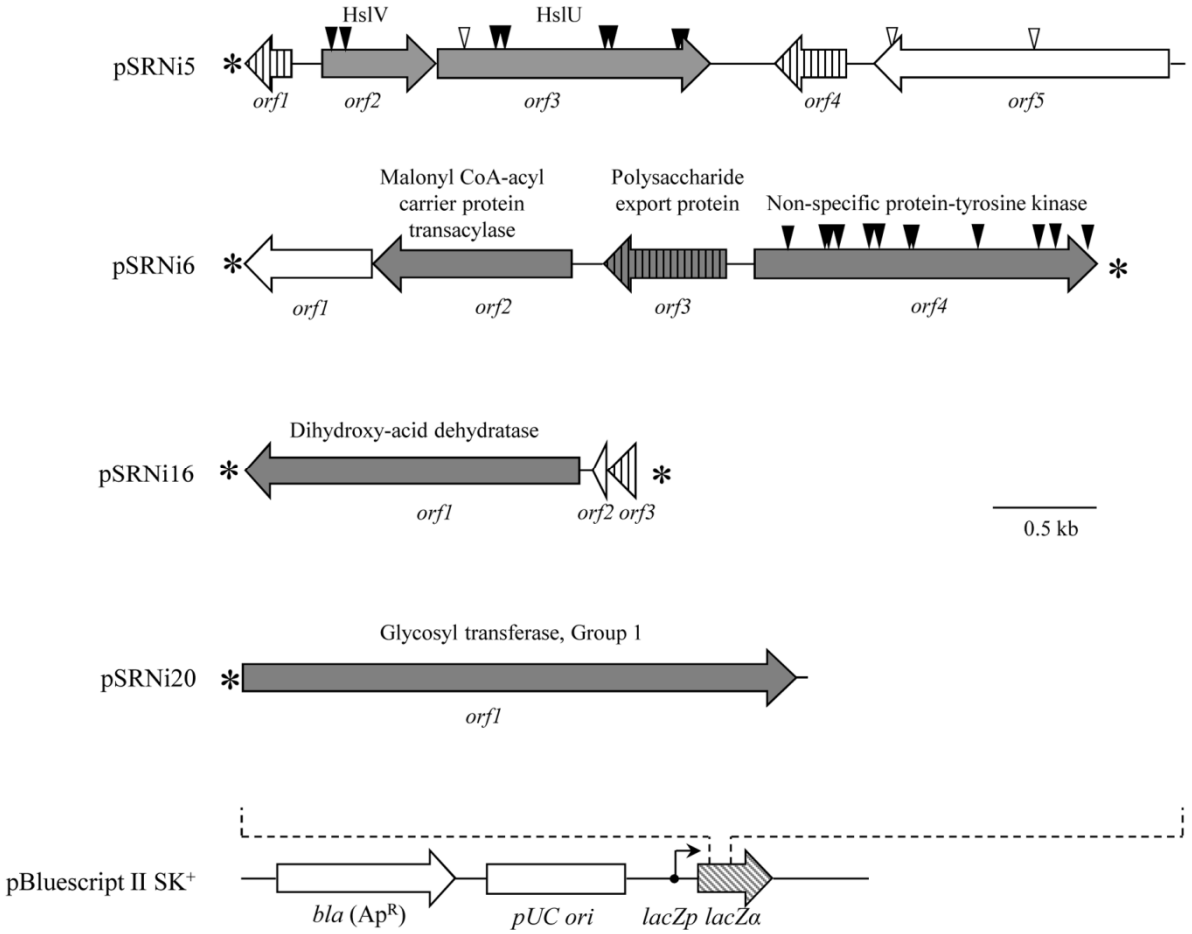

Figure 29. Genetic organization of the recombinant plasmids that confer Ni resistance to *E. coli*. ORFs involved in Ni resistance are shown in grey. ORFs with predicted transmembrane helices are shaded with vertical bars. Asterisks indicate incomplete ORFs. Vertical arrowheads indicate transposon insertions that either abolish the resistance phenotype (filled in black) or do not affect the resistance phenotype (not filled). The map of the vector (pBluescript®II SK+) is represented at the bottom. The scale bar represents 0.5 kb.

Clone (insert size)	GC content (%)	GenBank accession no.	ORF	Length (aa)	Proteins in *Acidiphilium* sp. PM using blastn (aa length), GenBank accession no. of the protein	Protein coverage (missing end)[1]	Function	TMH in the clone (TMH in the entire protein)[4]
pSRNi5 (4233 bp)	69	KC110840	1	75	Hypothetical protein (145), EGO96502	51% (C-term)	Unknown	2 (4)
			2	**183**	**ATP-dependent protease hsIV (183), EGO96503**	**100%**	**ATP-dependent protease HslVU**	**0 (0)**
			3	**439**	**ATP-dependent protease ATP-binding subunit HslU (439), EGO96504**	**100%**	**ATP-dependent protease HslVU**	**0 (0)**
			4	114	Hypothetical protein (114), EGO96505	100%	Unknown	2 (2)
			5	473	Amidase (473), EGO96506	100%	Hydrolysis of amides	0 (0)
pSRNi6 (4106 bp)	70	KC110841	1	209	3-oxoacyl-(acyl-carrier-protein) reductase (249), EGO95637	84% (C-term)	Dissociated (type II) fatty acid biosynthesis system	0 (0)
			2	**319**	**Malonyl CoA-acyl carrier protein transacylase (319), EGO95636**	**100%**	**Fatty-acid biosynthesis in bacteria**	**0 (0)**
			3	**196**	**Polysaccharide export protein (196), EGO95635**	**100%**	**Polysaccharide export**	**1 (1)**
			4	**551**	**Non-specific protein-tyrosine kinase (647), EGO95634**	**77% (C-term)[(2)]**	**Exopolysaccharide biosynthesis**	**0 (0)**
pSRNi16 (2281 bp)	69	KC110843	**1**	**537**	**Dihydroxy-acid dehydratase (617), EGO95524**	**87% (C-term)**	**Fourth step in the biosynthesis of Ile and Val**	**0 (0)**
			2	68	Hypothetical protein (68), EGO95523	100%	Unknown	0 (0)
			3	128	RND efflux transporter (107), EGO95522	20% (N-term)[(3)]	Involved in hopanoid biosynthesis	4 (12)
pSRNi20 (2728 bp)	63	KC110844	**1**	**889**	**Glycosyl transferase, Group 1, EGO96186**	**81% (N-term)**	**Cell envelope biogenesis, outer membrane**	**0 (0)**

Table 13. Description of the ORFs contained in the recombinant plasmids of the Ni^r clones. ORFs involved in Ni resistance are shown in bold type. [1] C-term and N-term represent carboxy and amino ends, respectively. [2] The amino acid sequence of non-specific protein-tyrosine kinase deposited in GenBank (EGO95634) is incomplete on the carboxy end. The full protein in *Acp. cryptum* JF-5 (ABQ30731) and *Acp. multivorum* AIU301 (BAJ80915) consists of 718 residues. [3] The amino acid sequence of RND efflux transporter deposited in GenBank (EGO95522) is incomplete on the amino end. The full protein in *Acp. cryptum* JF-5 (ABQ30260) and *Acp. multivorum* AIU301 (BAJ80194) consists of 858 residues. [4] TMH stands for transmembrane helixes.

The glycosyl transferase encoded in plasmid pSRNi20 belongs to the GT-B fold type of glycosyltransferases. It contains several conserved domains including a domain found in GT1 family of glycotransferases and two conserved RfaG domains. RfaG domains were named after protein RfaG of *E. coli*, an enzyme that catalyzes the addition of the first glucose to the core lipopolysaccharide (LPS), which forms part of the outer membrane (Parker *et al.*, 1992a; Parker *et al.*, 1992b). It is likely that the glycosyl transferase in pSRNi20 also participates in the biosynthesis of the LPS, hence contributing to an enhanced permeability barrier that helps maintain Ni ions outside the cell. Besides, there is evidence that sugars, including fructose, maltose and rhamnose, can coordinate Ni^{2+} ions (Sigel and Sigel, 2007). An enlarged LPS would therefore allow the formation of higher numbers of LPS-Ni^{2+} complexes, preventing Ni free ions from entering the cell. This would also explain the increased levels of cellular Ni observed in this clone (Figure 28).

In the case of pSRNi6, which harbours 4 ORFs, *in vitro* transposon mutagenesis was used to narrow down the candidates for Ni-resistance. The interruption of the non-specific protein-tyrosine kinase with Tn5 abolished the nickel-resistant phenotype. This protein contains several conserved domains (GumC, Wzz, eps_fam), all of which are found in proteins participating in exopolysaccharide or lipopolysaccharide biosynthesis. On the other hand, no insertion mutants were recovered that interrupted any of the three other ORFs present in pSRNi6 (Figure 29). Therefore, to discard their role in Ni resistance, a fragment that comprised *orf1-orf2-orf3* was subcloned. The resulting plasmid conferred a Ni-sensitive phenotype. Furthermore, plasmids which included only the kinase gene or a combination of the kinase and the polysaccharide export protein genes conferred only slight resistance to Ni (Figure 30). Overall, these results suggest that while the non-specific protein tyrosine kinase contributes to Ni resistance, the presence of at least the malonyl CoA-acyl carrier protein transacylase and the polysaccharide export protein is also necessary to explain the high levels of resistance to Ni observed in the clone bearing pSRNi6. Interestingly, the polysaccharide export protein contains a predicted transmembrane helix and it is therefore very likely embedded in the membrane, which would support its role in the biosynthesis of the lipopolysaccharide. As in the case of pSRNi20, we suggest that the overexpression of genes involved in the biosynthesis of cell envelope components might create a denser extracellular barrier that prevents Ni ions from entering the cell. The disparities in the cellular Ni content of pSRNi6 and pSRNi20 could be ascribed to the different Ni binding properties of the components of the cell envelope that each clone produces.

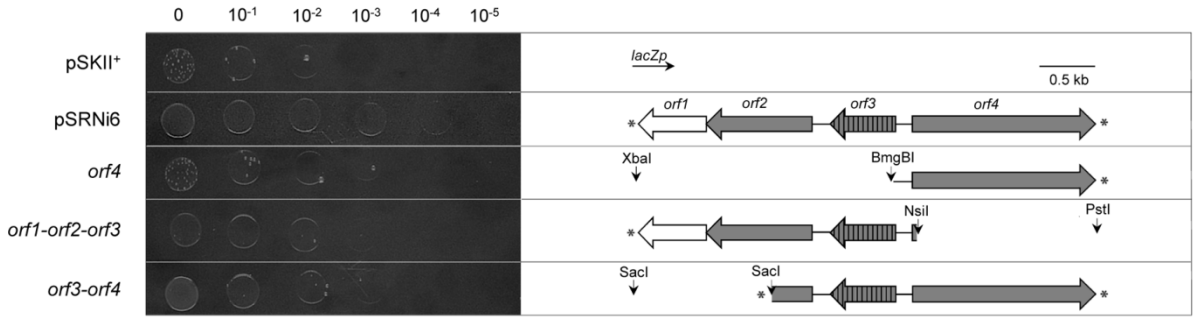

Figure 30. Identification of the ORFs involved in Ni resistance in pSRNi6 by subcloning. *orf4* was subcloned as follows: pSRNi6 was double-digested with XbaI and BmgBI, run in an agarose gel and the band containing *orf4* was excised and purified. Ends were then blunted using T4 DNA polymerase and religated with T4-DNA ligase. *orf1-orf2-orf3* was subcloned by double digestion of pSRNi6 with NsiI and PstI, then purified and religated with T4-DNA ligase. Finally, *orf3-orf4* was subcloned by digestion of pSRNi6 with SacI. Fragments were run in an agarose gel and the fragment containing *orf3-orf4* was excised, purified, and religated with T4-DNA ligase. These constructs were then transformed in *E. coli* DH10B as described in 3.4.9. Finally, serial dilutions of overnight cultures were plated in LB-Ap plates containing 2.25 mM Ni. *orf1*: 3-oxoacyl-(acyl-carrier-protein) reductase; *orf2*: malonyl CoA-acyl carrier protein transacylase; *orf3*: polysaccharide export protein; *orf4*: non-specific protein-tyrosine kinase. ORFs involved in Ni resistance are shown in grey. ORFs with predicted transmembrane helices are shaded with vertical bars. Asterisks indicate incomplete ORFs.

In pSRNi16, the Ni-resistance determinant was identified by subcloning the ORFs. Subcloning *orf1*, which encodes a putative dihydroxy-acid dehydratase, yielded cells with a resistance to Ni higher than those carrying the intact pSRNi16 (Figure 31). Additionally, subcloning both *orf2* and the complete *orf3* together in the direction of the lacZ promoter (lacZp) yielded a Ni-sensitive clone (Figure 31). Overall, these data indicated that the dihydroxy-acid dehydratase was the ORF responsible for the Ni^r phenotype observed in pSRNi16-bearing clones. Dihydroxy-acid dehydratases (EC 4.2.1.9) catalyze the third step in the biosynthesis of the branched-chain amino acids (BCAA) valine, leucine and isoleucine (Umbarger, 1978). Increased BCAA concentrations in response to both acid and metal stress have been reported previously (Tremaroli *et al.*, 2009; Santiago *et al.*, 2012) and might explain the increased Ni resistance observed when *E. coli* is transformed with pSRNi16. Moreover, dihydroxyacid dehydratases contain 4Fe-4S clusters in their active site, which are particularly susceptible to superoxide generated by Ni (Flint *et al.*, 1993; Geslin *et al.*, 2001; Cheng *et al.*, 2009). Thus, the overexpression of the dihydroxy acid dehydratase from *Acidiphilium* sp. PM could compensate the loss of function of the endogenous *E. coli* dehydratase by Ni.

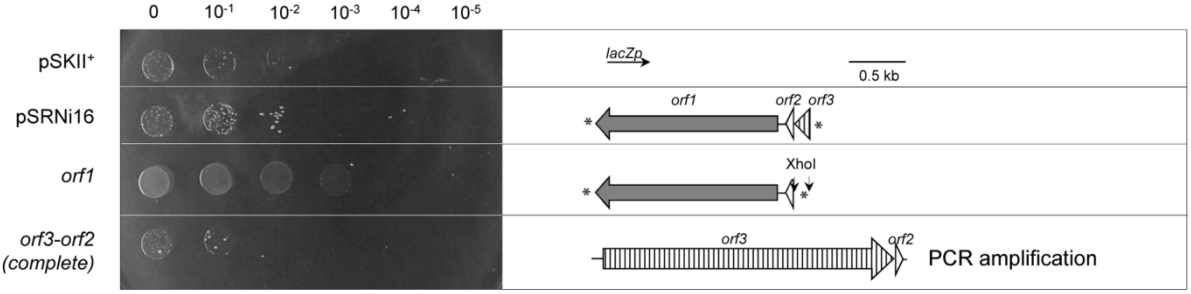

Figure 31. Identification of the ORFs involved in Ni resistance in pSRNi16 by subcloning. *orf1* was subcloned by digestion of pSRNi16 with XhoI followed by religation with T4-DNA ligase. *orf3-orf2* was PCR-amplified from genomic DNA using primers pSRNi16_*orf3*-2_F and pSRNi16_*orf3*-2_R (Table 4), checked on an agarose gel, then excised and purified. Amplicons were double-digested with XbaI and HindIII and ligated to equally-digested pSKII+. These constructs were then transformed in *E. coli* DH10B as described in 3.4.9. Finally, serial dilutions of overnight cultures were plated in LB-Ap plates containing 2.25 mM Ni. *orf1*: dihydroxy-acid dehydratase; *orf2*: hypothetical protein; *orf3*: RND efflux transporter. ORFs involved in Ni resistance are shown in grey. ORFs with predicted transmembrane helices are shaded with vertical bars. Asterisks indicate incomplete ORFs.

Plasmid pSRNi5 carries an insert encoding 5 ORFs. Transposon mutagenesis performed on pSRNi5 yielded eight Ni-sensitive mutants with insertions in *orf2* and *orf3* (Figure 29). On the other hand, two insertions in *orf5* (encoding an amidase) did not affect the resistant phenotype (Figure 29). *orf2* and *orf3* encode HslV and HslU proteins, which form an operon-encoded protease named HslVU (also known as ClpQY). The involvement of HslVU in the resistance to Ni was confirmed by subcloning *hslVU* (Figure 32). Indeed, the subcloned operon conferred the same level of resistance as the complete pSRNi5. On the other hand, the subcloning of the amidase yielded a Ni-sensitive clone (Figure 32). Overall, this data indicated that the *hslVU* operon was solely responsible for the resistance observed in the pSRNi5-bearing clone. The Ni cellular content of the transformants carrying pSRNi5 or an empty plasmid pSKII+ is similar, which indicates a possible intracellular protection, such as the recycling of misfolded, hence non-functional, proteins.

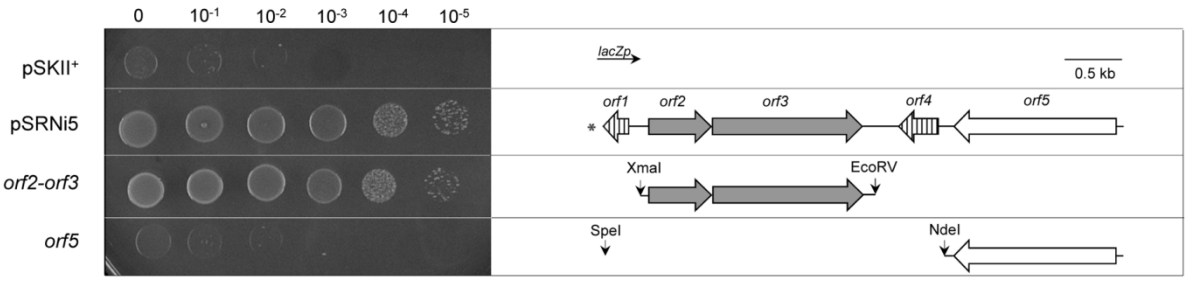

Figure 32. Identification of the ORFs involved in Ni resistance in pSRNi5 by subcloning. *orf2-orf3* was subcloned as follows: pSRNi5 was double-digested with XmaI and EcoRV, run on an agarose gel, and the band containing *or2-orf3* was excised and purified. This fragment was then ligated to an equally-digested pSKII+. To subclone *orf5*, pSRNi5 was double digested with SpeI and

NdeI, the fragments were run on an agarose gel and the band containing *orf5* was excised and purified. Ends were then blunted using T4 DNA polymerase and religated with T4 DNA ligase. These constructs were then transformed in *E. coli* DH10B as described in 3.4.9. Finally, serial dilutions of overnight cultures were plated in LB-Ap plates containing 2.25 mM Ni. *orf2*: ATP-dependent protease HsIV; *orf3*: ATP-dependent protease ATP-binding subunit HslU; *orf5*: amidase. ORFs involved in Ni resistance are shown in grey. ORFs with predicted transmembrane helices are shaded with vertical bars. Asterisks indicate incomplete ORFs.

Similarly to other caseinolytic proteases (Clp), HslVU is composed of an AAA+ ATPase responsible for the unfolding and protein recognition (HslU or ClpY) and a small peptidase (HslV or ClpQ) (Chuang *et al.*, 1993; Missiakas *et al.*, 1996; Rohrwild *et al.*, 1996). Together with Lon, ClpXP and ClpAP, HslVU is responsible for 70 to 80% of the protein degradation *in vivo* (Jain and Chan, 2007). Proteases are responsible for the degradation of misfolded proteins and those proteins no longer needed by the cell, which is crucial in adaptation to stress. The role of protein degradation in the response to metals has been reported in the past. In the presence of high intracellular Zn concentrations, *E. coli* Zn response regulator ZntR binds both Zn and DNA, activating ZntA (an ATPase essential for Zn export). However, when Zn concentrations are low, ZntR does not bind Zn or DNA, which makes it more unstable and susceptible to degradation by proteases ClpXP and Lon (Pruteanu *et al.*, 2007). Moreover, protease complex HslVU is considered to be the bacterial homolog of the proteasome (Rohrwild *et al.*, 1996), the main complex for protein degradation in eukaryotes and archaea. A study by Forzani and *et al.* (Forzani *et al.*, 2002) showed that the expression of the maize proteasome α subunit conferred resistance to Ni, Co and Cd in yeast. Similarly, we have observed that the proteasome homolog HslVU confers resistance to both Ni and Co but not to Cd, Cu or Zn (Figure 33).

Several recent reports suggest that chaperones and proteases from acidophiles could have major unknown roles in the resistance to specific environmental stresses: ClpB in the resistance to As (Morgante *et al.*, 2014), ClpXP in the resistance to acidic pH (Guazzaroni *et al.*, 2013), and HslVU (ClpQY) in resistance to Ni (this work).

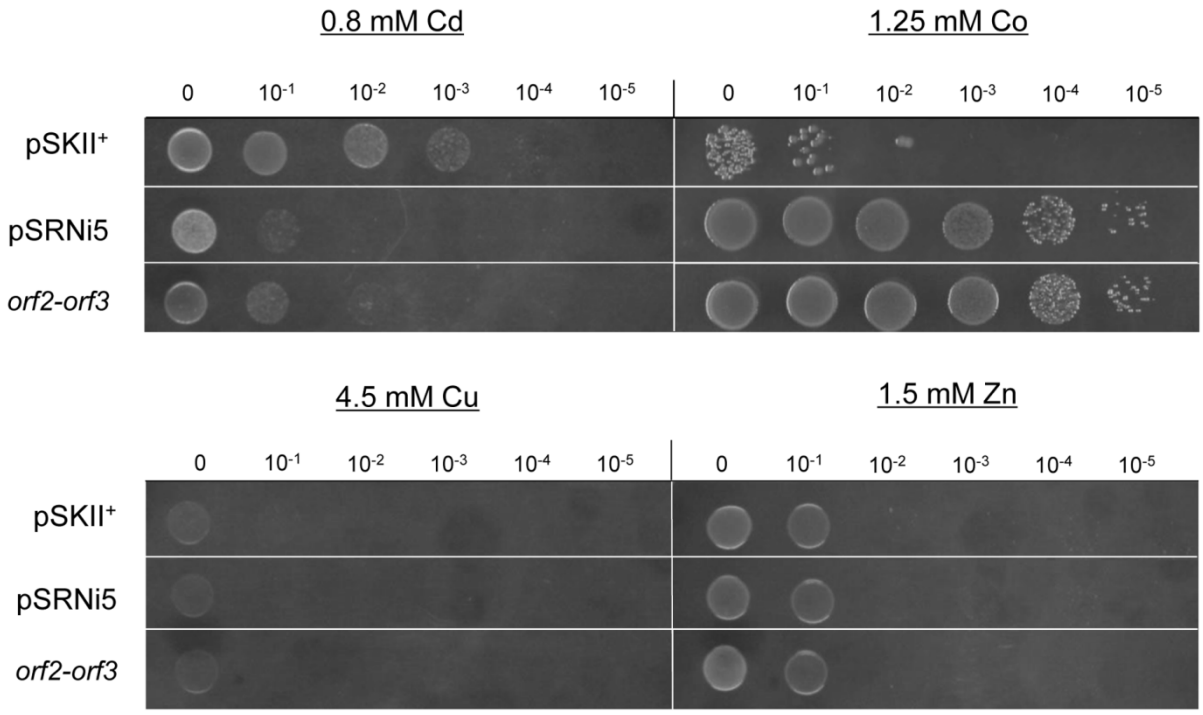

Figure 33. Heavy-metal cross-resistance of protease HslVU. Serial dilutions of overnight cultures were plated on LB-Ap plates containing 0.8 mM Cd, 1.25 mM Co, 4.5 mM Cu, or 1.5 mM Zn [the MICs for *E. coli* DH10B (pSKII+)].

4.3.5. Effect of the overexpression of protease HslVU under physico-chemical stress

Protease HslVU plays an important role in the heat shock response by controlling the *in vivo* turnover of both the heat shock sigma factor (σ^{32}) and abnormal proteins in *E. coli* (Kanemori *et al.*, 1997). At the same time, the transcription of *hslVU* is under the regulation of σ^{32} (Lien *et al.*, 2009). To test whether the overexpression of HslVU from *Acidiphilium* could confer greater resistance to heat shock in *E. coli*, cells carrying *hslVU* were grown to early exponential phase and exposed to 50 ºC. After a 30 min exposure, cells overexpressing HslVU had survival rates 42 times greater than the control, which carried an empty vector (pSKII+: 0.10 ± 0.05; HslVU: 4.11 ± 0.37) (Figure 34). This is in agreement with earlier reports which showed an increased transcription of operon *hslVU* upon heat shock induction (Lien *et al.*, 2009).

Interestingly, HslVU also plays a regulatory role in the response to oxidative stress by participating in the degradation of SulA, a cell division inhibitor activated in the SOS response in *E. coli* (Khattar, 1997; Seong *et al.*, 1999). To test whether overexpression of HslVU from *Acidiphilium* sp. PM could also confer resistance to oxidative stress in *E. coli*, the subclone bearing *hslVU* was exposed to UV radiation (λ = 254 nm) and to hydrogen

peroxide. After a five-second exposure to UV radiation, cells overexpressing HslVU did not show enhanced survival compared to control cells (Figure 34). Similarly, no differences were observed between the control and the HslVU-bearing clone when cells were exposed to 2.5 mM H_2O_2 (Fig. 5). Although H_2O_2 is known to trigger SOS response, overexpression of HslVU did not increase *E. coli* resistance to H_2O_2, probably because hydrogen peroxide causes further damages to the cell (*e.g.* lipid peroxidation) than can be repaired by the SOS response.

It has been reported that acidic conditions can lower intracellular pH, causing protein unfolding and uncoupling proton movement across the membrane from ATP synthesis (Goto *et al.*, 1990; Richard and Foster, 2004; Hong *et al.*, 2005). This damage can eventually lead to cell death. It has been recently published that the heterologous expression of *Terriglobus saanensis* protease ClpXP dramatically increases the survival of *E. coli* at pH 1.8 (Guazzaroni *et al.*, 2013). To test whether HslVU could also enable the growth of *E. coli* in acidic conditions, the clone carrying *hslVU* was exposed to pH 1.8 for one hour. No differences in the percentage of survival were observed between the *hslVU*-bearing clone and the control (Figure 34). This suggests that its contribution to the turnover of proteins is insufficient to maintain cell growth under acidic conditions.

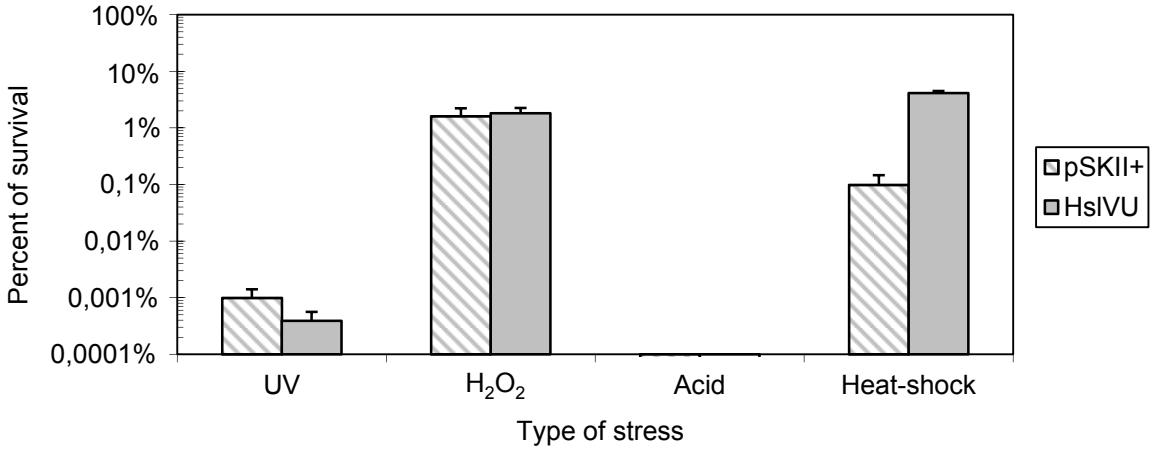

Figure 34. Effect of the overexpression of protease HslVU from *Acidiphilium* sp. PM. on the survival of *E. coli* to physico-chemical stresses. The graph shows the percentage of survival of *E.coli* DH10B bearing an empty pSKII+ vector (barred columns) or pSKII+ carrying operon *hslVU* (solid columns). Cells were exposed to the following stresses: 5-sec of germicidal UV light, 30 min in the presence of 2.5 mM H_2O_2, 1 h at pH 1.8 or 30 min at 50 ºC as described in 3.3.3. The percentage of survival was calculated as the number of colony forming units (cfu) per ml remaining after the treatment divided by the number of cfu/ml at time zero. Each experiment was repeated at least three times.

4.3.6. Phylogenetic analysis of HslVU

As explained above (4.2.2), microorganisms that share the same niche tend to exchange genes that are useful in adaptation to stress or changing conditions. A work by Cardenas *et al.* on rubrerythrin (a protein involved in response to oxidative stress) revealed that sequences from several distantly related acidophiles cluster together, separately from those of related non-acidophilic taxa. This suggests a horizontal gene transfer event (Cardenas *et al.*, 2012). The finding that the expression of HslVU enhances growth under different types of stress (presence of Ni and Co and heat shock), led us to explore the possibility that it had been acquired through HGT. A comparative analysis was performed using both acidic and non-acidic taxa. Acidic species included representatives of the three main genera found in Río Tinto (*Acidithiobacillus* spp., *Leptospirillum* spp. and *Acidiphilium* spp.) as well as other species found in acidic environments.

Phylogenetic trees were built using *16S rRNA* gene sequences and a concatenated amino acid sequence of HslV and HslU subunits. In both trees, sequences belonging to *Acidiphilium* spp. clustered together in a separate group from those of *Leptospirillum, Acidithiobacillus* and the rest of acidic species (APPENDIX II). The similarity in the topologies of HslVU-based and *16S rRNA*-based trees, suggests that operon *hslVU* of *Acidiphilium* was acquired through vertical transmission rather than horizontal transfer among the species tested.

This is the first attempt to identify genes involved in Ni resistance in *Acidiphilium*, one of the most conspicuous dwellers of acidic environments and a natural metal resister. Our screening revealed seven different genes that confer Ni resistance to *E. coli*. *Acidiphilium* sp. PM does not appear to rely on classic energy-dependent metal-efflux operons. Instead, Ni resistance could be a rather complex strategy involving several molecular mechanisms.

Atempts to conjugate or transform *Acidiphilium* sp. PM have been so far unsuccessful; hence the lack of mutants in this study. Further work is necessary to develop genetic tools for the manipulation of this strain. This would allow us to knock-out the genes identified in the screening and further explore their role in Ni resistance in *Acidiphilium* sp. PM.

4.4. CHARACTERIZATION OF THE EARLY RESPONSE TO Ni IN *Acidiphilium* sp. PM

As described earlier (4.1.4), most *Acidiphilium* sp. PM cells are moderately resistant to Ni (*ca*. 10 mM). A tiny fraction of them, however, is capable of bypassing or compensating for Ni toxicity and grows in 100-fold higher Ni concentrations (1 M).

As part of our goal to characterize Ni resistance in *Acidiphilium* sp. PM we aimed at identifying the primary targets of Ni toxicity by gaining knowledge of the general response to Ni in the cell. Whole-genome transcriptomics and proteomics were used to monitor early changes in gene expression upon addition of Ni.

4.4.1. Construction of a shotgun DNA microarray of *Acidiphilium* sp. PM

This tool was intended both for genome-wide transcriptional studies and for comparative genomic hybridization of *Acidiphilium* strains; hence, a shotgun DNA microarray design was chosen. The construction of shotgun DNA microarrays requires the existence of a collection of clones which contains the DNA fragments that will be amplified and printed onto the slides. In our case, these clones were contained in the random genomic library constructed for the functional screening (see section 4.3.1).

Recombinant clones from the genomic library were grown overnight and then lysed. The recombinant plasmids were used as templates for PCR amplification of the inserts as described in section 3.4.4. PCR products were then checked by agarose gel electrophoresis. Half of them were run in conventional 0.8% agarose gels, which allowed the estimation of the average insert size (I) (2.2 kb; range 0.5 to 7 kb). The overall efficiency of recombination was worked out to be 84% (69% of the inserts > 500 bp).

Clarke and Carbon's equation (Clarke and Carbon, 1976) is often used to calculate the number of clones (N) needed to have any given sequence represented in a genomic library with a certain probability (P) provided that the average insert size (I) and the genomic size (G) are known (Equation 1). Assuming a genome size of *ca.* 4 Mb, the amplification of 8500 clones yielded a *ca*. 98% probability (P) of any given sequence being represented in our microarray (*i.e.* 4-fold redundancy).

Equation 1

$$N = \frac{\ln(1-P)}{\ln\left(1-\frac{I}{G}\right)}$$

Thus, the inserts of 8544 library clones (contained in eighty-nine 96-well plates) were PCR-amplified, purified and printed onto slides. In addition, a set of 48 controls was included in the microarray to verify the quality of the hybridizations. Positive controls included twenty-two *Acidiphilium* sp. PM genes involved in catabolism, replication, transcription or heavy-metal detoxification as well as Sau3AI-digested genomic DNA. On the other hand, the inserts of several clones of a genomic library of *Leishmania infantum* and 1x spotting solution served as negative hybridization controls (see Table 9 and section 3.8).

A total of 8592 spots (including 48 control spots) constituted an individual array, which was printed in duplicate in each slide (Figure 35). Overall, these technical replicates had good correlation, thus confirming the quality of the spotting. The microarray configuration was deposited in NCBI's Gene Expression Omnibus database under accession number GPL17306).

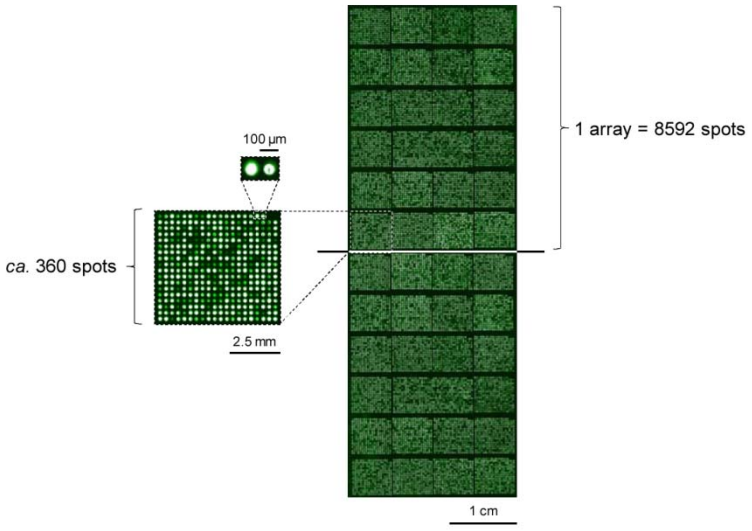

Figure 35. *Acidiphilium* sp. PM shotgun DNA microarray. Each slide contains two arrays printed in duplicate. The figure shows a slide hybridized with fragmented, Cy3-labelled genomic DNA of *Acidiphilium* sp. PM, which was used to control a batch of printed slides. The inset is a magnified view of one of twenty-four, 20x20-spot blocks that conform a full array. Each block was printed by a single pin. Upper to the inset is a 3X amplification of two control spots: *Acidiphilium* sp. PM *16S rRNA* (left) and Sau3AI-digested genomic DNA (right).

4.4.2. Transcriptomics of the early response to Ni in *Acidiphilium* sp. PM

4.4.2.1. Microarray hybridization and analysis

Cultures of *Acidiphilium* sp. PM were grown to early exponential phase and then exposed to 10 mM Ni for 0, 5 or 30 min. Cells were pelleted and their RNA was extracted and treated with DNase. The integrity of the RNA was then verified by capillary electrophoresis (Figure 36).

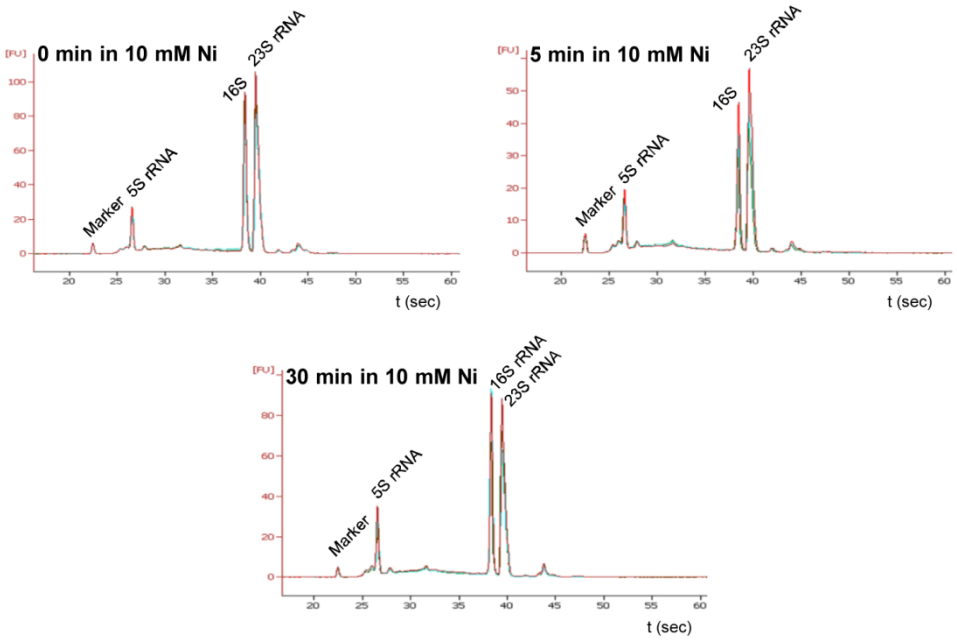

Figure 36. Early transcriptomic response to Ni. Quality of the RNAs used for microarray hybridization. RNA was extracted from cultures exposed to 10 mM Ni for 0, 5 and 30 min. The integrity of the RNAs was verified by capillary electrophoresis. Electropherograms show the RNA integrity of three of the six replicates used for each condition.

RNA was reverse-transcribed, then labelled as follows: cDNAs from cells challenged with Ni for 5 or for 30 min were labelled with Cy5 whereas cDNAs from unexposed cells were labelled with Cy3. Equimolar amounts of fluorescently-labelled cDNAs were hybridized against blocked *Acidiphilium* PM microarrays. Hybridized arrays were washed prior to scanning and analysis for Cy3 (532 nm) and Cy5 (635 nm) dyes (Figure 37). After subtraction of the background, fluorescence intensity (FI) values were normalized using *LOWESS per pin*. For each spot, the intensity ratios across six replicates were compared using a paired Student's t-test ($p < 0.05$) under the null hypothesis of absence of differential gene expression. The fold change / $\log_2$ (average intensity) (F/A) scatter plot (Figure 37) helped define the following criteria as indicative of significant differential expression: i) average signal intensity > 2000 FU (around 10 times the background intensity), ii) $p < 0.05$ and iii) For 0 vs 5 min Ni: $-2 > F > 2$. For 0 vs 30 min Ni: $-3.5 > F > 3$.

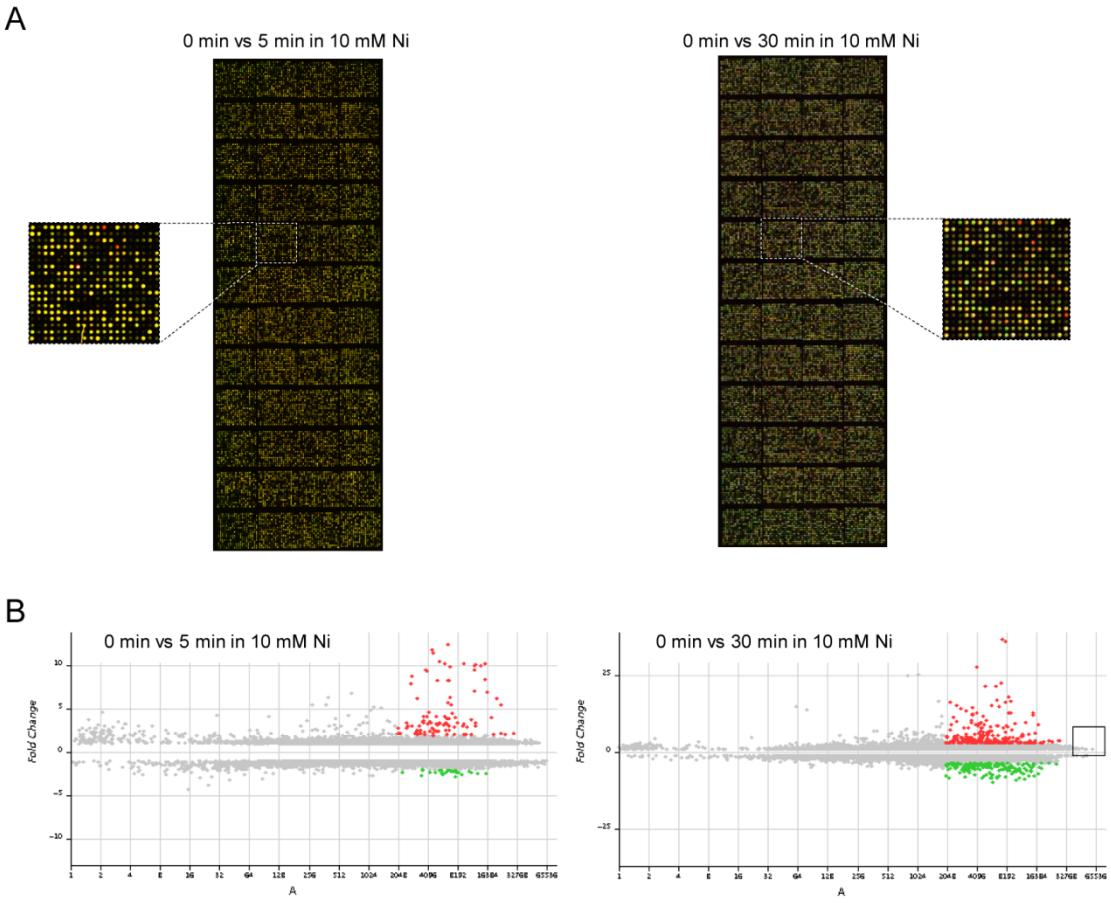

Figure 37. Early transcriptomic response to Ni. Microarray scanning and analysis. A) Microarrays were hybridized with Cy3-cDNA from unexposed cells and Cy5-cDNA from cells exposed to 10 mM Ni for 5 min (left) or 30 min (right). The microarray scan of one of six replicates is shown for each experiment. B) Fold change vs A scatter plot. These plots were used to establish the thresholds for spot selection. Selected spots have been coloured as follows: red dots indicate clones which contained genes significantly induced upon exposure to 10 mM Ni; green dots indicate clones with genes that were significantly repressed.

The quality of the hybridizations was checked using the internal controls of the microarray. *Acidiphilium* sp. PM control genes presented constitutive expression, with expressions ranging from the heavily-expressed *16S rRNA* and *rpoD* genes to the mild expression of PGC genes *pufL*, *bchC*, *bchH*. Only *MCAT* was found to meet the criteria for significant differential expression after addition of Ni for 30 min. On the other hand, negative control spots presented faint intensities comparable to the background (upper limit: 2.5 times the background signal) with high variation across replicates (Table 14). Data from the control spots confirms that the conditions used in the assays were stringent enough to avoid unspecific hybridization, yet sufficiently mild to allow annealing of complementary strands.

		0 vs 5 min in 10 mM Ni			0 vs 30 min in 10 mM Ni		
Spot	**Positive control**	**Fold Change**	**Log_2Ratio ± SD**	***p***	**Fold Change**	**Log_2Ratio ± SD**	***p***
90A1	*Apm 16S rRNA*	-1.70	-0.8 ± 0.4	0.004	-1.36	-0.4 ± 0.3	0.020
90A2	*Apm* Arsenate reductase	-1.04	-0.1 ± 0.3	0.650	2.60	1.4 ± 0.5	0.001
90A3	*Apm atpB*	1.16	0.2 ± 0.3	0.131	-2.61	-1.4 ± 0.4	0.000
90A4	*Apm* Cytochrome C oxidase subunit 3	-1.23	-0.3 ± 0.3	0.042	-1.35	-0.4 ± 0.2	0.006
90A5	*Apm GAPDH*	-1.18	-0.2 ± 0.4	0.173	-1.58	-0.7 ± 0.3	0.003
90A6	*Apm rpoD*	-1.14	-0.2 ± 0.2	0.116	-2.49	-1.3 ± 0.2	0.000
90A7	*Apm bchL*	-1.38	-0.5 ± 0.1	0.000	-1.41	-0.5 ± 0.2	0.004
90A8	*Apm trpB*	-1.17	-0.2 ± 0.3	0.109	-1.68	-0.7 ± 0.3	0.001
90A9	*Apm* Flavodoxin/nitric oxide synthase	-1.34	-0.4 ± 0.1	0.001	-2.04	-1.0 ± 0.3	0.000
90A10	*Apm* Arsenite oxidase large subunit	-1.23	-0.3 ± 0.4	0.136	2.69	1.4 ± 0.3	0.000
90A11	*Apm dnaK*	-1.18	-0.2 ± 0.2	0.030	-2.12	-1.1 ± 0.5	0.003
90A12	*Apm* Mercuric reductase	1.13	0.2 ± 0.4	0.281	1.25	0.3 ± 0.3	0.035
90B1	*Apm pufL*	-1.24	-0.3 ± 0.3	0.069	-1.28	-0.4 ± 0.3	0.021
90B2	*Apm* Fructose-1,6-Bisphosphatase (FBP)	-1.02	0.0 ± 0.2	0.676	2.83	1.5 ± 0.2	0.000
90B3	*Apm hydA*	-1.36	-0.4 ± 0.5	0.074	1.08	0.1 ± 0.1	0.113
90B4	***Apm MCAT***	-1.78	-0.8 ± 0.4	0.005	**-4.61**	**-2.2 ± 0.1**	**0.000**
90B5	*Apm bchC*	-1.18	-0.2 ± 0.3	0.120	1.19	0.3 ± 0.1	0.008
90B6	*Apm idh*	-1.47	-0.6 ± 0.3	0.005	-2.61	-1.4 ± 0.3	0.000
90B7	*Apm dnaE*	-1.57	-0.7 ± 0.2	0.001	-1.49	-0.6 ± 0.3	0.007
90B8	*Apm bchH*	-1.72	-0.8 ± 0.4	0.003	-1.28	-0.4 ± 0.3	0.038
90B9	*Apm* FUR family protein	-1.41	-0.5 ± 0.4	0.031	-1.52	-0.6 ± 0.1	0.000
90B10	*Apm* Molybdopterin oxidoreductase	-1.46	-0.5 ± 0.3	0.006	-1.38	-0.5 ± 0.5	0.093
90C1	*Apm* Sau3AI-digested gDNA	1.49	0.6 ± 0.2	0.002	1.44	0.5 ± 0.3	0.008
Spot	**Negative control**		**Average FI ± SD**			**Average FI ± SD**	
90B11	Spotting solution 1x		9 ± 10			8 ± 8	
90B12	Spotting solution 1x		10 ± 12			8 ± 8	
90C2	*Le. infantum* clone S30C8		88 ± 72			66 ± 44	
90C3	*Le. infantum* clone S18H12		93 ± 62			66 ± 41	
90C4	*Le. infantum* clone S31A9		133 ± 57			109 ± 51	
90C5	*Le. infantum* clone S13C5		162 ± 81			93 ± 26	
90C6	*Le. infantum* clone S31F5		266 ± 103			155 ± 55	
90C7	*Le. infantum* clone S19D9		132 ± 86			117 ± 69	
90C8	*Le. infantum* clone S15F1		63 ± 48			41 ± 29	
90C9	*Le. infantum* clone S21H8		32 ± 37			55 ± 33	
90C10	Spotting solution 1x		3 ± 1			8 ± 6	
90C11	Spotting solution 1x		3 ± 3			3 ± 1	
90C12	Spotting solution 1x		17 ± 12			17 ± 16	
90D1	Spotting solution 1x		106 ± 51			62 ± 27	
90D2	Spotting solution 1x		17 ± 15			6 ± 4	
90D3	Spotting solution 1x		31 ± 48			16 ± 15	
90D4	Spotting solution 1x		31 ± 25			68 ± 113	
90D5	Spotting solution 1x		6 ± 3			6 ± 11	
90D6	Spotting solution 1x		11 ± 15			11 ± 11	
90D7	Spotting solution 1x		8 ± 5			11 ± 21	
90D8	Spotting solution 1x		7 ± 5			6 ± 4	
90D9	Spotting solution 1x		11 ± 11			3 ± 1	
90D10	Spotting solution 1x		2 ± 1			2 ± 1	
90D11	Spotting solution 1x		4 ± 2			6 ± 5	
90D12	Spotting solution 1x		5 ± 10			2 ± 1	

Table 14. Early transcriptomic response to Ni. Microarray control spots. Control spots were used for the validation of microarray hybridizations. Data shown belongs to one of two replicates included in each slide. Data for the positive controls includes F, log_2F±SD and the associated p value. For the negative controls, the average fluorescence intensity (FI) values and their SD are shown. Data in bold type indicate significant differential gene expression as defined by the criteria explained in the text.

Seventy-one clones met the criteria for significant differential expression after cells were exposed to Ni for 5 min. This number rose to 243 when cells were exposed for 30 min. Interestingly, many of the clones induced/repressed by minute 5 were also induced/repressed after 30 min. A total of 270 unique clones had their inserts sequenced and 198 of these clones (73%) were successfully mapped against the genome of *Acidiphilium* sp. PM. The sequence of the remaining clones could not be defined because their reads i) had poor alignments (e values > 10^{-100}), ii) mapped in different contigs, iii) presented divergent orientation or, iv) did

not align with any of the contigs. Clones that were successfully mapped contained a total of 317 genes (or fragments of genes), distributed as shown in Table 15.

		Clones	Genes
0 min vs 5 min Ni	Induced	32	49
	Repressed	9	17
	Total	41	66
0 min vs 30 min Ni	Induced	95	137
	Repressed	89	154
	Total	184	291
	Non-redundant total	198	317

Table 15. Early transcriptomic response to Ni. Clone distribution. Classification of the clones (and genes contained within them) as induced/repressed attending to the experiment.

Oftentimes, several clones overlapped with the same gene. This redundancy, which arises from the microarray design, highlighted the relevance of that particular gene.

On the other hand, sometimes a single clone contained more than one gene. Hence, the up- or down-regulation of these genes needed further assessment with quantitative reverse-transcription PCR (qRT-PCR).

Data from the microarray hybridizations have been deposited in NCBI's Gene Expression Omnibus (Edgar *et al.*, 2002) and are accessible through GEO Series accession number GSE48042 (http://www.ncbi.nlm.nih.gov/geo/query/acc.cgi?acc=GSE48042).

4.4.2.2. Validation of the changes in gene expression via qRT-PCR

To validate the data from the hybridizations and study the up- or down-regulation of individual genes in clones containing multiple ORFs, qRT-PCR assays were performed.

100 ml-cultures of *Acidiphilium* sp. PM were grown to early exponential phase and then exposed to 10 mM Ni for 0, 5 or 30 min in triplicates. Next, RNA was extracted and treated with DNase. The absence of contaminant DNA was ascertained as the negative PCR amplification of *GAPDH*. The integrity of the RNA was verified by capillary electrophoresis (Figure 38).

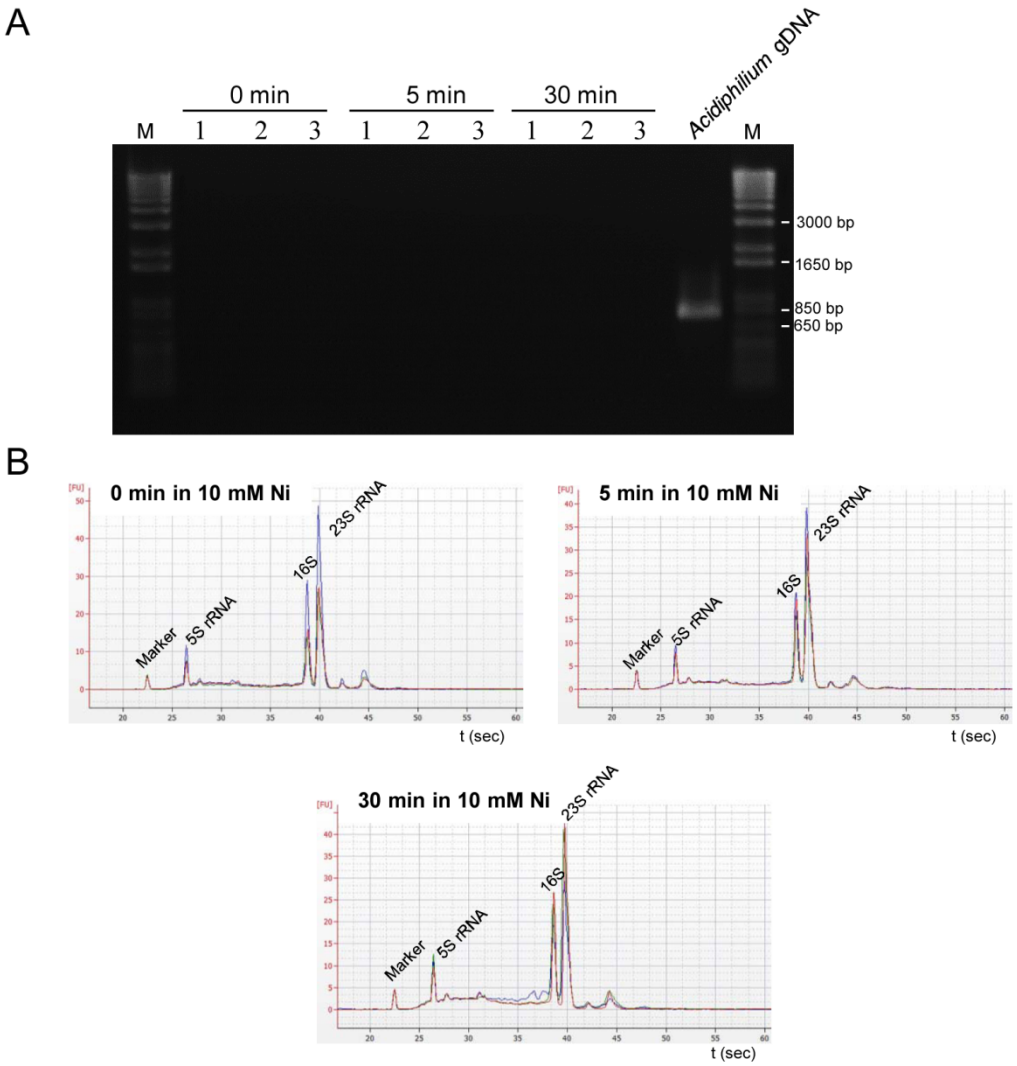

Figure 38. Early transcriptomic response to Ni. Quality of the RNAs used in the qRT-PCRs. RNA was extracted from cultures exposed to 10 mM Ni for 0, 5 and 30 min. A) The absence of contaminant DNA was ascertained by PCR amplification of *GAPDH*. *Acidiphilium* genomic DNA served as positive control. M indicates molecular weight marker (1 Kb Plus DNA Ladder). B) The integrity of the RNAs was verified by capillary electrophoresis.

Typical housekeeping genes (*e.g. 16S rRNA*, *GAPDH*, *rpoD*, *etc.*) are often used as endogenous controls for the normalization of qPCR assays. However, as seen in Table 14, these genes were significantly up- or down-regulated in the presence of Ni and thus could not be used for normalization. Microarray hybridization data was revisited to find a clone which contained a single gene with stable expression in all three conditions. The criteria used in this re-analysis were: i) average signal > 2000 (*i.e.* moderate to high gene expression), ii) $-1.2 < FC < 1.2$ (*i.e.* less than 20% variation in expression levels) and $p < 0.05$ (that is, statistically significantly stable). One clone (45B7) was found that met these criteria and was end-sequenced and mapped against the draft genome. Unfortunately, this clone turned out to be a chimera which contained fragments of 3 different genes.

Eventually, we decided to use external transcripts for normalization. In particular, 10^6 copies both of mouse β-actin antisense and of *Xenopus laevis* elongation factor 1α were added for every 2 ng of extracted RNAs prior to reverse-transcription. These spike-in controls were synthesized *in vitro* as described in 3.4.6 and allowed the normalization of both the reverse transcription and the qPCR itself.

The expression of *ca.* 1 in 4 genes (23%) obtained by microarray hybridization was further analysed by qPCR. In general, transcriptomic changes detected by microarray hybridization correlate well with those measured by qRT-PCR. Yet, qRT-PCR proved more sensitive in detecting large transcriptomic changes, such as the 100-fold change in the expression of toxin-antitoxin system *mazEF* after 30 min (Table 17). The fact that clones often harbour several genes makes their fold change a sort of average expression of all the genes in the clone, thus reducing the sensitivity to detect transcriptomic variations in a single gene.

In some cases, the expressions of several genes contained in the same clone were studied by qRT-PCR. Often times, these genes were found to have similar transcription levels, possibly indicating their belonging to the same operon (Table 16 and Table 17).

Frequently, the same gene was contained in several different clones and a single qRT-PCR was necessary for the validation. This redundancy stressed the importance of that gene.

Table 16. Significantly up- and down-regulated clones after 5 min in 10 mM Ni. Clones have been arranged on the basis of the function carried out by their genes. Clone data includes the clone library ID, its ratio of expression (F), the log_2F and its associated standard error as well as the p value. Genes which expression was further validated by qRT-PCR are shown in the same line. Clones induced/repressed both in Ni and Zn are coloured in pale blue, whereas clones whose expression was altered only in Ni are left uncoloured. Genes reported or suspected to conform operons are depicted by solid or discontinued vertical bars, respectively. Induction is shown in tones of red whereas repression is highlighted in shades of green.

128 64 32 16 8 4 2 1 | -1 -2 -4 -8 -16 -32 -64 -128

		Microarray hybridization						qRT-PCR		
	Clone	F	$Log_2F \pm SE$	p	Locus	Gene	F	$Log_2F \pm SE$	p
Replication, transcription, translation	42F4	3.19	1.7 ± 0.1	0.000	APM_2849	Transcriptional regulator/antitoxin, MazE	32.29	5.0 ± 0.1	0.004
					APM_2850	ATPase involved in chromosome partitioning-like protein	1.94	1.0 ± 0.1	0.005
					APM_2851	Hypothetical protein	1.85	0.9 ± 0.1	0.004
					APM_2852	Rep(pMBA19a)	1.37	0.5 ± 0.0	0.010
	05A3	2.25	1.2 ± 0.1	0.000	APM_3113	Putative ribonuclease BN	-1.38	-0.5 ± 0.0	0.000
					APM_3114	Ribonuclease R	-1.58	-0.7 ± 0.0	0.044
					APM_3115	C-terminal processing peptidase	-2.32	-1.2 ± 0.1	0.021
	47D11	2.22	1.1 ± 0.1	0.000	APM_3673	Transposase Tn3 family protein	N.D.		
	08B8	2.21	1.1 ± 0.1	0.000	APM_2850	ATPase involved in chromosome partitioning-like protein	1.94	1.0 ± 0.1	0.005
					APM_2851	Hypothetical protein	1.85	0.9 ± 0.1	0.004
	76H10	2.00	1.0 ± 0.1	0.000	APM_2856	Conjugal transfer protein traA	-1.20	-0.3 ± 0.1	0.056
	89C9	-2.14	-1.1 ± 0.1	0.000	APM_1367	Carbamoyl phosphate synthase small subunit	N.D.		
					APM_1368	Carbamoyl-phosphate synthase large chain	N.D.		
	41B1	-2.35	-1.2 ± 0.1	0.000	APM_1368	Carbamoyl-phosphate synthase large chain	N.D.		
	03A3	-2.46	-1.3 ± 0.1	0.000	APM_R0045	16S ribosomal RNA	N.D.		
Energy-yielding processes	69A3	5.87	2.6 ± 0.3	0.000	APM_0195	MmgE/PrpD family protein	9.02	3.2 ± 0.2	0.023
					APM_0196	Methylitaconate delta2-delta3-isomerase	4.51	2.2 ± 0.1	0.011
					APM_0198	Putative transcriptional regulator	1.71	0.8 ± 0.1	0.030
	11D7	4.16	2.1 ± 0.2	0.000	APM_0193	AraC family transcriptional regulator	-1.42	-0.5 ± 0.1	0.046
					APM_0195	MmgE/PrpD family protein	9.02	3.2 ± 0.2	0.023
	44F11	3.67	1.9 ± 0.3	0.000	APM_0196	Methylitaconate delta2-delta3-isomerase	4.51	2.2 ± 0.1	0.011
					APM_0198	Putative transcriptional regulator	1.71	0.8 ± 0.1	0.030
	61H9	3.49	1.8 ± 0.3	0.000	APM_0196	Methylitaconate delta2-delta3-isomerase	4.51	2.2 ± 0.1	0.011
					APM_0198	Putative transcriptional regulator	1.71	0.8 ± 0.1	0.030
					APM_0199	Tricarballylate dehydrogenase	1.18	0.2 ± 0.0	0.217
	79G9	2.20	1.1 ± 0.1	0.000	APM_1984	Putative transcriptional regulator	N.D.		
Metal homeostasis	78F6	11.37	3.5 ± 0.1	0.000	APM_0067	Natural resistance-associated macrophage protein	N.D.		
					APM_0068	Manganese transport regulator MntR	19.01	4.2 ± 0.1	0.009
	10F9	10.98	3.5 ± 0.1	0.000	APM_0066	MgtC/SapB transporter	4.32	2.1 ± 0.1	0.004
					APM_0067	Natural resistance-associated macrophage protein	N.D.		
					APM_0068	Manganese transport regulator MntR	19.01	4.2 ± 0.1	0.009
	39D8	10.42	3.4 ± 0.1	0.000	APM_0067	Natural resistance-associated macrophage protein	N.D.		
					APM_0068	Manganese transport regulator MntR	19.01	4.2 ± 0.1	0.009
					APM_0070	Natural resistance-associated macrophage protein	9.37	3.2 ± 0.1	0.009
	51F7	10.08	3.3 ± 0.0	0.000	APM_0067	Natural resistance-associated macrophage protein	N.D.		
					APM_0068	Manganese transport regulator MntR	19.01	4.2 ± 0.1	0.009
					APM_0070	Natural resistance-associated macrophage protein	9.37	3.2 ± 0.1	0.009
	49E11	10.00	3.3 ± 0.1	0.000	APM_0067	Natural resistance-associated macrophage protein	N.D.		
					APM_0068	Manganese transport regulator MntR	19.01	4.2 ± 0.1	0.009
					APM_0070	Natural resistance-associated macrophage protein	9.37	3.2 ± 0.1	0.009
	57G6	9.77	3.3 ± 0.2	0.000	APM_0067	Natural resistance-associated macrophage protein	N.D.		
					APM_0068	Manganese transport regulator MntR	19.01	4.2 ± 0.1	0.009
					APM_0070	Natural resistance-associated macrophage protein	9.37	3.2 ± 0.1	0.009
	74D6	9.15	3.2 ± 0.1	0.000	APM_0066	MgtC/SapB transporter	4.32	2.1 ± 0.1	0.004
					APM_0067	Natural resistance-associated macrophage protein	N.D.		
	88G6	8.79	3.1 ± 0.1	0.000	APM_0067	Natural resistance-associated macrophage protein	N.D.		
	26F12	8.29	3.1 ± 0.1	0.000	APM_0070	Natural resistance-associated macrophage protein	9.37	3.2 ± 0.1	0.009
	75D10	6.52	2.7 ± 0.1	0.000	APM_0068	Manganese transport regulator MntR	19.01	4.2 ± 0.1	0.009
					APM_0070	Natural resistance-associated macrophage protein	9.37	3.2 ± 0.1	0.009
	75C11	6.29	2.7 ± 0.1	0.000	APM_3430	Natural resistance-associated macrophage protein	N.D.		
	66H1	3.65	1.9 ± 0.1	0.000	APM_2362	Cation diffusion facilitator family transporter	1.56	0.6 ± 0.0	0.002
					APM_2363	Co/Zn/Cd cation transporter-like protein	2.20	1.1 ± 0.1	0.006
					APM_2364	MerR family transcriptional regulator	3.56	1.8 ± 0.0	0.000
					APM_2365	Cation diffusion facilitator family transporter	4.80	2.3 ± 0.1	0.001
	65A3	3.32	1.7 ± 0.1	0.000	APM_0250	Probable manganese transport protein mntH	4.15	2.1 ± 0.1	0.000
	17D2	3.09	1.6 ± 0.1	0.000	APM_3432	Major facilitator transporter	N.D.		
	84D4	2.67	1.4 ± 0.1	0.000	APM_2362	Cation diffusion facilitator family transporter	1.56	0.6 ± 0.0	0.002
					APM_2363	Co/Zn/Cd cation transporter-like protein	2.20	1.1 ± 0.1	0.006
					APM_2364	MerR family transcriptional regulator	3.56	1.8 ± 0.0	0.000
					APM_2365	Cation diffusion facilitator family transporter	4.80	2.3 ± 0.1	0.001
	60A12	-2.05	-1.0 ± 0.1	0.000	APM_1712	Periplasmic solute binding protein	N.D.		
					APM_1713	ABC transporter related	-2.34	-1.2 ± 0.0	0.021

				APM_1714	ABC-3 protein	N.D.			
				APM_1715	ABC-3 protein	N.D.			
03E1	-2.58	-1.4 ± 0.1	0.000	APM_2300	ABC transporter related	-1.57	-0.7 ± 0.1	0.030
38D1	-2.67	-1.4 ± 0.1	0.000	APM_0614	Natural resistance-associated macrophage protein	-1.74	-0.8 ± 0.0	0.100

Table 17. Significantly up- and down-regulated clones after 30 min in 10 mM Ni. Clones have been arranged on the basis of the function carried out by their genes. Clone data includes the clone library ID, its ratio of expression (F), the log_2F and its associated standard error as well as the p value. Genes which expression was further validated by qRT-PCR are shown in the same line. Clones induced/repressed both in Ni and Zn are coloured in pale blue, whereas clones whose expression was altered only in Ni are left uncoloured. Genes reported or suspected to conform operons are depicted by solid or discontinued vertical bars, respectively. Induction is shown in tones of red whereas repression is highlighted in shades of green.

128 64 32 16 8 4 2 1 | -1 -2 -4 -8 -16 -32 -64 -128

	Microarray hybridization						qRT-PCR		
	Clone	F	$Log_2F \pm SE$	p	Locus	Gene	F	$Log_2F \pm SE$	p
Replication, transcription, translation and related	80A7	5.97	2.6±0.2	0.000	APM_3510	Sigma 54 modulation protein/ribosomal protein S30EA	8.98	3.2±0.1	0.010
	42F4	5.65	2.5±0.1	0.000	APM_2849	Transcriptional regulator/antitoxin, MazE	107.14	6.7±0.1	0.004
					APM_2850	ATPase involved in chromosome partitioning-like protein	5.27	2.4±0.3	0.062
					APM_2851	Hypothetical protein	3.99	2.0±0.1	0.002
					APM_2852	Rep(pMBA19a)	3.46	1.8±0.1	0.019
	08B8	4.41	2.1±0.1	0.000	APM_2850	ATPase involved in chromosome partitioning-like protein	5.27	2.4±0.3	0.062
					APM_2851	Hypothetical protein	3.99	2.0±0.1	0.002
	40E9	4.39	2.1±0.1	0.000	APM_0372	Dihydropyrimidinase	N.D.		
	10C9	3.84	1.9±0.2	0.000	APM_0238	SirA family protein	3.19	1.7±0.1	0.008
	40D6	3.81	1.9±0.1	0.000	APM_0369	Dihydropyrimidine dehydrogenase	N.D.		
	49B12	3.60	1.8±0.1	0.000	APM_3260	MobA/MobL protein	N.D.		
	25F4	3.38	1.8±0.1	0.000	APM_1229	Helicase domain-containing protein	N.D.		
	14G1	3.38	1.8±0.0	0.000	APM_2041	ClpA homolog protein	3.56	1.8±0.1	0.002
	76H10	3.28	1.7±0.1	0.000	APM_2856	Conjugal transfer protein traA	1.30	0.4±0.0	0.004
	59B9	3.20	1.7±0.1	0.000	APM_3545	Transposase, IS4 family protein	N.D.		
	84E9	3.17	1.7±0.1	0.000	APM_0899	Hypothetical protein	N.D.		
	63D5	3.16	1.7±0.1	0.000	APM_3355	Hypothetical protein	N.D.		
					APM_3356	Hypothetical protein	3.25	1.7±0.1	0.006
	58H12	3.10	1.6±0.2	0.000	APM_3260	MobA/MobL protein	N.D.		
	21D5	3.07	1.6±0.1	0.000	APM_3512	Ppx/GppA phosphatase	N.D.		
	24E10	3.05	1.6±0.1	0.000	APM_3738	Phage integrase family protein	N.D.		
	87A6	-3.55	-1.8±0.1	0.000	APM_1648	tRNA (guanine-N(7)-)-methyltransferase	N.D.		
					APM_1650	Dihydrodipicolinate reductase	-3.00	-1.6±0.2	0.014
	81A12	-3.56	-1.8±0.1	0.000	APM_0396	Ribosomal protein S20	-2.63	-1.4±0.2	0.114
					APM_0397	Chromosomal replication initiation protein	-1.69	-0.8±0.1	0.036
	87H6	-3.58	-1.8±0.1	0.000	APM_3029	50S ribosomal protein L7/L12	N.D.		
					APM_3030	DNA-directed RNA polymerase subunit beta	-3.24	-1.7±0.1	0.001
	71G7	-3.63	-1.9±0.1	0.000	APM_0527	50S ribosomal protein L35	N.D.		
					APM_0529	50S ribosomal protein L20	-3.88	-2.0±0.2	0.007
	85G2	-3.66	-1.9±0.1	0.000	APM_1834	Ribonuclease D	-2.02	-1.0±0.2	0.006
					APM_1835	Aspartyl-tRNA synthetase	-2.99	-1.6±0.2	0.010
	03A3	-3.75	-1.9±0.1	0.000	APM_R0045	16S ribosomal RNA	N.D.		
	66G6	-3.81	-1.9±0.1	0.000	APM_3107	DNA gyrase subunit B	-1.89	-0.9±0.1	0.044
					APM_3108	Cytidylate kinase	-2.62	-1.4±0.1	0.014
					APM_3109	3-phosphoshikimate 1-carboxyvinyltransferase	N.D.		
	81F9	-3.81	-1.9±0.1	0.000	APM_3058	30S ribosomal protein S13	N.D.		
					APM_3059	30S ribosomal protein S11	N.D.		
					APM_3060	DNA-directed RNA polymerase subunit alpha	-5.65	-2.5±0.1	0.001
					APM_3061	50S ribosomal protein L17	N.D.		
	56F11	-3.90	-2.0±0.1	0.000	APM_0527	50S ribosomal protein L35	N.D.		
					APM_0529	50S ribosomal protein L20	-3.88	-2.0±0.2	0.007
	79C12	-3.91	-2.0±0.1	0.000	APM_3113	Putative ribonuclease BN	-2.31	-1.2±0.1	0.000
	71C7	-3.99	-2.0±0.1	0.000	APM_3108	Cytidylate kinase	-2.62	-1.4±0.1	0.014
	41B1	-4.04	-2.0±0.1	0.000	APM_1368	Carbamoyl-phosphate synthase large chain	N.D.		
	39A7	-4.06	-2.0±0.2	0.000	APM_2510	Deoxyribodipyrimidine photolyase-related protein	-1.27	-0.3±0.1	0.067
	57F7	-4.10	-2.0±0.1	0.000	APM_0516	30S ribosomal protein S16	N.D.		
	44D12	-4.13	-2.0±0.1	0.000	APM_0527	50S ribosomal protein L35	N.D.		
					APM_0529	50S ribosomal protein L20	-3.88	-2.0±0.2	0.007
	42D9	-4.16	-2.1±0.1	0.000	APM_3048	50S ribosomal protein L5	N.D.		
					APM_3049	30S ribosomal protein S14	-2.37	-1.2±0.1	0.023
	88H9	-4.18	-2.1±0.1	0.000	APM_2129	30S ribosomal protein S1	-5.56	-2.5±0.1	0.004
	57F4	-4.20	-2.1±0.1	0.000	APM_3048	50S ribosomal protein L5	N.D.		
					APM_3049	30S ribosomal protein S14	-2.37	-1.2±0.1	0.023
					APM_3050	30S ribosomal protein S8	N.D.		
					APM_3051	50S ribosomal protein L6	N.D.		
					APM_3052	50S ribosomal protein L18	N.D.		
					APM_3053	30S ribosomal protein S5	N.D.		
	70G5	-4.25	-2.1±0.0	0.000	APM_2129	30S ribosomal protein S1	-5.56	-2.5±0.1	0.004
	75E10	-4.26	-2.1±0.1	0.000	APM_1593	Phenylalanyl-tRNA synthetase beta chain	N.D.		
					APM_1594	Phenylalanyl-tRNA synthetase, alpha subunit	N.D.		
	58H5	-4.29	-2.1±0.1	0.000	APM_1834	Ribonuclease D	-2.02	-1.0±0.2	0.006
					APM_1835	Aspartyl-tRNA synthetase	-2.99	-1.6±0.2	0.010
	89C9	-4.51	-2.2±0.1	0.000	APM_1367	Carbamoyl phosphate synthase small subunit	N.D.		
					APM_1368	Carbamoyl-phosphate synthase large chain	N.D.		

28H12	-4.52	-2.2 ± 0.1	0.000	APM_1560	RNA methyltransferase	N.D.		
76G12	-4.67	-2.2 ± 0.1	0.000	APM_0433	50S ribosomal protein L36P	-2.48	-1.3 ± 0.2	0.183
69D6	-4.69	-2.2 ± 0.1	0.000	APM_1005	50S ribosomal protein L21	-2.46	-1.3 ± 0.2	0.028
79D1	-4.85	-2.3 ± 0.1	0.000	APM_1293	DNA polymerase I	1.07	0.1 ± 0.1	0.596
				APM_1294	Deoxycytidine triphosphate deaminase	N.D.		
45C2	-4.86	-2.3 ± 0.1	0.000	APM_1404	30S ribosomal protein S2	N.D.		
				APM_1405	Elongation factor Ts	-6.90	-2.8 ± 0.1	0.004
41G6	-4.86	-2.3 ± 0.0	0.000	APM_3061	50S ribosomal protein L17	N.D.		
59D2	-5.03	-2.3 ± 0.1	0.000	APM_0396	Ribosomal protein S20	-2.63	-1.4 ± 0.2	0.114
				APM_0397	Chromosomal replication initiation protein	-1.69	-0.8 ± 0.1	0.036
55G9	-5.04	-2.3 ± 0.1	0.000	APM_0527	50S ribosomal protein L35	N.D.		
				APM_0529	50S ribosomal protein L20	-3.88	-2.0 ± 0.2	0.007
81H10	-5.05	-2.3 ± 0.1	0.000	APM_0527	50S ribosomal protein L35	N.D.		
				APM_0529	50S ribosomal protein L20	-3.88	-2.0 ± 0.2	0.007
24C3	-5.16	-2.4 ± 0.1	0.000	APM_1294	Deoxycytidine triphosphate deaminase	N.D.		
49D7	-5.31	-2.4 ± 0.1	0.000	APM_1005	50S ribosomal protein L21	-2.46	-1.3 ± 0.2	0.028
05H1	-5.32	-2.4 ± 0.1	0.000	APM_3059	30S ribosomal protein S11	N.D.		
				APM_3060	DNA-directed RNA polymerase subunit alpha	-5.65	-2.5 ± 0.1	0.001
				APM_3061	50S ribosomal protein L17	N.D.		
65G6	-5.48	-2.5 ± 0.1	0.000	APM_1648	tRNA (guanine-N(7)-)-methyltransferase	N.D.		
24H9	-5.66	-2.5 ± 0.1	0.000	APM_3031	DNA-directed RNA polymerase subunit beta'	N.D.		
				APM_3032	30S ribosomal protein S12	N.D.		
				APM_3033	30S ribosomal protein S7	N.D.		
				APM_3034	Elongation factor Tu	N.D.		
56F1	-6.24	-2.6 ± 0.2	0.000	APM_3028	50S ribosomal protein L10	-2.87	-1.5 ± 0.1	0.072
				APM_3029	50S ribosomal protein L7/L12	N.D.		
				APM_3030	DNA-directed RNA polymerase subunit beta	-3.24	-1.7 ± 0.1	0.001
48E8	-6.41	-2.7 ± 0.1	0.000	APM_3034	Elongation factor Tu	N.D.		
				APM_3035	30S ribosomal protein S10	N.D.		
20B4	-6.56	-2.7 ± 0.1	0.000	APM_3046	50S ribosomal protein L14	N.D.		
				APM_3047	50S ribosomal protein L24	N.D.		
				APM_3048	50S ribosomal protein L5	N.D.		
				APM_3049	30S ribosomal protein S14	-2.37	-1.2 ± 0.1	0.023
				APM_3050	30S ribosomal protein S8	N.D.		
87H9	-6.58	-2.7 ± 0.1	0.000	APM_1404	30S ribosomal protein S2	N.D.		
				APM_1405	Elongation factor Ts	-6.90	-2.8 ± 0.1	0.004
06E9	-6.77	-2.8 ± 0.1	0.000	APM_1003	GTPase obg	-4.85	-2.3 ± 0.2	0.023
60A1	-6.96	-2.8 ± 0.1	0.000	APM_3033	30S ribosomal protein S7	N.D.		
				APM_3034	Elongation factor Tu	N.D.		
				APM_3035	30S ribosomal protein S10	N.D.		
				APM_3036	50S ribosomal protein L3	N.D.		
				APM_3037	50S ribosomal protein L4	N.D.		
				APM_3038	Ribosomal protein L25/L23	N.D.		
03D8	-7.01	-2.8 ± 0.1	0.000	APM_3033	30S ribosomal protein S7	N.D.		
				APM_3034	Elongation factor Tu	N.D.		
63H12	-7.27	-2.9 ± 0.1	0.000	APM_3037	50S ribosomal protein L4	N.D.		
				APM_3038	Ribosomal protein L25/L23	N.D.		
				APM_3039	50S ribosomal protein L2	-3.29	-1.7 ± 0.1	0.01
				APM_3040	30S ribosomal protein S19	N.D.		
				APM_3041	50S ribosomal protein L22	N.D.		
				APM_3042	30S ribosomal protein S3	-3.24	-1.7 ± 0.0	0.01
				APM_3043	50S ribosomal protein L16	N.D.		
				APM_3044	Ribosomal protein L29	N.D.		
				APM_3045	30S ribosomal protein S17	N.D.		
				APM_3046	50S ribosomal protein L14	N.D.		
02D7	-7.74	-3.0 ± 0.1	0.000	APM_0433	50S ribosomal protein L36P	-2.48	-1.3 ± 0.2	0.183
70A12	-8.00	-3.0 ± 0.1	0.000	APM_0516	30S ribosomal protein S16	N.D.		
				APM_0517	Ribosome maturation factor rimM	-5.62	-2.5 ± 0.1	0.052
				APM_0518	tRNA (guanine-N1)-methyltransferase	N.D.		
				APM_0519	50S ribosomal protein L19	N.D.		
12G5	-8.04	-3.0 ± 0.1	0.000	APM_3035	30S ribosomal protein S10	N.D.		
27F3	-8.16	-3.0 ± 0.1	0.000	APM_3033	30S ribosomal protein S7	N.D.		
				APM_3034	Elongation factor Tu	N.D.		
				APM_3035	30S ribosomal protein S10	N.D.		
				APM_3036	50S ribosomal protein L3	N.D.		
				APM_3037	50S ribosomal protein L4	N.D.		
25C1	-8.37	-3.1 ± 0.1	0.000	APM_0517	Ribosome maturation factor rimM	-5.62	-2.5 ± 0.1	0.052
				APM_0518	tRNA (guanine-N1)-methyltransferase	N.D.		
80D11	-8.67	-3.1 ± 0.1	0.000	APM_3037	50S ribosomal protein L4	N.D.		
				APM_3038	Ribosomal protein L25/L23	N.D.		
				APM_3039	50S ribosomal protein L2	-3.29	-1.7 ± 0.1	0.011
				APM_3040	30S ribosomal protein S19	N.D.		

Energy-yielding processes	69A3	36.31	5.2 ± 0.1	0.000	APM_0195	MmgE/PrpD family protein	47.64	5.6 ± 0.0	0.000
					APM_0196	Methylitaconate delta2-delta3-isomerase	33.04	5.0 ± 0.0	0.000
					APM_0197	Hypothetical protein	N.D.		
					APM_0198	Putative transcriptional regulator	21.48	4.4 ± 0.1	0.003
	61H9	24.38	4.6 ± 0.1	0.000	APM_0196	Methylitaconate delta2-delta3-isomerase	33.04	5.0 ± 0.0	0.000
					APM_0197	Hypothetical protein	N.D.		
					APM_0198	Putative transcriptional regulator	21.48	4.4 ± 0.1	0.003
					APM_0199	Tricarballylate dehydrogenase	32.26	5.0 ± 0.1	0.002
	44F11	22.06	4.5 ± 0.1	0.000	APM_0196	Methylitaconate delta2-delta3-isomerase	33.04	5.0 ± 0.0	0.000
					APM_0197	Hypothetical protein	N.D.		
					APM_0198	Putative transcriptional regulator	21.48	4.4 ± 0.1	0.003
	20E6	15.18	3.9 ± 0.1	0.000	APM_0197	Hypothetical protein	N.D.		
	11D7	15.00	3.9 ± 0.1	0.000	APM_0193	AraC family transcriptional regulator	2.07	1.1 ± 0.1	0.012
					APM_0195	MmgE/PrpD family protein	47.64	5.6 ± 0.0	0.000
	84D12	12.51	3.6 ± 0.1	0.000	APM_0133	Alanine dehydrogenase	3.88	2.0 ± 0.0	0.000
					APM_0134	XRE family transcriptional regulator	1.79	0.8 ± 0.1	0.002
	28D4	9.73	3.3 ± 0.1	0.000	APM_0199	Tricarballylate dehydrogenase	32.26	5.0 ± 0.1	0.002
	62A1	9.66	3.3 ± 0.1	0.000	APM_1444	NADH-quinone oxidoreductase subunit C/D	10.61	3.4 ± 0.1	0.004
					APM_1445	NADH-quinone oxidoreductase subunit C/D	N.D.		
					APM_1446	NADH-quinone oxidoreductase, E subunit	N.D.		
					APM_1447	NADH dehydrogenase (quinone)	N.D.		
					APM_1448	NADH-quinone oxidoreductase, chain G	N.D.		
	39D1	8.45	3.1 ± 0.1	0.000	APM_1443	NADH-quinone oxidoreductase subunit B 2	N.D.		
					APM_1444	NADH-quinone oxidoreductase subunit C/D	10.61	3.4 ± 0.1	0.004
	22B4	8.22	3.0 ± 0.1	0.000	APM_0133	Alanine dehydrogenase	3.88	2.0 ± 0.0	0.000
					APM_0134	XRE family transcriptional regulator	1.79	0.8 ± 0.1	0.002
	04D7	8.21	3.0 ± 0.1	0.000	APM_1443	NADH-quinone oxidoreductase subunit B 2	N.D.		
					APM_1444	NADH-quinone oxidoreductase subunit C/D	10.61	3.4 ± 0.1	0.004
					APM_1445	NADH-quinone oxidoreductase subunit C/D	N.D.		
					APM_1446	NADH-quinone oxidoreductase, E subunit	N.D.		
	47B2	5.49	2.5 ± 0.1	0.000	APM_1442	NADH-quinone oxidoreductase subunit A	N.D.		
					APM_1443	NADH-quinone oxidoreductase subunit B 2	N.D.		
					APM_1444	NADH-quinone oxidoreductase subunit C/D	10.61	3.4 ± 0.1	0.004
					APM_1445	NADH-quinone oxidoreductase subunit C/D	N.D.		
					APM_1446	NADH-quinone oxidoreductase, E subunit	N.D.		
	07A4	4.53	2.2 ± 0.1	0.000	APM_0133	Alanine dehydrogenase	3.88	2.0 ± 0.0	0.000
					APM_0134	XRE family transcriptional regulator	1.79	0.8 ± 0.1	0.002
					APM_0136	Glutamine synthetase, catalytic region	-1.32	-0.4 ± 0.1	0.021
	75D6	4.40	2.1 ± 0.1	0.000	APM_1442	NADH-quinone oxidoreductase subunit A	N.D.		
					APM_1443	NADH-quinone oxidoreductase subunit B 2	N.D.		
					APM_1444	NADH-quinone oxidoreductase subunit C/D	10.61	3.4 ± 0.1	0.004
					APM_1445	NADH-quinone oxidoreductase subunit C/D	N.D.		
	15F5	4.11	2.0 ± 0.1	0.000	APM_0197	Hypothetical protein	N.D.		
					APM_0198	Putative transcriptional regulator	21.48	4.4 ± 0.1	0.003
	07F10	3.87	2.0 ± 0.1	0.000	APM_2088	Cytochrome c-like protein	N.D.		
	83B7	3.84	1.9 ± 0.1	0.000	APM_1807	NAD-glutamate dehydrogenase	N.D.		
	71H3	3.34	1.7 ± 0.1	0.000	APM_0133	Alanine dehydrogenase	3.88	2.0 ± 0.0	0.000
	05B8	3.15	1.7 ± 0.1	0.000	APM_0273	Cytochrome c oxidase (B(O/a)3-type) chain II	N.D.		
					APM_0274	Cytochrome c oxidase, subunit I	N.D.		
	83D6	3.07	1.6 ± 0.1	0.000	APM_3780	5-aminolevulinate synthase	N.D.		
	22H8	-3.56	-1.8 ± 0.0	0.000	APM_1258	NADH-quinone oxidoreductase subunit D	N.D.		
					APM_1259	NADH (or F420H2) dehydrogenase, subunit C	N.D.		
					APM_1260	NADH-quinone oxidoreductase subunit B 1	N.D.		
					APM_1261	NADH-ubiquinone/plastoquinone oxidoreductase, chain 3	N.D.		
	52G7	-3.60	-1.8 ± 0.1	0.000	APM_3839	Glyceraldehyde-3-phosphate dehydrogenase, type I	-2.19	-1.1 ± 0.1	0.067
					APM_3840	Phosphoglycerate kinase	N.D.		
	26A8	-3.61	-1.9 ± 0.1	0.000	APM_1178	ATP synthase subunit a	-2.42	-1.3 ± 0.0	0.019
					APM_1179	H+-transporting two-sector ATPase, C subunit	N.D.		
					APM_1180	ATP synthase subunit b 2	N.D.		
					APM_1181	ATP synthase subunit b 1	N.D.		
	74B7	-3.63	-1.9 ± 0.1	0.000	APM_1255	NADH-quinone oxidoreductase subunit G	N.D.		
					APM_1256	NADH dehydrogenase [ubiquinone] flavoprotein 1, mitochondrial	N.D.		
					APM_1257	NADH-quinone oxidoreductase, E subunit	-2.14	-1.1 ± 0.1	0.001
					APM_1258	NADH-quinone oxidoreductase subunit D	N.D.		
	51D3	-3.79	-1.9 ± 0.1	0.000	APM_1094	2-oxoglutarate dehydrogenase E1 component	-2.21	-1.1 ± 0.1	0.010
					APM_1095	Succinyl-CoA synthetase, alpha subunit	N.D.		
	14F5	-3.82	-1.9 ± 0.1	0.000	APM_1255	NADH-quinone oxidoreductase subunit G	N.D.		
					APM_1256	NADH dehydrogenase [ubiquinone] flavoprotein 1, mitochondrial	N.D.		
					APM_1257	NADH-quinone oxidoreductase, E subunit	-2.14	-1.1 ± 0.1	0.001
					APM_1258	NADH-quinone oxidoreductase subunit D	N.D.		
					APM_1259	NADH (or F420H2) dehydrogenase, subunit C	N.D.		
					APM_1260	NADH-quinone oxidoreductase subunit B 1	N.D.		
	28A4	-3.97	-2.0 ± 0.1	0.000	APM_1256	NADH dehydrogenase [ubiquinone] flavoprotein 1, mitochondrial	N.D.		
					APM_1257	NADH-quinone oxidoreductase, E subunit	-2.14	-1.1 ± 0.1	0.001
	68C11	-4.34	-2.1 ± 0.0	0.000	APM_3406	Cytochrome c biogenesis protein transmembrane region	-1.63	-0.7 ± 0.1	0.029
					APM_3409	Redoxin domain-containing protein	1.68	0.7 ± 0.1	0.048
	02C11	-4.45	-2.2 ± 0.1	0.000	APM_1929	ATP synthase subunit beta	N.D.		
					APM_1930	ATP synthase gamma chain	-3.13	-1.6 ± 0.1	0.012
					APM_1931	ATP synthase subunit alpha	N.D.		
	51A3	-4.56	-2.2 ± 0.1	0.000	APM_1177	ATP synthase I chain	N.D.		
					APM_1178	ATP synthase subunit a	-2.42	-1.3 ± 0.0	0.019
	90B4	-4.82	-2.3 ± 0.1	0.000	APM_1530	Malonyl CoA-acyl carrier protein transacylase (MCT)	N.D.		

	08D5	-4.83	-2.3 ± 0.0	0.000	APM_1258	NADH-quinone oxidoreductase subunit D	N.D.		
					APM_1259	NADH (or F420H2) dehydrogenase, subunit C	N.D.		
					APM_1260	NADH-quinone oxidoreductase subunit B 1	N.D.		
					APM_1261	NADH-ubiquinone/plastoquinone oxidoreductase, chain 3	N.D.		
	89D6	-6.34	-2.7 ± 0.1	0.000	APM_1259	NADH (or F420H2) dehydrogenase, subunit C	N.D.		
					APM_1260	NADH-quinone oxidoreductase subunit B 1	N.D.		
					APM_1261	NADH-ubiquinone/plastoquinone oxidoreductase, chain 3	N.D.		
Metal homeostasis	78F6	17.30	4.1 ± 0.1	0.000	APM_0067	Natural resistance-associated macrophage protein	N.D.		
					APM_0068	Manganese transport regulator MntR	30.57	4.9 ± 0.1	0.008
	10F9	16.63	4.1 ± 0.1	0.000	APM_0066	MgtC/SapB transporter	4.85	2.3 ± 0.1	0.010
					APM_0067	Natural resistance-associated macrophage protein	N.D.		
					APM_0068	Manganese transport regulator MntR	30.57	4.9 ± 0.1	0.008
	51F7	12.85	3.7 ± 0.1	0.000	APM_0067	Natural resistance-associated macrophage protein	N.D.		
					APM_0068	Manganese transport regulator MntR	30.57	4.9 ± 0.1	0.008
					APM_0070	Natural resistance-associated macrophage protein	5.11	2.4 ± 0.1	0.001
	88G6	12.55	3.7 ± 0.1	0.000	APM_0067	Natural resistance-associated macrophage protein	N.D.		
	74D6	12.43	3.6 ± 0.1	0.000	APM_0066	MgtC/SapB transporter	4.85	2.3 ± 0.1	0.010
					APM_0067	Natural resistance-associated macrophage protein	N.D.		
	57G6	8.76	3.1 ± 0.1	0.000	APM_0067	Natural resistance-associated macrophage protein	N.D.		
					APM_0068	Manganese transport regulator MntR	30.57	4.9 ± 0.1	0.008
					APM_0070	Natural resistance-associated macrophage protein	5.11	2.4 ± 0.1	0.001
	09E11	8.44	3.1 ± 0.2	0.000	APM_3382	Transcriptional regulator, ArsR family	12.75	3.7 ± 0.1	0.001
	26F12	8.42	3.1 ± 0.1	0.000	APM_0070	Natural resistance-associated macrophage protein	5.11	2.4 ± 0.1	0.001
	49E11	6.87	2.8 ± 0.1	0.000	APM_0067	Natural resistance-associated macrophage protein	N.D.		
					APM_0068	Manganese transport regulator MntR	30.57	4.9 ± 0.1	0.008
					APM_0070	Natural resistance-associated macrophage protein	5.11	2.4 ± 0.1	0.001
	39D8	6.70	2.7 ± 0.1	0.000	APM_0067	Natural resistance-associated macrophage protein	N.D.		
					APM_0068	Manganese transport regulator MntR	30.57	4.9 ± 0.1	0.008
					APM_0070	Natural resistance-associated macrophage protein	5.11	2.4 ± 0.1	0.001
	19F8	5.92	2.6 ± 0.1	0.000	APM_0773	ModE family transcriptional regulator	N.D.		
					APM_0774	ABC-type molybdate transport system periplasmic component-like protein	7.21	2.9 ± 0.1	0.002
	75D10	5.81	2.5 ± 0.1	0.000	APM_0068	Manganese transport regulator MntR	30.57	4.9 ± 0.1	0.008
					APM_0070	Natural resistance-associated macrophage protein	5.11	2.4 ± 0.1	0.001
	84D4	5.32	2.4 ± 0.1	0.000	APM_2362	Cation diffusion facilitator family transporter	2.03	1.0 ± 0.1	0.003
					APM_2363	Co/Zn/Cd cation transporter-like protein	3.93	2.0 ± 0.2	0.014
					APM_2364	MerR family transcriptional regulator	2.87	1.5 ± 0.1	0.007
					APM_2365	Cation diffusion facilitator family transporter	7.80	3.0 ± 0.1	0.002
	71E2	4.50	2.2 ± 0.1	0.000	APM_0110	Major facilitator transporter	2.35	1.2 ± 0.1	0.005
	57B2	4.39	2.1 ± 0.1	0.000	APM_3385	Arsenite oxidase, large subunit	N.D.		
	74B1	4.20	2.1 ± 0.1	0.000	APM_0110	Major facilitator transporter	2.35	1.2 ± 0.1	0.005
	66H1	4.11	2.0 ± 0.0	0.000	APM_2362	Cation diffusion facilitator family transporter	2.03	1.0 ± 0.1	0.003
					APM_2363	Co/Zn/Cd cation transporter-like protein	3.93	2.0 ± 0.2	0.014
					APM_2364	MerR family transcriptional regulator	2.87	1.5 ± 0.1	0.007
					APM_2365	Cation diffusion facilitator family transporter	7.80	3.0 ± 0.1	0.002
	76C7	4.11	2.0 ± 0.1	0.000	APM_3385	Arsenite oxidase, large subunit	N.D.		
	88B1	3.88	2.0 ± 0.1	0.000	APM_2067	Major facilitator transporter	N.D.		
	47C8	3.87	2.0 ± 0.1	0.000	APM_1213	Hypothetical protein	N.D.		
	71C4	3.84	1.9 ± 0.1	0.000	APM_3385	Arsenite oxidase, large subunit	N.D.		
	14D8	3.72	1.9 ± 0.1	0.000	APM_0110	Major facilitator transporter	2.35	1.2 ± 0.1	0.005
	41E6	3.69	1.9 ± 0.1	0.000	APM_3385	Arsenite oxidase, large subunit	N.D.		
	53F5	3.20	1.7 ± 0.1	0.000	APM_0774	ABC-type molybdate transport system periplasmic component-like protein	7.21	2.9 ± 0.1	0.002
	89D1	3.17	1.7 ± 0.1	0.000	APM_3385	Arsenite oxidase, large subunit	N.D.		
	67H1	3.11	1.6 ± 0.1	0.000	APM_0893	Regulatory protein, ArsR	N.D.		
					APM_0894	Arsenate reductase	N.D.		
					APM_0895	Arsenical pump membrane protein	4.82	2.3 ± 0.1	0.000
	36C6	-3.70	-1.9 ± 0.1	0.000	APM_1490	Hydrophobe/amphiphile efflux-1 (HAE1) family protein	N.D.		
	88H4	-3.79	-1.9 ± 0.1	0.000	APM_2999	Hypothetical protein	N.D.		
	79A2	-3.81	-1.9 ± 0.0	0.000	APM_1490	Hydrophobe/amphiphile efflux-1 (HAE1) family protein	N.D.		
	28E12	-3.91	-2.0 ± 0.1	0.000	APM_1490	Hydrophobe/amphiphile efflux-1 (HAE1) family protein	N.D.		
Amino acid transport and biosynthesis	64B12	14.42	3.8 ± 0.2	0.000	APM_3715	Ornithine cyclodeaminase	2.14	1.1 ± 0.1	0.005
	29B5	-3.59	-1.8 ± 0.0	0.000	APM_0780	Amine oxidase	N.D.		
	41C1	-3.78	-1.9 ± 0.1	0.000	APM_1645	Inner-membrane translocator	N.D.		
					APM_1646	Inner-membrane translocator	N.D.		
	28G12	-3.79	-1.9 ± 0.1	0.000	APM_1643	ABC transporter related	N.D.		
					APM_1644	ABC transporter related	N.D.		
	28G12	-3.79	-1.9 ± 0.1	0.000	APM_1645	Inner-membrane translocator	N.D.		
	54F3	-3.97	-2.0 ± 0.1	0.000	APM_1643	ABC transporter related	N.D.		
					APM_1644	ABC transporter related	N.D.		
					APM_1645	Inner-membrane translocator	N.D.		
	35A9	-4.26	-2.1 ± 0.1	0.000	APM_0535	ABC transporter related	N.D.		
					APM_0536	ABC-type branched-chain amino acid transport systems periplasmic component-like protein	N.D.		
					APM_0537	Inner-membrane translocator	N.D.		
	10D6	-4.31	-2.1 ± 0.1	0.000	APM_0734	Glutamate synthase [NADPH] large chain	N.D.		
	76A1	-4.94	-2.3 ± 0.1	0.000	APM_1468	Ketol-acid reductoisomerase	N.D.		
	12F12	-5.15	-2.4 ± 0.1	0.000	APM_1664	Aspartate kinase	N.D.		
Other functions	53A11	6.97	2.8 ± 0.1	0.000	APM_3836	Glycosyl transferase family protein	N.D.		
	36F10	5.25	2.4 ± 0.1	0.000	APM_3547	Hypothetical protein	N.D.		
	30G11	5.10	2.3 ± 0.1	0.000	APM_1503	Nitrile hydratase	3.40	1.8 ± 0.0	0.000
	41E10	4.51	2.2 ± 0.1	0.000	APM_1503	Nitrile hydratase	3.40	1.8 ± 0.0	0.000
	74G7	3.45	1.8 ± 0.1	0.000	APM_3225	Beta alanine--pyruvate transaminase	3.15	1.7 ± 0.1	0.008

58D4	3.20	1.7 ± 0.1	0.000	APM_2411	Sulfotransferase	N.D.			
02D4	3.20	1.7 ± 0.1	0.000	APM_0355	Hypothetical protein	N.D.			
18H12	3.19	1.7 ± 0.0	0.000	APM_2516	2-nitropropane dioxygenase, NPD	N.D.			
34E11	3.11	1.6 ± 0.1	0.000	APM_3836	Glycosyl transferase family protein	N.D.			
40B5	3.10	1.6 ± 0.1	0.000	APM_3262	Hypothetical protein	N.D.			
73B7	3.01	1.6 ± 0.1	0.000	APM_2411	Sulfotransferase	N.D.			
54B4	-3.76	-1.9 ± 0.1	0.000	APM_0987	Serine-type D-Ala-D-Ala carboxypeptidase	-1.93	-0.9 ± 0.0	0.009	
05H9	-3.88	-2.0 ± 0.1	0.000	APM_1391	Fe-S metabolism associated SufE	-2.60	-1.4 ± 0.2	0.013	
34H12	-3.89	-2.0 ± 0.1	0.000	APM_2440	GTPase EngB	-3.03	-1.6 ± 0.1	0.030	
					Inner membrane protein oxaA	-2.54	-1.3 ± 0.0	0.024	
43G6	-4.79	-2.3 ± 0.0	0.000	APM_0890	Hypothetical protein	N.D.			
54G10	-5.03	-2.3 ± 0.1	0.000	APM_1922	FkbM family methyltransferase	N.D.			

4.4.2.3. Early transcriptomic changes in response to Ni

The addition of 10 mM Ni unleashed a rapid transcriptomic response that led to cell growth arrest (via the repression of DNA replication and transcription, protein biosynthesis, and synthesis of ATP). Among the up-regulated genes are many involved in cation homeostasis, stress response and survival, as well as an operon related to the 2-methylcitrate cycle.

Toxin-antitoxin systems

Plasmid-encoded antitoxin *mazE* is the most up-regulated gene in the presence of Ni. The expression of *mazE* increases 32-fold five minutes after the addition of Ni and rises to over 100-fold after thirty minutes. *mazE* is part of the operon-encoded toxin-antitoxin (TA) system *mazEF*, which was first described in *E. coli* (Aizenman *et al.*, 1996). Toxin MazF is a stable protein that inhibits translation through the cleavage of mRNAs, whereas antitoxin MazE is a labile protein that binds MazF, blocking its toxic effects. Under stress conditions the antitoxin is degraded by stress-induced proteases releasing the toxin and leading to cell growth arrest or even cell death. In *Acidiphilium* sp. PM, Ni induces the transcription of this TA system.

TA systems are known to mediate in many cellular processes including programed cell death, cell growth arrest, persistency, antibiotic tolerance and resistance, biofilm formation and general stress response. *E. coli* MazEF loci were originally believed to cause programmed cell death although recent evidence suggests it might indeed trigger cell growth arrest, leading to dormancy or persistency [reviewed in (Gerdes *et al.*, 2005; Yamaguchi *et al.*, 2011)].

Whether MazEF mediates programmed cell death or induces cell growth arrest and dormancy in response to Ni is unclear. However, as explained below, *Acidiphilium* sp. PM is actively inhibiting DNA replication and transcription, protein biosynthesis and central metabolism while favouring alternative production of energy, biosynthesis of amino acids and the synthesis of stress-related proteins. In our opinion, this seems more of an active

strategy to arrest cell growth than a programmed cell death. Moreover, programmed cell death usually occurs over a short period of time (typically hours). The fact that Ni induces cell death over a five-day period also suggests that *Acidiphilium* sp. PM is failing to cope with Ni toxicity rather than responding to a suicide signal.

Interestingly, an homologous MazEF TA system can be found in *Acp. cryptum* JF5 but not in *Acp. multivorum* AIU301. If (and how) these TA systems result in different tolerance to stress in various *Acidiphilium* strains is an intriguing question.

Alarmone (p)ppGpp

Two proteins known to interact with (p)ppGpp (GTPase obg and Ppx/GppA phosphatase) have significant changes in their expression upon addition of Ni.

Alarmone (p)ppGpp is a small nucleotide, first described as the master key in the stringent response that follows amino acid starvation. It is now known that (p)ppGpp can also signal fatty acid starvation, iron and phosphate limitation, heat shock and other stresses. (p)ppGpp acts at multiple levels; among others, it inhibits protein synthesis (and therefore cell growth), transcription of *rrn* operons (halting ribosome biogenesis), transcription of rRNA (inhibiting transcription) and redirects transcription to genes involved in stress response and survival and in amino acid biosynthesis [for reviews on the topic see (Potrykus and Cashel, 2008; Dalebroux and Swanson, 2012)].

A group of family protein exists that is responsible for (p)ppGpp synthesis and degradation. Two of these proteins present differential gene expression upon addition of Ni; The induced Ppx/GppA phosphatase is involved in the breakdown of guanosine pentaphosphate (pppGpp) to guanosine tetraphosphate (ppGpp) (Reizer *et al.*, 1993), which is eight times more efficient than pppGpp in triggering the stringent response. GTPase obg, on the other hand, binds ppGpp and contributes to the regulation of the stringent response to amino acid starvation (Persky *et al.*, 2009).

This finding is of particular interest because, as discussed below, much of the response of *Acidiphilium* sp. PM to Ni, resembles a classic stringent response triggered by the alarmone.

DNA replication

DNA replication initiator protein DnaA, primosome assembly protein PriA, DNA gyrase subunit B and DNA ligase, all which genes are key to DNA replication, were

repressed in the presence of Ni. On the other hand, the expression of *sirA* (which in *B. subtilis* inhibits replication by binding to DnaA (Wagner *et al.*, 2009)) was found to be up-regulated.

The pool of precursors necessary for the *de novo* synthesis of DNA and RNA was also compromised as deduced by the down-regulation of several pyrimidine biosynthesis genes (dCTP deaminase, cytidylate kinase, carbamoyl-phosphate synthase, orotate phosphoribosyltransferase) and the up-regulation of their catabolism (dihydropyriminidase and dihydropyrimidine dehydrogenase). Interestingly, the resulting imbalance in the pool of dNTPs could not only cause an overall drop in DNA replication but could lead to increased mutation rates, as reported in *E. coli* (Schaaper and Mathews, 2013). Moreover, a DNA glycosylase homolog to *E. coli*'s MutY (involved in DNA repair) is also down-regulated. Whether changes in the expression of these genes result in increased mutation rates, has not been tested. Yet, increased resistance to Ni as a result of a point mutation (in Mg^{2+} transport system CorA) has been described in *S. cerevisiae* (Sarikaya *et al.*, 2006).

On the other hand, a decrease in the initiating NTPs, is known to cause inefficient transcription of ribosomal RNA, hence hindering ribosome biogenesis (Gaal *et al.*, 1997).

Transcription and translation

Ribosomal protein (r-protein) operons account for a large portion of the genes repressed by Ni (Table 16 and Table 17). These evolutionary-conserved operons harbour genes involved in the synthesis of RNA, the assembly and maturation of the ribosome, the maturation of tRNAs and the elongation of the polypeptide chain, revealing an intricate, interdependent regulation of transcription and translation. Figure 39 illustrates the down-regulation of six of these operons caused by exposing *Acidiphilium* sp. PM cells to Ni.

The down-regulation of *rpoA*, *rpoB* and *rpoC* (encoding core RNA polymerase subunits α, β, and β', respectively) exposes an imminent drop in cell transcription levels, and ultimately in protein synthesis. Up-regulation of a σ^{54} transcriptional regulator (Fis family GAF modulated sigma54 specific transcriptional regulator) points to the transcription of genes alternative to those expressed by the housekeeping sigma factor, σ^{70}. Unlike other σ factors, σ^{54}- dependent promoters transcribe disparate genes with a variety of functions (Cases *et al.*, 2003).

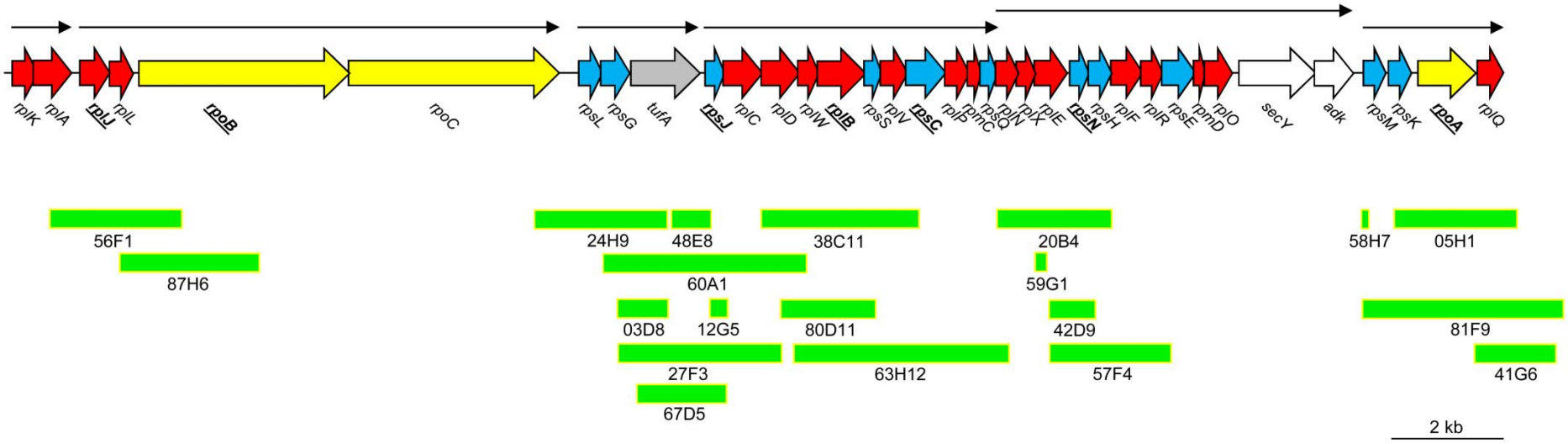

Figure 39. Down-regulation of ribosomal protein operons upon addition of Ni. The figure shows a *ca.* 28 kb fragment of ctg. 0604 (AFPR01000475) comprising 6 ribosomal protein operons (top). Microarray clones overlapping with that region are shown below. All the clones shown were found to be repressed after 30 min in Ni. The color code for the ORFs is as follows: turquoise: ribosomal proteins of the small (30S) subunit; red: ribosomal proteins of the large (50S) subunit; yellow: RNA polymerase subunits; grey: other genes involved in translation; white: genes with unrelated functions. Green rectangles represent microarray clones whose expression was repressed in the presence of Ni. Genes whose expression was further validated by qRT-PCR are shown in bold, underlined italics. Horizontal arrows on top of the ORFs illustrate transcriptional units (operons) in *E. coli* (Lemke *et al.*, 2011).

Protein synthesis is further compromised by deficient ribosome assembly. The expression of 37 of 55 r-proteins contained in the ribosome is repressed, and so are the transcription and maturation of the ribosome's structural rRNAs (16S rRNA and ribosomal RNA large subunit methyltransferase N). Other genes involved in the maturation of the ribosome (*rimM*) and the elongation of the polypeptide chain during translation (EF-Tu, EF-Ts and a translation-associated GTPase) were also found to be down-regulated.

Furthermore, the synthesis of aminoacyl-tRNAs is repressed as seen by the down-regulation of aspartyl- and phenylalanyl-tRNA synthetases and of several enzymes involved in the maturation of tRNAs (tRNA (guanine-N1)-methyltransferase, tRNA (guanine-N(7)-)-methyltransferase, ribonuclease D and putative ribonuclease BN). This reduction of aminoacyl-tRNAs triggers a reduction of the transcription and translation levels in the cell.

Overall, this data reveals a quick drop in protein synthesis. Yet, as noted by Maivali and co-workers, after entering stationary phase, intact ribosomes are still stable and enable the synthesis of proteins necessary for survival (Piir *et al.*, 2011).

Energy metabolism

The expression of glycolysis genes *gapdh* and *pgk* (encoding GAPDH and phosphoglycerate kinase, respectively), and of TCA cycle genes *lpd*, *sucA* and *sucD* (Lpd and SucA are part of 2-oxoglutarate dehydrogenase complex whereas *sucA* and *sucD* belong to the larger *sucABCD* operon encoding alpha-ketoglutarate dehydrogenase and succinyl coenzyme A synthetase) as well as of malonyl CoA-acyl carrier protein transacylase (biosynthesis of fatty acids) is repressed in the presence of Ni. On the other hand, isocitrate lyase (glyoxylate cycle) is induced. This suggests a repression of glycolysis and of classic TCA cycle in favour of the alternative glyoxylate shunt.

As mentioned above (4.2.3) *Acidiphilium* sp. PM harbours two *nuo* operons encoding two distinct complexes I of the respiratory chain. In the presence of Ni, the expression of one the operons is repressed in favour of the other, which indicates a preferential use of these complexes depending on environmental conditions. In addition, the synthesis of new ATP via oxidative phosphorylation is further compromised by the down-regulation of ATP synthase operons *atpHAGDC* and *atpIBEGF* (encoding F_1 and F_0 complexes, respectively) and of an insertase (inner membrane protein oxaA) required for the integration of the F_0 complex in the membrane. Paradoxically, Ni induces the expression of cytochrome c oxidase subunits I and

II and of the first gene in the synthesis of tetrapyrroles (5-aminolevulinate synthase), which includes heme groups such as those found in cyt c oxidase.

Unexpectedly, many of the clones with the largest and earliest up-regulation harbour five seemingly unrelated genes: a MmgE/PrpD family protein, a methylitaconate-Δ-isomerase (mmi) (homologs of which are also annotated as PrpF), a hypothetical protein, a putative transcriptional regulator and a tricarballylate dehydrogenase (TucA) (Table 16, Table 17, Figure 40). A detailed analysis of the annotated genes MmgE/PrpD, mmi/PrpF and tucA revealed that their substrates are structurally very similar. In addition, their products are further incorporated into the TCA cycle either directly or through intermediate steps (primarily via the 2-methylicitrate (2-MC) cycle) (Figure 40). The coincidental massive up-regulation of these adjacent genes and the relatedness of the reactions they catalyze, lead us to propose that these genes may conform an operon functioning within or in conjunction to the 2-MC and TCA cycles.

Based on the role played by these genes in other microorganisms, we propose two possible functions for this putative operon. In both scenarios, the accumulation of toxic 2-MC is likely (Figure 40).

1) Role in the methyl-citrate cycle

The first two genes in this putative operon are homologs to proteins that have been annotated PrpD and PrpF, respectively. Operon *prp* encodes enzymes of the 2-MC cycle, which is involved in the catabolism of toxic propionate or propionyl-CoA, the latter which is generated in the β-oxidation of odd-numbered fatty acids (Horswill and Escalante-Semerena, 1999). Interestingly, early experiments on *Acp. multivorum*, *Acp. cryptum* and *Acp. organovorum*, reported that 0.01% propionate completely inhibited their growth (Wakao *et al.*, 1994).

Studies in *Salmonella enterica* uncovered that, in fact, propionate's toxicity arises from its catabolism to the more toxic (2S,3S)-2-methylcitrate by PrpC (Horswill *et al.*, 2001). This intermediate is further catabolized to pyruvate by PrpD, TCA aconitase/PrpF and PrpB (or isocitrate lyase in *Mycobaterium tuberculosis*). TCA cycle enzyme citrate synthase is also known to produce toxic 2-methylcitrate. Yet, contrary to PrpC, which produces stereospecific (2S,3S)-2MC isomer, citrate synthase activity yields three different isomers of 2-MC (2S,3S; 2S,3R; and 2R,3S) (van Rooyen *et al.*, 1994). Only 2S,3S- isomer can be readily degraded by stereospecific PrpD, thus resulting in the accumulation of toxic 2S,3R and 2R,3S isomers.

Intermediates of the 2-methylcitrate cycle have been found to inhibit fructose-1,6-bisphosphatase and consequently gluconeogenesis, in *S. enterica* and *M. smegmatis* (Rocco and Escalante-Semerena, 2010; Eoh and Rhee, 2014) (Figure 40). Quite remarkably, gluconeogenic enzyme fructose-1,6-bisphosphate aldolase seems to be the primary target of Ni inhibition in *E. coli* (Macomber *et al.*, 2011).

In *M. smegmatis*, the deletion of isocitrate lyases resulted in the inability to catabolize 2-MC intermediates leading to a depletion of TCA intermediates, allosteric inhibition of gluconeogenic fructose-1,6-bisphosphatase as well as an imbalance of the NADH/NAD pool. Ultimately, this caused a 10 to 100-fold reduction in cell viability over 72 h. Supplementation with TCA intermediates and induction of an alternative propionate-degrading pathways allowed growth of *M. smegmatis* only after long lag phases (Eoh and Rhee, 2014).

2) Role in the catabolism of itaconic acid

An alternative scenario is the participation of these genes in the metabolism of itaconic acid (nicotinate metabolism). Mammalian IRG1 protein, a MmgE/PrpD protein that is highly expressed in macrophages, is a reported *cis*-aconitate decarboxylase that produces itaconic acid, a potent inhibitor of isocitrate lyase (Michelucci *et al.*, 2013). Despite belonging to organisms in separate domains, *Acidiphilium* sp. PM and mouse MmgE/PrpD are 23% identical (40% similar if conservative amino acid substitutions are considered). Interestingly, in addition to the isomerization of 3-methylitaconate, methylitaconate-Δ-isomerase (mmi) can isomerize itaconic acid to citraconate (albeit with higher K_m and lower k_{cat}) (Velarde *et al.*, 2009). That is, the two adjacent genes would catalyze two consecutive reactions of the metabolism of itaconic acid (Figure 40).

Inability to effectively degrade itaconic acid would quickly inhibit isocitrate lyase and, as mentioned above, inhibition of *M. smegmatis* isocitrate lyase by itaconic acid resembles the toxicity exerted by intermediates of the 2-MC cycle in other bacteria such as *S. enterica*. It is worth noticing that the inhibitory scenario observed in *M. smegmatis* Δ*icl* mutants is remarkably similar to the effect exerted by Ni in *Acidiphilium*, including the drop in cell viability and, especially, the long lag phases required for growth in the surviving subpopulation.

In summary, the two scenarios proposed are triggered by or cause an accumulation of toxic intermediates of the 2-MC cycle, which eventually inhibits growth and causes cell death. The exact mechanism of Ni toxicity is unclear, yet we propose that Ni cations may act

on specific enzymes of the TCA cycle (*e.g.* enhancing citrate synthase residual formation of 2-MC), the 2-MC cycle (*e.g.* inhibiting the enzymes downstream 2-MC) or by inhibiting the degradation of itaconic acid. Malfunctions in these enzymes may lead to the accumulation of toxic 2-MC and trigger the up-regulation of the putative operon in an attempt to limit the damage caused by 2-MC.

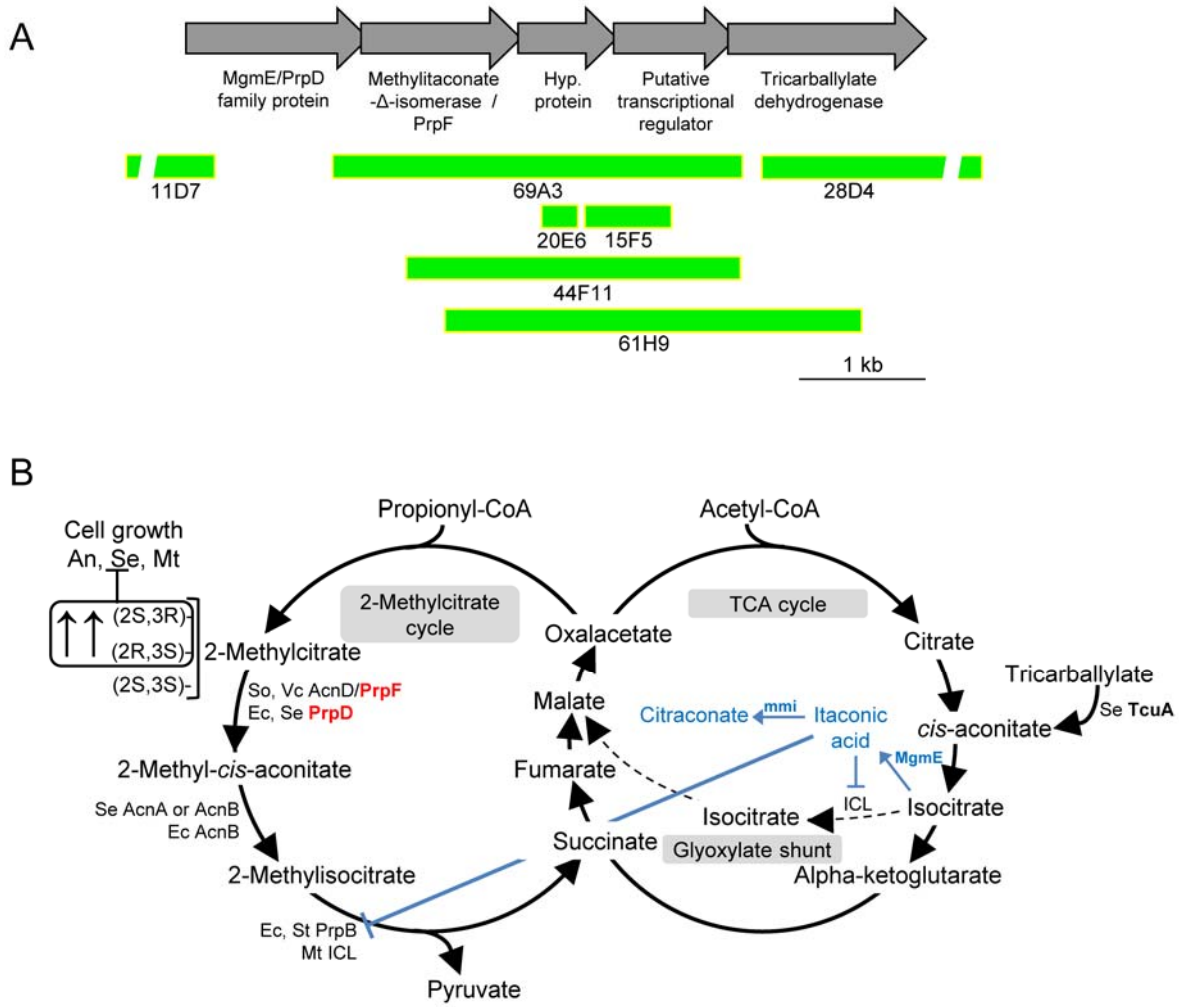

Figure 40. Enzymes related to the 2-MC and TCA cycles are possible targets of Ni toxicity. (A) Some of the clones with the earliest and greatest up-regulation contained five apparently disparate genes. Their similar up-regulation and the relatedness of their substrates and products lead us to propose that these genes actually conform an operon. (B) Two functions are contemplated for these genes: either they play a role in the 2-MC cycle (in red) or in the catabolism of itaconic acid (in blue). In both scenarios, malfunction in these or neighbouring enzymes may lead to the accumulation of toxic 2-methylcitrate, inhibiting cell growth a possibly causing cell death. Abbreviations: Acn: aconitase; MmgE / PrpD: MmgE/PrpD family protein; mmi / PrfF: methylitaconate-Δ-isomerase (homologous proteins are annotated PrpF); TucA: tricarballylate dehydrogenase; An: *Aspergillus nidulans*; Ec: *E. coli*; Mt: *M. tuberculosis*; So: *Shewanella oneidensis*; Se: *S. enterica*; St: *S. typhimurium*, Vc: *Vibrio cholerae*. Modified from (Michelucci *et al.*, 2013).

Ion homeostasis

Much as expected, the addition of Ni triggers the early expression of genes involved in cation homeostasis. In particular, a cluster of six genes encoded in one of the plasmids is found to be greatly up-regulated. This cluster includes a manganese transport regulator MntR up-regulated by 19-fold after 5 min, which rose to 31-fold after 30 min. This gene is flanked by two distinct natural resistance-associated macrophage protein (nramp) genes, a hypothetical protein exclusively found in acidophiles and a MgtC/SapB transporter (Mg^{2+} transport) (Table 16 and Table 17). MntR is a metal-responsive transcriptional regulator of the DtxR family. Representatives of this family act as repressors of genes involved in ion uptake (Pennella and Giedroc, 2005). The binding of the cation triggers a conformational change that allows binding of the repressor to DNA, hence impeding the transcription of specific uptake genes. MntR, and the two Nramp proteins have predicted Mn-binding domains, which suggest an active uptake of Mn^{2+} ions. Irving-William series predict that Mn^{2+} complexes are far less stable than Ni complexes (Irving and Williams, 1953). This could result in the displacement of Mn^{2+} ions from Mn-metalloproteins (*e.g.* superoxide dismutase), ruining their catalytic properties. The uptake of Mn^{2+} cations could therefore be a countermeasure to Ni cations flooding the cell. Indeed, a gene for a Mn transporter located outside this cluster also appears up-regulated.

Also early in the response to Ni, there is an up-regulation of a MerR transcriptional regulator, two adjacent cation diffusion facilitator family transporters and a Co/Zn/Cd cation transporter-like protein. MerR is a family of metal-binding transcriptional regulators involved in metal ion detoxification, efflux and sequestration. As opposed to ArsR/SmtB-type of regulators, MerR binding of the metal induces the activation of the resistance operon (Hobman *et al.*, 2005). Experimental evidence is required on the actual metal(s) bound by this protein; yet, significant up-regulation of this putative operon is also detected upon addition of Zn (Table 18).

Thirty minutes after the addition of Ni, an arsenite-oxidizing operon regulated by an ArsR-type regulator also appears induced. On the other hand, mild down-regulation is observed in other proteins (such as ABC transporters) which participate in the uptake of metals (Table 17).

Oxidative stress

Compared to other metals such as Fe or Cu, Ni is a poor generator of oxidative stress; yet, it is known to trigger the expression of catalase and peroxidase (as reviewed by (Macomber and Hausinger, 2011)). In *Acidiphilium* sp. PM, Ni does not increase transcription of these enzymes but it triggers the expression of rubrerythrin, a proposed H_2O_2-scavenging enzyme found in several acidophiles (Cárdenas *et al.*, 2012), and of an alkyl hydroperoxide reductase, the primary scavenger of endogenous H_2O_2 at low concentrations ($< 10^{-5}$ M) in *E. coli* (Seaver and Imlay, 2001). Interestingly, Cardenas *et al.* reported that rubrerythrin sequences from phylogenetically-distant acidophiles cluster together, indicating a possible acquisition by horizontal gene transfer (Cardenas *et al.*, 2012).

Amino acid transport and biosynthesis

The down-regulation of glutamate synthase (synthesis of glutamate), aspartate kinase (biosynthesis of lysine and proline), as well as the repression of several ABC transporters and translocators (similar to genes of the *liv* operon involved in the transport of BCAA) reveal a mild repression of the biosynthesis and import of some amino acids.

Biosynthesis of the cell wall

The slowdown in DNA replication provokes delayed cell division and, consequently, a decrease in cell wall biosynthesis is expected. Indeed, down-regulation is observed in two genes involved in the synthesis of the peptidoglycan: a serine-type D-Ala-D-Ala carboxypeptidase (involved in the crosslinking of peptidoglycan) and a rod shape-determining protein MreC (which couples the cytosolic and extracellular peptidoglycan-synthesis machinery).

N, S and Fe metabolism

The down-regulation of glutamate synthase (key for the incorporation of ammonium) together with the up-regulation of a nitrile hydratase is indicative of changes in the metabolism of N.

On the other hand, a sulfotransferase appears as the only S-related protein whose expression is modified. Taking into account that Ni was added as a SO_4^{2-} salt, which increased S availability by 66%, more S-related genes were expected to have their expression altered. The fact that S is already in excess in the defined media may account for this unexpected result.

Several down-regulated clones contained genes related to the assembly of [FeS] clusters, including Fe-S metabolism associated SufE. [FeS] clusters are found in a large number of proteins with various functions (*e.g.* complex I of the electron chain, succinate dehydrogenase, *etc.*); therefore, the implication of this slight down-regulation is uncertain.

4.4.3. Comparative transcriptomic response to Ni vs Zn in *Acidiphilium* sp. PM

To examine how specific the response to Ni was, *Acidiphilium* sp. PM cells were challenged with a different metal. Zn was chosen based on *Acidiphilium* sp. PM high tolerance to this metal (Figure 12). Cells were exposed to Zn, their RNA was then extracted, reverse-transcribed, labelled and hybridized as explained above. Hybridization data was subsequently analysed and selected clones were sequenced and mapped against the genome of *Acidiphilium* sp. PM. Unresolved clones were further analysed by qRT-PCR using fresh, DNA-free RNA. Figures illustrating these experiments can be found in APPENDIX VI. In particular, Table A 5 and Table A 6 summarize the transcriptomic changes detected 5 and 30 min after the addition of Zn. A comparison of the transcriptomic changes induced by Ni and Zn (as determined by qRT-PCR) is shown in Table 18.

Overall, transcriptomic responses to Ni and Zn were largely similar. To highlight these similarities, clones differentially expressed both with Ni and Zn are coloured blue throughout the tables (Table 17, Table 18, Table A 3, Table A 5, and Table A 6). Upon addition of either metal, the expression of genes involved in DNA replication, transcription and translation appeared down-regulated, and particularly so in the presence of Zn. In addition, Zn triggered the use of alternative heat-shock sigma factor (σ^{32}), which was uncalled for when cells were exposed to Ni. Interestingly, Zn did not trigger the massive expression of operon *mazEF* seen with Ni.

Negative regulation of rRNA expression (hence of ribosome biogenesis) can be mediated by ppGpp and amplified by the binding of DksA transcription factor to RNA polymerase. DksA also binds directly to RNA polymerase, inhibiting transcription initiation and transcript elongation (Paul *et al.*, 2004). While addition of Ni causes no major changes in *dksA* expression, Zn triggers a massive repression of TraR/DksA family transcriptional regulator after 30 min. Even though this may seem unexpected, *dksA* down-regulation could indicate that effective repression of transcription and ribosome biogenesis is readily achieved already 30 min after the addition of Zn. In this scenario, further repression of protein synthesis could be counterproductive since stress response proteins need to be synthesized.

Zn-induced mild down-regulation of ribonuclease R (which selectively degrades tRNA, rRNA, and mRNAs with extensive secondary structure) seems to support this hypothesis.

Other differences in the response to Ni vs Zn, are Zn-mediated up-regulation of a plasmid-encoded recombinase and of ribonucleotide-diphosphate reductase (critical for the regulation of DNA synthesis) and the down-regulation of genes encoding DNA polymerase I (crucial to replication), and RadA (which participates in DNA repair via homologous recombination). Moreover, larger up-regulation of several chaperone genes (*clpB*, *dnaK* and a gene encoding a ClpA homolog protein) induced by Zn may suggest that it could be causing greater damage to proteins than Ni. Zn also causes a major down-regulation of an RNaseE-domain containing ribonuclease (involved in ribosome maturation), of *tatC* (an enzyme of the Tat protein export pathway not affected by Ni) and of a C-terminal processing peptidase.

Regarding central metabolism, an overall drop in energy production is observed when either metal is added: genes encoding ATP synthase F_0 and F_1 complexes are down-regulated (particularly so in the presence of Zn), one *nuo* operon encoding NADH-dehydrogenase complex is repressed in favour of the other (possibly indicating a preferential use based on energy demand or on environmental conditions), and at least two TCA cycle (*lpd, sucA*) and two glycolytic genes (*gapdh* and *pgk*) are down-regulated. In addition, Zn triggers the repression of Entner-Doudoroff-specific *edd* and *eda* genes (encoding phosphogluconate dehydratase and ketohydroxyglutarate aldolase, respectively) and of gluconeogenic fructose-1,6-bisphosphatase. Interestingly, another enzyme of the gluconeogenesis pathway (fructose-1,6-bisphosphate aldolase) has been identified as the primary target of Ni toxicity in *E. coli* (Macomber *et al.*, 2011). Indirect energy-saving strategies are also observed in the presence of both Ni and Zn; for instance, AMP salvage reaction catalyzed by adenine phosphoribosyltransferase (as opposed to the costly *de novo* AMP synthesis). Alternative pathways, such as the glyoxylate shunt are activated, as deducted from the up-regulation of isocitrate lyase.

A major difference in *Acidiphilium* sp. PM response to Zn vs Ni is the massive up-regulation of 2-MC-related genes triggered by Ni but not by Zn. This supports our hypothesis that specific enzymes of the TCA and 2-MC cycles or the degradation of itaconic acid could be the primary targets of Ni toxicity. Indeed, enzyme poisoning by cations is rather metal-specific because metals have different affinities (*e.g.* Hg^{2+} and Cd^{2+} tend to bind thiol groups in cysteines).

As anticipated above, the expression profiles of genes involved in metal homeostasis is fundamentally different when *Acidiphilium* sp. PM is challenged with Ni or with Zn. As shown in Table 18, Ni-massively-induced MntR repressor (APM_0068) is greatly repressed with Zn, as is an adjacent MgtC/SapB (APM_0066). Yet, a nearby Nramp-protein (APM_0070) gene is greatly up-regulated both with Ni and Zn. On the other hand, while Ni prompts no significant changes in its expression, Zn induces a rapid 50-fold up-regulation of a MarR-type transcriptional regulator, adjacent to a 24-fold up-regulated transenvelope MFS transporter. The expression of other transcriptional regulators, such as one of the ArsR family, is induced both in the presence of Ni and Zn; yet this up-regulation is greater in the presence of Zn (Table 18). Similarly, a group of three efflux proteins (APM_2362, APM_2363, APM_2365) plus a transcriptional regulator (APM_2364), which resemble an RND efflux operon, are found up-regulated when either Zn or Ni metal is added. The expressions of a mercuric reductase, an arsenate reductase (Table A 5 and Table A 6) and a multicopper oxidase (Table 18) are up-regulated specifically by Zn.

Similarly to Ni, Zn is not a redox active metal and therefore does not directly generate reactive oxygen species (ROS) (Shahid *et al.*, 2014). However, the common Ni- and Zn-induction of *dnaK*, *clpB*, rubrerythrin, an alkyl hydroperoxide reductase and the Zn-specific induction of a peroxidase and of a 5-oxoprolinase involved in glutathione metabolism, suggest indirect generation of ROS. These ROS might be produced by stimulation of the activity of NADPH oxidases or by displacing metals from metalloenzyme active sites (Shahid *et al.*, 2014).

Regarding amino acid transport and biosynthesis, both metals repress the expression of aspartate kinase (involved in the biosynthesis of lysine and proline); however, while Ni down-regulates several operon *liv*-like genes (for the transport of BCAAs), Zn seems to trigger the transcription of an alternative BCAA transport system.

Similarly to Ni, Zn induces the expression of some N-related genes (namely, nitrile hydratase), represses the biosynthesis of cell wall components (*e.g.* lipid-A-disaccharide synthase or serine-type D-Ala-D-Ala carboxypeptidase), and of [FeS] clusters (*e.g.* Fe-S metabolism associated SufE).

However, unlike Ni, Zn represses the transcription of genes involved in the biosynthesis of flagella (*e.g.* flagellar hook capping protein), tetrapyrroles (*e.g.* siroheme synthase) and bacteriocins (*e.g.* colicin V production protein).

Table 18. Comparison of the early transcriptomic responses to Ni vs Zn after 5 and 30 min. Selected genes that were further validated with qRT-PCR are shown below. Only statistically significant values ($p < 0.05$) are color-coded (red tones indicate induction; green shades, repression).

			Ni 5		Ni 30		Zn 5		Zn 30	
	Locus	Gene	F	p	F	p	F	p	F	p
Genes relevant in the early (30 min) response to Ni	APM_2849	Transcriptional regulator/antitoxin, MazE	32.29	0.004	107.14	0.004	4.19	0.004	7.62	0.215
	APM_0195	MmgE/PrpD family protein	9.02	0.023	47.64	0.000	1.09	0.604	-2.70	0.022
	APM_0196	Methylitaconate delta2-delta3-isomerase	4.51	0.011	33.04	0.000	-1.04	0.853	-1.61	0.231
	APM_0199	Tricarballylate dehydrogenase	1.18	0.217	32.26	0.002	-1.07	0.533	-4.27	0.010
	APM_0068	Manganese transport regulator MntR	19.01	0.009	30.57	0.008	1.42	0.037	-13.33	0.004
	APM_0198	Putative transcriptional regulator	1.71	0.030	21.48	0.003	-1.01	0.984	-5.29	0.003
	APM_3382	Transcriptional regulator, ArsR family	1.32	0.120	12.75	0.001	48.02	0.007	30.88	0.109
	APM_1444	NADH-quinone oxidoreductase subunit C/D	1.16	0.218	10.61	0.004	1.03	0.901	12.90	0.219
	APM_3510	Sigma 54 modulation protein/ribosomal protein S30EA	1.64	0.044	8.98	0.010	2.29	0.007	4.53	0.027
	APM_2365	Cation diffusion facilitator family transporter	4.80	0.001	7.80	0.002	6.00	0.004	5.16	0.134
	APM_0774	ABC-type molybdate transport system periplasmic component-like protein	1.10	0.353	7.21	0.002	6.78	0.016	6.38	0.039
	APM_2517	Rubrerythrin	3.31	0.000	6.07	0.008	4.11	0.015	10.88	0.107
	APM_0070	Natural resistance-associated macrophage protein	9.37	0.009	5.11	0.001	9.16	0.007	12.14	0.028
	APM_3379	NADPH-dependent FMN reductase	-1.22	0.233	4.89	0.014	14.13	0.001	3.94	0.283
	APM_0066	MgtC/SapB transporter	4.32	0.004	4.85	0.010	-1.00	0.946	-3.77	0.020
	APM_0895	Arsenical pump membrane protein	1.03	0.900	4.82	0.000	13.27	0.021	1.66	0.092
	APM_0250	Probable manganese transport protein mntH	4.15	0.000	4.37	0.005	-1.16	0.503	-3.31	0.062
	APM_2300	ABC transporter related	-1.57	0.030	4.05	0.000	-2.00	0.011	-2.83	0.046
	APM_2851	Hypothetical protein	1.85	0.004	3.99	0.002	-1.08	0.521	1.62	0.248
	APM_2363	Co/Zn/Cd cation transporter-like protein	2.20	0.006	3.93	0.014	4.58	0.000	15.54	0.132
	APM_0133	Alanine dehydrogenase	-1.59	0.029	3.88	0.000	6.01	0.000	8.01	0.173
	APM_2041	ClpA homolog protein	1.14	0.651	3.56	0.002	1.82	0.057	2.19	0.192
	APM_2852	Rep(pMBA19a)	1.37	0.010	3.46	0.019	1.02	0.830	-1.12	0.673
	APM_2883	Fis family GAF modulated sigma54 specific transcriptional regulator	1.59	0.016	3.41	0.011	3.27	0.002	5.48	0.220
	APM_1503	Nitrile hydratase	-1.02	0.736	3.40	0.000	2.14	0.016	3.67	0.000
	APM_3356	Hypothetical protein	1.16	0.146	3.25	0.006	1.81	0.014	-1.78	0.031
	APM_0238	SirA family protein	1.00	0.906	3.19	0.008	1.64	0.017	-1.14	0.811
	APM_3225	Beta alanine--pyruvate transaminase	1.09	0.506	3.15	0.008	3.40	0.017	3.98	0.246
	APM_2007	Isocitrate lyase	2.17	0.010	3.09	0.004	2.66	0.009	22.16	0.067
	APM_2364	MerR family transcriptional regulator	3.56	0.000	2.87	0.007	3.96	0.085	1.43	0.175
	APM_0110	Major facilitator transporter	1.04	0.911	2.35	0.005	1.20	0.222	2.14	0.003
	APM_3715	Ornithine cyclodeaminase	1.04	0.685	2.14	0.005	1.22	0.281	2.49	0.006
	APM_0193	AraC family transcriptional regulator	-1.42	0.046	2.07	0.012	-1.21	0.079	-2.89	0.019
	APM_0087	Alkyl hydroperoxide reductase/ Thiol specific antioxidant/ Mal allergen	1.15	0.447	2.05	0.004	15.84	0.070	26.82	0.051
	APM_2362	Cation diffusion facilitator family transporter	1.56	0.002	2.03	0.003	2.68	0.001	5.99	0.158
	APM_1758	Rod shape-determining protein MreC (from incongruent clone)	-1.32	0.041	-2.01	0.002	-1.91	0.022	-4.83	0.008
	APM_1834	Ribonuclease D	-1.12	0.272	-2.02	0.006	-1.70	0.073	-6.37	0.021
	APM_1257	NADH-quinone oxidoreductase, E subunit	1.13	0.104	-2.14	0.001	-1.12	0.405	-4.13	0.011
	APM_0472	DNA ligase	-1.44	0.028	-2.14	0.005	-1.33	0.298	-7.25	0.015
	APM_1094	2-oxoglutarate dehydrogenase E1 component	-1.49	0.033	-2.21	0.010	-1.47	0.040	-14.08	0.007
	APM_1946	Orotate phosphoribosyltransferase	1.01	0.908	-2.24	0.008	-1.30	0.066	-10.10	0.002
	APM_0844	Hypothetical protein	-1.32	0.167	-2.28	0.035	-1.23	0.227	-2.70	0.016
	APM_3113	Putative ribonuclease BN	-1.38	0.000	-2.31	0.000	-1.21	0.220	-8.40	0.001
	APM_3049	30S ribosomal protein S14	-2.27	0.031	-2.37	0.023	-1.91	0.066	-2.99	0.026
	APM_1178	ATP synthase subunit a	1.05	0.710	-2.42	0.019	1.27	0.099	-18.52	0.002
	APM_1005	50S ribosomal protein L21	-1.15	0.401	-2.46	0.028	-1.15	0.323	-6.71	0.008
	APM_1173	Adenine phosphoribosyltransferase	-1.10	0.344	-2.48	0.002	-1.12	0.469	-22.22	0.016
	APM_2441	Inner membrane protein oxaA	-1.36	0.106	-2.54	0.024	-1.11	0.166	-4.57	0.014
	APM_1391	Fe-S metabolism associated SufE	1.14	0.547	-2.60	0.013	-1.16	0.610	-10.64	0.013
	APM_3108	Cytidylate kinase	-1.18	0.223	-2.62	0.014	-1.56	0.105	-6.67	0.022
	APM_2493	Ribosomal RNA large subunit methyltransferase N	-1.84	0.012	-2.76	0.010	-2.23	0.019	-11.36	0.006
	APM_3116	50S ribosomal protein L33P	1.13	0.297	-2.99	0.003	-2.12	0.162	-21.28	0.065
	APM_1835	Aspartyl-tRNA synthetase	-1.07	0.567	-2.99	0.010	-1.38	0.219	-13.16	0.030
	APM_1650	Dihydrodipicolinate reductase	-1.27	0.157	-3.00	0.014	-1.84	0.165	-34.48	0.053
	APM_2440	GTPase EngB	-1.65	0.086	-3.03	0.030	-1.57	0.043	-15.38	0.010
	APM_1930	ATP synthase gamma chain	-1.41	0.074	-3.13	0.012	-1.36	0.170	-10.53	0.017
	APM_3030	DNA-directed RNA polymerase subunit beta	-1.89	0.003	-3.24	0.001	-1.33	0.081	-1.80	0.168
	APM_3042	30S ribosomal protein S3	-2.72	0.013	-3.24	0.015	-2.67	0.032	-3.62	0.015
	APM_3039	50S ribosomal protein L2	-2.40	0.016	-3.29	0.011	-1.68	0.072	-4.13	0.016
	APM_0723	Primosome assembly protein PriA (from incongruent clone)	-1.64	0.078	-3.44	0.025	-1.54	0.044	-6.62	0.007
	APM_1291	HhH-GPD family protein	-1.57	0.019	-3.69	0.001	-1.85	0.136		
	APM_1713	ABC transporter related	-2.34	0.021	-3.70	0.008	-5.99	0.053	-8.93	0.032
	APM_0614	Natural resistance-associated macrophage protein	-1.74	0.100	-3.70	0.031	-4.76	0.010	-41.67	0.016
	APM_0529	50S ribosomal protein L20	-1.38	0.082	-3.88	0.007	-1.36	0.064	-16.39	0.004
	APM_1003	GTPase obg	-1.39	0.160	-4.85	0.023	-1.41		-10.64	0.009
	APM_0724	Translation-associated GTPase (from incongruent clone)	-1.51	0.054	-5.41	0.011	-1.58	0.062	-32.26	0.012
	APM_2129	30S ribosomal protein S1	-2.08	0.009	-5.56	0.004	-1.63	0.020	-28.57	0.003
	APM_3060	DNA-directed RNA polymerase subunit alpha	-1.75	0.002	-5.65	0.001	-1.49	0.129	-10.00	0.021

	APM_1405	Elongation factor Ts	-1.32	0.035	-6.90	0.004	-1.54		-9.26	0.002
Genes relevant ONLY in the early (30 min) response to Zn	APM_0179	Transcriptional regulator	-2.95	0.405	1.84	0.923	50.33	0.024	61.88	0.009
	APM_2361	Multicopper oxidase, type 2	-1.08	0.585	1.38	0.067	3.71	0.001	16.40	0.000
	APM_2997	RNA polymerase factor sigma-32	1.14	0.107	-1.47	0.009	2.81	0.141	5.24	0.000
	APM_3839	Glyceraldehyde-3-phosphate dehydrogenase, type I	-1.43	0.177	-2.19	0.067	-1.14	0.275	-2.44	0.019
	APM_1693	Formate dehydrogenase family accessory protein FdhD	-1.26	0.133	-1.62	0.035	-1.34	0.216	-3.07	0.032
	APM_0091	Transposase IS116/IS110/IS902 family protein	-1.38	0.098	-1.40	0.075	-1.26	0.234	-3.10	0.011
	APM_3413	Copper resistance protein	1.17	0.253	-1.13	0.364	1.74	0.026	-3.14	0.006
	APM_1293	DNA polymerase I	-1.14	0.331	1.07	0.596	-1.11	0.418	-3.27	0.020
	APM_3234	Leucyl-tRNA synthetase	1.07	0.410	-1.05	0.736	-1.10	0.580	-3.46	0.038
	APM_1092	Dihydrolipoamide dehydrogenase	-1.47	0.050	-1.93	0.026	-1.46	0.048	-3.53	0.014
	APM_1631	DNA repair protein RadC	-1.10	0.603	1.28	0.223	-1.07	0.606	-3.75	0.014
	APM_3182	2-dehydro-3-deoxyphosphogluconate aldolase/4-hydroxy-2-oxoglutarate aldolase	-1.18	0.085	-1.49	0.012	1.07	0.523	-4.20	0.005
	APM_0397	Chromosomal replication initiation protein	-1.23	0.179	-1.69	0.036	-1.54		-4.52	0.006
	APM_3117	Lipid-A-disaccharide synthase	-1.32	0.189	-1.22	0.293	-1.13	0.360	-5.21	0.007
	APM_3028	50S ribosomal protein L10	-1.61	0.164	-2.87	0.072	-2.29	0.021	-5.59	0.000
	APM_3406	Cytochrome c biogenesis protein transmembrane region	1.05	0.679	-1.63	0.029	-1.06	0.624	-5.68	0.009
	APM_0499	Siroheme synthase	-1.14	0.420	-1.34	0.187	-1.40	0.189	-6.10	0.010
	APM_0987	Serine-type D-Ala-D-Ala carboxypeptidase	-1.05	0.421	-1.93	0.009	1.05		-6.21	0.001
	APM_0011	Flagellar hook capping protein	-1.24	0.408	-1.18	0.462	1.02	0.599	-6.25	0.008
	APM_3114	Ribonuclease R	-1.58	0.044	1.20	0.334	-2.25	0.070	-6.33	0.028
	APM_3107	DNA gyrase subunit B	-1.14	0.380	-1.89	0.044	-1.35	0.129	-6.58	0.009
	APM_0517	Ribosome maturation factor rimM	-1.54	0.196	-5.62	0.052	-3.13		-7.81	0.041
	APM_1170	Colicin V production protein	-1.24	0.077	-1.71	0.013	-1.12	0.354	-11.90	0.003
	APM_3115	C-terminal processing peptidase	-2.32	0.021	1.20	0.243	-2.59	0.002	-12.35	0.001
	APM_1186	Ribonuclease	-1.73	0.014	-1.88	0.009	-2.48	0.053	-13.51	0.026
	APM_0396	Ribosomal protein S20	1.06	0.973	-2.63	0.114	-1.68	0.118	-17.54	0.028
	APM_1171	DNA repair protein RadA	-1.36	0.107	-1.88	0.020	-1.72	0.089	-21.74	0.019
	APM_0433	50S ribosomal protein L36P	1.16	0.838	-2.48	0.183	1.42	0.095	-23.81	0.029
	APM_0150	Sec-independent protein translocase, TatC subunit	-1.28	0.168	-1.91	0.045	-1.13	0.420	-43.48	0.000
	APM_0473	TraR/DksA family transcriptional regulator	1.08	0.673	-1.96	0.041	-1.25	0.144	-55.56	0.007
Other genes	APM_0290	Formate hydrogenlyase subunit 4-like protein	-1.13	0.464	1.17	0.371	1.04	0.876	-1.70	0.099
	APM_0180	MFS transporter	-2.15	0.382	-1.07	0.626	23.70	0.002	27.50	0.124
	APM_0136	Glutamine synthetase, catalytic region	-1.16	0.105	-1.32	0.021	-1.33	0.178	-1.83	0.132
	APM_2256	NUDIX hydrolase	-1.28	0.276	1.39	0.152	-1.24	0.137	-1.91	0.143
	APM_3422	Heavy metal translocating P-type ATPase	-1.06	0.579	-1.04	0.772	2.81	0.001	12.06	0.185
	APM_1409	Glutathione S-transferase domain-containing protein	-1.06	0.549	-1.16	0.179	1.45	0.157	1.25	0.197
	APM_3419	Alkyl hydroperoxide reductase/ Thiol specific antioxidant/ Mal allergen	1.01	0.926	1.09	0.304	1.89	0.003	2.59	0.237
	APM_0089	MerR family transcriptional regulator	-1.09	0.542	1.96	0.019	2.29	0.006	2.55	0.245
	APM_2850	ATPase involved in chromosome partitioning-like protein	1.94	0.005	5.27	0.062	1.11	0.431	1.96	0.266
	APM_3550	RecD/TraA family helicase	-1.33	0.086	-1.10	0.359	-1.47	0.049	-1.38	0.266
	APM_0294	NADH ubiquinone oxidoreductase, 20 kDa subunit	1.06	0.679	1.88	0.003	1.51	0.212	-1.27	0.305
	APM_1878	Endoribonuclease L-PSP	1.00	0.935	1.80	0.021	1.54	0.097	2.01	0.306
	APM_3421	Copper transporting ATPase	-1.07	0.605	-1.08	0.677	2.87	0.124	2.47	0.328
	APM_2257	DEAD/DEAH box helicase domain-containing protein	-1.40	0.059	1.31	0.071	1.02	0.844	-1.34	0.458
	APM_3409	Redoxin domain-containing protein	1.34	0.240	1.68	0.048	1.78	0.015	-1.43	0.472
	APM_0134	XRE family transcriptional regulator	-1.85	0.010	1.79	0.002	2.32	0.000	1.29	0.497
	APM_2798	Hypothetical protein	-1.02	0.823	1.59	0.014	1.10	0.533	-1.39	0.542
	APM_2856	Conjugal transfer protein traA	-1.20	0.056	1.30	0.004	-1.71	0.060	-1.26	0.564
	APM_2510	Deoxyribodipyrimidine photolyase-related protein	1.11	0.261	-1.27	0.067	1.03	0.950	1.16	0.683
	APM_3412	Peroxidase	1.00	0.849	1.08	0.958	3.50	0.011	1.21	0.714
	APM_2964	Replicative DNA helicase	-1.25	0.181	1.08	0.612	1.16	0.336	1.62	
	APM_1630	Endoribonuclease L-PSP	1.02	0.914	-1.01	0.961	2.15	0.033	-1.95	
	APM_1616	Permease for cytosine/purines, uracil, thiamine, allantoin	1.20	0.058	1.67	0.001	1.58	0.046	5.00	

The transcriptomic response to Zn and Ni is generally very similar. The addition of toxic concentrations of either metal prompts cell growth arrest through the rapid down-regulation of genes involved in DNA replication and transcription and in the synthesis of proteins. This cell growth arrest is accompanied by a decline in energy production. These results are in agreement with early growth experiments, where the addition of either metal resulted in extended lag phases (Figure 12). In the case of Zn, however, these changes do not appear to involve alarmone (p)ppGpp or MazEF toxin-antitoxin system.

Another major difference in the response to Ni vs Zn is the differential expression of genes in charge of metal sensing and metal homeostasis. Although, some of these genes are similarly induced/repressed by both metals, many others are clearly metal-specific.

The last big difference lies in the early, massive up-regulation of certain genes by Ni but not by Zn (Figure 40). Based on this evidence, we propose: i) that these genes conform an operon directly or indirectly related to the generation of 2-MC intermediates, and ii) that their up-regulation points to enzymes of the TCA or 2-MC cycles or the catabolism of itaconate as primary targets of Ni toxicity.

4.4.4. Proteomics of the early response to Ni in *Acidiphilium* sp. PM

To determine whether the transcriptomic changes induced by Ni were being reflected at the proteomic level we used two-dimensional differential in-gel electrophoresis (2D-DIGE).

A preculture of *Acidiphilium* sp. PM was grown to mid exponential phase and then split into 16 50-ml cultures as follows: 8 sub-cultures were grown untreated for 1h or 5h whereas the remaining 8 were incubated with 10 mM Ni for 1h or 5h. Four replicates were collected for each condition. Cells were pelleted and their proteins extracted and cleaned as described in 3.10.1. Protein samples were submitted to Parque Científico de Madrid (UCM-PCM) (Madrid, Spain), for comparative proteomic analysis using 2D-DIGE. The quality of the samples was checked in 10% SDS-PAGE gels (Figure 41). 2D-PAGE conditions were optimized and tested using a pool of proteins from each condition (Figure A 6 of APPENDIX VII). Proteins were labelled and loaded on 2D-gels according to the experimental design (Table 19).

	Label		
	Cy5	Cy3	Cy2
Gel 1	C_1h_rep1	Ni_1h_rep4	IS
Gel 2	C_1h_rep2	C_5h_rep4	IS
Gel 3	Ni_5h_rep1	C_1h_rep3	IS
Gel 4	C_5h_rep2	C_1h_rep4	IS
Gel 5	C_5h_rep3	Ni_1h_rep1	IS
Gel 6	Ni_1h_rep2	Ni_5h_rep3	IS
Gel 7	Ni_1h_rep3	Ni_5h_rep2	IS
Gel 8	Ni_5h_rep4	C_5h_rep1	IS

Table 19. Experimental design used in 2D-DIGE proteomic comparisons. The experimental design included a Cy2-labelled internal standard (IS) (50 μg) which contained an equal amount of protein from all replicates. Cy3/5 labelling and gel allocation was determined using a randomised trial that fulfilled this criterion: half the samples in each condition should be labelled with each dye (Cy3/Cy5). Treatment: control (C) vs Nickel (Ni); Incubation time: 1 hour (1h) vs 5 hours (5h). Rep stands for replicate.

After 2D-electrophoresis, gels were scanned (Figure A 7) and individual spots were identified and matched across gels using a master gel (Figure 41). Spot data was then normalized using the Cy2-labelled internal standard, and a treatment:control ratio was calculated using Student's t-test. 2-way ANOVA (with FDR correction) was applied to compare the effects of treatment (0 vs 10 mM Ni), time (1h vs 5 hours) and their interaction, on the proteome of *Acidiphilium* sp. PM. A total of 142 spots (10%) were found to be statistically significant in at least one of three criteria. 50 spots were selected, 47 of which could be successfully excised from 2D-DIGE gels stained with Coomassie Blue. The proteins contained in these spots were digested with trypsin prior to submission to MALDI-TOF/TOF analysis. Protein identification was achieved by peptide mass fingerprinting using MASCOT software and a database of predicted *Acidiphilium* sp. PM proteins.

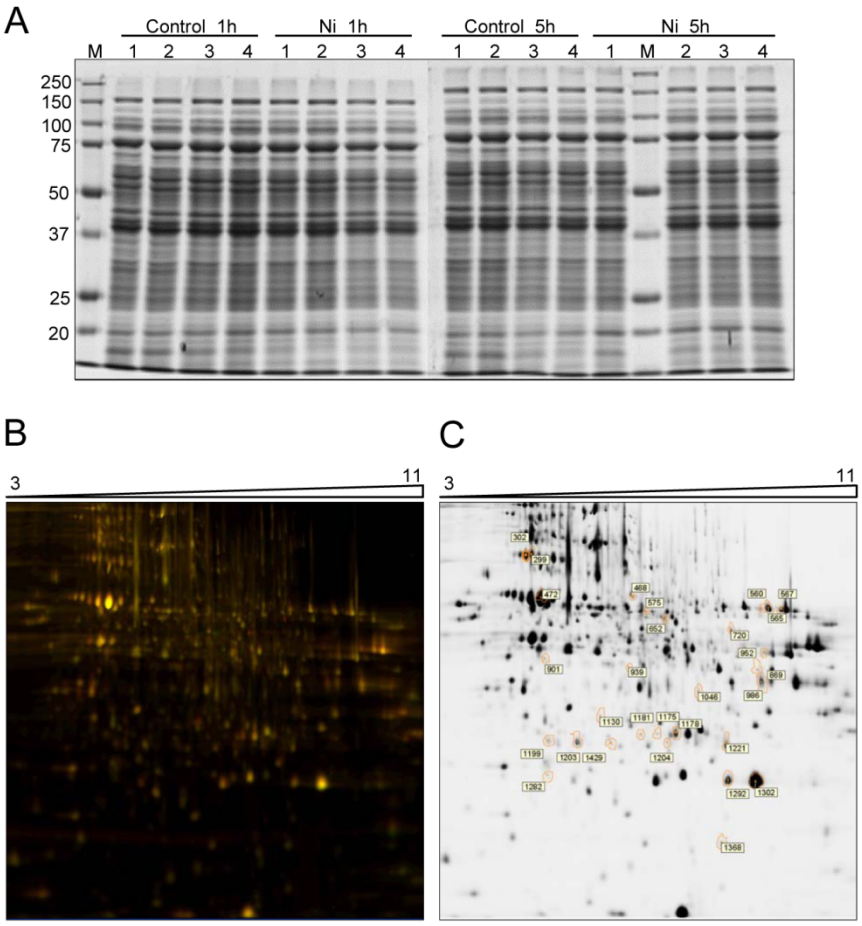

Figure 41. Study of the proteomic response to Ni using DIGE. Sixteen cultures in mid-exponential phase were incubated: with or without 10 mM Ni and for 1 h or 5 h. Cells were harvested, then proteins were extracted, cleaned and their quality checked in SDS-PAGE gels (A). Proteins were labelled and loaded onto 2D-gels according to the experimental design (Table 19). Gels were then scanned (picture B depicts Gel 4) and their spots were identified and matched across gels according to the master gel (C). Gel 4 was stained with Coomassie Blue and used as the master gel because this gel allowed the maximum recognition of Cy2-labelled protein spots (1429). Some spots of interest are highlighted in orange. M: molecular weight marker (in kDa; Precision Plus Protein™ Unstained standard). Treatment: control (C) vs Nickel (Ni); Incubation time: 1 hour (1h) vs 5 hours (5h).

The proteins contained in forty-four spots were readily identified (Table 20). Three other spots contained a mixture of two or more proteins and were not included in this analysis.

Changes at the proteomic level are more subtle than observed in the transcriptome. The rapid shut-down of ribosome biogenesis and the partial insight afforded by proteomics may be causing this buffered effect. Four genes (highlighted in blue in Table 20) had both their mRNA and protein levels significantly altered. Overall, the functions that were found to be altered at the transcriptomic and at proteomic level are (remarkably) fundamentally the same. Similarly to what was observed with qRT-PCR, DIGE revealed a compromise in the biosynthesis of proteins (primarily through a lack of elongation factors EF- G, EF-Ts, GreA) and enhanced chaperone folding activity (peptidyl-prolyl *cis-trans* isomerase, GROEL_2, protease Do). The addition of Ni also triggered significant changes in the expression of several proteins involved in central metabolism, including saccharide catabolism (*e.g.* monosaccharide-transporting ATPase, 6-phosphogluconate dehydrogenase of the pentose phosphate pathway) and fatty acids synthesis (3-oxoacyl-(acyl-carrier-protein) reductase) and oxidation (acyl-CoA dehydrogenase domain-containing protein). Interestingly, poly(hydroxyalcanoate) granule-associated proteins (Phasins) were also found to be more expressed with Ni. These proteins could be acting as transcriptional regulators of energy-storing PHA biosynthesis or degradation, as has been reported for other bacteria (Matsumoto *et al.*, 2002; Handrick *et al.*, 2004).

Rather excitingly, the protein with the largest change in expression was encoded by the massively Ni-induced MmgE/PrpD gene (4-fold protein increase after 5 h Ni; 48-fold mRNA increase after 30 min Ni). As explained above, this protein is suspected to play a role in the degradation of toxic 2-MC resulting from the degradation of propionyl-CoA. The down-regulation of methylmalonate-semialdehyde dehydrogenase (which catalyzes the NAD-dependent oxidation of methylmalonate semialdehyde to propionyl-CoA) further supports our hypothesis that Ni toxicity could be mediated by intermediates of the 2-MC cycle. Indeed, we suggest that the cell's strategy to cope with Ni stress could partially rely on minimizing the generation of toxic 2-MC intermediates and increasing its degradation rates.

Table 20. Significantly induced and repressed proteins after 1h and 5h in 10 mM Ni. Only statistically significant ($p < 0.05$) data is shown in black type. GenBank acc. No in blue show proteins whose transcription was seen to be altered in transcriptomic experiments. Induction is shown in tones of red whereas repression is highlighted in shades of green.

				Effect of treatment				Effect of time				2-way ANOVA		
				Ni/C after 1h		Ni/C after 5h		5h/1h in control		5h/1h in Ni		Treatment	Time	Treatment * Time
	Spot No.	Protein Id.	GenBank acc. no.	F	p	F	p	F	p	F	p	p	p	p
Protein synthesis and folding	299	Elongation factor G	EGO96166	-1.23	0.040	-1.20	0.310	-1.09	0.660	-1.06	0.670	0.003	0.290	0.320
	472	GroEL_2	EGO95091	-1.10	0.400	-1.18	0.023	1.02	0.910	-1.06	0.850	0.006	0.450	0.220
	577	Protease Do	EGO96297	1.24	0.230	1.72	0.260	1.11	0.770	1.54	0.610	0.010	0.170	0.140
	612	Protease Do	EGO96297	1.53	0.100	1.07	0.860	1.45	0.560	1.02	0.980	0.040	0.360	0.160
	1024	Tsf (elongation factor Ts)	EGO95773	-1.67	0.150	-1.14	0.790	-1.10	0.880	1.33	0.610	0.027	0.420	0.130
	1100	PpiC-type peptidyl-prolyl *cis-trans* isomerase	EGO93581	-2.61	0.140	-1.50	0.500	-1.25	0.820	1.38	0.850	0.013	0.480	0.200
	1337	GreA (Transcription elongation factor GreA)	EGO95802	-1.16	0.530	-1.61	0.270	1.07	0.960	-1.30	0.670	0.026	0.410	0.190
Energy metabolism	575	Methylmalonate-semialdehyde dehydrogenase	EGO96138	-1.17	0.036	-1.12	0.360	-1.08	0.560	-1.03	0.810	0.003	0.270	0.260
	652	MmgE/PrpD family protein	EGO96915	2.03	0.160	3.97	0.023	-1.24	0.880	1.57	0.060	0.000	0.440	0.120
	714	Aldehyde dehydrogenase	EGO93989	-2.06	0.300	1.93	0.280	-2.08	0.560	1.92	0.006	0.260	0.490	0.041
	717	GlyA (serine hydroxymethyltransferase)	EGO94992	-1.22	0.530	1.89	0.230	-1.66	0.560	1.40	0.370	0.068	0.450	0.041
	719	GlyA (serine hydroxymethyltransferase)	EGO94992	1.67	0.096	-1.74	0.440	1.77	0.560	-1.64	0.025	0.290	0.500	0.041
	720	Acyl-CoA dehydrogenase domain-containing protein	EGO93905	1.23	0.022	1.46	0.083	-1.01	0.970	1.18	0.370	0.000	0.320	0.100
	812	Monosaccharide-transporting ATPase	EGO96333	1.87	0.130	1.08	0.750	1.64	0.150	-1.05	0.980	0.011	0.200	0.061
	822	Monosaccharide-transporting ATPase	EGO96333	1.51	0.060	1.02	0.930	1.38	0.150	-1.07	0.870	0.006	0.200	0.035
	901	Tartrate dehydrogenase	EGO96097	1.26	0.140	1.49	0.023	1.08	0.650	1.28	0.260	0.000	0.070	0.130
	986	ABC-type sugar transport system periplasmic component-like protein	EGO94565	2.29	0.013	1.14	0.710	2.05	0.086	1.02	0.990	0.001	0.031	0.017
	1130	6-phosphogluconate dehydrogenase, NAD-binding	EGO96769	-1.05	0.300	1.63	0.002	-1.11	0.150	1.54	0.007	0.000	0.000	0.000
	1199	Carboxymethylenebutenolidase	EGO94942	1.49	0.013	1.48	0.028	1.27	0.150	1.26	0.210	0.000	0.004	0.350
	1203	Carboxymethylenebutenolidase	EGO94942	-1.29	0.040	-1.11	0.410	-1.15	0.440	1.01	0.960	0.002	0.320	0.097
	1204	3-oxoacyl-(acyl-carrier-protein) reductase	EGO95637	1.33	0.028	1.17	0.330	1.17	0.440	1.04	0.890	0.001	0.200	0.160
	1221	Acetoacetyl-CoA reductase	EGO95434	1.16	0.120	1.60	0.002	-1.08	0.420	1.28	0.050	0.000	0.072	0.001
	1292	Phasin family protein	EGO96239	1.22	0.160	1.77	0.005	1.01	0.960	1.48	0.016	0.000	0.017	0.015
	1301	Phasin family protein	EGO96239	1.30	0.250	1.51	0.083	1.18	0.590	1.36	0.370	0.003	0.093	0.250
	1302	Phasin family protein	EGO96239	1.18	0.270	1.79	0.005	-1.11	0.560	1.37	0.220	0.000	0.220	0.015
Other functions	432	Flavodoxin/nitric oxide synthase	EGO94310	-1.65	0.210	-1.19	0.750	-1.22	0.770	1.14	0.720	0.043	0.480	0.200
	468	Hypothetical protein	EGO95947	-1.40	0.040	-1.06	0.940	-1.07	0.860	1.23	0.370	0.046	0.440	0.120
	535	Pyrrolo-quinoline quinone	EGO96106	2.16	0.060	-1.04	0.990	2.12	0.160	-1.06	0.950	0.011	0.095	0.036
	554	Pyrrolo-quinoline quinone	EGO94306	1.57	0.052	-1.04	0.940	1.48	0.300	-1.10	0.790	0.028	0.320	0.043
	560	Pyrrolo-quinoline quinone	EGO94306	1.87	0.040	1.21	0.490	1.62	0.260	1.04	0.920	0.002	0.095	0.062
	565	Pyrrolo-quinoline quinone	EGO94306	1.38	0.009	1.08	0.760	1.25	0.560	-1.03	0.880	0.010	0.390	0.100
	567	Pyrrolo-quinoline quinone	EGO94306	1.69	0.013	1.69	0.130	1.37	0.180	1.37	0.390	0.000	0.017	0.360
	869	ABC-type branched-chain amino acid transport systems periplasmic component-like protein	EGO96613	1.51	0.040	-1.15	0.790	1.38	0.540	-1.25	0.560	0.090	0.470	0.047
	899	NADH:flavin oxidoreductase/NADH oxidase	EGO94218	1.23	0.250	1.53	0.220	1.25	0.530	1.55	0.260	0.006	0.041	0.200
	939	Glutathione synthetase	EGO93747	1.61	0.013	1.06	0.810	1.57	0.013	1.03	0.930	0.001	0.012	0.011
	1018	Thioredoxin reductase	EGO94106	-1.72	0.170	-1.24	0.610	-1.21	0.690	1.14	0.900	0.022	0.480	0.190
	1046	5,10-methylenetetrahydrofolate reductase	EGO94783	-1.28	0.051	1.31	0.023	-1.32	0.120	1.27	0.041	0.260	0.440	0.000
	1071	Hypothetical protein	EGO93388	-1.49	0.160	1.27	0.490	-1.15	0.790	1.65	0.220	0.220	0.390	0.045
	1128	Putative acetoacetate decarboxylase	EGO96208	-1.17	0.170	1.44	0.230	-1.22	0.560	1.38	0.035	0.087	0.440	0.029
	1137	FeS assembly ATPase SufC	EGO95521	-1.87	0.060	-1.17	0.780	-1.38	0.560	1.16	0.650	0.010	0.410	0.086
	1175	Short-chain dehydrogenase/reductase SDR	EGO94953	1.56	0.029	1.11	0.500	1.43	0.140	1.02	0.960	0.001	0.061	0.036
	1179	Short-chain dehydrogenase/reductase SDR	EGO94953	1.51	0.098	1.03	0.910	1.39	0.220	-1.05	0.930	0.014	0.250	0.058
	1181	Short-chain dehydrogenase/reductase SDR	EGO95611	1.24	0.130	1.67	0.002	-1.02	0.970	1.33	0.012	0.000	0.061	0.019

Ni also induces the expression of various other proteins, including pyrrolo-quinoline quinones (which function as redox cofactors of many enzymes), glutathione synthetase (involved in cell's antioxidant activity), BCAA transport proteins and short-chain dehydrogenase/reductases (SRDs) (SDRs are a functionally diverse family of oxidoreductases). On the other hand, Ni represses the expression of FeS assembly ATPase SufC (similarly to what was reported in the transcriptome) among other proteins.

Perhaps the most notable absence in this list of proteins is that of antitoxin/toxin proteins MazE/MazF. It is likely that the conditions used in the DIGE experiments led to the overlook of low molecular weight proteins (MazE, MazF < 12 kDa). Even though overexpression of MazF inhibits overall protein synthesis in *E. coli* (causing the death of most of the population), it allows the expression of a small portion of low-molecular weight proteins (particularly those without MazF cleaving target ACA) which increased the survivability of a small portion of the population (Amitai *et al.*, 2009). A similar phenomenon might be taking place in *Acidiphilium* sp. PM in response to Ni. In this scenario, Ni would trigger the expression of *mazEF*, yet it would still allow the synthesis of "survival proteins". This would explain the low yet rather constant rate of cell survival in the population.

Collectively, DIGE results indicate that transcriptomic techniques are more adequate for the interpretation of the cellular havoc triggered by Ni. Be it the result of protein synthesis arrest or plain cellular death, proteomics does not seem to reflect as sensitively the massive changes occurring in the cell.

A detailed examination of the proteome reveals changes in the protein synthesis machinery incompatible with normal cellular growth and replication.

4.5. GENERAL DISCUSSION ON Ni RESISTANCE

Acidiphilium sp. PM was isolated from a culture of *Acidiphilium* sp. 3.2 Sup 5. In voltammetry experiments, this strain provided large intensity currents and was selected for further in-depth characterization.

Heavy metal resistance tests performed on *Acidiphilium* sp. PM revealed an outstanding ability to grow in the presence of 1 M Ni after prolonged incubations. This extreme Ni resistance is unmatched in *Acidiphilium* and is only paralleled by an *A. ferrooxidans* strain isolated from a bioleaching tank (Dew *et al.*, 1999). Similar delayed growth following addition of large metal concentrations had been previously reported for some *Acidiphilium* species. For instance, some strains of "*Acidiphilium symbioticum*" and *Acp. cryptum* were reported to grow in 1 M Cd after lag phases exceeding 7 days (Mahapatra and Banerjee, 1996). However, contrary to these strains, where metal tolerance appeared to be homogeneous throughout the population, extreme Ni resistance in *Acidiphilium* sp. PM was constrained to a small fraction of the population. Indeed, only 1 in approximately 4000 cells (0.028%) was resistant to 20 mM Ni. Yet, the percentage of survivors remained constant when *Acidiphilium* sp. PM was challenged with up to 100 mM Ni (the highest concentration tested in plates).

Upon addition of 100 mM Ni to liquid cultures, cell viability dropped steadily (one $\log_{10}$ per day) for the first five days. Yet, a small proportion of *ca.* 1 in 10^6 cells remained viable after 10 days. This fraction of resistant cells very much resembled the persisters observed when bacterial cultures are exposed to lethal concentrations of antibiotics [a recent review on persistency can be found in (Balaban *et al.*, 2013)]. However, as opposed to persisters, the surviving *Acidiphilium* sp. PM cells lead to fully-grown cultures.

The sequencing and annotation of the genome of *Acidiphilium* sp. PM revealed multiple genes that are similar to operon-encoded ORFs involved in metal resistance in other bacteria. Unfortunately, it is not yet possible to determine the functionality and metal specificity of these metal transport systems based only on their protein sequence. Therefore, we cannot maintain that these ORFs are carrying out the same functions in *Acidiphilium* sp. PM.

Functional screenings of shotgun genomic libraries have been a traditional approach to uncovering genes involved in metal resistance. A screening of a genomic library of *Acidiphilium* sp. PM failed to uncover traditional operon-encoded efflux systems involved in

Ni resistance. Instead, several genes with various functions were isolated. While this could be the result of incompatibility between the host cell machinery and *Acidiphilium* genetic information, previous reports on genomic screenings of other acidophilic species seem to suggest otherwise (Mirete *et al.*, 2007; Tian *et al.*, 2007). Among other genes, an operon encoded protease (HslVU) was retrieved that afforded *E. coli* resistance to Ni and Co. Interestingly, recent screenings on metagenomes of acidic environments have retrieved similar chaperones/proteases that afford microorganisms resistance to As (Morgante *et al.*, 2014) and low pH (Guazzaroni *et al.*, 2013). Although preliminary, this line of evidence suggests that microorganisms inhabiting metal-rich environments could rely on broader adaptations to cope with metal toxicity. Other determinants retrieved in the screening include genes involved in the synthesis of the outer membrane as well as a gene involved in the biosynthesis of BCAA. Changes in the synthesis of BCAA upon exposure to acid and metals have been reported previously (Tremaroli *et al.*, 2009; Santiago *et al.*, 2012).

By exposing *Acidiphilium* sp. PM to 10 mM Ni (a concentration that is close to inhibitory for most of the population), we expected to understand the mechanisms that help this bacterium cope with Ni and possibly identify some targets of Ni toxicity. The addition of Ni triggered a rapid transcriptomic response that led to the repression of DNA replication and transcription, and to the arrest of protein synthesis (primarily through the down-regulation of ribosomal protein operons). However, changes in expression at the proteomic level were only mild, even 5 h after the addition of Ni. The repression of new ribosome assembly and the overall drop in protein synthesis may account for this buffered effect. Cell growth arrest was very likely mediated by toxin-antitoxin system MazEF, one of the earliest, most massively up-regulated Ni responders. In addition, as observed in response to other stresses, alarmone (p)ppGpp could be playing a key role in the cell shutdown. Indeed, the expression of MazEF is regulated by the levels of ppGpp in the cell (Aizenman *et al.*, 1996). Yet, differently to the stringent response, the alarmone did not lead to increased biosynthesis of amino acids. Energy-metabolism was also greatly altered: ATP synthesis by substrate-level phosphorylation (in glycolysis) and by ATP synthase (coupled to the electron transport chain) was repressed. Several genes and suspected operons involved in metal cation homeostasis were among the first responders. A comparison of the transcriptomic response to Ni versus Zn, exposed that some of these metal-responders were triggered specifically by Ni.

The coordinated and large up-regulation of a cluster of genes related to the TCA and 2-methylcitrate cycles leads us to propose that enzymes of these cycles or others involved in the degradation of the itaconic acid, could be the primary targets of Ni toxicity.

Delayed growth and dormancy seem appropriate strategies to limit Ni toxicity while conditions reset to normal. However, if toxic Ni remains, cell death may ensue as a result of Ni toxicity itself or by protein synthesis arrest leading to the loss of basic cell functions. The tiny fraction of resisters that emerge upon prolonged exposure to Ni, have obviously managed to bypass both deleterious scenarios. Whether these cells have evolved specific mutations or just display distinct regulations remains unclear and should be the subject of the next research in our laboratory. A preliminary comparison of the transcriptomes of the Ni^r fraction versus the entire population has shed little light on the mechanisms for Ni resistance (data not shown). Therefore, a genomic approach that uncovers mutations and genomic rearrangements in these cells is encouraged. Comparative genomic hybridization using *Acidiphilium* sp. PM microarray could rapidly identify any large genomic rearrangements whereas punctual mutations in genes, promoters, enhancers, etc. would require sequencing several Ni-resistant strains and a similar number of Ni-sensitive clones. Eventually, the confirmation that these mutations confer resistance to Ni (and that the hypothetical targets of Ni toxicity are indeed so), would require the mutation of "wild-type" *Acidiphilium* sp. PM cells. For that reason, establishing a genetic system that allows the introduction of exogenous DNA and its recombination with the chromosome or the plasmids, is of utmost importance.

5. CONCLUSIONS

The main conclusions drawn from this work are:

1. *Acidiphilium* sp. PM can grow heterotrophically on a variety of energy sources using both O_2 and Fe^{3+} as electron acceptors. Complete Fe^{3+} reduction is only achieved under microaerobic conditions.

2. *Acidiphilium* sp. PM contains one large chromosome and 9 plasmids. The chromosome is largely syntenous with those of *Acp. cryptum* JF-5 and *Acp. multivorum* AIU301; yet, it contains exclusive genomic islands including a 54-kb fragment probably acquired from *Acidithiobacillus* through horizontal gene transfer. Phylogenetically, *Acidiphilium* sp. PM falls in the same cluster as *Acp. cryptum*, *Acp. organovorum* and *Acp. multivorum*.

3. *Acidiphilium* sp. PM possesses complete Entner-Doudoroff and pentose phosphate pathways, a tricarboxylic acid cycle and essential enzymes of the Calvin-Benson-Bassham cycle. It also contains a *ca*. 38-kb photosynthetic gene cluster which encodes proteins of the reaction center and light-harvesting complex I, as well as enzymes for the biosynthesis of Zn-bacteriochlorophyll *a* and of the antenna pigment spirilloxanthin. No genes are found that explain the exchange of Mg by Zn as the metal center in Zn-Bchl *a*.

4. Unexposed cultures of *Acidiphilium* sp. PM evolve extreme Ni-resistant phenotypes after prolonged incubations with the metal. One in a million cells is capable of withstanding 1 M Ni, a fraction similar to that observed in persistency events. However, as opposed to persisters, *Acidiphilium* Ni-resisters eventually produce fully-grown cultures.

5. A functional screening of a genomic library of *Acidiphilium* sp. PM identified seven genes involved in Ni resistance, including operon-encoded protease HslVU and genes involved in the biosynthesis of branched amino acids and of the lipopolysaccharide.

6. The addition of Ni triggers a rapid transcriptomic response that leads to the repression of DNA replication and transcription, the arrest of protein synthesis and the shutdown of energy metabolism. These events, which are likely to be mediated by toxin-antitoxin system MazEF, ultimately lead to cell growth arrest.

7. Enzymes of the TCA or 2-methylcitrate cycles or others involved in the degradation of itaconic acid, are proposed to be primary targets of Ni toxicity.

Las principales conclusiones extraídas de este trabajo son:

1. *Acidiphilium* sp. PM es un heterótrofo capaz de crecer con una variedad de fuentes de energía utilizando O_2 y Fe^{3+} como aceptores de electrones. Sólo en condiciones de microaerobiosis se obtiene una reducción completa de Fe^{3+}.

2. El genoma de *Acidiphilium* sp. PM consiste en un cromosoma y 9 plásmidos. El cromosoma es altamente sinténico con los de *Acp. cryptum* JF-5 y *Acp. multivorum* AIU301; sin embargo, contiene islas genómicas exclusivas, como un fragmento de 54 kb probablemente adquirido de *Acidithiobacillus* mediante transferencia génica horizontal. Filogenéticamente, *Acidiphilium* sp. PM se agrupa con *Acp. cryptum*, *Acp. organovorum* y *Acp. multivorum*.

3. *Acidiphilium* sp. PM posee las rutas completas de Entner-Doudoroff, las pentosas fosfatos, el ciclo de los ácidos tricarboxílicos y enzimas clave del ciclo de Calvin-Benson-Bassham. Asímismo, tiene un cluster de genes fotosintéticos de *ca.* 38 kb que codifica para proteinas del centro de reacción y de la antena, así como para las enzimas necesarias en la biosíntesis de Zn-bacterioclorofila *a* y del pigmento antena espiriloxantina. No se han encontrado genes que expliquen el intercambio de Mg por Zn en el centro catalítico de la Zn-Bchl *a*.

4. Cultivos de *Acidiphilium* sp. PM que no han sido expuestos previamente a Ni desarrollan resistencias extremas tras incubaciones prolongadas con el metal. Una de cada millón de células es capaz de soportar 1 M Ni, una fracción similar a la observada en fenómenos de persistencia. Sin embargo, a diferencia de los persistentes, las células de *Acidiphilium* sp. PM resistentes a Ni, dan lugar a cultivos completamente crecidos.

5. Un análisis funcional de una genoteca de *Acidiphilium* sp. PM permitió identificar siete genes implicados en resistencia a Ni, como el operón que codifica para la proteasa HslVU y genes involucrados en la síntesis del lipopolisacárido y de aminoácidos de cadena ramificada.

6. La adición de Ni desencadena una rápida respuesta transcriptómica que reprime la replicación y transcripción del ADN, restringe la producción de proteínas y disminuye el metabolismo energético. Estos cambios, probablemente mediados por el sistema toxina-antitoxina MazEF, llevan en última instancia a una parada del crecimiento celular.

7. Algunas enzimas del ciclo de los ácidos tricarboxílicos o del 2-metilcitrato u otras implicadas en la degradación del ácido itacónico podrían ser las dianas principales de la toxicidad causada por el Ni.

6. REFERENCES

Acuña, L. G., Cárdenas, J. P., Covarrubias, P. C., Haristoy, J. J., Flores, R., Nuñez, H., Riadi, G., Shmaryahu, A., Valdés, J., Dopson, M., Rawlings, D. E., Banfield, J. F., Holmes, D. S. and Quatrini, R. (2013). "Architecture and gene repertoire of the flexible genome of the extreme acidophile *Acidithiobacillus caldus*." *PLoS One* **8**(11): e78237.

Adriano, D. (2001). Nickel. *Trace elements in terrestrial environments*, Springer New York**:** 677-705.

Aguilera, A., Manrubia, S. C., Gomez, F., Rodriguez, N. and Amils, R. (2006). "Eukaryotic community distribution and its relationship to water physicochemical parameters in an extreme acidic environment, Rio Tinto (southwestern Spain)." *Appl Environ Microbiol* **72**(8): 5325-5330.

Aizenman, E., Engelberg-Kulka, H. and Glaser, G. (1996). "An *Escherichia coli* chromosomal "addiction module" regulated by guanosine [corrected] 3',5'-bispyrophosphate: a model for programmed bacterial cell death." *Proc Natl Acad Sci U S A* **93**(12): 6059-6063.

Alcolea, P. J., Alonso, A., Sanchez-Gorostiaga, A., Moreno-Paz, M., Gomez, M. J., Ramos, I., Parro, V. and Larraga, V. (2009). "Genome-wide analysis reveals increased levels of transcripts related with infectivity in peanut lectin non-agglutinated promastigotes of *Leishmania infantum*." *Genomics* **93**(6): 551-564.

Altschul, S. F., Gish, W., Miller, W., Myers, E. W. and Lipman, D. J. (1990). "Basic Local Alignment Search Tool." *J Mol Biol* **215**(3): 403-410.

Altschul, S. F., Madden, T. L., Schaffer, A. A., Zhang, J., Zhang, Z., Miller, W. and Lipman, D. J. (1997). "Gapped BLAST and PSI-BLAST: a new generation of protein database search programs." *Nucleic Acids Res* **25**(17): 3389-3402.

Amils, R., González-Toril, E., Fernández-Remolar, D., Gómez, F., Aguilera, Á., Rodríguez, N., Malki, M., García-Moyano, A., Fairén, A. G., de la Fuente, V. and Luis Sanz, J. (2007). "Extreme environments as Mars terrestrial analogs: the Rio Tinto case." *Planet Space Sci* **55**(3): 370-381.

Amitai, S., Kolodkin-Gal, I., Hananya-Meltabashi, M., Sacher, A. and Engelberg-Kulka, H. (2009). "*Escherichia coli* MazF leads to the simultaneous selective synthesis of both "death proteins" and "survival proteins"." *PLoS Genet* **5**(3): e1000390.

Andersson, A. F. and Banfield, J. F. (2008). "Virus population dynamics and acquired virus resistance in natural microbial communities." *Science* **320**(5879): 1047-1050.

Baillet, F., Magnin, J. P., Cheruy, A. and Ozil, P. (1997). "Cadmium tolerance and uptake by a *Thiobacillus ferrooxidans* biomass." *Environ Technol* **18**(6): 631-637.

Baker-Austin, C., Dopson, M., Wexler, M., Sawers, R. G. and Bond, P. L. (2005). "Molecular insight into extreme copper resistance in the extremophilic archaeon 'Ferroplasma acidarmanus' Fer1." *Microbiology* **151**(Pt 8): 2637-2646.

Balaban, N. Q., Gerdes, K., Lewis, K. and McKinney, J. D. (2013). "A problem of persistence: still more questions than answers?" *Nat Rev Microbiol* **11**(8): 587-591.

Bartha, R. and Ordal, E. J. (1965). "Nickel-dependent chemolithotrophic growth of two hydrogenomonas strains." *J Bacteriol* **89**(4): 1015-1019.

Bhattacharyya, S., Banerjee, P. C. and Das, P. K. (1990). "A plasma-membrane associated ATPase from the acidophilic bacterium *Acidiphilium cryptum*." *Biochem Cell Biol* **68**(10): 1222-1225.

Blériot, C., Effantin, G., Lagarde, F., Mandrand-Berthelot, M. A. and Rodrigue, A. (2011). "RcnB Is a Periplasmic Protein Essential for Maintaining Intracellular Ni and Co Concentrations in *Escherichia coli*." *J Bacteriol* **193**(15): 3785-3793.

Boer, J. L., Mulrooney, S. B. and Hausinger, R. P. (2014). "Nickel-dependent metalloenzymes." *Arch Biochem Biophys* **544**: 142-152.

Bookout, A. L., Cummins, C. L., Mangelsdorf, D. J., Pesola, J. M. and Kramer, M. F. (2006). High-throughput real-time quantitative reverse transcription PCR. *Current Protocols in Molecular Biology*. **73:** Unit 15.

Borole, A. P., O'Neill, H., Tsouris, C. and Cesar, S. (2008). "A microbial fuel cell operating at low pH using the acidophile *Acidiphilium cryptum*." *Biotechnol Lett* **30**(8): 1367-1372.

Bradford, M. M. (1976). "A rapid and sensitive method for the quantitation of microgram quantities of protein utilizing the principle of protein-dye binding." *Anal Biochem* **72**(1–2): 248-254.

Brugger, K., Torarinsson, E., Redder, P., Chen, L. and Garrett, R. A. (2004). "Shuffling of *Sulfolobus* genomes by autonomous and non-autonomous mobile elements." *Biochem Soc Trans* **32**(Pt 2): 179-183.

Bruins, M. R., Kapil, S. and Oehme, F. W. (2000). "Microbial resistance to metals in the environment." *Ecotoxicol Environ Saf* **45**(3): 198-207.

Campbell, A. M., del Campillo-Campbell, A. and Villaret, D. B. (1985). "Molybdate reduction by *Escherichia coli* K-12 and its chl mutants." *Proc Natl Acad Sci U S A* **82**(1): 227-231.

Cardenas, J. P., Arenas, M., Quatrini, R. and Holmes, D. S. (2012). *Niche specific oxidative stress response in extreme acidophiles*. 9th International Congress On Extremophiles, Seville, Spain**:** 202.

Cárdenas, J. P., Moya, F., Covarrubias, P., Shmaryahu, A., Levicán, G., Holmes, D. S. and Quatrini, R. (2012). "Comparative genomics of the oxidative stress response in bioleaching microorganisms." *Hydrometallurgy* **127–128**(0): 162-167.

Carlin, A., Shi, W., Dey, S. and Rosen, B. P. (1995). "The *ars* operon of *Escherichia coli* confers arsenical and antimonial resistance." *J Bacteriol* **177**(4): 981-986.

Cases, I., Ussery, D. W. and De Lorenzo, V. (2003). "The σ^{54} regulon (sigmulon) of *Pseudomonas putida*." *Environ Microbiol* **5**(12): 1281-1293.

Clarke, L. and Carbon, J. (1976). "A colony bank containing synthetic Col El hybrid plasmids representative of the entire *E. coli* genome." *Cell* **9**(1): 91-99.

Cleveland, W. S., Diaconis, P. and McGill, R. (1982). "Variables on scatterplots look more highly correlated when the scales are increased." *Science* **216**(4550): 1138-1141.

Clugston, S. L., Barnard, J. F. J., Kinach, R., Miedema, D., Ruman, R., Daub, E. and Honek, J. F. (1998). "Overproduction and characterization of a dimeric non-zinc glyoxalase I from *Escherichia coli*: evidence for optimal activation by nickel ions." *Biochemistry* **37**(24): 8754-8763.

Cohen, S. N., Chang, A. C. and Hsu, L. (1972). "Nonchromosomal antibiotic resistance in bacteria: genetic transformation of *Escherichia coli* by R-factor DNA." *Proc Natl Acad Sci U S A* **69**(8): 2110-2114.

Coupland, K. and Johnson, D. B. (2008). "Evidence that the potential for dissimilatory ferric iron reduction is widespread among acidophilic heterotrophic bacteria." *FEMS Microbiol Lett* **279**(1): 30-35.

Cummings, D. E., Fendorf, S., Singh, N., Sani, R. K., Peyton, B. M. and Magnuson, T. S. (2007). "Reduction of Cr(VI) under acidic conditions by the facultative Fe(lll)-reducing bacterium *Acidiphilium cryptum*." *Environ Sci Technol* **41**(1): 146-152.

Chakravarty, R. and Banerjee, P. C. (2008). "Morphological changes in an acidophilic bacterium induced by heavy metals." *Extremophiles* **12**(2): 279-284.

Chen, Y. and Rosen, B. P. (1997). "Metalloregulatory properties of the ArsD repressor." *J Biol Chem* **272**(22): 14257-14262.

Cheng, Z., Wei, Y. Y., Sung, W. W., Glick, B. R. and McConkey, B. J. (2009). "Proteomic analysis of the response of the plant growth-promoting bacterium Pseudomonas putida UW4 to nickel stress." *Proteome Sci* **7**: 18.

Chuang, S. E., Burland, V., Plunkett, G., 3rd, Daniels, D. L. and Blattner, F. R. (1993). "Sequence analysis of four new heat-shock genes constituting the hslTS/ibpAB and hslVU operons in Escherichia coli." *Gene* **134**(1): 1-6.

Dai, Y., Wensink, P. C. and Abeles, R. H. (1999). "One protein, two enzymes." *J Biol Chem* **274**(3): 1193-1195.

Dalebroux, Z. D. and Swanson, M. S. (2012). "ppGpp: magic beyond RNA polymerase." *Nat Rev Microbiol* **10**(3): 203-212.

Delcher, A. L., Bratke, K. A., Powers, E. C. and Salzberg, S. L. (2007). "Identifying bacterial genes and endosymbiont DNA with Glimmer." *Bioinformatics* **23**(6): 673-679.

DeLong, E. (2000). "Extreme genomes." *Genome Biol* **1**(6): reviews1029.1021 - reviews1029.1023.

Dew, D. W., Muhlbauer, R. and van Buuren, C. (1999). *Bioleaching of copper sulphide concentrates with mesophiles and thermophiles*. ALTA Copper 1999: Copper Sulphides Symposium & Copper Hydrometallurgy Forum, Brisbane, Australia.

Diekert, G., Klee, B. and Thauer, R. (1980). "Nickel, a component of factor F_{430} from *Methanobacterium thermoautotrophicum*." *Arch Microbiol* **124**(1): 103-106.

Dixon, N. E., Gazzola, C., Blakeley, R. L. and Zerner, B. (1975). "Jack bean urease (EC 3.5.1.5). Metalloenzyme. Simple biological role for nickel." *J Am Chem Soc* **97**(14): 4131-4133.

Dopson, M., Baker-Austin, C., Koppineedi, P. R. and Bond, P. L. (2003). "Growth in sulfidic mineral environments: metal resistance mechanisms in acidophilic micro-organisms." *Microbiology* **149**(Pt 8): 1959-1970.

Dopson, M., Baker-Austin, C., Hind, A., Bowman, J. P. and Bond, P. L. (2004). "Characterization of *Ferroplasma* isolates and *Ferroplasma acidarmanus* sp. nov., extreme acidophiles from acid mine drainage and industrial bioleaching environments." *Appl Environ Microbiol* **70**(4): 2079-2088.

Drake, H. L., Hu, S. I. and Wood, H. G. (1980). "Purification of carbon monoxide dehydrogenase, a nickel enzyme from *Clostridium thermocaceticum*." *J Biol Chem* **255**(15): 7174-7180.

du Plessis, C. A., Slabbert, W., Hallberg, K. B. and Johnson, D. B. (2011). "Ferredox: a biohydrometallurgical processing concept for limonitic nickel laterites." *Hydrometallurgy* **109**(3–4): 221-229.

Eaton, K. A., Brooks, C. L., Morgan, D. R. and Krakowka, S. (1991). "Essential role of urease in pathogenesis of gastritis induced by *Helicobacter pylori* in gnotobiotic piglets." *Infect Immun* **59**(7): 2470-2475.

Edgar, R., Domrachev, M. and Lash, A. E. (2002). "Gene Expression Omnibus: NCBI gene expression and hybridization array data repository." *Nucleic Acids Res* **30**(1): 207-210.

Ellefson, W. L., Whitman, W. B. and Wolfe, R. S. (1982). "Nickel-containing factor F_{430}: chromophore of the methylreductase of *Methanobacterium*." *Proc Natl Acad Sci U S A* **79**(12): 3707-3710.

Englert, D. L., Adase, C. A., Jayaraman, A. and Manson, M. D. (2010). "Repellent taxis in response to nickel ion requires neither Ni^{2+} transport nor the periplasmic NikA binding protein." *J Bacteriol* **192**(10): 2633-2637.

Environmental Monitoring Systems Laboratory, U. S. E. P. A. (1996). Method 200.8 - Determination of trace elements in waters and wastes by inductively coupled plasma -

mass spectrometry. *Methods for the Determination of Metals in Environmental Samples*. E. M. S. Laboratory. Westwood, NJ, William Andrew Publishing**:** 88-145.

Eoh, H. and Rhee, K. Y. (2014). "Methylcitrate cycle defines the bactericidal essentiality of isocitrate lyase for survival of *Mycobacterium tuberculosis* on fatty acids." *Proc Natl Acad Sci U S A* **111**(13): 4976-4981.

Eppley, J. M., Tyson, G. W., Getz, W. M. and Banfield, J. F. (2007). "Genetic exchange across a species boundary in the archaeal genus *Ferroplasma*." *Genetics* **177**(1): 407-416.

Fernández-Remolar, D. C., Morris, R. V., Gruener, J. E., Amils, R. and Knoll, A. H. (2005). "The Río Tinto Basin, Spain: mineralogy, sedimentary geobiology, and implications for interpretation of outcrop rocks at Meridiani Planum, Mars." *Earth Planet Sci Lett* **240**(1): 149-167.

Fernandez, V. M., Amils, R., Garcia, J. L., Gomez, F., Ballester, A., Martin Gago, J. A. and Gomez, M. J. (2006). Empleo de bacterias reductoras de hierro en procesos energéticos y de descontaminación (Picomicro). Madrid, Comunidad de Madrid.

Ferry, J. G. (1995). "CO dehydrogenase." *Annu Rev Microbiol* **49**(1): 305-333.

Fischer, J., Quentmeier, A., Gansel, S., Sabados, V. and Friedrich, C. G. (2002). "Inducible aluminum resistance of *Acidiphilium cryptum* and aluminum tolerance of other acidophilic bacteria." *Arch Microbiol* **178**(6): 554-558.

Flint, D. H., Tuminello, J. F. and Emptage, M. H. (1993). "The inactivation of Fe-S cluster containing hydro-lyases by superoxide." *J Biol Chem* **268**(30): 22369-22376.

Fortin, D., Southam, G. and Beveridge, T. J. (1994). "Nickel sulfide, iron-nickel sulfide and iron sulfide precipitation by a newly isolated *Desulfotomaculum* species and its relation to nickel resistance." *FEMS Microbiol Ecol* **14**(2): 121-132.

Forzani, C., Lobreaux, S., Mari, S., Briat, J. F. and Lebrun, M. (2002). "Metal resistance in yeast mediated by the expression of a maize 20S proteasome α subunit." *Gene* **293**(1-2): 199-204.

Gaal, T., Bartlett, M. S., Ross, W., Turnbough, C. L. and Gourse, R. L. (1997). "Transcription regulation by initiating NTP concentration: rRNA synthesis in bacteria." *Science* **278**(5346): 2092-2097.

Garcia-Moyano, A. (2007). Fisiología y ecología del género *Leptospirillum*, responsable de las condiciones extremas de Río Tinto. Ph.D thesis, Universidad Autónoma de Madrid, Madrid, Spain.

Garcia-Moyano, A., Gonzalez-Toril, E., Aguilera, A. and Amils, R. (2007). "Prokaryotic community composition and ecology of floating macroscopic filaments from an extreme acidic environment, Rio Tinto (SW, Spain)." *Syst Appl Microbiol* **30**(8): 601-614.

Garcia-Moyano, A., Gonzalez-Toril, E., Aguilera, A. and Amils, R. (2012). "Comparative microbial ecology study of the sediments and the water column of the Rio Tinto, an extreme acidic environment." *FEMS Microbiol Ecol* **81**(2): 303-314.

Gerdes, K., Christensen, S. K. and Lobner-Olesen, A. (2005). "Prokaryotic toxin-antitoxin stress response loci." *Nat Rev Microbiol* **3**(5): 371-382.

Geslin, C., Llanos, J., Prieur, D. and Jeanthon, C. (2001). "The manganese and iron superoxide dismutases protect Escherichia coli from heavy metal toxicity." *Res Microbiol* **152**(10): 901-905.

Ghosh, S., Mahapatra, N. R. and Banerjee, P. C. (1997). "Metal resistance in *Acidocella* strains and plasmid-mediated transfer of this characteristic to *Acidiphilium multivorum* and *Escherichia coli*." *Appl Environ Microbiol* **63**(11): 4523-4527.

Gihring, T., Bond, P., Peters, S. and Banfield, J. (2003). "Arsenic resistance in the archaeon "*Ferroplasma acidarmanus*": new insights into the structure and evolution of the ars genes." *Extremophiles* **7**(2): 123-130.

Glenn, A. W., Roberto, F. F. and Ward, T. E. (1992). "Transformation of Acidiphilium by electroporation and conjugation." *Canadian Journal of Microbiology* **38**(5): 387-393.

Gonzalez-Toril, E., Llobet-Brossa, E., Casamayor, E. O., Amann, R. and Amils, R. (2003). "Microbial ecology of an extreme acidic environment, the Tinto River." *Appl Environ Microbiol* **69**(8): 4853-4865.

Goris, J., De Vos, P., Coenye, T., Hoste, B., Janssens, D., Brim, H., Diels, L., Mergeay, M., Kersters, K. and Vandamme, P. (2001). "Classification of metal-resistant bacteria from industrial biotopes as *Ralstonia campinensis* sp. nov., *Ralstonia metallidurans* sp. nov. and *Ralstonia basilensis* Steinle et al. 1998 emend." *Int J Syst Evol Microbiol* **51**(Pt 5): 1773-1782.

Goryshin, I. Y. and Reznikoff, W. S. (1998). "Tn5 *in vitro* transposition." *J Biol Chem* **273**(13): 7367-7374.

Goto, Y., Calciano, L. J. and Fink, A. L. (1990). "Acid-induced folding of proteins." *Proc Natl Acad Sci U S A* **87**(2): 573-577.

Graf, E.-G. and Thauer, R. K. (1981). "Hydrogenase from *Methanobacterium thermoautotrophicum*, a nickel-containing enzyme." *FEBS Lett* **136**(1): 165-169.

Grass, G., Grosse, C. and Nies, D. H. (2000). "Regulation of the cnr cobalt and nickel resistance determinant from Ralstonia sp. strain CH34." *J Bacteriol* **182**(5): 1390-1398.

Grass, G., Fan, B., Rosen, B. P., Lemke, K., Schlegel, H.-G. and Rensing, C. (2001). "NreB from *Achromobacter xylosoxidans* 31A is a nickel-induced transporter conferring nickel resistance." *J Bacteriol* **183**(9): 2803-2807.

Guay, R. and Silver, M. (1975). "*Thiobacillus acidophilus* sp. nov.; isolation and some physiological characteristics." *Can J Microbiol* **21**(3): 281-288.

Guazzaroni, M. E., Morgante, V., Mirete, S. and Gonzalez-Pastor, J. E. (2013). "Novel acid resistance genes from the metagenome of the Tinto River, an extremely acidic environment." *Environ Microbiol* **15**(4): 1088-1102.

Guldan, H., Sterner, R. and Babinger, P. (2008). "Identification and characterization of a bacterial glycerol-1-phosphate dehydrogenase: Ni^{2+}-dependent AraM from *Bacillus subtilis*." *Biochemistry* **47**(28): 7376-7384.

Hallberg, K. B., Grail, B. M., Plessis, C. A. d. and Johnson, D. B. (2011). "Reductive dissolution of ferric iron minerals: a new approach for bio-processing nickel laterites." *Miner Eng* **24**(7): 620-624.

Hanahan, D. (1983). "Studies on transformation of *Escherichia coli* with plasmids." *J Mol Biol* **166**(4): 557-580.

Handrick, R., Reinhardt, S., Schultheiss, D., Reichart, T., Schüler, D., Jendrossek, V. and Jendrossek, D. (2004). "Unraveling the function of the *Rhodospirillum rubrum* activator of polyhydroxybutyrate (PHB) degradation: the activator is a PHB-granule-bound protein (Phasin)." *J Bacteriol* **186**(8): 2466-2475.

Haritha, A., Sagar, K. P., Tiwari, A., Kiranmayi, P., Rodrigue, A., Mohan, P. M. and Singh, S. S. (2009). "MrdH, a novel metal resistance determinant of *Pseudomonas putida* KT2440, is flanked by metal-inducible mobile genetic elements." *J Bacteriol* **191**(19): 5976-5987.

Harrison, A. P. (1983). "Genomic and physiological comparisons between heterotrophic thiobacilli and *Acidiphilium cryptum*, *Thiobacillus versutus* sp. nov., and *Thiobacillus acidophilus* nom. rev." *Int J Syst Bacteriol* **33**(2): 211-217.

Harrison, A. P. (1984). "The acidophilic thiobacilli and other acidophilic bacteria that share their habitat." *Annu Rev Microbiol* **38**(1): 265-292.

Harrison, A. P. J. (1981). "*Acidiphilium cryptum* gen. nov., sp. nov., heterotrophic bacterium from acidic mineral environments." *Int J Syst Bacteriol* **31**(3): 327-332.

Harvey, P. I. and Crundwell, F. K. (1996). "The effect of As(III) on the growth of *Thiobacillus ferrooxidans* in an electrolytic cell under controlled redox potentials." *Miner Eng* **9**(10): 1059-1068.

Hiraishi, A., Nagashima, K. V., Matsuura, K., Shimada, K., Takaichi, S., Wakao, N. and Katayama, Y. (1998). "Phylogeny and photosynthetic features of *Thiobacillus acidophilus* and related acidophilic bacteria: its transfer to the genus *Acidiphilium* as *Acidiphilium acidophilum* comb. nov." *Int J Syst Bacteriol* **48 Pt 4**: 1389-1398.

Hiraishi, A. and Shimada, K. (2001). "Aerobic anoxygenic photosynthetic bacteria with zinc-bacteriochlorophyll." *J Gen Appl Microbiol* **47**(4): 161-180.

Hiraishi, A. and Imhoff, J. (2005). *Acidiphilium* Harrison 1981, 331 VP emend. Kishimoto, Kosako, Wakao, Tano and Hiraishi 1995b, 90. *Bergey's Manual® of Systematic Bacteriology*. D. Brenner, N. Krieg, G. Garrity*et al*, Springer US**:** 54-62.

Hobman, J. L., Wilkie, J. and Brown, N. L. (2005). "A design for life: prokaryotic metal-binding MerR family regulators." *Biometals* **18**(4): 429-436.

Holmes, D. S. and Haq, R. (1989). *Adaptation of Thiobacillus ferrooxidans for industrial applications*. Biohydrometallurgy, Jackson Hole, Wyoming, Canadian Centre for Mineral and Energy Technology**:** 116-127.

Hong, W., Jiao, W., Hu, J., Zhang, J., Liu, C., Fu, X., Shen, D., Xia, B. and Chang, Z. (2005). "Periplasmic protein HdeA exhibits chaperone-like activity exclusively within stomach pH range by transforming into disordered conformation." *J Biol Chem* **280**(29): 27029-27034.

Horswill, A. R. and Escalante-Semerena, J. C. (1999). "*Salmonella typhimurium* LT2 catabolizes propionate via the 2-methylcitric acid cycle." *J Bacteriol* **181**(18): 5615-5623.

Horswill, A. R., Dudding, A. R. and Escalante-Semerena, J. C. (2001). "Studies of propionate toxicity in *Salmonella enterica* identify 2-methylcitrate as a potent inhibitor of cell growth." *J Biol Chem* **276**(22): 19094-19101.

Horvath, P. and Barrangou, R. (2010). "CRISPR/Cas, the immune system of bacteria and archaea." *Science* **327**(5962): 167-170.

Huber, G., Spinnler, C., Gambacorta, A. and Stetter, K. O. (1989). "*Metallosphaera sedula* gen, and sp. nov. represents a new genus of aerobic, metal-mobilizing, thermoacidophilic archaebacteria." *Syst Appl Microbiol* **12**(1): 38-47.

Igarashi, N., Harada, J., Nagashima, S., Matsuura, K., Shimada, K. and Nagashima, K. V. P. (2001). "Horizontal transfer of the photosynthesis gene cluster and operon rearrangement in purple bacteria." *J Mol Evol* **52**(4): 333-341.

Imhoff, J. and Hiraishi, A. (2005). Aerobic bacteria containing bacteriochlorophyll and belonging to the *Alphaproteobacteria*. *Bergey's Manual® of Systematic Bacteriology*. D. Brenner, N. Krieg, J. Staley and G. Garrity, Springer US**:** 133-136.

Inagaki, K., Tomono, J., Kishimoto, N., Tano, T. and Tanaka, H. (1993a). "Cloning and sequence of the *recA* gene of *Acidiphilium facilis*." *Nucleic Acids Res* **21**(17): 4149.

Inagaki, K., Tomono, J., Kishimoto, N., Tano, T. and Tanaka, H. (1993b). "Transformation of the acidophilic heterotroph *Acidiphilium facilis* by electroporation." *Biosci Biotechnol Biochem* **57**(10): 1770-1771.

Inoue, H., Nojima, H. and Okayama, H. (1990). "High efficiency transformation of *Escherichia coli* with plasmids." *Gene* **96**(1): 23-28.

Irving, H. and Williams, R. J. P. (1953). "637. The stability of transition-metal complexes." *J Chem Soc*(0): 3192-3210.

Jain, R. and Chan, M. K. (2007). "Support for a potential role of E. coli oligopeptidase A in protein degradation." *Biochem Biophys Res Commun* **359**(3): 486-490.

Jaun, B. and Thauer, R. K. (2007). Methyl-coenzyme M reductase and its nickel corphin coenzyme F_{430} in methanogenic archaea. *Nickel and its surprising impact in nature*. A. Sigel, H. Sigel and R. K. O. Sigel. Chichester, West Sussex, England, John Wiley & Sons Ltd.**:** 323-356.

Johnson, D. B. and McGinness, S. (1991). "Ferric iron reduction by acidophilic heterotrophic bacteria." *Appl Environ Microbiol* **57**(1): 207-211.

Johnson, D. B., Ghauri, M. A. and Said, M. F. (1992). "Isolation and characterization of an acidophilic, heterotrophic bacterium capable of oxidizing ferrous iron." *Appl Environ Microbiol* **58**(5): 1423-1428.

Johnson, D. B. (1998). "Biodiversity and ecology of acidophilic microorganisms." *FEMS Microbiol Ecol* **27**(4): 307-317.

Johnson, D. B. and Bridge, T. A. (2002). "Reduction of ferric iron by acidophilic heterotrophic bacteria: evidence for constitutive and inducible enzyme systems in *Acidiphilium* spp." *J Appl Microbiol* **92**(2): 315-321.

Joho, M., Inouhe, M., Tohoyama, H. and Murayama, T. (1995a). "Nickel resistance mechanisms in yeasts and other fungi." *Journal of Industrial Microbiology* **14**(2): 164-168.

Joho, M., Inouhe, M., Tohoyama, H. and Murayama, T. (1995b). "Nickel resistance mechanisms in yeasts and other fungi." *J Ind Microbiol* **14**(2): 164-168.

Kaluarachchi, H., Chan Chung, K. C. and Zamble, D. B. (2010). "Microbial nickel proteins." *Nat Prod Rep* **27**(5): 681-694.

Kanemori, M., Nishihara, K., Yanagi, H. and Yura, T. (1997). "Synergistic roles of HslVU and other ATP-dependent proteases in controlling in vivo turnover of σ32 and abnormal proteins in Escherichia coli." *J Bacteriol* **179**(23): 7219-7225.

Karp, P. D., Paley, S. and Romero, P. (2002). "The Pathway Tools software." *Bioinformatics* **18 Suppl 1**: S225-232.

Khattar, M. M. (1997). "Overexpression of the hslVU operon suppresses SOS-mediated inhibition of cell division in Escherichia coli." *FEBS Lett* **414**(2): 402-404.

Kishimoto, N. and Tano, T. (1987). "Acidophilic heterotrophic bacteria isolated from acidic mine drainage, sewage, and soils." *J Gen Appl Microbiol* **33**(1): 11-25.

Kishimoto, N., Fukaya, F., Inagaki, K., Sugio, T., Tanaka, H. and Tano, T. (1995a). "Distribution of bacteriochlorophyll *a* among aerobic and acidophilic bacteria and light-enhanced CO_2-incorporation in *Acidiphilium rubrum*." *FEMS Microbiol Ecol* **16**(4): 291-296.

Kishimoto, N., Kosako, Y., Wakao, N., Tano, T. and Hiraishi, A. (1995b). "Transfer of *Acidiphilium facilis* and *Acidiphilium aminolytica* to the genus *Acidocella* gen. nov., and emendation of the genus *Acidiphilium*." *Syst Appl Microbiol* **18**(1): 85-91.

Kobayashi, M., Yamamura, M., Akiyama, M., Kise, H., Inoue, K., Hara, M., Wakao, N., Yahara, K. and Watanabe, T. (1998). "Acid resistance of Zn-Bacteriochlorophyll *a* from an acidophilic bacterium *Acidiphilium rubrum*." *Analyt Sci* **14**(6): 1149-1152.

Kondratyeva, T. F., Muntyan, L. N. and Karavaiko, G. I. (1995). "Zinc- and arsenic-resistant strains of *Thiobacillus ferrooxidans* have increased copy numbers of chromosomal resistance genes." *Microbiology* **141**(5): 1157-1162.

Kontur, W. S., Schackwitz, W. S., Ivanova, N., Martin, J., Labutti, K., Deshpande, S., Tice, H. N., Pennacchio, C., Sodergren, E., Weinstock, G. M., Noguera, D. R. and

Donohue, T. J. (2012). "Revised sequence and annotation of the *Rhodobacter sphaeroides* 2.4.1 genome." *J Bacteriol* **194**(24): 7016-7017.

Kusel, K., Dorsch, T., Acker, G. and Stackebrandt, E. (1999). "Microbial reduction of Fe(III) in acidic sediments: isolation of *Acidiphilium cryptum* JF-5 capable of coupling the reduction of Fe(III) to the oxidation of glucose." *Appl Environ Microbiol* **65**(8): 3633-3640.

Kusel, K., Roth, U. and Drake, H. L. (2002). "Microbial reduction of Fe(III) in the presence of oxygen under low pH conditions." *Environ Microbiol* **4**(7): 414-421.

Leduc, L. G., Ferroni, G. D. and Trevors, J. T. (1997). "Resistance to heavy metals in different strains of *Thiobacillus ferrooxidans*." *World J Microbiol Biotechnol* **13**(4): 453-455.

Leistel, J. M., Marcoux, E., Thiéblemont, D., Quesada, C., Sánchez, A., Almodóvar, G. R., Pascual, E. and Sáez, R. (1997). "The volcanic-hosted massive sulphide deposits of the Iberian Pyrite Belt." *Miner Deposita* **33**(1-2): 2-30.

Lemke, J. J., Sanchez-Vazquez, P., Burgos, H. L., Hedberg, G., Ross, W. and Gourse, R. L. (2011). "Direct regulation of *Escherichia coli* ribosomal protein promoters by the transcription factors ppGpp and DksA." *Proc Natl Acad Sci U S A* **108**(14): 5712-5717.

Lennox, E. S. (1955). "Transduction of linked genetic characters of the host by bacteriophage P1." *Virology* **1**(2): 190-206.

Li, Y. and Zamble, D. B. (2009). "Nickel homeostasis and nickel regulation: an overview." *Chem Rev* **109**(10): 4617-4643.

Lien, H. Y., Yu, C. H., Liou, C. M. and Wu, W. F. (2009). "Regulation of clpQ+Y+ (hslV+U+) Gene Expression in Escherichia coli." *Open Microbiol J* **3**: 29-39.

Liesegang, H., Lemke, K., Siddiqui, R. A. and Schlegel, H. G. (1993). "Characterization of the inducible nickel and cobalt resistance determinant cnr from pMOL28 of Alcaligenes eutrophus CH34." *J Bacteriol* **175**(3): 767-778.

Lightfoot, D. A., Baron, A. J. and Wootton, J. C. (1988). "Expression of the *Escherichia coli* glutamate dehydrogenase gene in the cyanobacterium *Synechococcus* PCC6301 causes ammonium tolerance." *Plant Mol Biol* **11**(3): 335-344.

Lo, I., Denef, V. J., Verberkmoes, N. C., Shah, M. B., Goltsman, D., DiBartolo, G., Tyson, G. W., Allen, E. E., Ram, R. J., Detter, J. C., Richardson, P., Thelen, M. P., Hettich, R. L. and Banfield, J. F. (2007). "Strain-resolved community proteomics reveals recombining genomes of acidophilic bacteria." *Nature* **446**(7135): 537-541.

Lobos, J. H., Chisolm, T. E., Bopp, L. H. and Holmes, D. S. (1986). "*Acidiphilium organovorum* sp. nov., an acidophilic heterotroph isolated from a *Thiobacillus ferrooxidans* culture." *Int J Syst Bacteriol* **36**(2): 139-144.

Lopez-Archilla, A. I., Marin, I. and Amils, R. (2001). "Microbial community composition and ecology of an acidic aquatic environment: the Tinto River, Spain." *Microb Ecol* **41**(1): 20-35.

López de Saro, F. J., Gómez, M. J., González-Tortuero, E. and Parro, V. (2013). The dynamic genomes of acidophiles. *Polyextremophiles*. J. Seckbach, A. Oren and H. Stan-Lotter, Springer Netherlands. **27:** 81-97.

Lovley, D. R. (2006). "Bug juice: harvesting electricity with microorganisms." *Nat Rev Microbiol* **4**(7): 497-508.

Lovley, D. R. (2012). "Electromicrobiology." *Annu Rev Microbiol* **66**(1): 391-409.

Lowe, T. M. and Eddy, S. R. (1997). "tRNAscan-SE: a program for improved detection of transfer RNA genes in genomic sequence." *Nucleic Acids Res* **25**(5): 955-964.

Ludwig, W., Strunk, O., Westram, R., Richter, L., Meier, H., Yadhukumar, Buchner, A., Lai, T., Steppi, S., Jobb, G., Förster, W., Brettske, I., Gerber, S., Ginhart, A. W., Gross,

O., Grumann, S., Hermann, S., Jost, R., König, A., Liss, T., Lüßmann, R., May, M., Nonhoff, B., Reichel, B., Strehlow, R., Stamatakis, A., Stuckmann, N., Vilbig, A., Lenke, M., Ludwig, T., Bode, A. and Schleifer, K. H. (2004). "ARB: a software environment for sequence data." *Nucleic Acids Research* **32**(4): 1363-1371.

Macomber, L., Elsey, S. P. and Hausinger, R. P. (2011). "Fructose-1,6-bisphosphate aldolase (class II) is the primary site of nickel toxicity in *Escherichia coli*." *Mol Microbiol* **82**(5): 1291-1300.

Macomber, L. and Hausinger, R. P. (2011). "Mechanisms of nickel toxicity in microorganisms." *Metallomics* **3**(11): 1153-1162.

Maezato, Y., Johnson, T., McCarthy, S., Dana, K. and Blum, P. (2012). "Metal resistance and lithoautotrophy in the extreme thermoacidophile *Metallosphaera sedula*." *J Bacteriol* **194**(24): 6856-6863.

Mahapatra, N. R. and Banerjee, P. C. (1996). "Extreme tolerance to cadmium and high resistance to copper, nickel and zinc in different *Acidiphilium* strains." *Lett Appl Microbiol* **23**(6): 393-397.

Mahapatra, N. R., Ghosh, S., Deb, C. and Banerjee, P. C. (2002a). "Resistance to Cadmium and Zinc in Acidiphilium symbioticum KM2 Is Plasmid Mediated." *Current Microbiology* **45**(3): 180-186.

Mahapatra, N. R., Ghosh, S., Deb, C. and Banerjee, P. C. (2002b). "Resistance to cadmium and zinc in Acidiphilium symbioticum KM2 is plasmid mediated." *Curr Microbiol* **45**(3): 180-186.

Mahapatra, N. R., Ghosh, S., Sarkar, P. K. and Banerjee, P. C. (2003). "Generation of novel plasmids in *Escherichia coli* S17-1(pSUP106)." *Curr Microbiol* **46**(5): 318-323.

Malki, M. (2003). *Acidithiobacillus ferrooxidans* y su papel en la geomicrobiología del ciclo del hierro en el Río Tinto. Ph.D thesis, Universidad Autónoma de Madrid, Madrid, Spain.

Malki, M., De Lacey, A. L., Rodriguez, N., Amils, R. and Fernandez, V. M. (2008). "Preferential use of an anode as an electron acceptor by an acidophilic bacterium in the presence of oxygen." *Appl Environ Microbiol* **74**(14): 4472-4476.

Marchler-Bauer, A., Zheng, C., Chitsaz, F., Derbyshire, M. K., Geer, L. Y., Geer, R. C., Gonzales, N. R., Gwadz, M., Hurwitz, D. I., Lanczycki, C. J., Lu, F., Lu, S., Marchler, G. H., Song, J. S., Thanki, N., Yamashita, R. A., Zhang, D. and Bryant, S. H. (2013). "CDD: conserved domains and protein three-dimensional structure." *Nucleic Acids Res* **41**(D1): D348-D352.

Marmur, J. (1961). "A procedure for the isolation of deoxyribonucleic acid from micro-organisms." *J Mol Biol* **3**(2): 208-218.

Marrero, J., Auling, G., Coto, O. and Nies, D. H. (2007). "High-level resistance to cobalt and nickel but probably no transenvelope efflux: metal resistance in the Cuban *Serratia marcescens* strain C-1." *Microb Ecol* **53**(1): 123-133.

Matsumoto, K. i., Matsusaki, H., Taguchi, K., Seki, M. and Doi, Y. (2002). "Isolation and characterization of polyhydroxyalkanoates inclusions and their associated proteins in *Pseudomonas* sp. 61-3." *Biomacromolecules* **3**(4): 787-792.

Mergeay, M., Nies, D., Schlegel, H. G., Gerits, J., Charles, P. and Van Gijsegem, F. (1985). "*Alcaligenes eutrophus* CH34 is a facultative chemolithotroph with plasmid-bound resistance to heavy metals." *J Bacteriol* **162**(1): 328-334.

Mergeay, M., Monchy, S., Vallaeys, T., Auquier, V., Benotmane, A., Bertin, P., Taghavi, S., Dunn, J., van der Lelie, D. and Wattiez, R. (2003). "*Ralstonia metallidurans*, a bacterium specifically adapted to toxic metals: towards a catalogue of metal-responsive genes." *FEMS Microbiol Rev* **27**(2-3): 385-410.

Merkens, H., Kappl, R., Jakob, R. P., Schmid, F. X. and Fetzner, S. (2008). "Quercetinase QueD of *Streptomyces* sp. FLA, a monocupin dioxygenase with a preference for nickel and cobalt." *Biochemistry* **47**(46): 12185-12196.

Michelucci, A., Cordes, T., Ghelfi, J., Pailot, A., Reiling, N., Goldmann, O., Binz, T., Wegner, A., Tallam, A., Rausell, A., Buttini, M., Linster, C. L., Medina, E., Balling, R. and Hiller, K. (2013). "Immune-responsive gene 1 protein links metabolism to immunity by catalyzing itaconic acid production." *Proc Natl Acad Sci U S A* **110**(19): 7820-7825.

Mier, J. L., Ballester, A., Gonzalez, F., Blazquez, M. L. and Gomez, E. (1996). "The influence of metallic ions on the activity of *Sulfolobus* BC." *J Chem Technol Biotechnol* **65**(3): 272-280.

Miller, K. W., Risanico, S. S. and Bruno Risatti, J. (1992). "Differential tolerance of *Sulfolobus* strains to transition metals." *FEMS Microbiol Lett* **93**(1): 69-73.

Mirete, S., de Figueras, C. G. and Gonzalez-Pastor, J. E. (2007). "Novel nickel resistance genes from the rhizosphere metagenome of plants adapted to acid mine drainage." *Appl Environ Microbiol* **73**(19): 6001-6011.

Missiakas, D., Schwager, F., Betton, J. M., Georgopoulos, C. and Raina, S. (1996). "Identification and characterization of HsIV HsIU (ClpQ ClpY) proteins involved in overall proteolysis of misfolded proteins in Escherichia coli." *EMBO J* **15**(24): 6899-6909.

Monchy, S., Benotmane, M. A., Janssen, P., Vallaeys, T., Taghavi, S., van der Lelie, D. and Mergeay, M. (2007). "Plasmids pMOL28 and pMOL30 of *Cupriavidus metallidurans* are specialized in the maximal viable response to heavy metals." *J Bacteriol* **189**(20): 7417-7425.

Moran, N. A. and Plague, G. R. (2004). "Genomic changes following host restriction in bacteria." *Curr Opin Genet Dev* **14**(6): 627-633.

Moreno, R., Martínez-Gomariz, M., Yuste, L., Gil, C. and Rojo, F. (2009). "The *Pseudomonas putida* Crc global regulator controls the hierarchical assimilation of amino acids in a complete medium: evidence from proteomic and genomic analyses." *Proteomics* **9**(11): 2910-2928.

Morgante, V., Mirete, S., de Figueras, C. G., Postigo Cacho, M. and González-Pastor, J. E. (2014). "Exploring the diversity of arsenic resistance genes from acid mine drainage microorganisms." *Environ Microbiol*: doi: 10.1111/1462-2920.12505.

Moy, E. C. (2007). Prohibition on the exportation, melting, or treatment of 5-cent and one-cent coins. T. United States Mint, Federal Register. **31 CFR Part 82**.

Mulrooney, S. B. and Hausinger, R. P. (2003). "Nickel uptake and utilization by microorganisms." *FEMS Microbiol Rev* **27**(2-3): 239-261.

Munkelt, D., Grass, G. and Nies, D. H. (2004). "The chromosomally encoded cation diffusion facilitator proteins DmeF and FieF from *Wautersia metallidurans* CH34 are transporters of broad metal specificity." *J Bacteriol* **186**(23): 8036-8043.

Nagashima, S. and Nagashima, K. V. P. (2013). Chapter Five - Comparison of photosynthesis gene clusters retrieved from total genome sequences of purple bacteria. *Advances in Botanical Research*. J. T. Beatty, Academic Press. **Volume 66:** 151-178.

Naylor, G., Addlesee, H., Gibson, L. and Hunter, C. (1999). "The photosynthesis gene cluster of *Rhodobacter sphaeroides*." *Photosynth Res* **62**(2): 121-139.

Nieminen, T. M., Ukonmaanaho, L., Rausch, N. and Shotyk, W. (2007). Biogeochemistry of nickel and its release into the environment. *Nickel and Its Surprising Impact in Nature*, John Wiley & Sons, Ltd**:** 1-29.

Nies, D. H. (1999). "Microbial heavy-metal resistance." *Appl Microbiol Biotechnol* **51**(6): 730-750.

Nies, D. H. (2003). "Efflux-mediated heavy metal resistance in prokaryotes." *FEMS Microbiol Rev* **27**(2-3): 313-339.

Nriagu, J. O. (1990). "Global metal pollution - poisoning the biosphere." *Environment* **32**(7): 6-&.

Östlund, G., Schmitt, T., Forslund, K., Köstler, T., Messina, D. N., Roopra, S., Frings, O. and Sonnhammer, E. L. L. (2010). "InParanoid 7: new algorithms and tools for eukaryotic orthology analysis." *Nucleic Acids Res* **38**(suppl 1): D196-D203.

Papke, R. T., Koenig, J. E., Rodríguez-Valera, F. and Doolittle, W. F. (2004). "Frequent recombination in a saltern population of *Halorubrum*." *Science* **306**(5703): 1928-1929.

Park, J. E., Schlegel, H. G., Rhie, H. G. and Lee, H. S. (2004). "Nucleotide sequence and expression of the ncr nickel and cobalt resistance in Hafnia alvei 5-5." *Int Microbiol* **7**(1): 27-34.

Park, J. S., Lee, S. J., Rhie, H. G. and Lee, H. S. (2008). "Characterization of a chromosomal nickel resistance determinant from *Klebsiella oxytoca* CCUG 15788." *J Microbiol Biotechnol* **18**(6): 1040-1043.

Parker, C. T., Kloser, A. W., Schnaitman, C. A., Stein, M. A., Gottesman, S. and Gibson, B. W. (1992a). "Role of the rfaG and rfaP genes in determining the lipopolysaccharide core structure and cell surface properties of Escherichia coli K-12." *J Bacteriol* **174**(8): 2525-2538.

Parker, C. T., Pradel, E. and Schnaitman, C. A. (1992b). "Identification and sequences of the lipopolysaccharide core biosynthetic genes rfaQ, rfaP, and rfaG of Escherichia coli K-12." *J Bacteriol* **174**(3): 930-934.

Parro, V. and Moreno-Paz, M. (2003). "Gene function analysis in environmental isolates: the *nif* regulon of the strict iron oxidizing bacterium *Leptospirillum ferrooxidans*." *Proc Natl Acad Sci U S A* **100**(13): 7883-7888.

Paul, B. J., Ross, W., Gaal, T. and Gourse, R. L. (2004). "rRNA transcription in *Escherichia coli*." *Annu Rev Genet* **38**(1): 749-770.

Pennella, M. A. and Giedroc, D. P. (2005). "Structural determinants of metal selectivity in prokaryotic metal-responsive transcriptional regulators." *Biometals* **18**(4): 413-428.

Perkins, D. N., Pappin, D. J., Creasy, D. M. and Cottrell, J. S. (1999). "Probability-based protein identification by searching sequence databases using mass spectrometry data." *Electrophoresis* **20**(18): 3551-3567.

Persky, N. S., Ferullo, D. J., Cooper, D. L., Moore, H. R. and Lovett, S. T. (2009). "The ObgE/CgtA GTPase influences the stringent response to amino acid starvation in *Escherichia coli*." *Mol Microbiol* **73**(2): 253-266.

Piir, K., Paier, A., Liiv, A., Tenson, T. and Maivali, U. (2011). "Ribosome degradation in growing bacteria." *EMBO Rep* **12**(5): 458-462.

Potrykus, K. and Cashel, M. (2008). "(p)ppGpp: still magical?" *Annu Rev Microbiol* **62**: 35-51.

Pronk, J. T., Meesters, P. J. W., Dijken, J. P., Bos, P. and Kuenen, J. G. (1990). "Heterotrophic growth of *Thiobacillus acidophilus* in batch and chemostat cultures." *Arch Microbiol* **153**(4): 392-398.

Pruitt, K. D., Tatusova, T., Brown, G. R. and Maglott, D. R. (2012). "NCBI Reference Sequences (RefSeq): current status, new features and genome annotation policy." *Nucleic Acids Res* **40**(D1): D130-D135.

Pruteanu, M., Neher, S. B. and Baker, T. A. (2007). "Ligand-controlled proteolysis of the Escherichia coli transcriptional regulator ZntR." *J Bacteriol* **189**(8): 3017-3025.

Quentmeier, A. and Friedrich, C. G. (1994). "Transfer and expression of degradative and antibiotic resistance plasmids in acidophilic bacteria." *Appl Environ Microbiol* **60**(3): 973-978.

Ragsdale, S. W. and Kumar, M. (1996). "Nickel-containing carbon monoxide dehydrogenase/acetyl-CoA synthase." *Chem Rev* **96**(7): 2515-2540.

Rastorguev, S. M., Zavil'gel'skii, G. B., Suzuki, K. and Sakka, K. (2001). "[Alleviation of type I restriction in *Escherichia coli* K12 in the presence of the *arsR* gene from pKW301 of *Acidiphilium multivorum* AIU 301]." *Mol Biol (Mosk)* **35**(1): 79-82.

Rawlings, D. (2007). Relevance of cell physiology and genetic adaptability of biomining microorganisms to industrial processes. *Biomining*. D. Rawlings and D. B. Johnson, Springer Berlin Heidelberg**:** 177-198.

Rawlings, D. E. (2002). "Heavy metal mining using microbes." *Annu Rev Microbiol* **56**: 65-91.

Reimann, C., Norges geologiske, u., Geologian, t. and Central Kola, E. (1998). *Environmental geochemical atlas of the central Barents region*. Trondheim, Norway, Geological Survey of Norway.

Reizer, J., Reizer, A., Saier Jr, M. H., Bork, P. and Sander, C. (1993). "Exopolyphosphate phosphatase and guanosine pentaphosphate phosphatase belong to the sugar kinase/actin/hsp70 superfamily." *Trends Biochem Sci* **18**(7): 247-248.

Rice, P., Longden, I. and Bleasby, A. (2000). "EMBOSS: The European Molecular Biology Open Software Suite." *Trends Genet* **16**(6): 276-277.

Richard, H. and Foster, J. W. (2004). "Escherichia coli glutamate- and arginine-dependent acid resistance systems increase internal pH and reverse transmembrane potential." *J Bacteriol* **186**(18): 6032-6041.

Rocco, C. J. and Escalante-Semerena, J. C. (2010). "In *Salmonella enterica*, 2-methylcitrate blocks gluconeogenesis." *J Bacteriol* **192**(3): 771-778.

Rodrigue, A., Effantin, G. and Mandrand-Berthelot, M. A. (2005). "Identification of *rcnA* (*yohM*), a nickel and cobalt resistance gene in *Escherichia coli*." *J Bacteriol* **187**(8): 2912-2916.

Rohrwild, M., Coux, O., Huang, H. C., Moerschell, R. P., Yoo, S. J., Seol, J. H., Chung, C. H. and Goldberg, A. L. (1996). "HslV-HslU: A novel ATP-dependent protease complex in Escherichia coli related to the eukaryotic proteasome." *Proc Natl Acad Sci U S A* **93**(12): 5808-5813.

Rubio-Sanz, L., Prieto, R. I., Imperial, J., Palacios, J. M. and Brito, B. (2013). "Functional and expression analysis of the metal-inducible *dmeRF* system from *Rhizobium leguminosarum* bv. viciae." *Appl Environ Microbiol* **79**(20): 6414-6422.

Ruepp, A., Graml, W., Santos-Martinez, M.-L., Koretke, K. K., Volker, C., Mewes, H. W., Frishman, D., Stocker, S., Lupas, A. N. and Baumeister, W. (2000). "The genome sequence of the thermoacidophilic scavenger *Thermoplasma acidophilum*." *Nature* **407**(6803): 508-513.

Sambrook, J. and Russell, D. W. (2001). *Molecular cloning: a laboratory manual*. Cold Spring Harbor, New York, Cold Spring Harbor Laboratory Press.

Sampson, M. I. and Phillips, C. V. (2001). "Influence of base metals on the oxidising ability of acidophilic bacteria during the oxidation of ferrous sulfate and mineral sulfide concentrates, using mesophiles and moderate thermophiles." *Miner Eng* **14**(3): 317-340.

San Martin-Uriz, P., Gomez, M. J., Arcas, A., Bargiela, R. and Amils, R. (2011). "Draft genome sequence of the electricigen *Acidiphilium* sp. strain PM (DSM 24941)." *J Bacteriol* **193**(19): 5585-5586.

Sanchez-Andrea, I., Rodriguez, N., Amils, R. and Sanz, J. L. (2011). "Microbial diversity in anaerobic sediments at Rio Tinto, a naturally acidic environment with a high heavy metal content." *Appl Environ Microbiol* **77**(17): 6085-6093.

Sanchez-Andrea, I., Knittel, K., Amann, R., Amils, R. and Sanz, J. L. (2012). "Quantification of Tinto River sediment microbial communities: importance of sulfate-reducing bacteria and their role in attenuating acid mine drainage." *Appl Environ Microbiol* **78**(13): 4638-4645.

Sanger, F., Nicklen, S. and Coulson, A. R. (1977). "DNA sequencing with chain-terminating inhibitors." *Proc Natl Acad Sci U S A* **74**(12): 5463-5467.

SantaLucia, J. (1998). "A unified view of polymer, dumbbell, and oligonucleotide DNA nearest-neighbor thermodynamics." *Proc Natl Acad Sci U S A* **95**(4): 1460-1465.

Santiago, B., MacGilvray, M., Faustoferri, R. C. and Quivey, R. G., Jr. (2012). "The branched-chain amino acid aminotransferase encoded by *ilvE* is involved in acid tolerance in *Streptococcus mutans*." *J Bacteriol* **194**(8): 2010-2019.

Sarikaya, A., Akman, G. and Temizkan, G. (2006). "Nickel resistance in fission yeast associated with the magnesium transport system." *Mol Biotechnol* **32**(2): 139-145.

Schaaper, R. M. and Mathews, C. K. (2013). "Mutational consequences of dNTP pool imbalances in *E. coli*." *DNA Repair (Amst)* **12**(1): 73-79.

Schippers, A. and Sand, W. (1999). "Bacterial leaching of metal sulfides proceeds by two indirect mechanisms via thiosulfate or via polysulfides and sulfur." *Appl Environ Microbiol* **65**(1): 319-321.

Schmidt, T., Stoppel, R.-D. and Schlegel, H. G. (1991). "High-level nickel resistance in *Alcaligenes xylosoxydans* 31A and *Alcaligenes eutrophus* KTO2." *Appl Environ Microbiol* **57**(11): 3301-3309.

Schmidt, T. and Schlegel, H. G. (1994). "Combined nickel-cobalt-cadmium resistance encoded by the *ncc* locus of *Alcaligenes xylosoxidans* 31A." *J Bacteriol* **176**(22): 7045-7054.

Schönheit, P., Moll, J. and Thauer, R. (1979). "Nickel, cobalt, and molybdenum requirement for growth of *Methanobacterium thermoautotrophicum*." *Arch Microbiol* **123**(1): 105-107.

Schonknecht, G., Chen, W. H., Ternes, C. M., Barbier, G. G., Shrestha, R. P., Stanke, M., Brautigam, A., Baker, B. J., Banfield, J. F., Garavito, R. M., Carr, K., Wilkerson, C., Rensing, S. A., Gagneul, D., Dickenson, N. E., Oesterhelt, C., Lercher, M. J. and Weber, A. P. (2013). "Gene transfer from bacteria and archaea facilitated evolution of an extremophilic eukaryote." *Science* **339**(6124): 1207-1210.

Schwartz, D. C. and Cantor, C. R. (1984). "Separation of yeast chromosome-sized DNAs by pulsed field gradient gel electrophoresis." *Cell* **37**(1): 67-75.

Schwartz, E. and Friedrich, B. (2006). The H_2-metabolizing prokaryotes. *The Prokaryotes*. M. Dworkin, S. Falkow, E. Rosenberg, K.-H. Schleifer and E. Stackebrandt, Springer New York**:** 496-563.

Seaver, L. C. and Imlay, J. A. (2001). "Alkyl hydroperoxide reductase is the primary scavenger of endogenous hydrogen peroxide in *Escherichia coli*." *J Bacteriol* **183**(24): 7173-7181.

Seong, I. S., Oh, J. Y., Yoo, S. J., Seol, J. H. and Chung, C. H. (1999). "ATP-dependent degradation of SulA, a cell division inhibitor, by the HslVU protease in Escherichia coli." *FEBS Lett* **456**(1): 211-214.

Shahid, M., Pourrut, B., Dumat, C., Nadeem, M., Aslam, M. and Pinelli, E. (2014). "Heavy-metal-induced reactive oxygen species: phytotoxicity and physicochemical changes in plants." *Rev Environ Contam Toxicol* **232**: 1-44.

Shuttleworth, K. L., Unz, R. F. and Wichlacz, P. L. (1985). "Glucose catabolism in strains of acidophilic, heterotrophic bacteria." *Appl Environ Microbiol* **50**(3): 573-579.

Sigel, R. K. O. and Sigel, H. (2007). Complex formation of nickel(II) and related metal ions with sugar residues, nucleobases, phosphates, nucleotides, and nucleic acids. *Nickel and its surprising impact in nature*. A. Sigel, H. Sigel and R. K. O. Sigel. Chichester, West Sussex, England, John Wiley & Sons Ltd.**:** 109-180.

Siguier, P., Perochon, J., Lestrade, L., Mahillon, J. and Chandler, M. (2006). "ISfinder: the reference centre for bacterial insertion sequences." *Nucleic Acids Res* **34**(suppl 1): D32-D36.

Silver, S. and Phung le, T. (2005). "A bacterial view of the periodic table: genes and proteins for toxic inorganic ions." *J Ind Microbiol Biotechnol* **32**(11-12): 587-605.

Simmons, S. L., Dibartolo, G., Denef, V. J., Goltsman, D. S., Thelen, M. P. and Banfield, J. F. (2008). "Population genomic analysis of strain variation in *Leptospirillum* group II bacteria involved in acid mine drainage formation." *PLoS Biol* **6**(7): e177.

Singh, S. K. and Banerjee, P. C. (2007). "Nucleotide sequence analysis of cryptic plasmid pAM5 from *Acidiphilium multivorum*." *Plasmid* **58**(2): 101-114.

Snow, E. T., Xu, L.-S. and Kinney, P. L. (1993). "Effects of nickel ions on polymerase activity and fidelity during DNA replication in vitro." *Chem Biol Interact* **88**(2–3): 155-173.

Souza-Egipsy, V., Gonzalez-Toril, E., Zettler, E., Amaral-Zettler, L., Aguilera, A. and Amils, R. (2008). "Prokaryotic community structure in algal photosynthetic biofilms from extreme acidic streams in Rio Tinto (Huelva, Spain)." *Int Microbiol* **11**(4): 251-260.

Stahler, F. N., Odenbreit, S., Haas, R., Wilrich, J., Van Vliet, A. H., Kusters, J. G., Kist, M. and Bereswill, S. (2006). "The novel *Helicobacter pylori* CznABC metal efflux pump is required for cadmium, zinc, and nickel resistance, urease modulation, and gastric colonization." *Infect Immun* **74**(7): 3845-3852.

Stein, L. D., Mungall, C., Shu, S., Caudy, M., Mangone, M., Day, A., Nickerson, E., Stajich, J. E., Harris, T. W., Arva, A. and Lewis, S. (2002). "The Generic Genome Browser: a building block for a Model Organism System Database." *Genome Res* **12**(10): 1599-1610.

Stoppel, R.-D., Meyer, M. and Schlegel, H. (1995). "The nickel resistance determinant cloned from the enterobacterium *Klebsiella oxytoca*: conjugational transfer, expression, regulation and DNA homologies to various nickel-resistant bacteria." *Biometals* **8**(1): 70-79.

Sugio, T., Domatsu, C., Tano, T. and Imai, K. (1984). "Role of ferrous ions in synthetic cobaltous sulfide leaching of *Thiobacillus ferrooxidans*." *Appl Environ Microbiol* **48**(3): 461-467.

Suzuki, K., Wakao, N., Sakurai, Y., Kimura, T., Sakka, K. and Ohmiya, K. (1997). "Transformation of *Escherichia coli* with a large plasmid of *Acidiphilium multivorum* AIU 301 encoding arsenic resistance." *Appl Environ Microbiol* **63**(5): 2089-2091.

Suzuki, K., Wakao, N., Kimura, T., Sakka, K. and Ohmiya, K. (1998a). "Expression and regulation of the arsenic resistance operon of *Acidiphilium multivorum* AIU 301 plasmid pKW301 in *Escherichia coli*." *Appl Environ Microbiol* **64**(2): 411-418.

Suzuki, K., Wakao, N., Kimura, T., Sakka, K. and Ohmiya, K. (1998b). "Metalloregulatory properties of the ArsR and ArsD repressors of *Acidiphilium multivorum* AIU 301." *J Ferment Bioeng* **85**(6): 623-626.

Tabita, F. R., Hanson, T. E., Li, H., Satagopan, S., Singh, J. and Chan, S. (2007). "Function, structure, and evolution of the RubisCO-Like proteins and their RubisCO homologs." *Microbiol Mol Biol Rev* **71**(4): 576-599.

Tamura, K., Peterson, D., Peterson, N., Stecher, G., Nei, M. and Kumar, S. (2011). "MEGA5: molecular evolutionary genetics analysis using maximum likelihood, evolutionary distance, and maximum parsimony methods." *Mol Biol Evol* **28**(10): 2731-2739.

Thompson, J. D., Higgins, D. G. and Gibson, T. J. (1994). "CLUSTAL W: improving the sensitivity of progressive multiple sequence alignment through sequence weighting, position-specific gap penalties and weight matrix choice." *Nucleic Acids Res* **22**(22): 4673-4680.

Tian, J., Wu, N., Li, J., Liu, Y., Guo, J., Yao, B. and Fan, Y. (2007). "Nickel-resistant determinant from Leptospirillum ferriphilum." *Appl Environ Microbiol* **73**(7): 2364-2368.

Tibazarwa, C., Wuertz, S., Mergeay, M., Wyns, L. and van Der Lelie, D. (2000). "Regulation of the cnr cobalt and nickel resistance determinant of Ralstonia eutropha (Alcaligenes eutrophus) CH34." *J Bacteriol* **182**(5): 1399-1409.

Torma, A. (1977). The role of *Thiobacillus ferrooxidans* in hydrometallurgical processes. *Advances in Biochemical Engineering, Volume 6*. T. K. Ghose, A. Fiechter and N. Blakebrough, Springer Berlin Heidelberg. **6:** 1-37.

Tremaroli, V., Workentine, M. L., Weljie, A. M., Vogel, H. J., Ceri, H., Viti, C., Tatti, E., Zhang, P., Hynes, A. P., Turner, R. J. and Zannoni, D. (2009). "Metabolomic investigation of the bacterial response to a metal challenge." *Appl Environ Microbiol* **75**(3): 719-728.

Tso, W.-W. and Adler, J. (1974). "Negative chemotaxis in *Escherichia coli*." *J Bacteriol* **118**(2): 560-576.

Tuffin, I. M., de Groot, P., Deane, S. M. and Rawlings, D. E. (2005). "An unusual Tn*21*-like transposon containing an *ars* operon is present in highly arsenic-resistant strains of the biomining bacterium *Acidithiobacillus caldus*." *Microbiology* **151**(9): 3027-3039.

Tuffin, I. M., Hector, S. B., Deane, S. M. and Rawlings, D. E. (2006). "Resistance determinants of a highly arsenic-resistant strain of *Leptospirillum ferriphilum* isolated from a commercial biooxidation tank." *Appl Environ Microbiol* **72**(3): 2247-2253.

Tuovinen, O. H., Niemelä, S. I. and Gyllenberg, H. G. (1971). "Tolerance of *Thiobacillus ferrooxidans* to some metals." *Anton Leeuw Int J G* **37**(1): 489-496.

Umbarger, H. E. (1978). "Amino acid biosynthesis and its regulation." *Annu Rev Biochem* **47**: 532-606.

Valdés, J., Cárdenas, J. P., Quatrini, R., Esparza, M., Osorio, H., Duarte, F., Lefimil, C., Sepulveda, R., Jedlicki, E. and Holmes, D. S. (2010). "Comparative genomics begins to unravel the ecophysiology of bioleaching." *Hydrometallurgy* **104**(3–4): 471-476.

van Rooyen, J. P., Mienie, L. J., Erasmus, E., De Wet, W. J., Ketting, D., Duran, M. and Wadman, S. K. (1994). "Identification of the stereoisomeric configurations of methylcitric acid produced by si-citrate synthase and methylcitrate synthase using capillary gas chromatography-mass spectrometry." *J Inherit Metab Dis* **17**(6): 738-747.

Vandamme, P. and Coenye, T. (2004). "Taxonomy of the genus *Cupriavidus*: a tale of lost and found." *Int J Syst Evol Microbiol* **54**(Pt 6): 2285-2289.

Vartanyan, N. S., Karavaiko, G. I., Pivovarova, T. A. and Dorofeev, A. G. (1990). "Resistance of *Sulfobacillus thermosulfidooxidans* subspecies *asporogenes* to Cu^{2+}, Zn^{2+} and Ni^{2+} ions." *Mikrobiologiia*(59): 399-404.

Velarde, M., Macieira, S., Hilberg, M., Broker, G., Tu, S. M., Golding, B. T., Pierik, A. J., Buckel, W. and Messerschmidt, A. (2009). "Crystal structure and putative mechanism of 3-methylitaconate-delta-isomerase from *Eubacterium barkeri*." *J Mol Biol* **391**(3): 609-620.

Wagner, J. K., Marquis, K. A. and Rudner, D. Z. (2009). "SirA enforces diploidy by inhibiting the replication initiator DnaA during spore formation in *Bacillus subtilis*." *Mol Microbiol* **73**(5): 963-974.

Wakao, N., Nagasawa, N., Matsuura, T., Matsukura, H., Matsumoto, T., Hiraishi, A., Sakurai, Y. and Shiota, H. (1994). "*Acidiphilium multivorum* sp. nov., an acidophilic chemoorganotrophic bacterium from pyrtic acid mine drainage." *J Gen Appl Microbiol* **40**(2): 143-159.

Ward, T. E., Bruhn, D. F. and Bulmer, D. (1992). Lysogenic bacteriophage isolated from *Acidophilium*. I. EG&G Idaho. United States, The United States Department of Energy. **5132221**.

Ward, T. E., Bruhn, D. F., Shean, M. L., Watkins, C. S., Bulmer, D. and Winston, V. (1993). "Characterization of a new bacteriophage which infects bacteria of the genus *Acidiphilium*." *J Gen Virol* **74**(11): 2419-2425.

Watkin, E. L. J., Keeling, S. E., Perrot, F. A., Shiers, D. W., Palmer, M. L. and Watling, H. R. (2009). "Metals tolerance in moderately thermophilic isolates from a spent copper sulfide heap, closely related to *Acidithiobacillus caldus*, *Acidimicrobium ferrooxidans* and *Sulfobacillus thermosulfidooxidans*." *J Ind Microbiol Biotechnol* **36**(3): 461-465.

Watling, H. R. (2008). "The bioleaching of nickel-copper sulfides." *Hydrometallurgy* **91**(1–4): 70-88.

Whitman, W. B. and Wolfe, R. S. (1980). "Presence of nickel in factor F_{430} from *Methanobacterium bryantii*." *Biochem Biophys Res Commun* **92**(4): 1196-1201.

Wichlacz, P. L., Unz, R. F. and Langworthy, T. A. (1986). "*Acidiphilium angustum* sp. nov., *Acidiphilium facilis* sp. nov., and *Acidiphilium rubrum* sp. nov.: acidophilic heterotrophic bacteria isolated from acidic coal mine drainage." *Int J Syst Bacteriol* **36**(2): 197-201.

Wolin, E. A., Wolin, M. J. and Wolfe, R. S. (1963). "Formation of methane by bacterial extracts." *J Biol Chem* **238**: 2882-2886.

Xu, A. L., Xia, J. L., Liu, K. K., Li, L., Yang, Y., Nie, Z. Y. and Qiu, G. Z. (2010). "Real-time PCR analysis of metabolic pathway of PHB in *Acidiphilium cryptum* DX1-1." *J Microbiol Biotechnol* **20**(1): 71-77.

Xu, A. L., Xia, J. L., Song, Z. W., Jiang, P., Xia, Y., Wan, M. X., Zhang, R. Y., Yang, Y. and Liu, K. K. (2013a). "The effect of energy substrates on PHB accumulation of *Acidiphilium cryptum* DX1-1." *Curr Microbiol* **67**(3): 379-387.

Xu, Y., Yin, H., Jiang, H., Liang, Y., Guo, X., Ma, L., Xiao, Y. and Liu, X. (2013b). "Comparative study of nickel resistance of pure culture and co-culture of *Acidithiobacillus thiooxidans* and *Leptospirillum ferriphilum*." *Arch Microbiol* **195**(9): 637-646.

Yamaguchi, Y., Park, J.-H. and Inouye, M. (2011). "Toxin-antitoxin systems in Bacteria and Archaea." *Annu Rev Genet* **45**(1): 61-79.

Yang, Y. H., Dudoit, S., Luu, P., Lin, D. M., Peng, V., Ngai, J. and Speed, T. P. (2002). "Normalization for cDNA microarray data: a robust composite method addressing single and multiple slide systematic variation." *Nucleic Acids Res* **30**(4): e15.

Ye, J., Coulouris, G., Zaretskaya, I., Cutcutache, I., Rozen, S. and Madden, T. L. (2012). "Primer-BLAST: a tool to design target-specific primers for polymerase chain reaction." *BMC Bioinformatics* **13**: 134.

Yong, N. K., Oshima, M., Blake Ii, R. C. and Sugio, T. (1997). "Isolation and some properties of an iron-oxidizing bacterium *Thiobacillus ferrooxidans* resistant to molybdenum ion." *Biosci Biotechnol Biochem* **61**(9): 1523-1526.

Yoshizawa, Y., Toyoda, K., Arai, H., Ishii, M. and Igarashi, Y. (2004). "CO_2-responsive expression and gene organization of three Ribulose-1,5-Bisphosphate

Carboxylase/Oxygenase enzymes and carboxysomes in *Hydrogenovibrio marinus* strain MH-110." *J Bacteriol* **186**(17): 5685-5691.

Youn, H.-D., Youn, H., Lee, J.-W., Yim, Y.-I., Lee, J. K., Hah, Y. C. and Kang, S.-O. (1996a). "Unique isozymes of superoxide dismutase in *Streptomyces griseus*." *Arch Biochem Biophys* **334**(2): 341-348.

Youn, H. D., Kim, E. J., Roe, J. H., Hah, Y. C. and Kang, S. O. (1996b). "A novel nickel-containing superoxide dismutase from *Streptomyces* spp." *Biochem. J.* **318**(3): 889-896.

Zadvornyy, O. A., Allen, M., Brumfield, S. K., Varpness, Z., Boyd, E. S., Zorin, N. A., Serebriakova, L., Douglas, T. and Peters, J. W. (2009). "Hydrogen enhances nickel tolerance in the purple sulfur bacterium *Thiocapsa roseopersicina*." *Environ Sci Technol* **44**(2): 834-840.

Zhu, T., Tian, J., Zhang, S., Wu, N. and Fan, Y. (2011). "Identification of the transcriptional regulator NcrB in the nickel resistance determinant of *Leptospirillum ferriphilum* UBK03." *PLoS One* **6**(2): e17367.

7. APPENDIXES

APPENDIX I. *16S rRNA*-based phylogenetic tree of the strains contained in a culture of *Acidiphilium* sp. 3.2 Sup 5

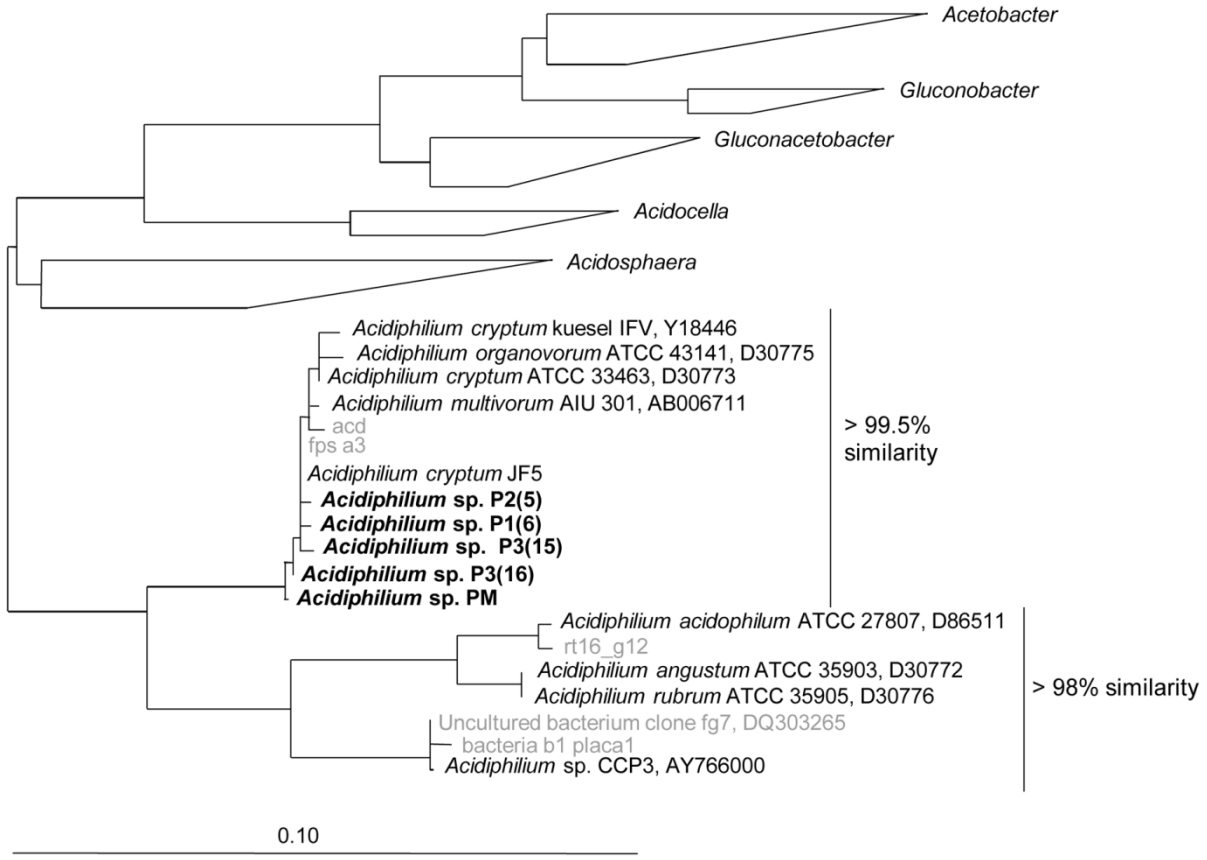

Figure A 1. *16S rRNA*-based phylogenetic tree of the strains contained in a culture of *Acidiphilium* sp. 3.2 Sup 5 (bold type). Other clones isolated from Río Tinto are shown in grey. Type and reference strains are shown for comparison. The scale bar represents a 10% nucleotide substitution rate.

APPENDIX II. Exploring horizontal gene transfer of operon *hslVU* among acidophiles

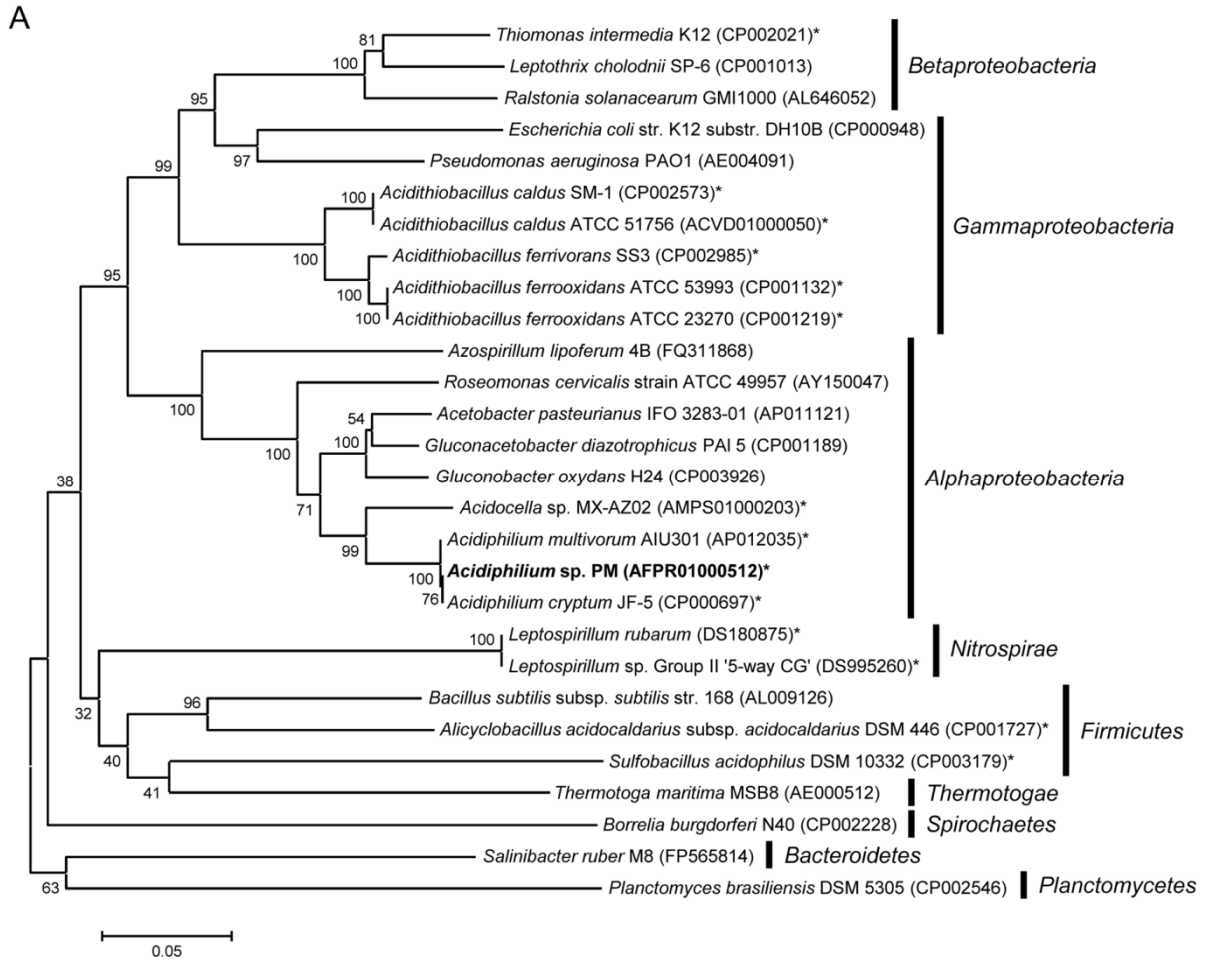

B

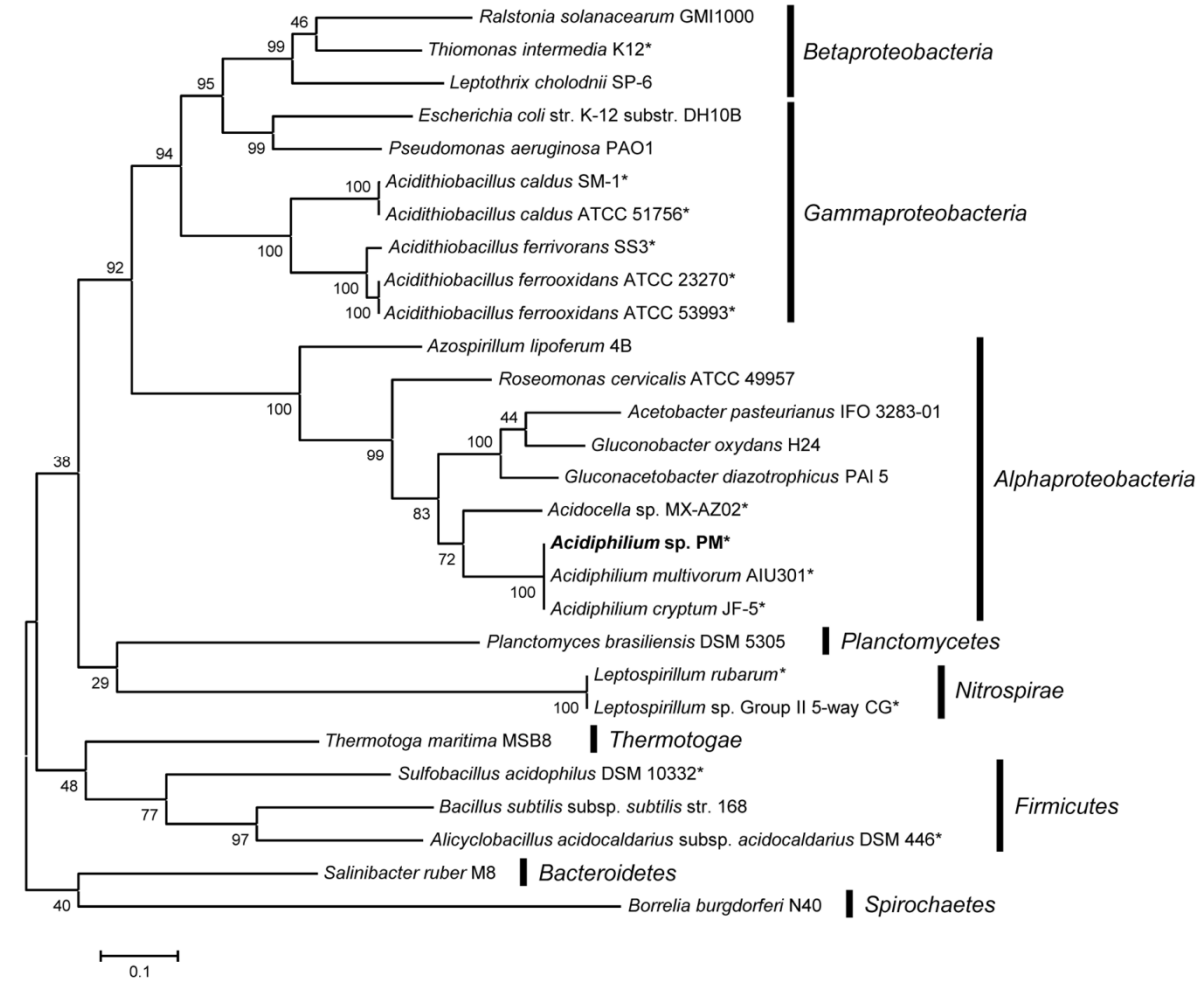

Figure A 2. Exploring horizontal gene transfer of operon *hslVU*. Phylogenetic trees of 14 acidic and 14 non-acidic species are shown as reconstructed from the *16S rRNA* gene (A), and the concatenated amino acid sequences of HslV and HslU (B). Sequences belonging to *Acidiphilium* sp. PM are shown in bold text and those of acidic species are denoted by asterisks. Bootstrap values are indicated at the nodes. Scale bars correspond to 5% (A) or 10% (B) sequence divergence. The amino acid sequences for HslV and HslU used in the analysis are the following: *Rhodospirillum rubrum* F11, AEO50144 and AEO50145; *Escherichia coli* str. K-12 substr. DH10B, ACB04944 and ACB04943; *Pseudomonas aeruginosa* PAO1, AAG08438.1 and AAG08439; *Bacillus subtilis* subsp. *subtilis* str. 168, CAB13488 and CAB13489; *Salinibacter ruber* M8, CBH24765 and CBH24767; *Ralstonia solanacearum* GMI1000, CAD13571 and CAD13570; *Borrelia burgdorferi* N40, ADQ29063 and ADQ29174; *Thermotoga maritima* MSB8, AAD35606 and AAD35607; *Planctomyces brasiliensis* DSM 5305, ADY60041 and ADY60040; *Acidithiobacillus ferrooxidans* ATCC 23270, ACK80450 and ACK79019; *Acidithiobacillus ferrooxidans* ATCC 53993, ACH84568 and ACH84569; *Acidithiobacillus ferrivorans* SS3, AEM46768 and AEM46767; *Acidithiobacillus caldus* SM-1, AEK57130 and AEK57129; *Acidithiobacillus caldus* ATCC 51756, EET27426 and EET27425; *Acidiphilium multivorum* AIU301, BAJ80804 and BAJ80803; *Acidiphilium* sp. PM, EGO96503 and EGO96504; *Acidiphilium cryptum* JF-5, ABQ30620 and ABQ30619; *Leptospirillum rubarum*, EAY57767 and EAY57766; *Leptospirillum* sp. Group II '5-way CG', EDZ39580 and EDZ39579; *Acidocella* sp. MX-AZ02, EKM99984 and EKM99983; *Acetobacter pasteurianus* IFO 3283-01, BAH99172 and BAH99173; *Gluconacetobacter diazotrophicus* PAl 5, ACI52812 and ACI52813; *Gluconobacter oxydans* H24, AFW01689 and AFW01690; *Roseomonas cervicalis* ATCC 49957, EFH12145 and EFH12146; *Azospirillum lipoferum* 4B, CBS88212 and CBS88211; *Thiomonas intermedia* K12, ADG31586 and ADG31587; *Sulfobacillus acidophilus* DSM 10332, AEW05868 and AEW05867; *Alicyclobacillus acidocaldarius* subsp. *acidocaldarius* DSM 446, ACV58411 and ACV58412; *Leptothrix cholodnii* SP-6, ACB36091 and ACB36092.

APPENDIX III. Re-calculation of F, $Log_2F \pm SE$ and p values to merge data from two replicates of the same microarray

Fold change: $F_{1,2} = \sqrt[2]{F_1 \cdot F_2}$

Or $F_{1,2} = -\left(\sqrt[2]{F_1 \cdot F_2}\right)$ when $F_1, F_2 < 0$.

Log_2F: $\mathrm{Log}_2 F_{1,2} = \frac{\log_2 F_1 + \log_2 F_2}{2}$

SE (log_2F): $\mathrm{SE}_{1,2} = \frac{SD_{1,2}}{\sqrt{n}}$

where: n is the total number of replicates (12)

$SD_{1,2} = \sqrt[2]{(Var_{1,2})}$

$Var_{1,2} = \left(\frac{Var_1 + Var_2}{2}\right) + \left(\frac{\log_2 F_1 - \log_2 F_2}{2}\right)^2$

p was re-calculated in Excel using *fx=T.DIST(ABS(t value);11 DF;2 tails)*

where: $t_{1,2} = \frac{\mathrm{Log}_2 F_{1,2}}{SE_{1,2}}$

Degrees of freedom: DF= n-1

APPENDIX IV. Oligonucleotides and probes used in qRT-PCR

Table A 1. Oligonucleotides and probes used in the qRT-PCR analysis of genes differentially expressed upon addition of metals. TaqMan probes contained 6-carboxyfluorescein (FAM) as the reporter dye in 5' and minor groove binder-nonfluorescent quencher (MGB-NFQ) as the quencher in 3'.

Locus	Gene	Assay ID	Forward Primer Sequence	Reverse Primer Sequence	Reporter Sequence
APM_0011	Flagellar hook capping protein	AIWR2PB	CGGCGACCTGACCCA	GATGTAGCGGTCACCTTGCT	TCCCAGCATCGAACTC
APM_0066	MgtC/SapB transporter	AIVI4I7	CGGCTGCGGCTTTCC	GGCGAGGATGAAACCTGTGA	CACGGTCGCTTCCGCT
APM_0068	Manganese transport regulator MntR	AIWR2PF	GAAAGCGATCAATCGGCTCAAG	GGTGAGAAAGACACTGCGATAGG	CCTTCACGAGCCCTTC
APM_0070	Natural resistance-associated macrophage protein	AIX00VN	CTGCGTGGTCGATAAGGGTAT	CGATAACGCCGAGCATCAGAT	TTGCCGCAGGATATC
APM_0087	Alkyl hydroperoxide reductase/ Thiol specific antioxidant/ Mal allergen	AIMSHBN	CCACCTGGTGTCCAAGCT	CCTGATGCTGTGCGAAGGT	CTGAGCCCGGCCTTG
APM_0089	MerR family transcriptional regulator	AIN1FHV	GGAACTCGGCTTCTCTCTTGAC	GCAGGGCCGCTCTTTCT	CAGTCCGCGCACCTC
APM_0091	Transposase IS116/IS110/IS902 family protein	AIPADN3	GGCAGCAAATCAGCAAATACCT	TGATCCGGGCGATCTTGTTG	CACCGCGATCTTGC
APM_0110	Major facilitator transporter	AIQJBUB	GGCATGGCCACGATTGG	GCGTGTCGCGCACA	TCGCCACGATCACCCG
APM_0133	Alanine dehydrogenase	AIX00VJ	GGCGCCGATGTCACCAT	CGCGGCCCGTAGAGATC	TCGCCCGCCTCGCCCA
APM_0134	XRE family transcriptional regulator	AIY9Y1R	GCCGGAGGATGTGTTCTTCA	GCTCGTCGAAGGCGATTTC	CCGCCGACCTTACC
APM_0136	Glutamine synthetase, catalytic region	AI0IW7Z	CGAGGTCACGCTGCACTAC	TGCTTGCGGGCGATGT	CAGCACCGCATCGTC
APM_0150	Sec-independent protein translocase, TatC subunit	AI1RVD7	GCTGCTGCCCTTCCTGAT	CCAGGCATTTGGAAATATGACATAATATGC	CCGGTGCTGTTCTTC
APM_0179	Transcriptional regulator	AI20TKF	GACATCGAGGAGACGCATCT	GCGCTCGACCTCGATCAG	CCGCCGCCAGCTTG
APM_0180	4-methylmuconolactone transporter	AI39RQN	CGCAGGCGATCGTGTTTTC	GCGCCGATCGCGAAC	TCACCCGCCAGGCAAT
APM_0193	AraC family transcriptional regulator	AI5IPWV	TGCCGTCGTTGCCACTA	GGGTCCTGGAAATAGGGAACATC	TCGACGCCGATCCTG
APM_0195	MmgE/PrpD family protein	AI6RN23	GCATGGCCAAGCCTTTCAG	GCTGCGCGCCATGATC	CATGCCGTTCATCGCC
APM_0196	Methylitaconate delta2-delta3-isomerase	AI70L9B	TGCTGCCCACCGGTAAC	CGTCGACCAGCGAGACC	ATGACCGCATCTCCC
APM_0198	Putative transcriptional regulator	AI89KFJ	TGGATCAAGGCGCACGAA	CGAGGGATCGCCGAAGAC	CATCGTCCCGCGCTTC
APM_0199	Fumarate reductase/succinate dehydrogenase flavoprotein-like protein	AIAAZLC	TGGGACCTCGCGAAAGTC	GGCAGCCGGACCAGT	TCCCCTCGCCGTTATT
APM_0238	SirA family protein	AIBJXRK	GGCTGCGCGTGCTC	GTGGCCGGCATCGC	CTGTCGTCGATTTTC
APM_0250	Probable manganese transport protein mntH	AICSVXS	GGCGCCACGGTAATGC	CCGGAGAGGCCGGAATG	CACGCGCTGTTCCTG
APM_0290	Formate hydrogenlyase subunit 4-like protein	AID1T30	GCGGTCATCGGCATTCTC	TCGAGCGCGCGAACA	TCGTCGGCATCACCC
APM_0294	NADH ubiquinone oxidoreductase, 20 kDa subunit	AIFAR98	GCGCAGCCTGCATGTG	GCAGGTTGTAGAACGGGTTGTT	TTCGCAGCCATTGCAG
APM_0396	Ribosomal protein S20	AIGJQGG	GCGACGGGCAATCACATC	CGCGCTGCAGTTCGG	ATGCCGTCCGCGCCTC
APM_0397	Chromosomal replication initiation protein	AIHSOMO	ACGACCTGCAGTTCCTGATC	CGCATTGAAGGTGTGGAAGAATT	TCCTGCGTGCCATCCT
APM_0433	50S ribosomal protein L36P	AII1MSW	GCCCGCGACAAGAACTG	GCGGGTTCTTCTTGTTGATCAC	TCATGGCCGCGTCTAC
APM_0472	DNA ligase	AIKAKY4	GCGCCCGGCTCGAT	TCGCGTGGCTGACCAG	CCGCCGACATTCACCG
APM_0473	TraR/DksA family transcriptional regulator	AILJI5C	GGCATTCTCGAACCCGACATTA	CCGGGTGCGCAATTCG	CCAGCGTCGAAACCG
APM_0499	Siroheme synthase	AIRR90J	CGCGTGCTGGTGAATGTC	GCGCCACGGAATGAAAGTC	ACCGCCTGCCCGACTG
APM_0517	Ribosome maturation factor rimM	AIMSHBK	CGAGGCCGCCACGAT	GCCCGGCGCACATAGA	AAGCTGACCAATCTTC
APM_0529	50S ribosomal protein L20	AIN1FHS	GGAACAAGAAGCGCGAGTT	GCGATGAACTGGCTGTAGGT	ATCCAGCGCATCAACG
APM_0614	Natural resistance-associated macrophage protein	AIPADN0	CGTCGCCGCCAATATCG	CGCCGATTGCTGGTAGAAGAT	ATCCACGGCATGATCA
APM_0723	Primosome assembly protein PriA	AIQJBT8	TCGGCCGGCGCAT	GCTCCGGCACGTCGT	ACACCACGCCATGCAC

APM_0724	Translation-associated GTPase	AIRR90G	CCGCTTCTGAAAGTCCTCGAA	GCACCGCCTCCTCCTC	CACCGCGATTCCCG
APM_0774	ABC-type molybdate transport system periplasmic component-like protein	AIS076O	CGAGCACGGCGATGGT	GGCCGCCTCGAAATCCT	CACTCGCGCTTCCGCA
APM_0844	Hypothetical protein	AIT96CW	CACCGATGGCGGCTTTC	TGGGACGCACGTGATAGG	ACAGCGCCGAAATC
APM_0895	Arsenical pump membrane protein	AIVI4I4	GCAATCCGCGACCATGTC	TGACGAAATAGGCCACGAACAG	TCTTCCGCGCTGCCTG
APM_0987	Serine-type D-Ala-D-Ala carboxypeptidase	AIWR2PC	GTCCGTACCTATCCGCAGTTC	ATCTTGTCGAAGGTGAAGTGCTT	CTTGACCGAAATCTTC
APM_1003	GTPase obg	AIX00VK	GCGGCTCAAGCTGATTGC	AGGTCGATTTCCCTGCATTCG	CAGCCCGACCAGCCC
APM_1005	50S ribosomal protein L21	AIY9Y1S	CCGTTGTCGAGGGTGCAA	ATGATGACCGTATCGAGCTTGTC	CTGCGCGATCACCG
APM_1092	Dihydrolipoamide dehydrogenase	AI0IW70	AGAAAACCCTCGGCAAGCT	GCACCGGTGACCTTGGT	CCGAGCTTGAACTTC
APM_1094	2-oxoglutarate dehydrogenase E1 component	AI1RVD8	CCAGCCGCTGATGTACCA	CGAGGCGCTCGGCATA	ACGACCCGCACCCTC
APM_1170	Colicin V production protein	AI20TKG	GTTCGATGGTGCGGGATTC	GCGAGCCCCAGCGT	ACGCCTGAAAGCACC
APM_1171	DNA repair protein RadA	AI39RQO	TTGGCCATGTGACCAAGGA	CGCGATCACCTTCGAAGTG	CAGCACCACATCCACC
APM_1173	Adenine phosphoribosyltransferase	AI5IPWW	GCCGCGGCTTCATCCT	CGCTTGCGCAGCATGAT	CCGCTCGCCCTCAAG
APM_1178	ATP synthase subunit a	AI6RN24	CCAGCCACATCGCGATCA	CCGTGATACCAGAAACCTACCA	CCTGGCGCTTTTCGTC
APM_1186	Ribonuclease	AI70L9C	CGCTGCGGACCAATCTG	AGCCCCGCGAGGTC	CAACTGCCGCGCCACT
APM_1257	NADH-quinone oxidoreductase, E subunit	AI89KFK	CCAGGTCTGCACCACGAC	CAGGCCGACATCACCTCATC	CCGCGCAGCCAACAC
APM_1291	HhH-GPD family protein	AIAAZLD	GCGAAGGACGCGATTGC	AAGTCACCTGGGCTGGATTG	CCGCTGCCCGCCTTG
APM_1293	DNA polymerase I	AIBJXRL	TCGGCGTTGCATCTCGAT	GGTTCCTGTCACCTCATCGT	CATCGGCCCATTTCC
APM_1391	Fe-S metabolism associated SufE	AICSVXT	GCCCGGCTGCCAGA	GCGCCGGCGAAATAGAG	CCGCCTTCCAGCTTC
APM_1405	Elongation factor Ts	AID1T31	GTCGGCGAGAACATGTCGAT	GCGCCATGCACGTATGAC	AACGCCGTCCTTCACC
APM_1409	Glutathione S-transferase domain-containing protein	AIFAR99	GCTCTATCTCGCGGAGAAGTTC	AGCCAGGAGAGGCATTCG	CCTGCCGAAGGACCTC
APM_1444	NADH-quinone oxidoreductase subunit C/D	AIGJQGH	TCGAGGGCGAGGAAATCG	GCGGTGATGAAAGCCGATCT	TCGACGCCGTGCCCG
APM_1503	Nitrile hydratase	AIHSOMP	ACGCCGGGCATCCA	GTAGCAGCTGCACAGGGT	CCACCTCGTCGTCTGC
APM_1616	Permease for cytosine/purines, uracil, thiamine, allantoin	AII1MSX	CCGGCCGATACCTCGTT	GCACCGAGCCGAGATAGG	ATGCGCCGAACTGC
APM_1630	Endoribonuclease L-PSP	AIKAKY5	ACGCGCTGCTCGAACA	CGTCGATCGATTTCAGCCAGAT	ACAACACGCGCCTTC
APM_1631	DNA repair protein RadC	AILJI5D	TGGCGGCGATCAAGCT	GCCGCTCCCAGTTGTTCA	TCGGCCATCCGCCTCG
APM_1650	Dihydrodipicolinate reductase	AIMSHBL	GGGCGTGAACCTGGTGATC	TGGTGCATCTCGAGGATTTCG	CCGCCGAGACCCACG
APM_1693	Formate dehydrogenase family accessory protein FdhD	AIN1FHT	GCGGGCTGGAAAGCCT	GGTTCAGCTCCTGCTGCAT	TCCCGCGCATCACC
APM_1713	ABC transporter related	AIPADN1	GCAGCAGCGGGTGATGA	CCAGCGGCTCGTCGA	TCCGCCGCCCCGACGT
APM_1758	Rod shape-determining protein MreC	AIQJBT9	TCTCGGCGGGCTTTATGC	CGCGTCGCGGACATC	CAGCGTCACCATCACC
APM_1834	Ribonuclease D	AIRR90H	CTGGGTGGCCGAGGAA	GGCGCCAGGCATCCT	CCGATCCCGCGACCTA
APM_1835	Aspartyl-tRNA synthetase	AIS076P	TCGGACAAGCCGGACCTA	ACGCCTCGGTCACGTC	CCGCTGCTGATCACC
APM_1878	Endoribonuclease L-PSP	AIT96CX	GCGGGCCTGTTTCATCAAC	TGGGCAACGGCATCGA	CATGCGCCTCGATCTG
APM_1916	Diguanylate cyclase with PAS/PAC sensor	AIVI4I5	CGGGCAGCTGACCCT	CTTGAACCCGTCGAGATCGA	CCTCGCCGCTGCTTC
APM_1930	ATP synthase gamma chain	AIWR2PD	GACATGCGCGAGAAGATCATC	TCGGCGAACTCGATCGT	TCTTGCCGACGAAATT
APM_1946	Orotate phosphoribosyltransferase	AIX00VL	GCATGGGCCTGCCGAT	ACGTCGCCCTCGATCTG	CCCTTCGGCTTCTTG
APM_2007	Isocitrate lyase	AIY9Y1T	GAGGACGGCGTGATCGT	CGAATAGGCGATCTGCTTGGT	CCGCACCGACTCGCT
APM_2041	ClpA homolog protein	AI0IW71	TCGAGCTTTCGGCGAAATACA	CGCCAACCTCATCGATCACAT	TCCACGACCGCAAACT
APM_2129	30S ribosomal protein S1	AI1RVD9	ACCGATCCGTGGGAAGGT	CCGTAGTCGGTGATGTTGGT	ATTCCCGGCGGATACT
APM_2256	NUDIX hydrolase	AI20TKH	GGCGGGCAGGAGCT	GCGATGGATCGAGTCCACATG	TCCTCGCGCAGTTCC
APM_2257	DEAD/DEAH box helicase domain-containing protein	AI39RQP	GCGGGTCTATTGGGTGTGT	CGGCGGCGATGTCCAT	CTCGCTCTCGGCCACC
APM_2300	ABC transporter related	AI5IPWX	GCTCGCCTGGATCATCGA	ACGTCGCCGGGACTC	CCGCTGGCTCGACCAT
APM_2361	Multicopper oxidase, type 2	AI6RN25	CGGCATGACCATGGATGTGAA	CGAGCGTGCGGTCGTT	ACGACGCCTTCCTCG

APM_2362	Cation diffusion facilitator family transporter	AI70L9D	TCACCGCCTGGCTGTT	GTCATAGGCCATGTGCTGGAA	TCCGACATCAATATCC
APM_2363	Co/Zn/Cd cation transporter-like protein	AI89KFL	GGCGGGCTGCTGTTC	GAACGCCGCCATGATGAC	CCCTTGCCGCCTCTGT
APM_2364	MerR family transcriptional regulator	AIAAZLE	GGGCGTCTCCGCTTCAT	CGTGCCGATACGGTCGAT	CCCTCGGCTTCCCG
APM_2365	Cation diffusion facilitator family transporter	AIBJXRM	GACGCACCTCGTGACGAT	GCGGCACGCCATCCT	CCTCGGCATTTTCG
APM_2440	GTPase EngB	AICSVXU	TCGACATGCCGGGCTATG	CGCAGGTAGCGGAACATCA	CTGCCAGTCCCGCTTC
APM_2441	Inner membrane protein oxaA	AID1T32	CGCGAAGCCCGTCGAT	CTCAGGATGCTCAGCACCTT	CACGACCCACGTCTTC
APM_2493	Ribosomal RNA large subunit methyltransferase N	AIFASAA	CGGCTGCTCTCCACCAT	GGCGACGTTCTCGTAATTGTAGA	CCCATGCCCATCAGCA
APM_2510	Deoxyribodipyrimidine photolyase-related protein	AIGJQGI	CCGGCTTCGGCGACT	CAGCGAGTGGAACATGAAATCC	CCGCCATCGCGTCCTG
APM_2517	Rubrerythrin	AIHSOMQ	GGCGGAGGCCGATCAC	GACTTCCTCGGTCAGGTTCTC	CTCGCCGACCGTCTCG
APM_2798	Hypothetical protein	AI5IPWZ	GGAAACGGCTTCAGGATCAGATC	GCTAGATCGCTCTTCCGTTGAG	CCGACACGCAAGCTAT
APM_2849	Transcriptional regulator/antitoxin, MazE	AIY9Y1V	GGCCTGACCGTCGATAACG	CGAGCAGTTCGGACATGATG	TAGTGCGGCCTAGCCC
APM_2850	ATPase involved in chromosome partitioning-like protein	AI0IW73	GGCACTGATTCTGTCCGATGT	GCCCACACGTCGTAGGA	CTGGTGCCCTTTGCC
APM_2851	Hypothetical protein	AI1RVEB	AGGGCGTGGCGAAAGG	CGCGGCGCAGCAAAT	ACAAGCGGCAGATCAG
APM_2852	Rep(pMBA19a)	AI20TKJ	CGTGCTGATGGGTGTTTCTCA	CCCAGACCAGCACGATAGC	ACGGAAGCCATGAACC
APM_2856	Conjugal transfer protein traA	AI39RQR	CAGCTTTCCCGGTTCATCAC	TGCAGCTGCTCGGGATC	CCCACCAGCACGATCT
APM_2883	Fis family GAF modulated sigma54 specific transcriptional regulator	AII1MSY	TGGCCGGCGAAACAGA	CTCCACCAGCGCATTGC	CCCGCGCCGTCGTC
APM_2964	Replicative DNA helicase	AIKAKY6	GCCCGCGCCGAGAA	GCTCGGCGCTCATTTCAAG	ACGCACTGCTTTGCC
APM_2997	RNA polymerase factor sigma-32	AILJI5E	CTGCGCCGCCTCAAG	GGCGATCTTTTCCACCTGTTC	CATGTCGCCATCCTC
APM_3028	50S ribosomal protein L10	AIMSHBM	GACTGAAGCCGATGCTGAAG	CACGAACTTCTCGTTGGTCTTG	TCGCCACCGCCACCG
APM_3030	DNA-directed RNA polymerase subunit beta	AIN1FHU	GATTTCCGCCTGGTCAAACC	GCGGCAACCGAGACGA	TCGCCGTGACCTCGTC
APM_3039	50S ribosomal protein L2	AIPADN2	GCGATCCCGGTTGGCA	GCGCCGGCCTTCAG	ATCGTCCACAATATCG
APM_3042	30S ribosomal protein S3	AIQJBUA	CATCGAGGTGCTCAAGAAGGA	GCGGATCTCGACGATGTTCAG	ACGTCGGCCTTCGCC
APM_3049	30S ribosomal protein S14	AIRR90I	CGTGGAGGATCGGTTCGA	CGCACGCGGGTCTTC	AAGCTCGCGCAACTC
APM_3060	DNA-directed RNA polymerase subunit alpha	AIS076Q	CCGGTCGACTCGATCTACTC	GCGGGTCGGCTCGA	CCGCCGCGTGTCCTA
APM_3107	DNA gyrase subunit B	AIT96CY	GTGATCACCGCCGAGGAT	TGGTCTGGCCCTGGAATTG	AACAGCGAGAGCTTG
APM_3108	Cytidylate kinase	AIVI4I6	GCCGTCGCCTCGATCAA	CCGCCCGTCCAGCA	CCAGCGCCGATTCG
APM_3113	Putative ribonuclease BN	AIWR2PE	AAACGCGCGGCTTCTTC	GCATGGCAATCAGCGTCATC	ACCGCCTGAAACTC
APM_3114	Ribonuclease R	AIX00VM	TGCCTGTTCGTCGAGATGATC	GCGAAGCTGCGCATCAG	CTGAGCCACAAATTC
APM_3115	C-terminal processing peptidase	AIY9Y1U	CGGCAGCATGATCGATCTGA	GCCCGGTGACGCTCT	CCGCAGACGATCACC
APM_3116	50S ribosomal protein L33P	AI0IW72	ACTGTTCAGATCAAACTGGTTTCCA	GCGTTCTTCTTCGTCACGTAGA	CCGACACCGGCTTCT
APM_3117	Lipid-A-disaccharide synthase	AI1RVEA	CGGCCTGGCGGAGT	GCTGCCAGGCATCAGGAT	CAGCGCGTTCCCTG
APM_3182	2-dehydro-3-deoxyphosphogluconate aldolase/4-hydroxy-2-oxoglutarate aldolase	AI20TKI	CGCGGCGGCGAAAAG	CGGTCGGCGTTGCG	CCGCGTGCCATTCC
APM_3225	Beta alanine--pyruvate transaminase	AI39RQQ	CCATCGCCGCCTGCAT	CGCAGCCGCTCCAGATAG	CAGCACGCCCGTCGAT
APM_3234	Leucyl-tRNA synthetase	AI5IPWY	TCGCCGAGCTCGAATCG	CGCAGGCGCCAGTTG	ACCACGCCCTTGCCG
APM_3356	Hypothetical protein	AIS076R	GAACAGCACCGCGACATG	CGCATCGCGTCGTTGTC	ACCTGCGTCATCAATG
APM_3379	NADPH-dependent FMN reductase	AI6RN26	CTGGATCCCGCTGGAAGTC	TGTTCACCGCGTTGAAGCT	CATCACCGCGAGCACC
APM_3382	Transcriptional regulator, ArsR family	AI70L9E	AAGCGCACCGGCAATG	GGTTGACCGGGCCAGATG	CCGTGAACACGAAATC
APM_3406	Cytochrome c biogenesis protein transmembrane region	AI89KFM	ACTGCGATTCACGCTGGAA	CCGGAGTTGCCGAAAACG	CCGCAGCCAATCCGTT
APM_3409	Redoxin domain-containing protein	AIAAZLF	GGCTCCAAGCCCGACTT	CATAGAATTTCCTGACCGCTTCCA	CCGGCACCACTTCGAA
APM_3412	Peroxidase	AIBJXRN	GAATGATCCACCCGGAAGCT	AGCCGAACCTTCTTGTTTGGA	CACGCTCCGAACCGT
APM_3413	Hypothetical protein	AICSVXV	CGAAACCATCAACCGGCATTT	GCCATGGCTGACGGTCTTT	TCGGCCCTTGGACCAC

APM_3419	Alkyl hydroperoxide reductase/ Thiol specific antioxidant/ Mal allergen	AID1T33	GCAGAGGCGCCGTATCTC	GGCGATGCCCCAGACAT	CAGCCCCGATTTCG
APM_3421	Copper transporting ATPase	AIFASAB	CGCGACCTTCAACAAGATTCG	AGCGGAATGCCAACGACAT	ACGCCCAGAACAGTCC
APM_3422	Heavy metal translocating P-type ATPase	AIGJQGJ	TCGATGCTGACGGGAGAGA	CCGCCAGTGACCTTGTGA	CCGGTGACCAAGAGTG
APM_3427	OmpR family two-component response regulator	AIHSOMR	CGGATCAGGGCGGTTCTG	CCAGCGATCGAAGCGGTATC	CCGCGCCCCGTTTG
APM_3510	Sigma 54 modulation protein/ribosomal protein S30EA	AII1MSZ	CCGCCGAGCACATTGC	CGGGCATGGTCGTTCAC	CTCCGGCGCTATCG
APM_3550	RecD/TraA family helicase	AIT96CZ	GCGTATCCTCGCTGCAAAAT	CCGTCGTCTCGGCAAGA	CCGTCCGCATTCTGCT
APM_3715	Ornithine cyclodeaminase	AIKAKY7	GCGGCAACGCGGAAAT	GCAGGGCGTGATGTCGAA	CATCCGCAACCTCG
APM_3839	Glyceraldehyde-3-phosphate dehydrogenase, type I	AILJI5F	CGCCGATGGCGATGGT	TGGTCGCCGGTGTAGGA	TCGAGCGCGGCTACAT
	Putative plasmid maintenance system killer	AI89KFN	CAGTGGGTGCAGCTTAAACG	GCATTCTTGGCCTTTTGGATGTG	CCTGCGGCGTTTGC
	Putative VapI-like plasmid maintenance system antidote protein	AIAAZLG	GCCGGATCGCCAAATCAG	CCGCGCAGCGTTGTC	CAGCCCTGGCGTTCAA
Normalization 1	Beta-actin antisense (mouse)	AI6RN27	ACAGGATTCCATACCCAAGAAGGA	CAGGTCATCACTATTGGCAACGA	CCCTGAGGCTCTTTTC
Normalization 2	Elongation factor 1-alpha chain (*Xenopus laevis*)	AI70L9F	CTGCCTCTGCAGGATGTCTAC	CCACACGACCAACTGGTACAG	CAATACCGCCAATTTT

APPENDIX V. Transcriptomic response to Ni in *Acidiphilium* sp. PM. Unresolved clones and genes.

Table A 2. Unresolved clones and non-validated genes with significant up- or down-regulation after 5 min in 10 mM Ni. Clones which were up- or down-regulated both in Ni and Zn are coloured in pale blue, whereas clones whose expression was altered only in Ni are left uncoloured. Induction is shown in tones of red whereas repression is highlighted in shades of green.

	Microarray hybridization				
Clone	**F**	**$Log_2F \pm SE$**	**p**	**Locus**	**Gene**
78F6	11.37	3.5 ± 0.1	0.000	APM_0069	Hypothetical protein
10F9	10.98	3.5 ± 0.1	0.000	APM_0069	Hypothetical protein
39D8	10.42	3.4 ± 0.1	0.000	APM_0069	Hypothetical protein
51F7	10.08	3.3 ± 0.0	0.000	APM_0069	Hypothetical protein
49E11	10.00	3.3 ± 0.1	0.000	APM_0069	Hypothetical protein
57G6	9.77	3.3 ± 0.2	0.000	APM_0069	Hypothetical protein
26F12	8.29	3.1 ± 0.1	0.000	APM_0069	Hypothetical protein
75D10	6.52	2.7 ± 0.1	0.000	APM_0069	Hypothetical protein
69A3	5.87	2.6 ± 0.3	0.000	APM_0197	Hypothetical protein
11D7	4.16	2.1 ± 0.2	0.000	APM_0192	Transposase, IS4 family protein
				APM_0194	Hypothetical protein Rru_A0535
31G4	4.14	2.0 ± 0.1	0.000	APM_0574	Hypothetical protein
				APM_0575	Hypothetical protein
				APM_0576	Hypothetical protein
44F11	3.67	1.9 ± 0.3	0.000	APM_0197	Hypothetical protein
61H9	3.49	1.8 ± 0.3	0.000	APM_0197	Hypothetical protein
45A1	3.39	1.8 ± 0.1	0.000	APM_2724	Hypothetical protein
				APM_2725	Glycosyl transferase, group 1
65A3	3.32	1.7 ± 0.1	0.000	APM_0251	ABC transporter related
				APM_0252	ABC transporter related
43B2	3.28	1.7 ± 0.1	0.000	APM_3427	OmpR family two-component response regulator
				APM_3428	Signal transduction histidine kinase
26F11	3.23	1.7 ± 0.1	0.000	APM_1193	Dihydrodipicolinate synthetase
				APM_1194	D-isomer specific 2-hydroxyacid dehydrogenase, NAD-binding
				APM_1195	Dihydroxy-acid dehydratase
04D4	3.04	1.6 ± 0.1	0.000	APM_3848	Carbohydrate porin, OprB family protein
				APM_3849	Integrase catalytic region
				APM_3850	Transposase IS3/IS911 family protein
77E7	2.96	1.6 ± 0.0	0.000	APM_3427	OmpR family two-component response regulator
				APM_3428	Signal transduction histidine kinase
				APM_3429	Hypothetical protein
84D4	2.67	1.4 ± 0.1	0.000	APM_2366	Hypothetical protein
76H10	2.00	1.0 ± 0.1	0.000	APM_2857	Hypothetical protein
06A5	-2.27	-1.2 ± 0.1	0.000	APM_1916	Diguanylate cyclase with PAS/PAC sensor
				APM_1917	Hypothetical protein
				APM_1918	Hypothetical protein
				APM_1919	Acyl-CoA dehydrogenase domain-containing protein
80B5	-2.30	-1.2 ± 0.0	0.000	APM_1915	Diguanylate cyclase/phosphodiesterase with PAS/PAC and GAF sensor(s)
				APM_1916	Diguanylate cyclase with PAS/PAC sensor
				APM_1917	Hypothetical protein
				APM_1918	Hypothetical protein
35H9	-2.31	-1.2 ± 0.1	0.000	APM_1917	Hypothetical protein
				APM_1918	Hypothetical protein
				APM_1919	Acyl-CoA dehydrogenase domain-containing protein
03E1	-2.58	-1.4 ± 0.1	0.000	APM_2301	Glycosyl transferase, group 1
38D1	-2.67	-1.4 ± 0.1	0.000	APM_0612	Amidase
				APM_0613	Acetylornithine deacetylase

Table A 3. Unresolved clones and non-validated genes with significant up- or down-regulation after 30 min in 10 mM Ni. Clones which were up- or down-regulated both in Ni and Zn are coloured in pale blue, whereas clones whose expression was altered only in Ni are left uncoloured. Induction is shown in tones of red whereas repression is highlighted in shades of green.

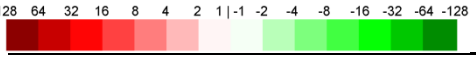

	Microarray hybridization				
Clone	F	$Log_2F \pm SE$	p	Locus	Gene
78F6	17.30	4.1 ± 0.1	0.000	APM_0069	Hypothetical protein
10F9	16.63	4.1 ± 0.1	0.000	APM_0069	Hypothetical protein
11D7	15.00	3.9 ± 0.1	0.000	APM_0192	Transposase, IS4 family protein
				APM_0194	Hypothetical protein
64B12	14.42	3.8 ± 0.2	0.000	APM_3714	Alpha/beta hydrolase fold protein
				APM_3716	Arginase
51F7	12.85	3.7 ± 0.1	0.000	APM_0069	Hypothetical protein
28D4	9.73	3.3 ± 0.1	0.000	APM_0200	Hypothetical protein
57G6	8.76	3.1 ± 0.1	0.000	APM_0069	Hypothetical protein
45A1	8.71	3.1 ± 0.1	0.000	APM_2724	Hypothetical protein
				APM_2725	Glycosyl transferase, group 1
09E11	8.44	3.1 ± 0.2	0.000	APM_3383	Regulatory protein, ArsR
				APM_3384	Arsenite oxidase, small subunit
26F12	8.42	3.1 ± 0.1	0.000	APM_0069	Hypothetical protein
22B4	8.22	3.0 ± 0.1	0.000	APM_0135	Putative aminotransferase
49E11	6.87	2.8 ± 0.1	0.000	APM_0069	Hypothetical protein
39D8	6.70	2.7 ± 0.1	0.000	APM_0069	Hypothetical protein
68B5	6.19	2.6 ± 0.1	0.000	APM_0254	Inner-membrane translocator
				APM_0255	Extracellular ligand-binding receptor
80A7	5.97	2.6 ± 0.2	0.000	APM_3511	Pyruvate dehydrogenase (acetyl-transferring)
75D10	5.81	2.5 ± 0.1	0.000	APM_0069	Hypothetical protein
89E6	5.67	2.5 ± 0.1	0.000	APM_0202	Binding-protein-dependent transport systems inner membrane component
				APM_0203	Sulfonate ABC transporter, ATP-binding protein
84D4	5.32	2.4 ± 0.1	0.000	APM_2366	Hypothetical protein
30G11	5.10	2.3 ± 0.1	0.000	APM_1501	Hypothetical protein
				APM_1502	Hypothetical protein
				APM_1504	MscS mechanosensitive ion channel
31G4	5.08	2.3 ± 0.1	0.000	APM_0574	Hypothetical protein
				APM_0575	Hypothetical protein
				APM_0576	Hypothetical protein
07A4	4.53	2.2 ± 0.1	0.000	APM_0135	Putative aminotransferase
41E10	4.51	2.2 ± 0.1	0.000	APM_1502	Hypothetical protein
				APM_1504	MscS mechanosensitive ion channel
71E2	4.50	2.2 ± 0.1	0.000	APM_0109	Beta-lactamase domain-containing protein
75D6	4.40	2.1 ± 0.1	0.000	APM_1441	ATPase, P-type (transporting), HAD superfamily, subfamily IC
40E9	4.39	2.1 ± 0.1	0.000	APM_0373	NCS1 nucleoside transporter
43E2	4.29	2.1 ± 0.1	0.000	APM_3574	Putative urea amidolyase related protein
				APM_3575	Allophanate hydrolase subunit 1
74B1	4.20	2.1 ± 0.1	0.000	APM_0109	Beta-lactamase domain-containing protein
79E8	3.94	2.0 ± 0.1	0.000	APM_1319	Small multidrug resistance protein
				APM_1320	Substrate-binding region of ABC-type glycine betaine transport system
				APM_1321	Binding-protein-dependent transport systems inner membrane component
10C9	3.84	1.9 ± 0.2	0.000	APM_0237	Histone deacetylase superfamily protein
02F11	3.75	1.9 ± 0.1	0.000	APM_2105	HpcH/HpaI aldolase
				APM_2106	Pyrrolidone-carboxylate peptidase
14D8	3.72	1.9 ± 0.1	0.000	APM_0109	Beta-lactamase domain-containing protein
				APM_0111	Secretion protein HlyD family
26F11	3.65	1.9 ± 0.1	0.000	APM_1193	Dihydrodipicolinate synthetase
				APM_1194	D-isomer specific 2-hydroxyacid dehydrogenase, NAD-binding
				APM_1195	Dihydroxy-acid dehydratase
87B8	3.65	1.9 ± 0.1	0.000	APM_3546	MobA/MobL protein
				APM_3547	Hypothetical protein
57H2	3.63	1.9 ± 0.2	0.000	APM_3261	MobA/MobL protein
				APM_3262	Hypothetical protein
89C5	3.60	1.8 ± 0.1	0.000	APM_3261	MobA/MobL protein
				APM_3262	Hypothetical protein
43G2	3.47	1.8 ± 0.1	0.000	APM_2105	HpcH/HpaI aldolase
				APM_2106	Pyrrolidone-carboxylate peptidase
74G7	3.45	1.8 ± 0.1	0.000	APM_3226	Aldehyde dehydrogenase
14G1	3.38	1.8 ± 0.0	0.000	APM_2042	Hypothetical protein
71H3	3.34	1.7 ± 0.1	0.000	APM_0130	Binding-protein-dependent transport systems inner membrane component
				APM_0131	Binding-protein-dependent transport systems inner membrane component
				APM_0132	Spermidine/putrescine ABC transporter ATPase subunit
14D6	3.30	1.7 ± 0.1	0.000	APM_0670	Methionine aminopeptidase, type I
				APM_0671	Major facilitator transporter
				APM_0672	Rhodanese domain-containing protein
45E7	3.30	1.7 ± 0.1	0.000	APM_2085	Short-chain dehydrogenase/reductase SDR
				APM_2086	FkbM family methyltransferase
42B11	3.28	1.7 ± 0.1	0.000	APM_1704	Thioesterase superfamily protein
				APM_1705	Branched-chain amino acid aminotransferase
				APM_1706	MarR family transcriptional regulator
76H10	3.28	1.7 ± 0.1	0.000	APM_2857	Hypothetical protein
60G9	3.22	1.7 ± 0.1	0.000	APM_3574	Putative urea amidolyase related protein
				APM_3575	Allophanate hydrolase subunit 1
53F5	3.20	1.7 ± 0.1	0.000	APM_0775	Binding-protein-dependent transport systems inner membrane component

36C11	3.20	1.7 ± 0.1	0.000	APM_1811	Acetamidase/formamidase
				APM_1812	Short-chain dehydrogenase/reductase SDR
04D4	3.18	1.7 ± 0.1	0.000	APM_3848	Carbohydrate porin, OprB family protein
				APM_3849	Integrase catalytic region
				APM_3850	Transposase IS3/IS911 family protein
89D1	3.17	1.7 ± 0.1	0.000	APM_3386	Hypothetical protein
				APM_3387	Hypothetical protein
63D5	3.16	1.7 ± 0.1	0.000	APM_3357	Transposase, IS4 family protein
01G4	3.12	1.6 ± 0.1	0.000	APM_1213	Hypothetical protein
				APM_1214	Hypothetical protein
				APM_1215	Virulence protein, SciE type
67H1	3.11	1.6 ± 0.1	0.000	APM_0892	Diguanylate phosphodiesterase
74B2	3.04	1.6 ± 0.1	0.000	APM_2984	Diguanylate cyclase/phosphodiesterase
				APM_2985	Hypothetical protein
				APM_2987	Glutathione-dependent formaldehyde-activating, GFA
87A5	3.03	1.6 ± 0.1	0.000	APM_1356	Nitrilase/cyanide hydratase and apolipoprotein N-acyltransferase
				APM_1357	NAD(+) kinase
35D2	-3.50	-1.8 ± 0.2	0.000	APM_1053	Iron-sulfur cluster assembly accessory protein
				APM_1054	Hypothetical protein
				APM_1055	NifU family SUF system FeS assembly protein
87A6	-3.55	-1.8 ± 0.1	0.000	APM_1647	Extracellular ligand-binding receptor
				APM_1649	S-adenosylmethionine synthetase
				APM_1652	GCN5-related N-acetyltransferase
85B2	-3.56	-1.8 ± 0.1	0.000	APM_1009	Glycosyl transferase, group 1
				APM_1010	Sua5/YciO/YrdC/YwlC family protein
81A12	-3.56	-1.8 ± 0.1	0.000	APM_0395	O-succinylhomoserine sulfhydrylase
53G1	-3.59	-1.8 ± 0.0	0.000	APM_1533	3-oxoacyl-(acyl carrier protein) synthase II
				APM_1534	Aminodeoxychorismate lyase
				APM_1535	Hypothetical protein
78D8	-3.59	-1.8 ± 0.1	0.000	APM_0530	Glycosyl transferase, group 1
				APM_0531	Metallophosphoesterase
26A8	-3.61	-1.9 ± 0.1	0.000	APM_1182	Phosphoribosylaminoimidazole-succinocarboxamide synthase
71G7	-3.63	-1.9 ± 0.1	0.000	APM_0528	Glycosyl transferase family protein
				APM_0530	Glycosyl transferase, group 1
				APM_0531	Metallophosphoesterase
				APM_0532	Hypothetical protein
				APM_0533	Alcohol dehydrogenase
28G5	-3.65	-1.9 ± 0.1	0.000	APM_3597	2-dehydro-3-deoxyphosphooctonate aldolase
				APM_3598	CTP synthase
50C12	-3.68	-1.9 ± 0.1	0.000	APM_0733	Putative oxidoreductase
				APM_0734	Glutamate synthase [NADPH] large chain
54B4	-3.76	-1.9 ± 0.1	0.000	APM_0986	Signal peptidase I
79A2	-3.81	-1.9 ± 0.0	0.000	APM_1491	Pyridoxal-dependent decarboxylase
81F9	-3.81	-1.9 ± 0.1	0.000	APM_3062	M3 family oligoendopeptidase
05H9	-3.88	-2.0 ± 0.1	0.000	APM_1392	Glycosyl transferase family protein
34H12	-3.89	-2.0 ± 0.1	0.000	APM_2439	Acetylglutamate kinase
10D9	-3.90	-2.0 ± 0.1	0.000	APM_1302	Inner-membrane translocator
				APM_1303	Inner-membrane translocator
56F11	-3.90	-2.0 ± 0.1	0.000	APM_0528	Glycosyl transferase family protein
				APM_0530	Glycosyl transferase, group 1
				APM_0531	Metallophosphoesterase
79C12	-3.91	-2.0 ± 0.1	0.000	APM_3109	3-phosphoshikimate 1-carboxyvinyltransferase
				APM_3110	Hypothetical protein
				APM_3111	L-carnitine dehydratase/bile acid-inducible protein F
				APM_3112	Hypothetical protein
28E12	-3.91	-2.0 ± 0.1	0.000	APM_1491	Pyridoxal-dependent decarboxylase
71C7	-3.99	-2.0 ± 0.1	0.000	APM_3109	3-phosphoshikimate 1-carboxyvinyltransferase
49E1	-4.02	-2.0 ± 0.1	0.000	APM_2194	Hypothetical protein
				APM_2195	Hypothetical protein
39A7	-4.06	-2.0 ± 0.2	0.000	APM_2511	Hypothetical protein
				APM_2512	COG2062, SixA, Phosphohistidine phosphatase SixA
57F7	-4.10	-2.0 ± 0.1	0.000	APM_0515	Signal recognition particle protein
44D12	-4.13	-2.0 ± 0.1	0.000	APM_0528	Glycosyl transferase family protein
				APM_0530	Glycosyl transferase, group 1
88H9	-4.18	-2.1 ± 0.1	0.000	APM_2128	DNA uptake lipoprotein-like protein
70G5	-4.25	-2.1 ± 0.0	0.000	APM_2130	Hypothetical protein
58H5	-4.29	-2.1 ± 0.1	0.000	APM_1836	Alcohol dehydrogenase
68C11	-4.34	-2.1 ± 0.0	0.000	APM_3407	Hypothetical protein
				APM_3408	Classical-complement-pathway C3/C5 convertase
				APM_3410	Hypothetical protein
76G12	-4.67	-2.2 ± 0.1	0.000	APM_0432	FAD linked oxidase domain-containing protein
				APM_0434	Hypothetical protein
69D6	-4.69	-2.2 ± 0.1	0.000	APM_1006	Hypothetical protein
				APM_1007	Ribose/xylose/arabinose/galactoside ABC-type transporter permease
				APM_1008	FkbM family methyltransferase
45C2	-4.86	-2.3 ± 0.1	0.000	APM_1403	Coproporphyrinogen III oxidase
41G6	-4.86	-2.3 ± 0.0	0.000	APM_3062	M3 family oligoendopeptidase
55G9	-5.04	-2.3 ± 0.1	0.000	APM_0528	Glycosyl transferase family protein
				APM_0530	Glycosyl transferase, group 1
81H10	-5.05	-2.3 ± 0.1	0.000	APM_0528	Glycosyl transferase family protein
				APM_0530	Glycosyl transferase, group 1
49D7	-5.31	-2.4 ± 0.1	0.000	APM_1006	Hypothetical protein
				APM_1007	Ribose/xylose/arabinose/galactoside ABC-type transporter permease
				APM_1008	FkbM family methyltransferase
05H1	-5.32	-2.4 ± 0.1	0.000	APM_3062	M3 family oligoendopeptidase
08B6	-5.50	-2.5 ± 0.1	0.000	APM_0839	Hypothetical protein
				APM_0840	Hypothetical protein

56F1	-6.24	-2.6 ± 0.2	0.000	APM_3027	50S ribosomal protein L1
06E9	-6.77	-2.8 ± 0.1	0.000	APM_1002	Gamma-glutamyl kinase
02D7	-7.74	-3.0 ± 0.1	0.000	APM_0432	FAD linked oxidase domain-containing protein
				APM_0434	Hypothetical protein

APPENDIX VI. Early transcriptomic response to 10 mM Zn in *Acidiphilium* sp. PM.

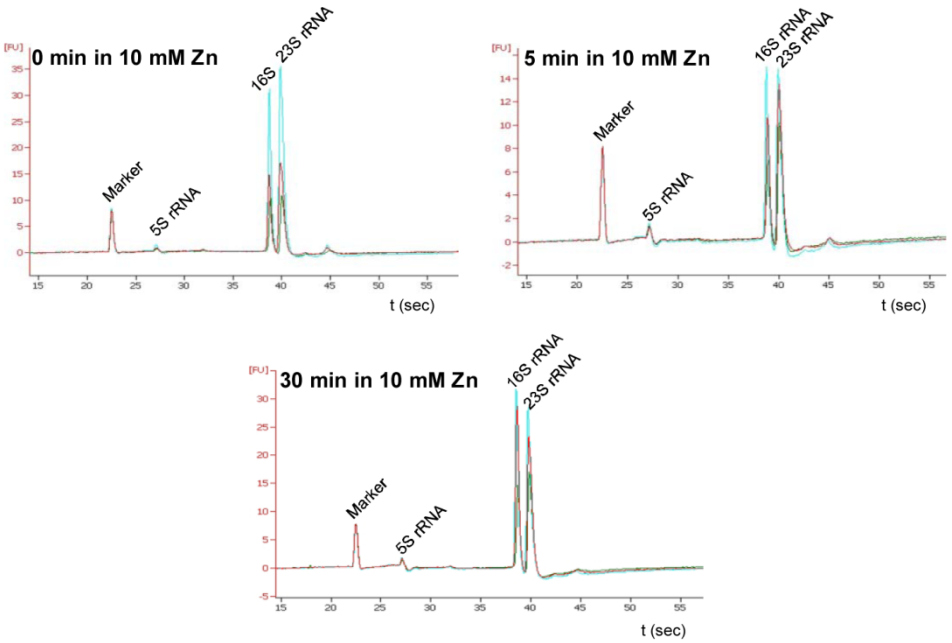

Figure A 3. Early transcriptomic response to Zn. Quality of the RNAs used for microarray hybridization. RNA was extracted from cultures exposed to 10 mM Zn for 0, 5 and 30 min. The integrity of the RNAs was verified by capillary electrophoresis. Electropherograms show the RNA integrity of the three replicates used for each condition.

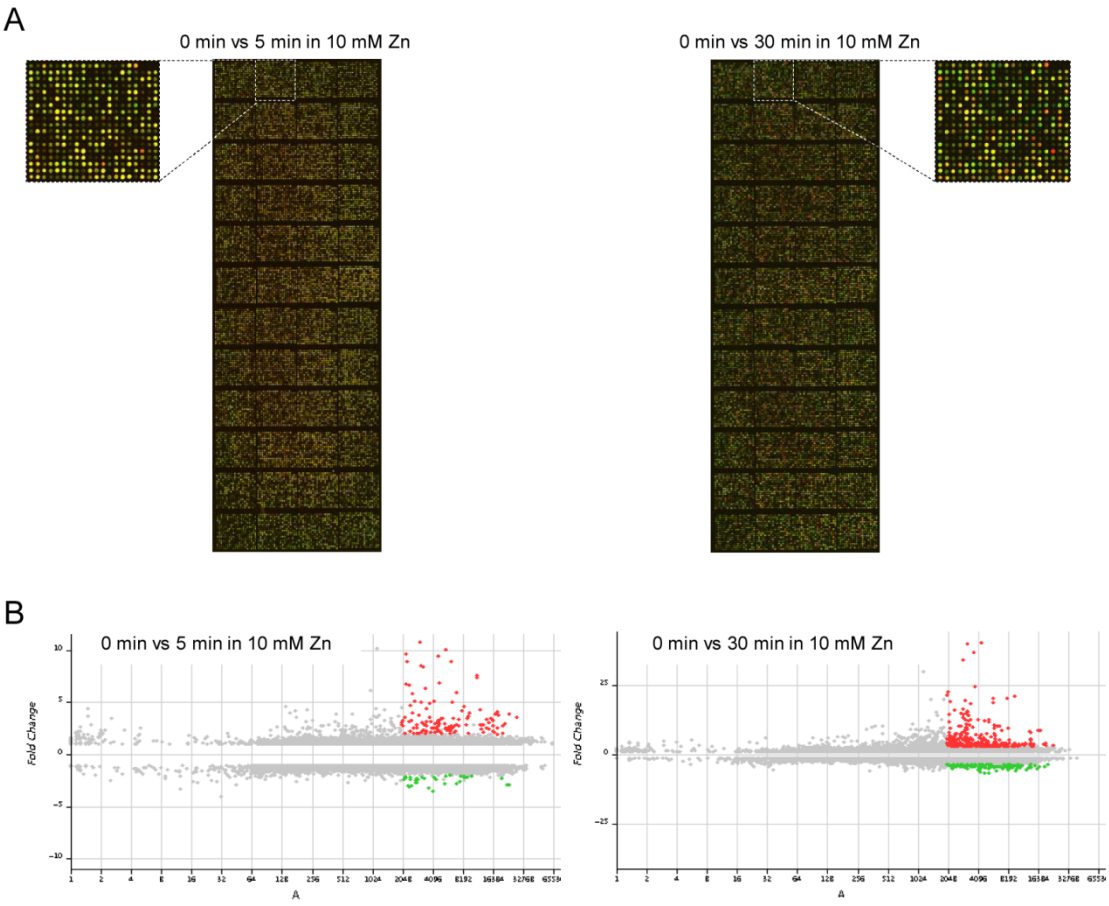

Figure A 4. Early transcriptomic response to Zn. Microarray scanning and analysis. A) Microarrays were hybridized with Cy3-cDNA from unexposed cells and Cy5-cDNA from cells exposed to 10 mM Zn for 5 min (left) or 30 min (right). The microarray scan of one of three replicates is shown for each experiment. B) Fold change vs A scatter plot. These plots were used to establish the thresholds for spot selection: i) average signal intensity > 2000 FU, ii) $p < 0.05$ for statistical significance, and iii) For 0 vs 5 min Ni (left): -2 > Fold change > 2. For 0 vs 30 min Ni (right): -3.5 > Fold change > 3. Selected spots are coloured: red dots indicate clones which contained genes significantly induced upon exposure to 10 mM Zn whereas green dots indicate clones with genes that were significantly repressed.

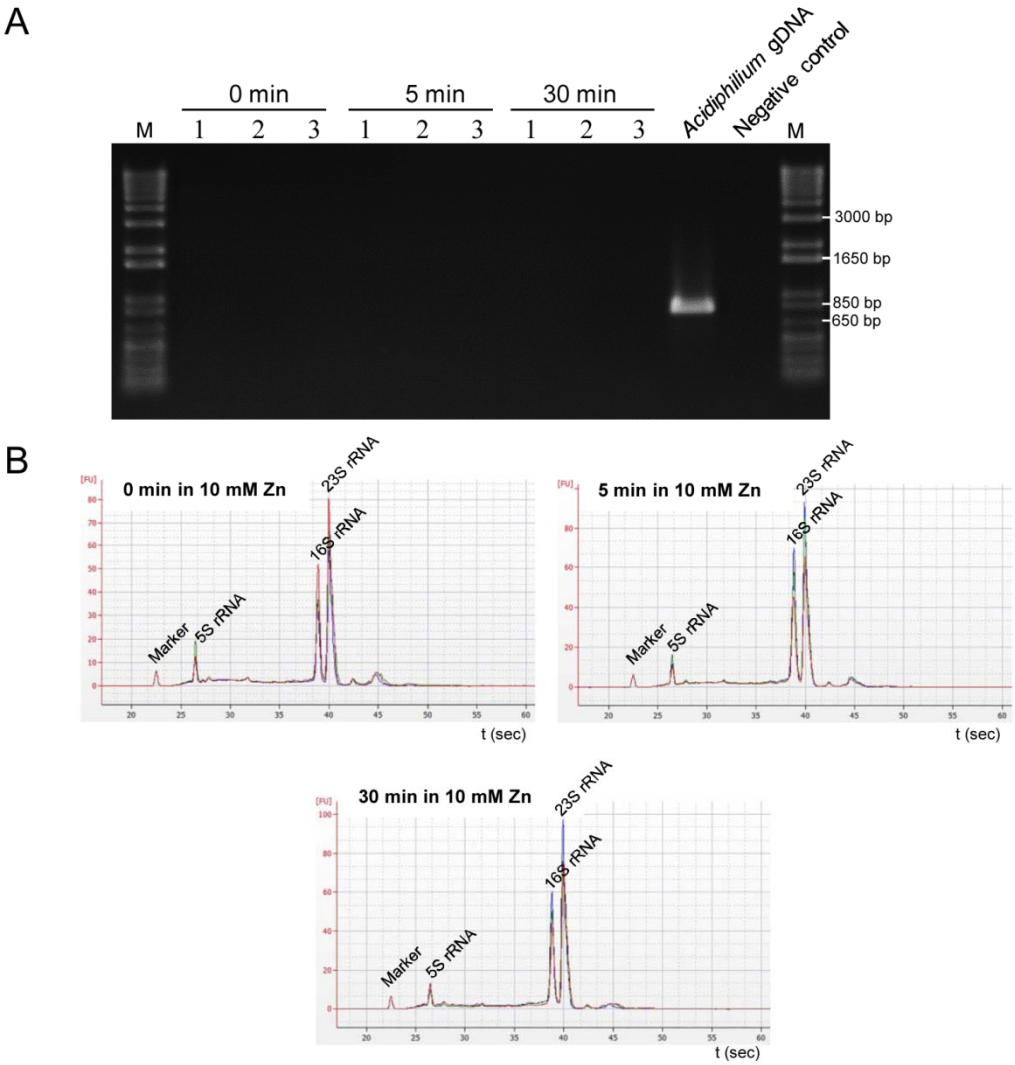

Figure A 5. Early transcriptomic response to Zn. Quality of the RNAs used in the qRT-PCRs. A) The absence of contaminant DNA was ascertained by PCR amplification of *GAPDH*. *Acidiphilium* genomic DNA served as positive control while ultrapure H_20 served as negative control. M indicates molecular weight marker (1 Kb Plus DNA Ladder). B) The integrity of the RNAs was verified by capillary electrophoresis.

Table A 4. Early transcriptomic response to Zn. Microarray control spots. Data shown belongs to one of two replicates included in each slide. Data for the positive controls includes F, log_2F±SD and the associated p value. For the negative controls, the average fluorescence intensity (FI) values and their SD are shown. Data in bold indicate significant differential gene expression as defined by the following criteria: i) average signal intensity > 2000 FU (*ca*. 10 times the background intensity), ii) $p < 0.05$ and iii) For 0 vs 5 min Ni: $-2 > F > 2$. For 0 vs 30 min Ni: $-3.5 > F > 3$.

		0 vs 5 min in 10 mM Zn			0 vs 30 min in 10 mM Zn		
Spot	**Positive control**	**Fold Change**	**Log_2Ratio ± SD**	***p***	**Fold Change**	**Log_2Ratio ± SD**	***p***
90A1	*Apm 16S rRNA*	-1.38	-0.5 ± 0.5	0.216	-1.08	-0.1 ± 0.4	0.694
90A2	***Apm* Arsenate reductase**	1.99	1.0 ± 0.1	0.004	**7.91**	**3.0 ± 0.2**	**0.001**
90A3	*Apm atpB*	-1.33	-0.4 ± 0.4	0.228	-2.27	-1.2 ± 0.4	0.028
90A4	*Apm* Cytochrome C oxidase subunit 3	-1.21	-0.3 ± 0.3	0.288	-1.81	-0.9 ± 0.4	0.060
90A5	*Apm GAPDH*	-1.20	-0.3 ± 0.5	0.456	-1.32	-0.4 ± 0.1	0.036
90A6	*Apm rpoD*	-1.26	-0.3 ± 0.1	0.014	-2.93	-1.5 ± 0.3	0.011
90A7	*Apm bchL*	-1.08	-0.1 ± 0.2	0.393	-1.28	-0.4 ± 0.3	0.180
90A8	*Apm trpB*	-1.38	-0.5 ± 0.4	0.194	-1.84	-0.9 ± 0.2	0.012
90A9	*Apm* Flavodoxin/nitric oxide synthase	1.48	0.6 ± 0.0	0.002	-1.29	-0.4 ± 0.5	0.312
90A10	***Apm* Arsenite oxidase large subunit**	**3.40**	**1.8 ± 0.2**	**0.004**	**3.87**	**2.0 ± 0.1**	**0.001**
90A11	***Apm dnaK***	1.49	0.6 ± 0.2	0.026	**8.00**	**3.0 ± 0.3**	**0.002**
90A12	***Apm* Mercuric reductase**	**7.38**	**2.9 ± 0.2**	**0.002**	**20.29**	**4.3 ± 0.2**	**0.001**
90B1	*Apm pufL*	-1.21	-0.3 ± 0.2	0.188	-1.49	-0.6 ± 0.3	0.066
90B2	*Apm* Fructose-1,6-Bisphosphatase (FBP)	-1.27	-0.3 ± 0.1	0.038	5.10	2.4 ± 0.4	0.010
90B3	*Apm hydA*	-1.14	-0.2 ± 0.2	0.232	-1.33	-0.4 ± 0.4	0.190
90B4	*Apm MCAT*	-1.48	-0.6 ± 0.1	0.006	-4.52	-2.2 ± 0.4	0.010
90B5	*Apm bchC*	-1.12	-0.2 ± 0.2	0.267	-1.09	-0.1 ± 0.4	0.688
90B6	*Apm idh*	-1.40	-0.5 ± 0.1	0.014	-1.64	-0.7 ± 0.2	0.030
90B7	*Apm dnaE*	-1.48	-0.6 ± 0.3	0.062	-1.69	-0.8 ± 0.5	0.102
90B8	*Apm bchH*	-1.33	-0.4 ± 0.1	0.014	-1.23	-0.3 ± 0.2	0.150
90B9	*Apm* FUR family protein	-1.35	-0.4 ± 0.1	0.027	-1.54	-0.6 ± 0.3	0.080
90B10	*Apm* Molybdopterin oxidoreductase	-1.31	-0.4 ± 0.2	0.084	-1.41	-0.5 ± 0.3	0.090
90C1	*Apm* Sau3AI-digested gDNA	1.58	0.7 ± 0.5	0.151	1.89	0.9 ± 0.2	0.014
Spot	**Negative control**		**Average FI ± SD**			**Average FI ± SD**	
90B11	Spotting solution 1x		3 ± 2			10 ± 13	
90B12	Spotting solution 1x		7 ± 7			2 ± 0	
90C2	*Le. infantum* clone S30C8		75 ± 56			60 ± 4	
90C3	*Le. infantum* clone S18H12		32 ± 38			33 ± 18	
90C4	*Le. infantum* clone S31A9		119 ± 76			100 ± 59	
90C5	*Le. infantum* clone S13C5		113 ± 44			112 ± 60	
90C6	*Le. infantum* clone S31F5		172 ± 78			110 ± 69	
90C7	*Le. infantum* clone S19D9		129 ± 60			106 ± 35	
90C8	*Le. infantum* clone S15F1		26 ± 34			22 ± 13	
90C9	*Le. infantum* clone S21H8		40 ± 40			26 ± 16	
90C10	Spotting solution 1x		5 ± 1			3 ± 1	
90C11	Spotting solution 1x		4 ± 4			4 ± 3	
90C12	Spotting solution 1x		36 ± 28			33 ± 14	
90D1	Spotting solution 1x		74 ± 18			29 ± 8	
90D2	Spotting solution 1x		5 ± 2			5 ± 1	
90D3	Spotting solution 1x		6 ± 0			11 ± 0	
90D4	Spotting solution 1x		45 ± 28			15 ± 13	
90D5	Spotting solution 1x		4 ± 2			2 ± 1	
90D6	Spotting solution 1x		6 ± 0			2 ± 1	
90D7	Spotting solution 1x		4 ± 1			4 ± 2	
90D8	Spotting solution 1x		5 ± 1			3 ± 1	
90D9	Spotting solution 1x		2 ± 1			1 ± 0	
90D10	Spotting solution 1x		1 ± 0			5 ± 6	
90D11	Spotting solution 1x		9 ± 10			7 ± 6	
90D12	Spotting solution 1x		4 ± 5			1 ± 0	

Table A 5. Significantly up- and down-regulated clones after 5 minutes in 10 mM Zn. Clones have been arranged on the basis of the function carried out by their genes. Clones which contain genes with unrelated functions are classified as "others". Clone data includes the clone library ID, its ratio of expression (F), the log_2F and its associated standard error as well as the p value. Genes whose expression was further validated by qRT-PCR are shown in the same line. Clones which were up- or down-regulated both in Zn and Ni are coloured in pale blue, whereas clones whose expression was altered only in Zn are left uncoloured. Induction is shown in tones of red whereas repression is highlighted in shades of green.

		Microarray hybridization					qRT-PCR		
	Clone	F	Log_2F±SE	p	Locus	Gene	F	Log_2F±SE	p
Replication, transcription, translation and related	69A8	2.55	1.3± 0.1	0.000	APM_0091	Transposase IS116/IS110/IS902 family protein	-1.26	-0.3± 0.2	0.234
					APM_0092	Type III restriction protein res subunit	N.D.		
	74F11	2.48	1.3± 0.1	0.000	APM_3199	Ribonucleotide-diphosphate reductase subunit alpha	N.D.		
					APM_3200	Ribonucleotide-diphosphate reductase subunit beta	N.D.		
	49B12	2.10	1.1± 0.1	0.002	APM_3260	MobA/MobL protein	N.D.		
	85E3	2.07	1.0± 0.1	0.008	APM_0896	Relaxase/primase-like fusion protein	N.D.		
	41B1	-2.03	-1.0± 0.0	0.000	APM_1368	Carbamoyl-phosphate synthase large chain	N.D.		
	78B9	-2.06	-1.0± 0.0	0.000	APM_3114	Ribonuclease R	-2.25	-1.2± 0.1	0.070
					APM_3115	C-terminal processing peptidase	-2.59	-1.4± 0.1	0.002
	87H9	-2.26	-1.2± 0.1	0.004	APM_1404	30S ribosomal protein S2	N.D.		
					APM_1405	Elongation factor Ts	-1.54	-0.6± 0.0	
Energy-yielding processes	70B2	3.24	1.7± 0.1	0.000	APM_0292	NADH dehydrogenase (quinone)	N.D.		
					APM_0293	NADH-ubiquinone oxidoreductase, chain 49kDa	N.D.		
					APM_0294	NADH ubiquinone oxidoreductase, 20 kDa subunit	1.51	0.6± 0.3	0.212
					APM_0295	NADH/ubiquinone/plastoquinone (complex I)	N.D.		
	84D12	3.00	1.6± 0.1	0.000	APM_0133	Alanine dehydrogenase	6.01	2.6± 0.1	0.000
					APM_0134	XRE family transcriptional regulator	2.32	1.2± 0.0	0.000
	22B4	2.47	1.3± 0.1	0.000	APM_0133	Alanine dehydrogenase	6.01	2.6± 0.1	0.000
					APM_0134	XRE family transcriptional regulator	2.32	1.2± 0.0	0.000
					APM_0135	Putative aminotransferase	N.D.		
	71H3	2.27	1.2± 0.1	0.005	APM_0130	Binding-protein-dependent transport systems inner membrane component	N.D.		
					APM_0131	Binding-protein-dependent transport systems inner membrane component	N.D.		
					APM_0132	Spermidine/putrescine ABC transporter ATPase subunit	N.D.		
					APM_0133	Alanine dehydrogenase	6.01	2.6± 0.1	0.000
Metal homeostasis	09E11	10.11	3.3± 0.1	0.000	APM_3382	Transcriptional regulator, ArsR family	48.02	5.6± 0.1	0.007
					APM_3383	Regulatory protein, ArsR	N.D.		
					APM_3384	Arsenite oxidase, small subunit	N.D.		
	25C12	9.29	3.2± 0.1	0.000	APM_0088	Mercuric reductase	N.D.		
	54E3	8.97	3.2± 0.1	0.000	APM_0088	Mercuric reductase	N.D.		
	90A12	7.51	2.9± 0.1	0.000	APM_0088	Mercuric reductase	N.D.		
	81H4	7.33	2.9± 0.1	0.000	APM_0088	Mercuric reductase	N.D.		
	70D1	5.92	2.6± 0.1	0.000	APM_0179	Transcriptional regulator	50.33	5.7± 0.2	0.024
					APM_0180	4-methylmuconolactone transporter	23.70	4.6± 0.1	0.002
	57B2	5.08	2.3± 0.2	0.008	APM_3385	Arsenite oxidase, large subunit	N.D.		
	49E11	4.27	2.1± 0.1	0.000	APM_0067	Natural resistance-associated macrophage protein	N.D.		
					APM_0068	Manganese transport regulator MntR	1.42	0.5± 0.1	0.037
					APM_0069	Hypothetical protein	N.D.		
					APM_0070	Natural resistance-associated macrophage protein	9.16	3.2± 0.1	0.007
	66H1	4.18	2.1± 0.1	0.000	APM_2362	Cation diffusion facilitator family transporter	2.68	1.4± 0.0	0.001
					APM_2363	Co/Zn/Cd cation transporter-like protein	4.58	2.2± 0.1	0.000
					APM_2364	MerR family transcriptional regulator	3.96	2.0± 0.3	0.085
					APM_2365	Cation diffusion facilitator family transporter	6.00	2.6± 0.1	0.004
	51F7	4.04	2.0± 0.1	0.000	APM_0067	Natural resistance-associated macrophage protein	N.D.		
					APM_0068	Manganese transport regulator MntR	1.42	0.5± 0.1	0.037
					APM_0069	Hypothetical protein	N.D.		
					APM_0070	Natural resistance-associated macrophage protein	9.16	3.2± 0.1	0.007
	57G6	3.78	1.9± 0.1	0.000	APM_0067	Natural resistance-associated macrophage protein	N.D.		
					APM_0068	Manganese transport regulator MntR	1.42	0.5± 0.1	0.037
					APM_0069	Hypothetical protein	N.D.		
					APM_0070	Natural resistance-associated macrophage protein	9.16	3.2± 0.1	0.007
	75D10	3.78	1.9± 0.1	0.000	APM_0068	Manganese transport regulator MntR	1.42	0.5± 0.1	0.037
					APM_0069	Hypothetical protein	N.D.		
					APM_0070	Natural resistance-associated macrophage protein	9.16	3.2± 0.1	0.007
	26F12	3.57	1.8± 0.1	0.000	APM_0069	Hypothetical protein	N.D.		
					APM_0070	Natural resistance-associated macrophage protein	9.16	3.2± 0.1	0.007
	39D8	3.45	1.8± 0.1	0.000	APM_0067	Natural resistance-associated macrophage protein	N.D.		
					APM_0068	Manganese transport regulator MntR	1.42	0.5± 0.1	0.037
					APM_0069	Hypothetical protein	N.D.		
					APM_0070	Natural resistance-associated macrophage protein	9.16	3.2± 0.1	0.007
	89D1	3.36	1.7± 0.1	0.000	APM_3385	Arsenite oxidase, large subunit	N.D.		
					APM_3386	Hypothetical protein	N.D.		
					APM_3387	Hypothetical protein	N.D.		

	67H1	3.34	1.7± 0.0	0.000	APM_0892	Diguanylate phosphodiesterase	N.D.			
					APM_0893	Regulatory protein, ArsR	N.D.			
					APM_0894	Arsenate reductase	N.D.			
					APM_0895	Arsenical pump membrane protein	13.27	3.7± 0.2	0.021	
	19F8	3.28	1.7± 0.1	0.000	APM_0773	ModE family transcriptional regulator	N.D.			
					APM_0774	ABC-type molybdate transport system periplasmic component-like protein	6.78	2.8± 0.2	0.016	
	78F6	3.18	1.7± 0.0	0.000	APM_0067	Natural resistance-associated macrophage protein	N.D.			
					APM_0068	Manganese transport regulator MntR	1.42	0.5± 0.1	0.037	
					APM_0069	Hypothetical protein	N.D.			
	90A10	3.12	1.6± 0.2	0.000	APM_3385	Arsenite oxidase large subunit	N.D.			
	84D4	3.11	1.6± 0.1	0.000	APM_2362	Cation diffusion facilitator family transporter	2.68	1.4± 0.0	0.001	
					APM_2363	Co/Zn/Cd cation transporter-like protein	4.58	2.2± 0.1	0.000	
					APM_2364	MerR family transcriptional regulator	3.96	2.0± 0.3	0.085	
					APM_2365	Cation diffusion facilitator family transporter	6.00	2.6± 0.1	0.004	
					APM_2366	Hypothetical protein	N.D.			
	41E6	3.04	1.6± 0.1	0.000	APM_3385	Arsenite oxidase, large subunit	N.D.			
	71C4	2.88	1.5± 0.1	0.000	APM_3385	Arsenite oxidase, large subunit	N.D.			
	10F9	2.84	1.5± 0.1	0.000	APM_0066	MgtC/SapB transporter	-1.00	0.0± 0.1	0.946	
					APM_0067	Natural resistance-associated macrophage protein	N.D.			
					APM_0068	Manganese transport regulator MntR	1.42	0.5± 0.1	0.037	
					APM_0069	Hypothetical protein	N.D.			
	74D6	2.81	1.5± 0.1	0.000	APM_0066	MgtC/SapB transporter	-1.00	0.0± 0.1	0.946	
					APM_0067	Natural resistance-associated macrophage protein	N.D.			
	43B2	2.76	1.5± 0.1	0.000	APM_3427	OmpR family two-component response regulator	N.D.			
					APM_3428	Signal transduction histidine kinase	N.D.			
	77E7	2.66	1.4± 0.1	0.000	APM_3427	OmpR family two-component response regulator	N.D.			
					APM_3428	Signal transduction histidine kinase	N.D.			
					APM_3429	Hypothetical protein	N.D.			
	53F5	2.64	1.4± 0.1	0.000	APM_0774	ABC-type molybdate transport system periplasmic component-like protein	6.78	2.8± 0.2	0.016	
					APM_0775	Binding-protein-dependent transport systems inner membrane component	N.D.			
	88G6	2.32	1.2± 0.0	0.000	APM_0067	Natural resistance-associated macrophage protein	N.D.			
	43H2	2.05	1.0± 0.1	0.004	APM_2361	Multicopper oxidase, type 2	3.71	1.9± 0.1	0.001	
					APM_2362	Cation diffusion facilitator family transporter	2.68	1.4± 0.0	0.001	
					APM_2363	Co/Zn/Cd cation transporter-like protein	4.58	2.2± 0.1	0.000	
	60A12	-2.28	-1.2± 0.1	0.000	APM_1712	Cation ABC transporter substrate-binding protein	N.D.			
					APM_1713	ABC transporter related	-5.99	-2.6± 0.1	0.053	
					APM_1714	Cation ABC transporter permease	N.D.			
					APM_1715	ABC-3 protein	N.D.			
	03E1	-2.63	-1.4± 0.1	0.002	APM_2300	ABC transporter related	-2.00	-1.0± 0.1	0.011	
					APM_2301	Glycosyl transferase, group 1	N.D.			
	30H1	6.74	2.8± 0.2	0.000	APM_0178	5-oxoprolinase	N.D.			
					APM_0179	Transcriptional regulator	50.33	5.7± 0.2	0.024	
					APM_0180	MFS transporter	23.70	4.6± 0.1	0.002	
	53A11	5.47	2.5± 0.1	0.000	APM_3836	Glycosyl transferase family protein	N.D.			
	43D9	4.37	2.1± 0.1	0.000	APM_0178	5-oxoprolinase	N.D.			
					APM_0179	Transcriptional regulator	50.33	5.7± 0.2	0.024	
					APM_0180	MFS transporter	23.70	4.6± 0.1	0.002	
	03F2	3.79	1.9± 0.1	0.000	APM_1586	ABC transporter related	N.D.			
					APM_1587	ABC transporter related	N.D.			
	45C3	3.65	1.9± 0.1	0.003	APM_3377	Hypothetical protein	N.D.			
					APM_3378	Hypothetical protein	N.D.			
					APM_3379	NADPH-dependent FMN reductase	14.13	3.8± 0.1	0.001	
					APM_3380	Arsenical pump membrane protein	N.D.			
	35G1	3.20	1.7± 0.1	0.000	APM_0895	Arsenical pump membrane protein	13.27	3.7± 0.2	0.021	
					APM_0896	Relaxase/primase-like fusion protein	N.D.			
	53E3	3.01	1.6± 0.1	0.000	APM_3398	Mercuric reductase	N.D.			
					APM_3399	Alkyl hydroperoxide reductase	N.D.			
Others	17H5	2.85	1.5± 0.1	0.000	APM_0180	4-methylmuconolactone transporter	23.70	4.6± 0.1	0.002	
					APM_0181	Integrase catalytic subunit	N.D.			
					APM_0182	Transposase IS3/IS911 family protein	N.D.			
	25C11	2.82	1.5± 0.1	0.000	APM_0178	5-oxoprolinase	N.D.			
	31D9	2.58	1.4± 0.1	0.000	APM_3377	Hypothetical protein	N.D.			
					APM_3378	Hypothetical protein	N.D.			
					APM_3379	NADPH-dependent FMN reductase	14.13	3.8± 0.1	0.001	
	02B4	2.56	1.4± 0.2	0.000	APM_0177	Amidohydrolase 2	N.D.			
					APM_0178	5-oxoprolinase	N.D.			
	11C12	2.35	1.2± 0.1	0.000	APM_2892	Sulfite reductase subunit beta	N.D.			
					APM_2893	Phosphoadenosine phosphosulfate reductase	N.D.			
	26F11	2.30	1.2± 0.1	0.000	APM_1193	Dihydrodipicolinate synthetase	N.D.			
					APM_1194	D-isomer specific 2-hydroxyacid dehydrogenase, NAD-binding	N.D.			
					APM_1195	Dihydroxy-acid dehydratase	N.D.			
	85G7	2.27	1.2± 0.1	0.009	APM_2892	Sulfite reductase subunit beta	N.D.			
					APM_2893	Phosphoadenosine phosphosulfate reductase	N.D.			
	30F7	2.06	1.0± 0.1	0.003	APM_0086	Hypothetical protein	N.D.			
					APM_0087	Alkyl hydroperoxide reductase/ Thiol specific antioxidant/ Mal allergen	15.84	4.0± 0.4	0.070	
					APM_0088	Mercuric reductase	N.D.			

				APM_0089	MerR family transcriptional regulator	2.29	1.2± 0.0	0.006
82H2	-2.17	-1.1± 0.1	0.004	APM_0977	HAD family hydrolase	N.D.		
				APM_0978	Alpha/beta hydrolase fold	N.D.		
				APM_0979	Hypothetical protein	N.D.		
14C9	-2.18	-1.1± 0.1	0.010	APM_1916	Diguanylate cyclase with PAS/PAC sensor	N.D.		
				APM_1917	Hypothetical protein	N.D.		
				APM_1918	Hypothetical protein	N.D.		
				APM_1919	Acyl-CoA dehydrogenase domain-containing protein	N.D.		
35H9	-2.41	-1.3± 0.1	0.000	APM_1917	Hypothetical protein	N.D.		
				APM_1918	Hypothetical protein	N.D.		
				APM_1919	Acyl-CoA dehydrogenase domain-containing protein	N.D.		
80B5	-2.67	-1.4± 0.1	0.000	APM_1915	Diguanylate cyclase/phosphodiesterase with PAS/PAC and GAF sensor(s)	N.D.		
				APM_1916	Diguanylate cyclase with PAS/PAC sensor	N.D.		
				APM_1917	Hypothetical protein	N.D.		
				APM_1918	Hypothetical protein	N.D.		
70B10	-2.89	-1.5± 0.0	0.000	APM_3234	Leucyl-tRNA synthetase	-1.10	-0.1± 0.1	0.580
				APM_3235	Hypothetical protein	N.D.		
				APM_3236	Hypothetical protein	N.D.		
				APM_3237	Thiamine monophosphate synthase	N.D.		
06A5	-3.11	-1.6± 0.1	0.000	APM_1916	Diguanylate cyclase with PAS/PAC sensor	N.D.		
				APM_1917	Hypothetical protein	N.D.		
				APM_1918	Hypothetical protein	N.D.		
				APM_1919	Acyl-CoA dehydrogenase domain-containing protein	N.D.		

Table A 6. Significantly up- and down-regulated clones after 30 minutes in 10 mM Zn. Clones have been arranged on the basis of the function carried out by their genes. Clones which contain genes with unrelated functions are classified as "others". Clone data includes the clone library ID, its ratio of expression (F), the log_2F and its associated standard error as well as the p value. Genes whose expression was further validated by qRT-PCR are shown in the same line. Clones which were up- or down-regulated both in Zn and Ni are coloured in pale blue, whereas clones whose expression was altered only in Zn are left uncoloured. Induction is shown in tones of red whereas repression is highlighted in shades of green.

		Microarray					qPCR		
	Clone	F	$Log_2F \pm SE$	p	Locus	Gene	F	$Log_2F \pm SE$	p
Replication, transcription, translation and related	34C6	22.96	4.5 ± 0.1	0.000	APM_3828	Chaperone protein clpB	N.D.		
	82G3	11.79	3.6 ± 0.2	0.002	APM_0279	Recombinase	N.D.		
	90A11	8.48	3.1 ± 0.1	0.000	APM_0410	Chaperone protein dnaK	N.D.		
	02C7	5.46	2.4 ± 0.1	0.000	APM_0279	Recombinase	N.D.		
	69A8	5.40	2.4 ± 0.1	0.000	APM_0091	Transposase IS116/IS110/IS902 family protein	-3.10	-1.6 ± 0.1	0.011
					APM_0092	Type III restriction protein res subunit	N.D.		
	80A7	4.48	2.2 ± 0.1	0.000	APM_3510	Sigma 54 modulation protein/ribosomal protein S30EA	4.53	2.2 ± 0.1	0.027
					APM_3511	Pyruvate dehydrogenase (acetyl-transferring)	N.D.		
	74F11	4.44	2.2 ± 0.1	0.000	APM_3199	Ribonucleotide-diphosphate reductase subunit alpha	N.D.		
					APM_3200	Ribonucleotide-diphosphate reductase subunit beta	N.D.		
	59B9	4.09	2.0 ± 0.0	0.000	APM_3545	Transposase, IS4 family protein	N.D.		
	05A10	3.77	1.9 ± 0.1	0.000	APM_3255	Transposase	N.D.		
	40E9	3.75	1.9 ± 0.1	0.001	APM_0372	Dihydropyrimidinase	N.D.		
					APM_0373	NCS1 nucleoside transporter	N.D.		
	32A1	3.66	1.9 ± 0.2	0.000	APM_0279	Recombinase	N.D.		
	29F7	3.56	1.8 ± 0.1	0.000	APM_2997	RNA polymerase factor sigma-32	5.24	2.4 ± 0.0	0.000
	14G1	3.49	1.8 ± 0.1	0.001	APM_2041	ClpA homolog protein	2.19	1.1 ± 0.3	0.192
					APM_2042	Hypothetical protein	N.D.		
	39B6	3.37	1.8 ± 0.1	0.000	APM_1877	Hypothetical protein	N.D.		
					APM_1878	Endoribonuclease L-PSP	2.01	1.0 ± 0.4	0.306
	10C9	3.34	1.7 ± 0.1	0.000	APM_0237	Histone deacetylase superfamily protein	N.D.		
					APM_0238	SirA family protein	-1.14	-0.2 ± 0.4	0.811
	05C12	3.30	1.7 ± 0.1	0.000	APM_2997	RNA polymerase factor sigma-32	5.24	2.4 ± 0.0	0.000
	36F10	3.22	1.7 ± 0.2	0.009	APM_3547	Hypothetical protein	N.D.		
	12B2	3.19	1.7 ± 0.1	0.000	APM_1877	Vitamin B12-dependent ribonucleotide reductase	N.D.		
	79H2	3.15	1.7 ± 0.1	0.000	APM_3199	Ribonucleotide-diphosphate reductase subunit alpha	N.D.		
					APM_3200	Ribonucleotide-diphosphate reductase subunit beta	N.D.		
					APM_3201	DNA modification methylase	N.D.		
	85E3	3.09	1.6 ± 0.1	0.005	APM_0896	Relaxase/primase-like fusion protein	N.D.		
	72E9	3.04	1.6 ± 0.1	0.004	APM_1630	Endoribonuclease L-PSP	-1.95	-1.0 ±	
					APM_1631	DNA repair protein RadC	-3.75	-1.9 ± 0.5	0.014
	75E10	-3.53	-1.8 ± 0.1	0.001	APM_1593	Phenylalanyl-tRNA synthetase beta chain	N.D.		
					APM_1594	Phenylalanyl-tRNA synthetase, alpha subunit	N.D.		
	45G1	-3.58	-1.8 ± 0.1	0.003	APM_1243	Prolyl-tRNA synthetase	N.D.		
	71G7	-3.66	-1.9 ± 0.1	0.005	APM_0527	50S ribosomal protein L35	N.D.		
					APM_0528	Glycosyl transferase family protein	N.D.		
					APM_0529	50S ribosomal protein L20	-16.39	-4.0 ± 0.1	0.004
					APM_0530	Glycosyl transferase, group 1	N.D.		
					APM_0531	Metallophosphoesterase	N.D.		
					APM_0532	Hypothetical protein	N.D.		
					APM_0533	Alcohol dehydrogenase	N.D.		
	44D12	-3.73	-1.9 ± 0.1	0.001	APM_0527	50S ribosomal protein L35	N.D.		
					APM_0528	Glycosyl transferase family protein	N.D.		
					APM_0529	50S ribosomal protein L20	-16.39	-4.0 ± 0.1	0.004
					APM_0530	Glycosyl transferase, group 1	N.D.		
	55G9	-3.74	-1.9 ± 0.1	0.000	APM_0527	50S ribosomal protein L35	N.D.		
					APM_0528	Glycosyl transferase family protein	N.D.		
					APM_0529	50S ribosomal protein L20	-16.39	-4.0 ± 0.1	0.004
					APM_0530	Glycosyl transferase, group 1	N.D.		
	24H9	-3.79	-1.9 ± 0.1	0.000	APM_3031	DNA-directed RNA polymerase subunit beta'	N.D.		
					APM_3032	30S ribosomal protein S12	N.D.		
					APM_3033	30S ribosomal protein S7	N.D.		
					APM_3034	Elongation factor Tu	N.D.		
	85B2	-3.80	-1.9 ± 0.1	0.000	APM_1009	Glycosyl transferase, group 1	N.D.		
					APM_1010	Sua5/YciO/YrdC/YwlC family protein	N.D.		
	10F8	-3.80	-1.9 ± 0.2	0.008	APM_3098	Transposase, IS4 family protein	N.D.		
	69D6	-3.81	-1.9 ± 0.0	0.000	APM_1005	50S ribosomal protein L21	-6.71	-2.7 ± 0.0	0.008
					APM_1006	Hypothetical protein	N.D.		
					APM_1007	Ribose/xylose/arabinose/galactoside ABC-type transporter permease	N.D.		
					APM_1008	FkbM family methyltransferase	N.D.		
	81F9	-3.82	-1.9 ± 0.1	0.000	APM_3058	30S ribosomal protein S13	N.D.		
					APM_3059	30S ribosomal protein S11	N.D.		
					APM_3060	DNA-directed RNA polymerase subunit alpha	-10.00	-3.3 ± 0.4	0.021
					APM_3061	50S ribosomal protein L17	N.D.		
					APM_3062	M3 family oligoendopeptidase	N.D.		

	02D7	-3.84	-1.9 ± 0.1	0.000	APM_0432	FAD linked oxidase domain-containing protein	N.D.		
					APM_0433	50S ribosomal protein L36P	-23.81	-4.6 ± 0.5	0.029
					APM_0434	Hypothetical protein	N.D.		
	49D7	-3.90	-2.0 ± 0.1	0.002	APM_1005	50S ribosomal protein L21	-6.71	-2.7 ± 0.0	0.008
					APM_1006	Hypothetical protein	N.D.		
					APM_1007	Ribose/xylose/arabinose/galactoside ABC-type transporter permease	N.D.		
					APM_1008	FkbM family methyltransferase	N.D.		
	88H9	-3.91	-2.0 ± 0.1	0.000	APM_2128	DNA uptake lipoprotein-like protein	N.D.		
					APM_2129	30S ribosomal protein S1	-28.57	-4.8 ± 0.2	0.003
	27F3	-4.01	-2.0 ± 0.0	0.000	APM_3033	30S ribosomal protein S7	N.D.		
					APM_3034	Elongation factor Tu	N.D.		
					APM_3035	30S ribosomal protein S10	N.D.		
					APM_3036	50S ribosomal protein L3	N.D.		
					APM_3037	50S ribosomal protein L4	N.D.		
	03D8	-4.04	-2.0 ± 0.1	0.000	APM_3033	30S ribosomal protein S7	N.D.		
					APM_3034	Elongation factor Tu	N.D.		
	45C2	-4.04	-2.0 ± 0.1	0.001	APM_1403	Coproporphyrinogen III oxidase	N.D.		
					APM_1404	30S ribosomal protein S2	N.D.		
					APM_1405	Elongation factor Ts	-9.26	-3.2 ± 0.0	0.002
	79D1	-4.13	-2.0 ± 0.1	0.000	APM_1293	DNA polymerase I	-3.27	-1.7 ± 0.4	0.020
					APM_1294	Deoxycytidine triphosphate deaminase	N.D.		
	70A12	-4.20	-2.1 ± 0.1	0.000	APM_0516	30S ribosomal protein S16	N.D.		
					APM_0517	Ribosome maturation factor rimM	-7.81	-3.0 ± 0.4	0.041
					APM_0518	tRNA (guanine-N1)-methyltransferase	N.D.		
					APM_0519	50S ribosomal protein L19	N.D.		
	25C1	-4.24	-2.1 ± 0.1	0.001	APM_0517	Ribosome maturation factor rimM	-7.81	-3.0 ± 0.4	0.041
					APM_0518	tRNA (guanine-N1)-methyltransferase	N.D.		
	81H10	-4.25	-2.1 ± 0.2	0.000	APM_0527	50S ribosomal protein L35	N.D.		
					APM_0528	Glycosyl transferase family protein	N.D.		
					APM_0529	50S ribosomal protein L20	-16.39	-4.0 ± 0.1	0.004
					APM_0530	Glycosyl transferase, group 1	N.D.		
	08B10	-4.27	-2.1 ± 0.1	0.003	APM_1173	Adenine phosphoribosyltransferase	-22.22	-4.5 ± 0.3	0.016
	79C12	-4.30	-2.1 ± 0.0	0.000	APM_3109	3-phosphoshikimate 1-carboxyvinyltransferase	N.D.		
					APM_3110	Hypothetical protein	N.D.		
					APM_3111	L-carnitine dehydratase/bile acid-inducible protein F	N.D.		
					APM_3112	Hypothetical protein	N.D.		
					APM_3113	Putative ribonuclease BN	-8.40	-3.1 ± 0.3	0.001
	60A1	-4.33	-2.1 ± 0.1	0.000	APM_3033	30S ribosomal protein S7	N.D.		
					APM_3034	Elongation factor Tu	N.D.		
					APM_3035	30S ribosomal protein S10	N.D.		
					APM_3036	50S ribosomal protein L3	N.D.		
					APM_3037	50S ribosomal protein L4	N.D.		
					APM_3038	Ribosomal protein L25/L23	N.D.		
	56F1	-4.40	-2.1 ± 0.1	0.001	APM_3027	50S ribosomal protein L1	N.D.		
					APM_3028	50S ribosomal protein L10	-5.59	-2.5 ± 0.1	0.000
					APM_3029	50S ribosomal protein L7/L12	N.D.		
					APM_3030	DNA-directed RNA polymerase subunit beta	-1.80	-0.8 ± 0.4	0.168
	80D11	-4.44	-2.1 ± 0.1	0.000	APM_3037	50S ribosomal protein L4	N.D.		
					APM_3038	Ribosomal protein L25/L23	N.D.		
					APM_3039	50S ribosomal protein L2	-4.13	-2.0 ± 0.3	0.016
					APM_3040	30S ribosomal protein S19	N.D.		
	41B1	-4.47	-2.2 ± 0.1	0.000	APM_1368	Carbamoyl-phosphate synthase large chain	N.D.		
	87H9	-4.87	-2.3 ± 0.1	0.000	APM_1404	30S ribosomal protein S2	N.D.		
					APM_1405	Elongation factor Ts	-9.26	-3.2 ± 0.0	0.002
	81A12	-4.95	-2.3 ± 0.2	0.000	APM_0395	O-succinylhomoserine sulfhydrylase	N.D.		
					APM_0396	Ribosomal protein S20	-17.54	-4.1 ± 0.4	0.028
					APM_0397	Chromosomal replication initiation protein	-4.52	-2.2 ± 0.3	0.006
	24C3	-4.96	-2.3 ± 0.2	0.000	APM_1294	Deoxycytidine triphosphate deaminase	N.D.		
	20B4	-4.99	-2.3 ± 0.1	0.000	APM_3046	50S ribosomal protein L14	N.D.		
					APM_3047	50S ribosomal protein L24	N.D.		
					APM_3048	50S ribosomal protein L5	N.D.		
					APM_3049	30S ribosomal protein S14	-2.99	-1.6 ± 0.3	0.026
	20B4	-4.99	-2.3 ± 0.1	0.000	APM_3050	30S ribosomal protein S8	N.D.		
	41G6	-5.00	-2.3 ± 0.0	0.000	APM_3061	50S ribosomal protein L17	N.D.		
					APM_3062	M3 family oligoendopeptidase	N.D.		
	05H1	-5.47	-2.5 ± 0.1	0.000	APM_3059	30S ribosomal protein S11	N.D.		
					APM_3060	DNA-directed RNA polymerase subunit alpha	-10.00	-3.3 ± 0.4	0.021
					APM_3061	50S ribosomal protein L17	N.D.		
					APM_3062	M3 family oligoendopeptidase	N.D.		
	59D2	-5.61	-2.5 ± 0.2	0.000	APM_0396	Ribosomal protein S20	-17.54	-4.1 ± 0.4	0.028
					APM_0397	Chromosomal replication initiation protein	-4.52	-2.2 ± 0.3	0.006
Energy-yielding processes	41G10	15.51	4.0 ± 0.1	0.000	APM_1290	Isocitrate lyase	N.D.		
	84D12	15.06	3.9 ± 0.3	0.005	APM_0133	Alanine dehydrogenase	8.01	3.0 ± 0.4	0.173
					APM_0134	XRE family transcriptional regulator	1.29	0.4 ± 0.4	0.497
	22B4	13.79	3.8 ± 0.1	0.000	APM_0133	Alanine dehydrogenase	8.01	3.0 ± 0.4	0.173
					APM_0134	XRE family transcriptional regulator	1.29	0.4 ± 0.4	0.497
					APM_0135	Putative aminotransferase	N.D.		
	39D1	9.95	3.3 ± 0.1	0.000	APM_1443	NADH-quinone oxidoreductase subunit B 2	N.D.		
					APM_1444	NADH-quinone oxidoreductase subunit C/D	12.90	3.7 ± 0.5	0.219
	04D7	7.79	3.0 ± 0.1	0.000	APM_1443	NADH-quinone oxidoreductase subunit B 2	N.D.		
					APM_1444	NADH-quinone oxidoreductase subunit C/D	12.90	3.7 ± 0.5	0.219
					APM_1445	NADH-quinone oxidoreductase subunit C/D	N.D.		

					APM_1446	NADH-quinone oxidoreductase, E subunit	N.D.		
	70B2	6.84	2.8 ± 0.0	0.000	APM_0292	NADH dehydrogenase (quinone)	N.D.		
					APM_0293	NADH-ubiquinone oxidoreductase, chain 49kDa	N.D.		
					APM_0294	NADH ubiquinone oxidoreductase, 20 kDa subunit	-1.27	-0.3 ± 0.2	0.305
					APM_0295	NADH/ubiquinone/plastoquinone (complex I)	N.D.		
	75D6	6.78	2.8 ± 0.2	0.000	APM_1441	ATPase, P-type (transporting), HAD superfamily, subfamily IC	N.D.		
					APM_1442	NADH-quinone oxidoreductase subunit A	N.D.		
					APM_1443	NADH-quinone oxidoreductase subunit B 2	N.D.		
					APM_1444	NADH-quinone oxidoreductase subunit C/D	12.90	3.7 ± 0.5	0.219
					APM_1445	NADH-quinone oxidoreductase subunit C/D	N.D.		
	90B2	6.62	2.7 ± 0.2	0.008	APM_1676	Fructose-1,6-bisphosphatase class 1	N.D.		
	83B7	6.55	2.7 ± 0.1	0.000	APM_1807	NAD-glutamate dehydrogenase	N.D.		
	47B2	6.52	2.7 ± 0.1	0.000	APM_1442	NADH-quinone oxidoreductase subunit A	N.D.		
					APM_1443	NADH-quinone oxidoreductase subunit B 2	N.D.		
					APM_1444	NADH-quinone oxidoreductase subunit C/D	12.90	3.7 ± 0.5	0.219
					APM_1445	NADH-quinone oxidoreductase subunit C/D	N.D.		
					APM_1446	NADH-quinone oxidoreductase, E subunit	N.D.		
	07F10	6.31	2.7 ± 0.1	0.002	APM_2088	Cytochrome c-like protein	N.D.		
	69B12	6.03	2.6 ± 0.1	0.003	APM_1019	Putative glycosidase	N.D.		
					APM_1020	Trehalose synthase	N.D.		
	24F10	5.79	2.5 ± 0.1	0.000	APM_0288	Hypothetical protein	N.D.		
					APM_0289	Hypothetical protein	N.D.		
					APM_0290	Formate hydrogenlyase subunit 4-like protein	-1.70	-0.8 ± 0.3	0.099
					APM_0291	Hydrogenase-4 component E	N.D.		
	56E3	5.25	2.4 ± 0.2	0.007	APM_1019	Putative glycosidase	N.D.		
					APM_1020	Trehalose synthase	N.D.		
	07A4	4.67	2.2 ± 0.2	0.000	APM_0133	Alanine dehydrogenase	8.01	3.0 ± 0.4	0.173
					APM_0134	XRE family transcriptional regulator	1.29	0.4 ± 0.4	0.497
					APM_0135	Putative aminotransferase	N.D.		
					APM_0136	Glutamine synthetase, catalytic region	-1.83	-0.9 ± 0.4	0.132
	71H3	4.19	2.1 ± 0.1	0.000	APM_0130	Binding-protein-dependent transport systems inner membrane component	N.D.		
					APM_0131	Binding-protein-dependent transport systems inner membrane component	N.D.		
					APM_0132	Spermidine/putrescine ABC transporter ATPase subunit	N.D.		
					APM_0133	Alanine dehydrogenase	8.01	3.0 ± 0.4	0.173
	05C2	3.82	1.9 ± 0.1	0.000	APM_1020	Alpha-amylase	N.D.		
					APM_1021	1,4-alpha-glucan-branching enzyme	N.D.		
	50F7	3.77	1.9 ± 0.2	0.000	APM_1020	Trehalose synthase	N.D.		
	05B8	3.75	1.9 ± 0.1	0.000	APM_0273	Cytochrome c oxidase (B(O/a)3-type) chain II	N.D.		
					APM_0274	Cytochrome c oxidase, subunit I	N.D.		
	84E1	3.14	1.7 ± 0.1	0.000	APM_1019	Putative glycosidase	N.D.		
					APM_1020	Trehalose synthase	N.D.		
	54E1	3.08	1.6 ± 0.1	0.001	APM_1692	Hypothetical protein	N.D.		
					APM_1693	Formate dehydrogenase family accessory protein FdhD	-3.07	-1.6 ± 0.3	0.032
					APM_1694	Formate dehydrogenase, alpha subunit	N.D.		
	90B4	-3.56	-1.8 ± 0.1	0.004	APM_1530	Malonyl CoA-acyl carrier protein transacylase (MCT)	N.D.		
	64H1	-3.70	-1.9 ± 0.1	0.000	APM_3179	Sorbitol dehydrogenase	N.D.		
					APM_3180	Glucose-6-phosphate 1-dehydrogenase	N.D.		
					APM_3181	Phosphogluconate dehydratase	N.D.		
	68C11	-3.93	-2.0 ± 0.1	0.000	APM_3406	Cytochrome c biogenesis protein transmembrane region	-5.68	-2.5 ± 0.7	0.009
					APM_3407	Hypothetical protein	N.D.		
					APM_3408	Classical-complement-pathway C3/C5 convertase	N.D.		
					APM_3409	Redoxin domain-containing protein	-1.43	-0.5 ± 0.5	0.472
					APM_3410	Hypothetical protein	N.D.		
	11C11	-4.34	-2.1 ± 0.1	0.003	APM_3180	Glucose-6-phosphate 1-dehydrogenase	N.D.		
					APM_3181	Phosphogluconate dehydratase	N.D.		
					APM_3182	Ketohydroxyglutarate aldolase	-4.20	-2.1 ± 0.3	0.005
					APM_3183	Sugar transporter	N.D.		
	02C11	-4.38	-2.1 ± 0.1	0.000	APM_1929	ATP synthase subunit beta	N.D.		
					APM_1930	ATP synthase gamma chain	-10.53	-3.4 ± 0.3	0.017
					APM_1931	ATP synthase subunit alpha	N.D.		
Metal homeostasis	25C12	40.17	5.3 ± 0.1	0.000	APM_0088	Mercuric reductase	N.D.		
	54E3	35.54	5.2 ± 0.1	0.000	APM_0088	Mercuric reductase	N.D.		
	81H4	20.74	4.4 ± 0.1	0.000	APM_0088	Mercuric reductase	N.D.		
	90A12	20.62	4.4 ± 0.2	0.000	APM_0088	Mercuric reductase	N.D.		
	09E11	18.82	4.2 ± 0.2	0.000	APM_3382	Transcriptional regulator, ArsR family	30.88	4.9 ± 0.2	0.109
					APM_3383	Regulatory protein, ArsR	N.D.		
					APM_3384	Arsenite oxidase, small subunit	N.D.		
	70D1	15.23	3.9 ± 0.2	0.000	APM_0179	Transcriptional regulator	61.88	6.0 ± 0.0	0.009
					APM_0180	MFS transporter	27.50	4.8 ± 0.3	0.124
	57B2	14.35	3.8 ± 0.1	0.000	APM_3385	Arsenite oxidase, large subunit	N.D.		
	41E6	11.40	3.5 ± 0.1	0.000	APM_3385	Arsenite oxidase, large subunit	N.D.		
	43H2	9.57	3.3 ± 0.1	0.000	APM_2361	Multicopper oxidase, type 2	16.40	4.0 ± 0.0	0.000
					APM_2362	Cation diffusion facilitator family transporter	5.99	2.6 ± 0.3	0.158
					APM_2363	Co/Zn/Cd cation transporter-like protein	15.54	4.0 ± 0.3	0.132
	89D1	8.51	3.1 ± 0.0	0.000	APM_3385	Arsenite oxidase, large subunit	N.D.		
					APM_3386	Hypothetical protein	N.D.		
					APM_3387	Hypothetical protein	N.D.		
	71C4	8.47	3.1 ± 0.1	0.000	APM_3385	Arsenite oxidase, large subunit	N.D.		
	90A2	7.72	2.9 ± 0.1	0.000	APM_3381	Arsenate reductase	N.D.		
	19F8	7.63	2.9 ± 0.2	0.006	APM_0773	ModE family transcriptional regulator	N.D.		
					APM_0774	ABC-type molybdate transport system periplasmic component-like protein	6.38	2.7 ± 0.1	0.039
	26F12	7.03	2.8 ± 0.1	0.000	APM_0069	Hypothetical protein	N.D.		

					APM_0070	Natural resistance-associated macrophage protein	12.14	3.6 ± 0.1	0.028
	53F5	6.64	2.7 ± 0.1	0.000	APM_0774	ABC-type molybdate transport system periplasmic component-like protein	6.38	2.7 ± 0.1	0.039
					APM_0775	Binding-protein-dependent transport systems inner membrane component	N.D.		
	01B4	6.41	2.7 ± 0.1	0.000	APM_3398	Mercuric reductase	N.D.		
	68B5	5.70	2.5 ± 0.1	0.000	APM_0254	Inner-membrane translocator	N.D.		
					APM_0255	Extracellular ligand-binding receptor	N.D.		
	51F7	5.56	2.5 ± 0.2	0.000	APM_0067	Natural resistance-associated macrophage protein	N.D.		
					APM_0068	Manganese transport regulator MntR	-13.33	-3.7 ± 0.4	0.004
					APM_0069	Hypothetical protein	N.D.		
					APM_0070	Natural resistance-associated macrophage protein	12.14	3.6 ± 0.1	0.028
	74B1	4.48	2.2 ± 0.1	0.000	APM_0109	Beta-lactamase domain-containing protein	N.D.		
					APM_0110	Major facilitator transporter	2.14	1.1 ± 0.0	0.003
	47C8	4.47	2.2 ± 0.2	0.000	APM_1213	Hypothetical protein	N.D.		
	53B5	4.30	2.1 ± 0.1	0.001	APM_0185	Response regulator receiver protein	N.D.		
	49E11	4.27	2.1 ± 0.1	0.000	APM_0067	Natural resistance-associated macrophage protein	N.D.		
					APM_0068	Manganese transport regulator MntR	-13.33	-3.7 ± 0.4	0.004
					APM_0069	Hypothetical protein	N.D.		
					APM_0070	Natural resistance-associated macrophage protein	12.14	3.6 ± 0.1	0.028
	75D10	4.26	2.1 ± 0.1	0.000	APM_0068	Manganese transport regulator MntR	-13.33	-3.7 ± 0.4	0.004
					APM_0069	Hypothetical protein	N.D.		
					APM_0070	Natural resistance-associated macrophage protein	12.14	3.6 ± 0.1	0.028
	84D4	4.15	2.1 ± 0.1	0.002	APM_2362	Cation diffusion facilitator family transporter	5.99	2.6 ± 0.3	0.158
					APM_2363	Co/Zn/Cd cation transporter-like protein	15.54	4.0 ± 0.3	0.132
					APM_2364	MerR family transcriptional regulator	1.43	0.5 ± 0.2	0.175
					APM_2365	Cation diffusion facilitator family transporter	5.16	2.4 ± 0.3	0.134
					APM_2366	Hypothetical protein	N.D.		
	57G6	4.10	2.0 ± 0.1	0.000	APM_0067	Natural resistance-associated macrophage protein	N.D.		
					APM_0068	Manganese transport regulator MntR	-13.33	-3.7 ± 0.4	0.004
					APM_0069	Hypothetical protein	N.D.		
					APM_0070	Natural resistance-associated macrophage protein	12.14	3.6 ± 0.1	0.028
	66H1	4.05	2.0 ± 0.1	0.000	APM_2362	Cation diffusion facilitator family transporter	5.99	2.6 ± 0.3	0.158
					APM_2363	Co/Zn/Cd cation transporter-like protein	15.54	4.0 ± 0.3	0.132
					APM_2364	MerR family transcriptional regulator	1.43	0.5 ± 0.2	0.175
					APM_2365	Cation diffusion facilitator family transporter	5.16	2.4 ± 0.3	0.134
	71E2	4.00	2.0 ± 0.2	0.000	APM_0109	Beta-lactamase domain-containing protein	N.D.		
					APM_0110	Major facilitator transporter	2.14	1.1 ± 0.0	0.003
	90A10	3.81	1.9 ± 0.1	0.000	APM_3385	Arsenite oxidase large subunit	N.D.		
	01G4	3.30	1.7 ± 0.1	0.000	APM_1213	Hypothetical protein	N.D.		
					APM_1214	Hypothetical protein	N.D.		
					APM_1215	Virulence protein, SciE type	N.D.		
	67H1	3.11	1.6 ± 0.1	0.000	APM_0892	Diguanylate phosphodiesterase	N.D.		
					APM_0893	Regulatory protein, ArsR	N.D.		
					APM_0894	Arsenate reductase	N.D.		
					APM_0895	Arsenical pump membrane protein	1.66	0.7 ± 0.2	0.092
Amino acid transport & biosynthesis	64B12	14.46	3.9 ± 0.2	0.003	APM_3714	Alpha/beta hydrolase fold protein	N.D.		
					APM_3715	Ornithine cyclodeaminase	2.49	1.3 ± 0.1	0.006
					APM_3716	Arginase	N.D.		
	03F2	7.50	2.9 ± 0.1	0.001	APM_1586	ABC transporter related	N.D.		
					APM_1587	ABC transporter related	N.D.		
	77F11	3.53	1.8 ± 0.2	0.000	APM_1590	Branched-chain amino acid ABC transporter substrate binding protein	N.D.		
					APM_1592	Extracellular ligand-binding receptor	N.D.		
	06D12	3.23	1.7 ± 0.1	0.000	APM_1588	Branched-chain amino acid ABC transporter permease	N.D.		
					APM_1589	ABC transporter permease	N.D.		
					APM_1590	Branched-chain amino acid ABC transporter substrate binding protein	N.D.		
	10D9	-3.57	-1.8 ± 0.1	0.000	APM_1302	Inner-membrane translocator	N.D.		
					APM_1303	Inner-membrane translocator	N.D.		
	12F12	-3.97	-2.0 ± 0.2	0.000	APM_1664	Aspartate kinase	N.D.		
Cell wall and flagella	29G11	3.14	1.7 ± 0.1	0.004	APM_3699	Peptidoglycan glycosyltransferase	N.D.		
	08D8	-3.62	-1.9 ± 0.2	0.009	APM_0010	Hypothetical protein	N.D.		
					APM_0011	Flagellar hook capping protein	-6.25	-2.6 ± 0.1	0.008
					APM_0012	Hypothetical protein	N.D.		
	20H6	-4.19	-2.1 ± 0.1	0.004	APM_3648	Glycosyl transferase family protein	N.D.		
					APM_3649	Hypothetical protein	N.D.		
	53G11	-5.79	-2.5 ± 0.2	0.000	APM_3647	Acyltransferase 3	N.D.		
					APM_3648	Glycosyl transferase family protein	N.D.		
Heme	51C9	-3.80	-1.9 ± 0.1	0.002	APM_0497	Molybdopterin oxidoreductase	N.D.		
					APM_0498	Uroporphyrin-III C-methyltransferase	N.D.		
					APM_0499	Siroheme synthase	-6.10	-2.6 ± 0.4	0.010
Nitrogen metab.	30G11	6.00	2.6 ± 0.1	0.000	APM_1501	Hypothetical protein	N.D.		
					APM_1502	Hypothetical protein	N.D.		
					APM_1503	Nitrile hydratase	3.67	1.9 ± 0.0	0.000
					APM_1504	MscS mechanosensitive ion channel	N.D.		
	41E10	3.26	1.7 ± 0.1	0.000	APM_1502	Hypothetical protein	N.D.		
					APM_1503	Nitrile hydratase	3.67	1.9 ± 0.0	0.000
					APM_1504	MscS mechanosensitive ion channel	N.D.		
Others	26D8	18.26	4.2 ± 0.1	0.000	APM_2012	Hypothetical protein	N.D.		
	85E9	12.29	3.6 ± 0.1	0.000	APM_2006	Hypothetical protein	N.D.		
					APM_2007	Isocitrate lyase	22.16	4.5 ± 0.1	0.067
					APM_2008	TetR family transcriptional regulator	N.D.		
	25C11	11.69	3.5 ± 0.2	0.000	APM_0178	5-oxoprolinase	N.D.		
	02B4	9.73	3.3 ± 0.3	0.000	APM_0177	Amidohydrolase 2	N.D.		
					APM_0178	5-oxoprolinase	N.D.		

53A11	8.21	3.0 ± 0.2	0.000	APM_3836	Glycosyl transferase family protein	N.D.		
55A12	7.31	2.9 ± 0.1	0.000	APM_1290	Isocitrate lyase	N.D.		
				APM_1291	DNA glycosylase	N.D.		
				APM_1292	Hypothetical protein	N.D.		
				APM_1293	DNA polymerase I	-3.27	-1.7 ± 0.4	0.020
17H5	6.95	2.8 ± 0.2	0.000	APM_0180	MFS transporter	27.50	4.8 ± 0.3	0.124
				APM_0181	Integrase catalytic subunit, transposase	N.D.		
				APM_0182	Transposase IS3/IS911 family protein	N.D.		
59B1	6.52	2.7 ± 0.2	0.000	APM_0177	Amidohydrolase 2	N.D.		
				APM_0178	5-oxoprolinase	N.D.		
45C3	5.86	2.6 ± 0.1	0.000	APM_3377	DNA primase	N.D.		
				APM_3378	Hypothetical protein	N.D.		
				APM_3379	NADPH-dependent FMN reductase	3.94	2.0 ± 0.6	0.283
				APM_3380	Arsenical pump membrane protein	N.D.		
23A11	5.80	2.5 ± 0.1	0.000	APM_3418	Cytochrome c oxidase, subunit II	N.D.		
				APM_3419	Cytochrome C biogenesis protein	2.59	1.4 ± 0.4	0.237
				APM_3420	Heavy metal-dependent transcription regulator 2	N.D.		
				APM_3421	Copper transporting ATPase	2.47	1.3 ± 0.5	0.328
17C4	5.80	2.5 ± 0.1	0.002	APM_0177	Amidohydrolase 2	N.D.		
				APM_0178	5-oxoprolinase	N.D.		
44C5	5.79	2.5 ± 0.1	0.000	APM_2255	Putative sulfite oxidase subunit YedY	N.D.		
				APM_2256	NUDIX hydrolase	-1.91	-0.9 ± 0.4	0.143
				APM_2257	DEAD/DEAH box helicase domain-containing protein	-1.34	-0.4 ± 0.4	0.458
34G3	5.48	2.5 ± 0.1	0.002	APM_3529	Hypothetical protein	N.D.		
				APM_3530	Transglycosylase-associated protein	N.D.		
65C5	5.28	2.4 ± 0.1	0.000	APM_1143	Hypothetical protein	N.D.		
				APM_1144	Hypothetical protein	N.D.		
				APM_1145	Hypothetical protein	N.D.		
				APM_1146	NADPH:quinone reductase	N.D.		
58A4	5.18	2.4 ± 0.2	0.005	APM_1773	NADH:flavin oxidoreductase/NADH oxidase	N.D.		
				APM_1775	Regulatory protein, ArsR	N.D.		
36C11	4.80	2.3 ± 0.2	0.000	APM_1811	Acetamidase/formamidase	N.D.		
				APM_1812	Short-chain dehydrogenase/reductase SDR	N.D.		
11F11	4.22	2.1 ± 0.1	0.000	APM_1773	NADH:flavin oxidoreductase/NADH oxidase	N.D.		
				APM_1774	3-ketoacyl-(acyl-carrier-protein) reductase	N.D.		
				APM_1775	Regulatory protein, ArsR	N.D.		
74G7	4.22	2.1 ± 0.1	0.000	APM_3225	Beta alanine--pyruvate transaminase	3.98	2.0 ± 0.5	0.246
				APM_3226	Aldehyde dehydrogenase	N.D.		
65B11	4.16	2.1 ± 0.1	0.000	APM_2255	Putative sulfite oxidase subunit YedY	N.D.		
				APM_2256	NUDIX hydrolase	-1.91	-0.9 ± 0.4	0.143
				APM_2257	DEAD/DEAH box helicase domain-containing protein	-1.34	-0.4 ± 0.4	0.458
78D6	4.16	2.1 ± 0.0	0.000	APM_1408	Methyl-accepting chemotaxis sensory transducer	N.D.		
				APM_1409	Glutathione S-transferase domain-containing protein	1.25	0.3 ± 0.0	0.197
59A6	4.15	2.1 ± 0.1	0.002	APM_2513	Glycosyl transferase family protein	N.D.		
				APM_2514	Glycine cleavage T-protein, C-terminal barrel	N.D.		
				APM_2515	Glutathione S-transferase domain-containing protein	N.D.		
				APM_2516	2-nitropropane dioxygenase, NPD	N.D.		
24B2	4.14	2.0 ± 0.1	0.000	APM_3229	Anti-ECFsigma factor, ChrR	N.D.		
				APM_3230	Carbon-monoxide dehydrogenase (acceptor)	N.D.		
52D8	4.01	2.0 ± 0.1	0.000	APM_3230	Carbon-monoxide dehydrogenase (acceptor)	N.D.		
27G2	4.01	2.0 ± 0.1	0.000	APM_2254	Nucleoside triphosphate pyrophosphohydrolase	N.D.		
				APM_2255	Putative sulfite oxidase subunit YedY	N.D.		
				APM_2256	NUDIX hydrolase	-1.91	-0.9 ± 0.4	0.143
				APM_2257	DEAD/DEAH box helicase domain-containing protein	-1.34	-0.4 ± 0.4	0.458
73F5	3.86	1.9 ± 0.1	0.000	APM_1615	Hypothetical protein	N.D.		
				APM_1616	Permease for cytosine/purines, uracil, thiamine, allantoin	5.00	2.3 ±	
30F6	3.73	1.9 ± 0.2	0.007	APM_0701	Aldo/keto reductase	N.D.		
				APM_0702	Major facilitator transporter	N.D.		
73B7	3.65	1.9 ± 0.1	0.000	APM_2411	Sulfotransferase	N.D.		
21C1	3.64	1.9 ± 0.2	0.000	APM_3515	NUDIX hydrolase	N.D.		
				APM_3516	Hypothetical protein	N.D.		
66E9	3.59	1.8 ± 0.0	0.000	APM_3062	M3 family oligoendopeptidase	N.D.		
				APM_3063	Glutathione S-transferase	N.D.		
49E2	3.57	1.8 ± 0.1	0.000	APM_0356	Hypothetical protein	N.D.		
56H12	3.56	1.8 ± 0.2	0.007	APM_2097	Aminotransferase	N.D.		
				APM_2098	Hypothetical protein	N.D.		
				APM_2099	Hypothetical protein	N.D.		
				APM_2100	Poly(R)-hydroxyalkanoic acid synthase, class I	N.D.		
49G2	3.53	1.8 ± 0.1	0.000	APM_3515	NUDIX hydrolase	N.D.		
				APM_3516	Hypothetical protein	N.D.		
				APM_3517	ATPase	N.D.		
24E5	3.53	1.8 ± 0.1	0.000	APM_1687	ABC transporter ATP-binding protein	N.D.		
				APM_1688	Nitrate ABC transporter ATPase	N.D.		
				APM_1689	Nitrate ABC transporter substrate-binding	N.D.		
				APM_1690	Hypothetical protein	N.D.		
				APM_1691	Formate/nitrite transporter	N.D.		
21D11	3.53	1.8 ± 0.1	0.004	APM_3408	Classical-complement-pathway C3/C5 convertase	N.D.		
				APM_3409	Redoxin domain-containing protein	-1.43	-0.5 ± 0.5	0.472
				APM_3410	Hypothetical protein	N.D.		
				APM_3411	Hypothetical protein	N.D.		
				APM_3412	Peroxidase	1.21	0.3 ± 0.2	0.714
				APM_3413	Copper resistance protein	-3.14	-1.7 ± 0.2	0.006

				APM_3414	Hypothetical protein	N.D.			
32H12	3.52	1.8 ± 0.1	0.000	APM_2425	Hypothetical protein	N.D.			
59D6	3.46	1.8 ± 0.1	0.000	APM_2209	Diguanylate cyclase/phosphodiesterase with PAS/PAC and GAF sensor(s)	N.D.			
				APM_2210	Signal-transduction protein	N.D.			
				APM_2211	Proton-translocating NADH-quinone oxidoreductase, chain N	N.D.			
06A11	3.45	1.8 ± 0.0	0.000	APM_3148	Aldehyde dehydrogenase	N.D.			
				APM_3149	Hypothetical protein	N.D.			
				APM_3150	Hypothetical protein	N.D.			
31D9	3.39	1.8 ± 0.1	0.000	APM_3377	DNA primase	N.D.			
				APM_3378	Hypothetical protein	N.D.			
				APM_3379	NADPH-dependent FMN reductase	3.94	2.0 ± 0.6	0.283	
82G4	3.34	1.7 ± 0.2	0.009	APM_3148	Aldehyde dehydrogenase	N.D.			
				APM_3149	Hypothetical protein	N.D.			
57F11	3.31	1.7 ± 0.1	0.002	APM_1783	Hypothetical protein	N.D.			
				APM_1784	Molybdenum cofactor biosynthesis protein A	N.D.			
05C12	3.30	1.7 ± 0.1	0.000	APM_2992	Probable chemoreceptor glutamine deamidase cheD	N.D.			
				APM_2993	Hypothetical protein	N.D.			
				APM_2994	Hypothetical protein	N.D.			
				APM_2995	Hypothetical protein	N.D.			
				APM_2996	Beta-lactamase domain-containing protein	N.D.			
13G12	3.29	1.7 ± 0.0	0.000	APM_0891	Transposase	N.D.			
				APM_0892	Diguanylate phosphodiesterase	N.D.			
				APM_0893	Regulatory protein, ArsR	N.D.			
				APM_0894	Arsenate reductase	N.D.			
				APM_0895	Arsenical pump membrane protein	1.66	0.7 ± 0.2	0.092	
83G7	3.28	1.7 ± 0.2	0.000	APM_0089	MerR family transcriptional regulator	2.55	1.4 ± 0.4	0.245	
				APM_0090	Putative transposase	N.D.			
41A6	3.27	1.7 ± 0.1	0.004	APM_1143	Hypothetical protein	N.D.			
				APM_1144	Hypothetical protein	N.D.			
				APM_1145	Hypothetical protein	N.D.			
				APM_1146	NADPH:quinone reductase	N.D.			
39A11	3.25	1.7 ± 0.1	0.004	APM_2963	Hypothetical protein	N.D.			
				APM_2964	Replicative DNA helicase	1.62	0.7 ±		
46F9	3.22	1.7 ± 0.1	0.001	APM_0938	Hypothetical protein	N.D.			
				APM_0939	OmpA/MotB domain-containing protein	N.D.			
				APM_0940	ATP-dependent helicase HrpB	N.D.			
68F1	3.11	1.6 ± 0.1	0.000	APM_3293	Protein ydeP	N.D.			
45C10	3.11	1.6 ± 0.1	0.000	APM_3422	Heavy metal translocating P-type ATPase	12.06	3.6 ± 0.4	0.185	
				APM_3423	Cysteine synthase A	N.D.			
10F2	3.08	1.6 ± 0.1	0.002	APM_0088	Mercuric reductase	N.D.			
				APM_0089	MerR family transcriptional regulator	2.55	1.4 ± 0.4	0.245	
				APM_0090	Putative transposase	N.D.			
				APM_0091	Transposase IS116/IS110/IS902 family protein	-3.10	-1.6 ± 0.1	0.011	
30E10	3.06	1.6 ± 0.1	0.000	APM_2881	Hypothetical protein	N.D.			
				APM_2883	Fis family GAF modulated sigma54 specific transcriptional regulator	5.48	2.5 ± 0.4	0.220	
59A2	3.03	1.6 ± 0.0	0.001	APM_2796	Hypothetical protein	N.D.			
				APM_2797	Hypothetical protein	N.D.			
				APM_2798	Hypothetical protein	-1.39	-0.5 ± 0.5	0.542	
41G11	3.03	1.6 ± 0.1	0.008	APM_1170	Colicin V production protein	-11.90	-3.6 ± 0.2	0.003	
				APM_1171	DNA repair protein RadA	-21.74	-4.4 ± 0.3	0.019	
				APM_1172	Hypothetical protein	N.D.			
39B1	3.02	1.6 ± 0.2	0.009	APM_0772	TspO and MBR like protein	N.D.			
				APM_0773	ModE family transcriptional regulator	N.D.			
				APM_0774	ABC-type molybdate transport system periplasmic component-like protein	6.38	2.7 ± 0.1	0.039	
				APM_0775	Binding-protein-dependent transport systems inner membrane component	N.D.			
				APM_0776	PEBP family protein	N.D.			
				APM_0777	Acyl-CoA dehydrogenase domain-containing protein	N.D.			
13B2	3.01	1.6 ± 0.1	0.001	APM_0183	Hypothetical protein	N.D.			
				APM_0184	Hypothetical protein	N.D.			
				APM_0185	Response regulator receiver protein	N.D.			
28G5	-3.52	-1.8 ± 0.1	0.004	APM_3597	2-dehydro-3-deoxyphosphooctonate aldolase	N.D.			
				APM_3598	CTP synthase	N.D.			
79E11	-3.53	-1.8 ± 0.1	0.005	APM_1241	ABC transporter related	N.D.			
				APM_1242	LolC/E family lipoprotein releasing system, transmembrane protein	N.D.			
				APM_1243	Prolyl-tRNA synthetase	N.D.			
65B10	-3.54	-1.8 ± 0.1	0.000	APM_2492	Hypothetical protein	N.D.			
				APM_2493	Ribosomal RNA large subunit methyltransferase N	-11.36	-3.5 ± 0.4	0.006	
				APM_2494	Short-chain dehydrogenase/reductase SDR	N.D.			
				APM_2495	50S ribosomal protein L28	N.D.			
81A10	-3.57	-1.8 ± 0.2	0.007	APM_1125	Major facilitator transporter	N.D.			
				APM_1126	Integral membrane sensor signal transduction histidine kinase	N.D.			
16E1	-3.57	-1.8 ± 0.1	0.005	APM_0148	Putative transcriptional regulator	N.D.			
				APM_0149	Sec-independent protein translocase TatB	N.D.			
				APM_0150	Sec-independent protein translocase, TatC subunit	-43.48	-5.4 ± 0.6	0.000	
11A2	-3.64	-1.9 ± 0.1	0.006	APM_3115	C-terminal processing peptidase	-12.35	-3.6 ± 0.5	0.001	
				APM_3116	50S ribosomal protein L33P	-21.28	-4.4 ± 0.8	0.065	
				APM_3117	Lipid-A-disaccharide synthase	-5.21	-2.4 ± 0.3	0.007	
				APM_3118	Nitrilase/cyanide hydratase and apolipoprotein N-acyltransferase	N.D.			
70B10	-3.66	-1.9 ± 0.1	0.000	APM_3234	Leucyl-tRNA synthetase	-3.46	-1.8 ± 0.5	0.038	
				APM_3235	Hypothetical protein	N.D.			
				APM_3236	Hypothetical protein	N.D.			
				APM_3237	Thiamine monophosphate synthase	N.D.			

73A2	-3.78	-1.9 ± 0.1	0.000	APM_0472	DNA ligase	-7.25	-2.9 ± 0.4	0.015
				APM_0473	TraR/DksA family transcriptional regulator	-55.56	-5.8 ± 0.3	0.007
				APM_0474	Hypothetical protein	N.D.		
				APM_0475	Flagellar basal body P-ring protein	N.D.		
54G10	-3.83	-1.9 ± 0.1	0.000	APM_1922	FkbM family methyltransferase	N.D.		
80H1	-3.87	-2.0 ± 0.1	0.002	APM_1945	Diguanylate cyclase	N.D.		
				APM_1946	Orotate phosphoribosyltransferase	-10.10	-3.3 ± 0.4	0.002
				APM_1947	Isocitrate dehydrogenase	N.D.		
65B2	-3.93	-2.0 ± 0.2	0.010	APM_0798	Histone family protein DNA-binding protein	N.D.		
				APM_0799	Hypothetical protein	N.D.		
				APM_0800	Cell division topological specificity factor	N.D.		
				APM_R0008	tRNA-Phe	N.D.		
63C9	-3.99	-2.0 ± 0.1	0.002	APM_1244	Acyltransferase 3	N.D.		
				APM_1245	Beta-lactamase domain-containing protein	N.D.		
87C7	-4.07	-2.0 ± 0.0	0.001	APM_2312	Hypothetical protein	N.D.		
				APM_2313	S-adenosylmethionine decarboxylase related	N.D.		
				APM_2314	Spermidine synthase	N.D.		
18D2	-4.23	-2.1 ± 0.1	0.001	APM_1170	Colicin V production protein	-11.90	-3.6 ± 0.2	0.003
				APM_1171	DNA repair protein RadA	-21.74	-4.4 ± 0.3	0.019
				APM_1172	Hypothetical protein	N.D.		
				APM_1173	Adenine phosphoribosyltransferase	-22.22	-4.5 ± 0.3	0.016
08B10	-4.27	-2.1 ± 0.1	0.003	APM_1170	Colicin V production protein	-11.90	-3.6 ± 0.2	0.003
				APM_1171	DNA repair protein RadA	-21.74	-4.4 ± 0.3	0.019
				APM_1172	Hypothetical protein	N.D.		
26C11	-4.27	-2.1 ± 0.2	0.000	APM_1242	LolC/E family lipoprotein releasing system, transmembrane protein	N.D.		
				APM_1243	Prolyl-tRNA synthetase	N.D.		
36A6	-4.29	-2.1 ± 0.1	0.000	APM_1184	Voltage-gated potassium channel	N.D.		
				APM_1185	Hypothetical protein	N.D.		
				APM_1186	Ribonuclease	-13.51	-3.8 ± 0.3	0.026
08B6	-4.74	-2.2 ± 0.1	0.000	APM_0839	Hypothetical protein	N.D.		
				APM_0840	Hypothetical protein	N.D.		

APPENDIX VII. Proteomic response to Ni in *Acidiphilium* sp. PM

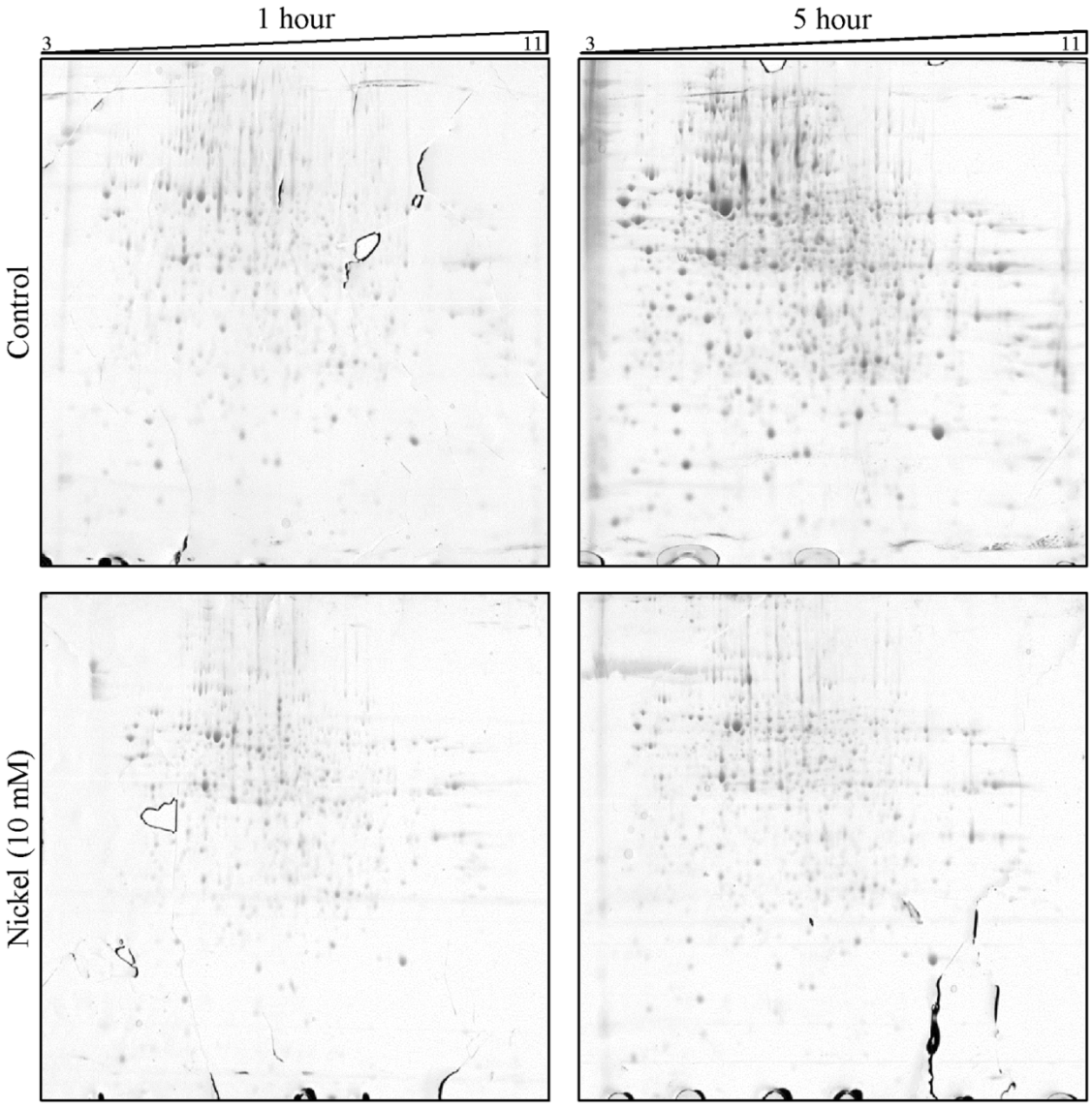

Figure A 6. Optimization of two-dimensional gel electrophoresis. The conditions of the 2D-electrophoresis were optimized using pools of proteins from each condition: 1D (isoelectric focusing) was performed at 20 ºC in strips with a pH gradient 3-11 using the following voltage steps: 120 V for 1 h; 500 V for 2 h; 500-2000V gradient along 2 h; 1000–5000V gradient along 6 h; 5000V for 12 h (totalling 71200 Vhs); 2D was performed by applying the reduced-, alkylated- strip on top of a 12% T, 2.6% C polyacrylamide gel (15W per gel; 20 ºC). For a detailed description of the protocol, see 3.10.2.

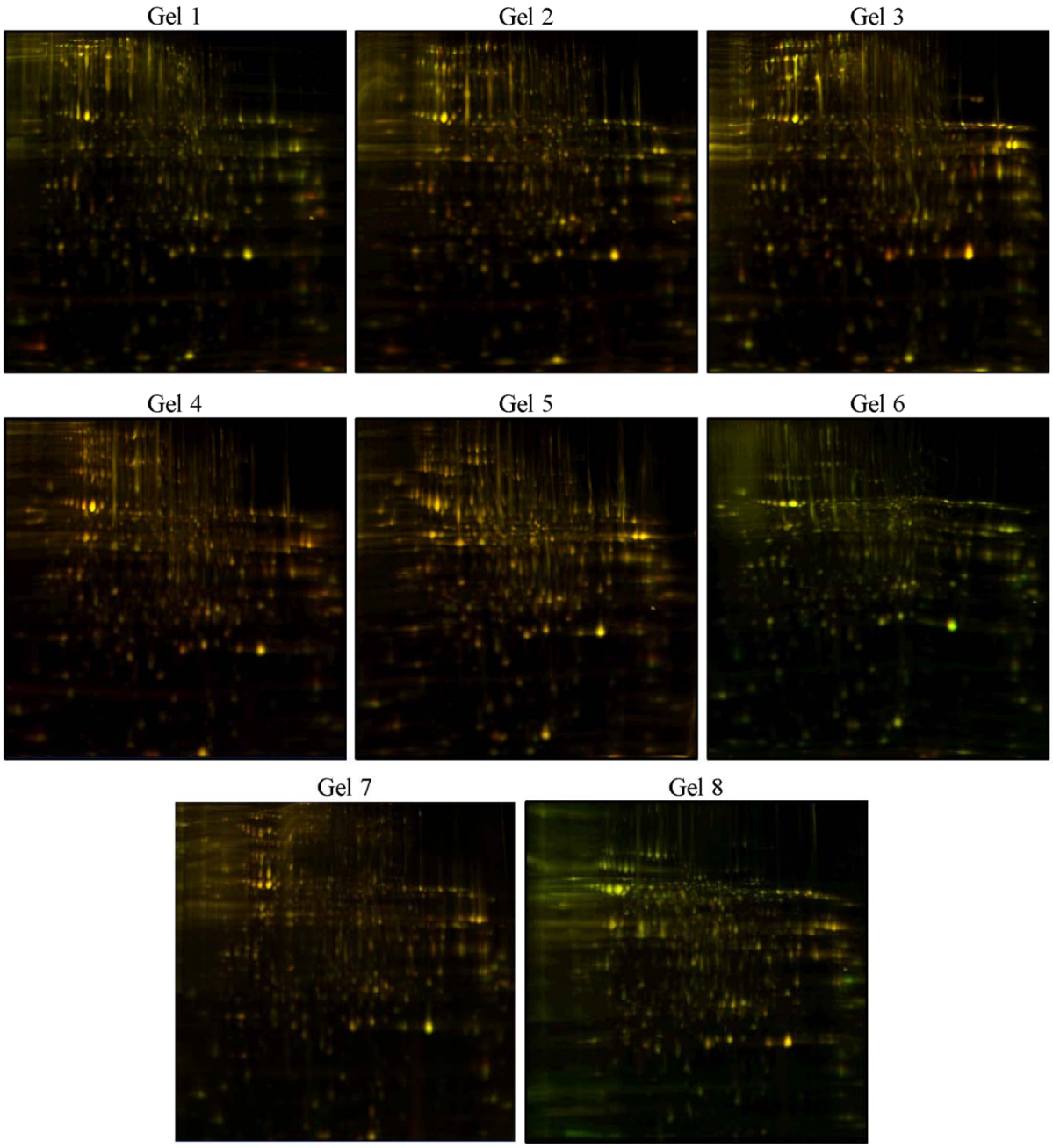

Figure A 7. DIGE gels of the proteomic response to Ni. Proteins were labelled using Cy2 (for the internal standard) and Cy3 or Cy5, and loaded in 8 separate 2D-gels according to the experimental design shown in (Table 19). After 2D electrophoresis, gels were scanned for Cy2, Cy3 and Cy5 emission wavelengths. Images are composites of the three channels.

33. Tamura K, Peterson D, Peterson N, Stecher G, Nei M, et al. (2011) MEGA5: molecular evolutionary genetics analysis using maximum likelihood, evolutionary distance, and maximum parsimony methods. Mol Biol Evol 28: 2731–2739.
34. Thompson JD, Higgins DG, Gibson TJ (1994) CLUSTAL W: improving the sensitivity of progressive multiple sequence alignment through sequence weighting, position-specific gap penalties and weight matrix choice. Nucleic Acids Res 22: 4673–4680.
35. Dew DW, Muhlbauer R, van Buuren C (1999) Bioleaching of copper sulphide concentrates with mesophiles and thermophiles; Brisbane, Australia.
36. Rodrigue A, Effantin G, Mandrand-Berthelot MA (2005) Identification of *rcnA* (*yohM*), a nickel and cobalt resistance gene in *Escherichia coli*. J Bacteriol 187: 2912–2916.
37. Park JE, Schlegel HG, Rhie HG, Lee HS (2004) Nucleotide sequence and expression of the *ncr* nickel and cobalt resistance in *Hafnia alvei* 5–5. Int Microbiol 7: 27–34.
38. Mahapatra NR, Ghosh S, Deb C, Banerjee PC (2002) Resistance to cadmium and zinc in *Acidiphilium symbioticum* KM2 is plasmid mediated. Curr Microbiol 45: 180–186.
39. Parker CT, Kloser AW, Schnaitman CA, Stein MA, Gottesman S, et al. (1992) Role of the *rfaG* and *rfaP* genes in determining the lipopolysaccharide core structure and cell surface properties of *Escherichia coli* K-12. J Bacteriol 174: 2525–2538.
40. Parker CT, Pradel E, Schnaitman CA (1992) Identification and sequences of the lipopolysaccharide core biosynthetic genes *rfaQ*, *rfaP*, and *rfaG* of *Escherichia coli* K-12. J Bacteriol 174: 930–934.
41. Sigel RKO, Sigel H (2007) Complex formation of nickel(II) and related metal ions with sugar residues, nucleobases, phosphates, nucleotides, and nucleic acids. In: Sigel A, Sigel H, Sigel RKO, editors. Nickel and its surprising impact in nature. Chichester, West Sussex, England: John Wiley & Sons Ltd. pp. 109–180.
42. Umbarger HE (1978) Amino acid biosynthesis and its regulation. Annu Rev Biochem 47: 532–606.
43. Santiago B, MacGilvray M, Faustoferri RC, Quivey RG Jr (2012) The branched-chain amino acid aminotransferase encoded by *ilvE* is involved in acid tolerance in *Streptococcus mutans*. J Bacteriol 194: 2010–2019.
44. Tremaroli V, Workentine ML, Weljie AM, Vogel HJ, Ceri H, et al. (2009) Metabolomic investigation of the bacterial response to a metal challenge. Appl Environ Microbiol 75: 719–728.
45. Cheng Z, Wei YY, Sung WW, Glick BR, McConkey BJ (2009) Proteomic analysis of the response of the plant growth-promoting bacterium *Pseudomonas putida* UW4 to nickel stress. Proteome Sci 7: 18.
46. Flint DH, Tuminello JF, Emptage MH (1993) The inactivation of Fe-S cluster containing hydro-lyases by superoxide. J Biol Chem 268: 22369–22376.
47. Geslin C, Llanos J, Prieur D, Jeanthon C (2001) The manganese and iron superoxide dismutases protect *Escherichia coli* from heavy metal toxicity. Res Microbiol 152: 901–905.
48. Chuang SE, Burland V, Plunkett G III, Daniels DL, Blattner FR (1993) Sequence analysis of four new heat-shock genes constituting the *hslTS/ibpAB* and *hslVU* operons in *Escherichia coli*. Gene 134: 1–6.
49. Missiakas D, Schwager F, Betton JM, Georgopoulos C, Raina S (1996) Identification and characterization of HsIV HsIU (ClpQ ClpY) proteins involved in overall proteolysis of misfolded proteins in *Escherichia coli*. EMBO J 15: 6899–6909.
50. Rohrwild M, Coux O, Huang HC, Moerschell RP, Yoo SJ, et al. (1996) HslV-HslU: A novel ATP-dependent protease complex in *Escherichia coli* related to the eukaryotic proteasome. Proc Natl Acad Sci U S A 93: 5808–5813.
51. Jain R, Chan MK (2007) Support for a potential role of *E. coli* oligopeptidase A in protein degradation. Biochem Biophys Res Commun 359: 486–490.
52. Pruteanu M, Neher SB, Baker TA (2007) Ligand-controlled proteolysis of the *Escherichia coli* transcriptional regulator ZntR. J Bacteriol 189: 3017–3025.
53. Kanemori M, Nishihara K, Yanagi H, Yura T (1997) Synergistic roles of HslVU and other ATP-dependent proteases in controlling in vivo turnover of σ^{32} and abnormal proteins in *Escherichia coli*. J Bacteriol 179: 7219–7225.
54. Lien HY, Yu CH, Liou CM, Wu WF (2009) Regulation of *clpQ*$^{+}$*Y*$^{+}$ (*hslV*$^{+}$*U*$^{+}$) Gene Expression in *Escherichia coli*. Open Microbiol J 3: 29–39.
55. Seong IS, Oh JY, Yoo SJ, Seol JH, Chung CH (1999) ATP-dependent degradation of SulA, a cell division inhibitor, by the HslVU protease in *Escherichia coli*. FEBS Lett 456: 211–214.
56. Khattar MM (1997) Overexpression of the *hslVU* operon suppresses SOS-mediated inhibition of cell division in *Escherichia coli*. FEBS Lett 414: 402–404.
57. Goto Y, Calciano LJ, Fink AL (1990) Acid-induced folding of proteins. Proc Natl Acad Sci U S A 87: 573–577.
58. Hong W, Jiao W, Hu J, Zhang J, Liu C, et al. (2005) Periplasmic protein HdeA exhibits chaperone-like activity exclusively within stomach pH range by transforming into disordered conformation. J Biol Chem 280: 27029–27034.
59. Richard H, Foster JW (2004) *Escherichia coli* glutamate- and arginine-dependent acid resistance systems increase internal pH and reverse transmembrane potential. J Bacteriol 186: 6032–6041.
60. Schonknecht G, Chen WH, Ternes CM, Barbier GG, Shrestha RP, et al. (2013) Gene transfer from bacteria and archaea facilitated evolution of an extremophilic eukaryote. Science 339: 1207–1210.
61. Morgante V, Mirete S, Gonzalez de Figueras C, Postigo Cacho M, Gonzalez-Pastor JE (2014) Exploring the diversity of arsenic resistance genes from acid mine drainage microorganisms. Environ Microbiol: In press.